# PHASE DIFFERENCE/TIME DELAY TRACE FUNCTIONS AND THEIR APPLICATION TO BEARING ESTIMATION IN ARRAYS

Shmuel C. Shelef

# NAVAL POSTGRADUATE SCHOOL
## Monterey, California


# THESIS

PHASE DIFFERENCE/TIME DELAY
TRACE FUNCTIONS AND THEIR
APPLICATION TO BEARING ESTIMATION
IN ARRAYS

by

Shmuel C. Shelef

December 1979

Thesis Advisor: G. L. Sackman

Approved for public release; distribution unlimited.

| REPORT DOCUMENTATION PAGE | | READ INSTRUCTIONS BEFORE COMPLETING FORM |
|---|---|---|
| 1. REPORT NUMBER | 2. GOVT ACCESSION NO. | 3. RECIPIENT'S CATALOG NUMBER |
| 4. TITLE (and Subtitle)<br>PHASE DIFFERENCE/TIME DELAY TRACE FUNCTIONS AND THEIR APPLICATION TO BEARING ESTIMATION IN ARRAYS | | 5. TYPE OF REPORT & PERIOD COVERED<br>Doctoral Dissertation; December 1979<br>6. PERFORMING ORG. REPORT NUMBER |
| 7. AUTHOR(s)<br>Shmuel C. Shelef | | 8. CONTRACT OR GRANT NUMBER(s) |
| 9. PERFORMING ORGANIZATION NAME AND ADDRESS<br>Naval Postgraduate School<br>Monterey, California 93940 | | 10. PROGRAM ELEMENT, PROJECT, TASK AREA & WORK UNIT NUMBERS |
| 11. CONTROLLING OFFICE NAME AND ADDRESS<br>Naval Postgraduate School<br>Monterey, California 93940 | | 12. REPORT DATE<br>December 1979<br>13. NUMBER OF PAGES |
| 14. MONITORING AGENCY NAME & ADDRESS(if different from Controlling Office) | | 15. SECURITY CLASS. (of this report)<br>UNCLASSIFIED<br>15a. DECLASSIFICATION/DOWNGRADING SCHEDULE |

16. DISTRIBUTION STATEMENT (of this Report)

Approved for public release; distribution unlimited

17. DISTRIBUTION STATEMENT (of the abstract entered in Block 20, if different from Report)

18. SUPPLEMENTARY NOTES

19. KEY WORDS (Continue on reverse side if necessary and identify by block number)

Array Processing, Bearing Estimation, Passive Sonar, Phase Differences, Trace Function, Time Delay

20. ABSTRACT (Continue on reverse side if necessary and identify by block number)

A new concept called here the "trace function" was formulated and developed in this work.

The notion is that the phase differences/time delays of the signals received from an array of sensors which has a given defined geometry describe a certain "trace function" which is constant for that array at a given look direction. If one can find a geometry for which the trace function's basic shape is not dependent on the

look direction, but only some of its parameters are, then one has a powerful method to correlate (compare) the trace function of the received signal to a stored replica.

The concept of the trace function was formalized and its application to some typical array geometries was demonstrated. Furthermore, it was shown that for highly symmetric arrays like the circular and linear arrays the trace function reduces to a particularly simple form.

This characteristic was used to derive a relatively simple and manageable MMSE estimator for the bearing of the incoming signal. The estimator is applicable to either narrow band signals by use of phase difference trace functions or to a wide band signal using the time delay trace function.

The performance of the estimator was checked by simulation and compared to the CRLB as adapted to this application.

Finally, a system configuration applying trace function principles was outlined and the major problem areas caused by the specific application were identified, reviewed and some suggestions to solutions were made. The principle can be applied to any other situation in which phase differences and/or time delays within an array of sensors can be measured.

Approved for public release; distribution unlimited.

# PHASE DIFFERENCE/TIME DELAY TRACE FUNCTIONS AND THEIR APPLICATION TO BEARING ESTIMATION IN ARRAYS

by

Shmuel C. Shelef
Lieutenant Commander, Israeli Navy
B.S., Technion, Israel Institute of Technology, 1974

Submitted in partial fulfillment of the
requirements for the degree of

DOCTOR OF PHILOSOPHY

from the
NAVAL POSTGRADUATE SCHOOL
December 1979

ABSTRACT

A new concept called here the "trace function" was formulated and developed in this work.

The notion is that the phase differences/time delays of the signals received from an array of sensors which has a given defined geometry describe a certain "trace function" which is constant for that array at a given look direction. If one can find a geometry for which the trace function's basic shape is not dependent on the look direction, but only some of its parameters are, then one has a powerful method to correlate (compare) the trace function of the received signal to a stored replica.

The concept of the trace function was formalized and its application to some typical array geometries was demonstrated. Furthermore, it was shown that for highly symmetric arrays like the circular and linear arrays the trace function reduces to a particularly simple form.

This characteristic was used to derive a relatively simple and manageable MMSE estimator for the bearing of the incoming signal. The estimator is applicable to either narrow band signals by use of phase difference trace functions or to a wide band signal using the time delay trace function.

The performance of the estimator was checked by simulation and compared to the CRLB as adapted to this application.

Finally, a system configuration applying trace function principles was outlined and the major problem areas caused by the specific application were identified, reviewed and some suggestions to solutions were made. The principle can be applied to any other situation in which phase differences and/or time delays within an array of sensors can be measured.

TABLE OF CONTENTS

ACKNOWLEDGEMENTS

I wish to express sincere thanks to the Israeli Navy who by sending me to the Naval Postgraduate School made possible this work.

I am grateful to Professor G. L. Sackman for suggesting the original approach and for his committed assistance during this work.

I also want to thank Professor R. W. Hamming and J. Rockmore for the stimulating discussions which greatly helped to refine the concept. In addition I want to express my appreciation to my doctoral committee which closely followed my work during its evolution.

I would also like to acknowledge the great help of Shirley Strickland, whose assistance was essential in securing the computer, without which this thesis could not have been completed in the time available.

Special thanks are due to Elaine Christian for the devoted and tireless typing of the entire thesis .

Last but not least I want thank my wife Miriam and my children Lital and Yuval for their patience and forbearance during the last two years.

# I. INTRODUCTION

## A. PURPOSE

The estimation of the bearing, frequency and amplitude of acoustic signals for passive sonar is normally accomplished with an array of sensors which has a defined geometrical arrangement. In most cases there are several factors which influence the geometry, of which the most prominent are the size, number of elements and frequency coverage, versus the desired performance. As a result of various tradeoffs, traditionally three main geometrical configurations have been applied:

- the linear array
- the circular or spherical array
- the conformal array.

The linear array is typically applied in fixed sites and in towed configurations and as such the size (length) is not the dominant limitation. The circular or spherical array and the conformal array are applied normally in moving platforms and the size limitations (maximum aperture) is a major factor in the design. The size limitation implies a limitation of angular accuracy and resolution at low frequencies. The extent of the performance limitation can be reduced by proper processing of the array outputs.

To achieve the desired performance, the processing of array data is done in two domains: space domain and time

domain and their derived (by transform) versions; spatial and temporal frequency.

Several approaches have been taken to the above processing, from the simplest one which is the delay and sum beamformer [35, 37, 33] through the correlation processor [17, 21] to the optimal processing [ 1, 2 , 5 , 13, 20, 24, 39] with adaptive version as the "ultimate" processor [12, 20, 42]. All those techniques solve to some extent the processing problem of arrays whose size is such that the interelement spacing is on the order of $\lambda/2$ for the lowest frequencies of interest, and have enough elements to sample adequately the space/time field.

Attempts to overcome the spatial resolution problem have been made by applying the "superdirective array" concept. Although this technique gives infinitely good spatial resolution for noise free environment, it has not been found to be practical because of poor aperture efficiency and sensitivity of the solution to tolerances in implementation [11 , 35 , 37 ]. Recently some constrained sensitivity solutions to the superdirective arrays were presented which give a less sensitive and more efficient array [10 , 24 ].

Some of the above processors are implemented as "beamformers" while the others are considered as estimators of the incoming signal direction. As a general conclusion it can be said that an adequate solution to the problem of small arrays at low frequencies has not yet been fully derived. The aim of this dissertation was to develop such a solution.

## B. MOTIVATION

The practical situation which motivated the initiation of this work was the small circular and cylindrical arrays found in a great number of submarines and surface ships. These arrays are constrained in size to few meters diameter which in turn limits their ability to perform spatial processing of low frequency signals. The size of the whole array is small compared to the wavelength at frequencies of 100 Hz or less.

However, those low frequencies are the very ones which offer longer detection ranges and better classification means. The spatial processing problem can be solved by adding a long line array (towed in general) which will give the needed aperture for the low frequency spatial resolution. For small platforms this approach may not be practical and a different way has to be found by signal processing of the small circular array.

## C. OUTLINE OF THE DISSERTATION

A novel idea which is believed to be original is used as the basis for this dissertation. This idea is basically a new way to look at the available information from an array of sensors called the "trace function" by the author.

It is based on the fact that the directional information of an incoming plane wave is mainly contained in the received signal phases, or to be more precise, in the relative phase differences between received signals at the various elements of the array.

Those phase differences are representative of the time delay of the plane wave between the elements of the array. The notion is that the phase differences/time delays of the signals received from an array of sensors which has a given defined geometry describes a certain "trace function" which is constant for that array at a given look direction. If one can find a geometry for which the trace function's basic shape is not dependent on the look direction, but only some of its parameters are, then one has a powerful method to correlate (compare) the trace function of the received signal to a stored replica.

Fortunately one such geometry is provided by the circular array, which was the motivation behind this work and whose phase difference trace function is a simple two dimensional sine-cosine "wave" of exactly one period of each dimension.

The apparent "phase" of this trace function is indicative of the bearing of the incoming plane wave signal. The trace function idea can be used with array geometries other than the circular one, however, it will be less efficient as the symmetry is broken. For example, it will be shown in later chapters how it applies to linear arrays.

General Definition - A trace function is a discrete plot of phase difference/time delay versus element indices for all element pairs.

Fig. I-1 shows such a trace function for a random array while Figs. I-2 and (-3 show one each for a linear and circular array.

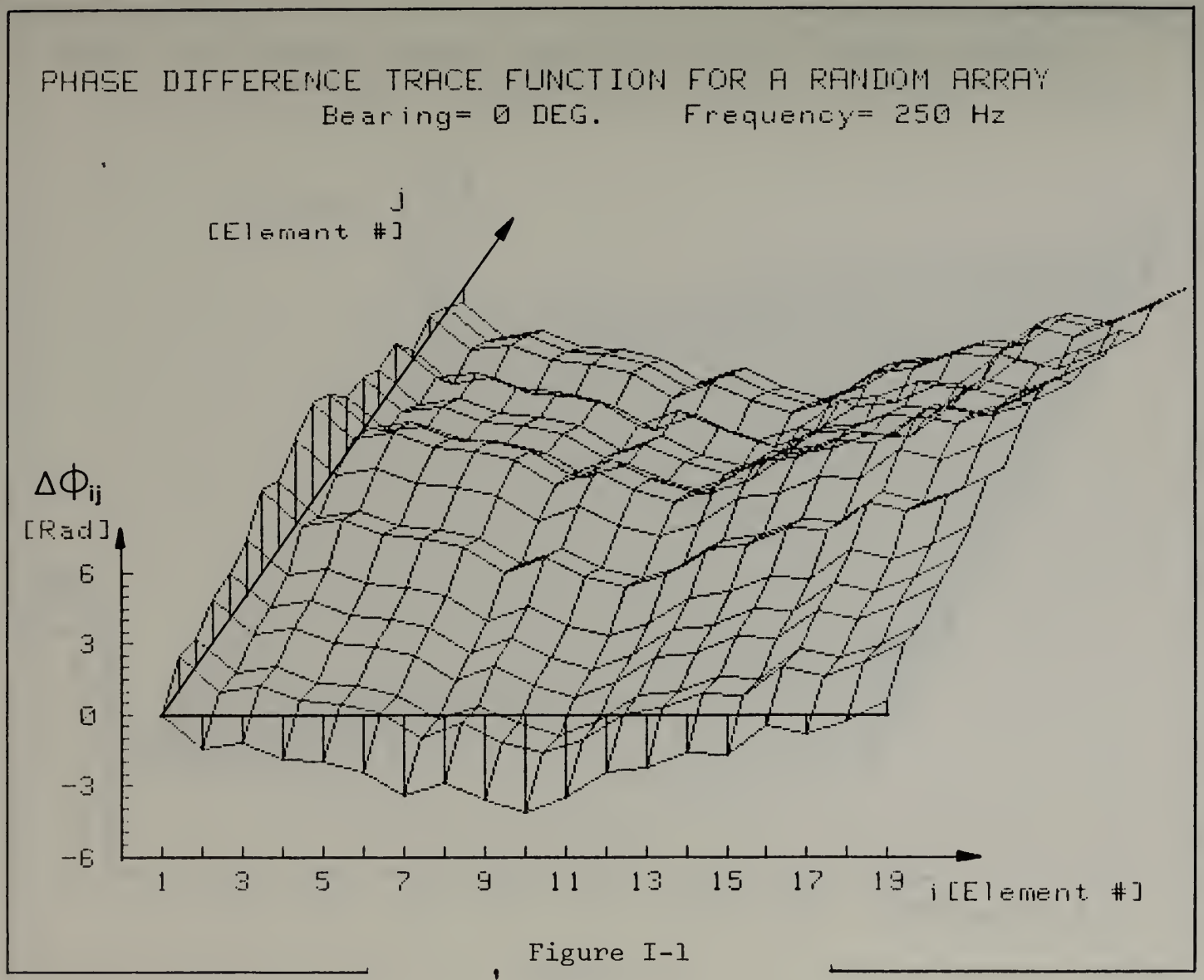
PHASE DIFFERENCE TRACE FUNCTION FOR A RANDOM ARRAY
Bearing= 0 DEG. Frequency= 250 Hz
j
[Elemant #]
$\Delta\Phi_{ij}$
[Rad]
6
3
0
-3
-6
1
3
5
7
9
11
13
15
17
19
i[Element #]

Figure I-1

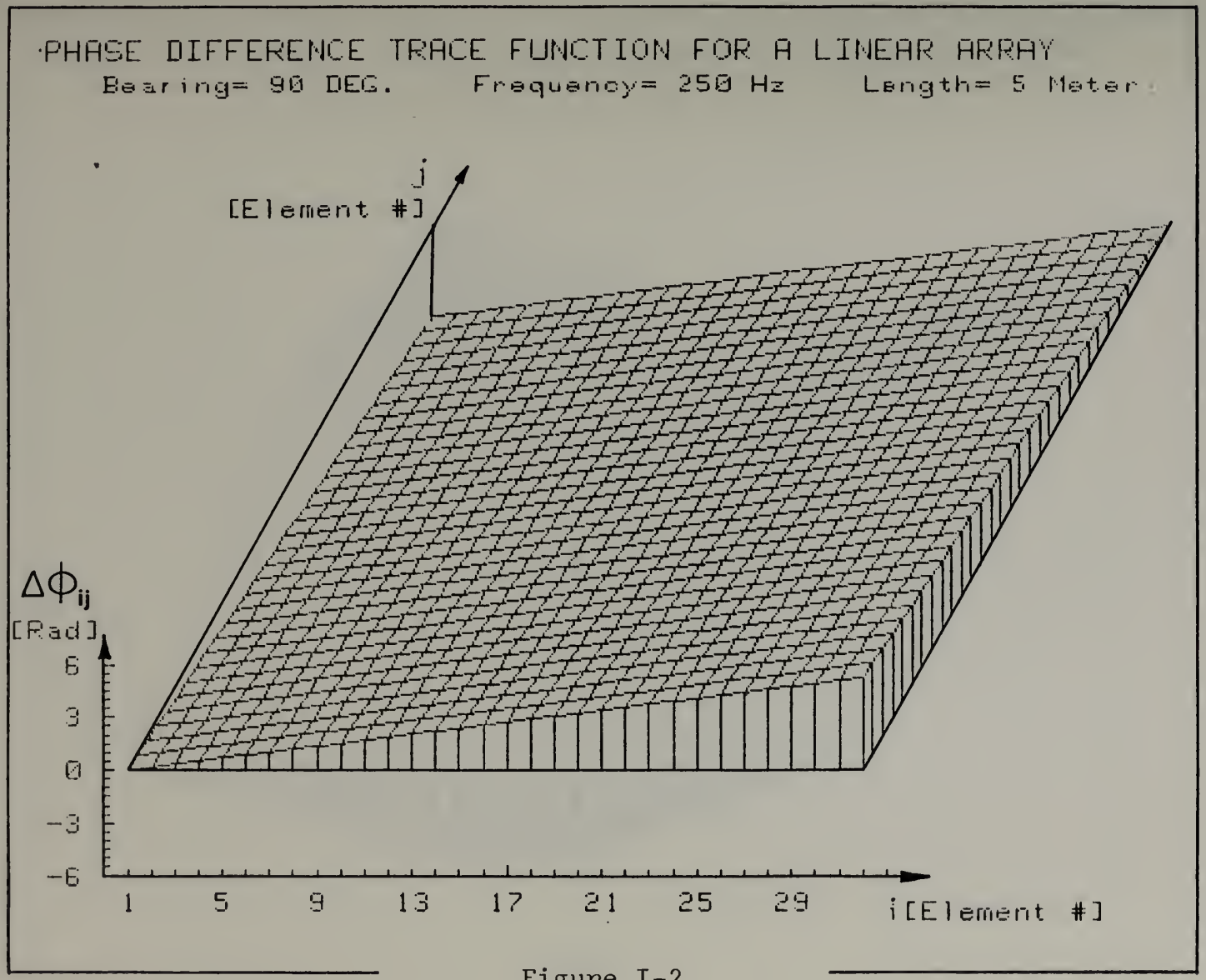
PHASE DIFFERENCE TRACE FUNCTION FOR A LINEAR ARRAY
Bearing= 90 DEG.
Frequency= 250 Hz
Length= 5 Meter
j
[Element #]
$\Delta\phi_{ij}$
[Rad]
6
3
0
-3
-6
1
5
9
13
17
21
25
29
i[Element #]

Figure I-2

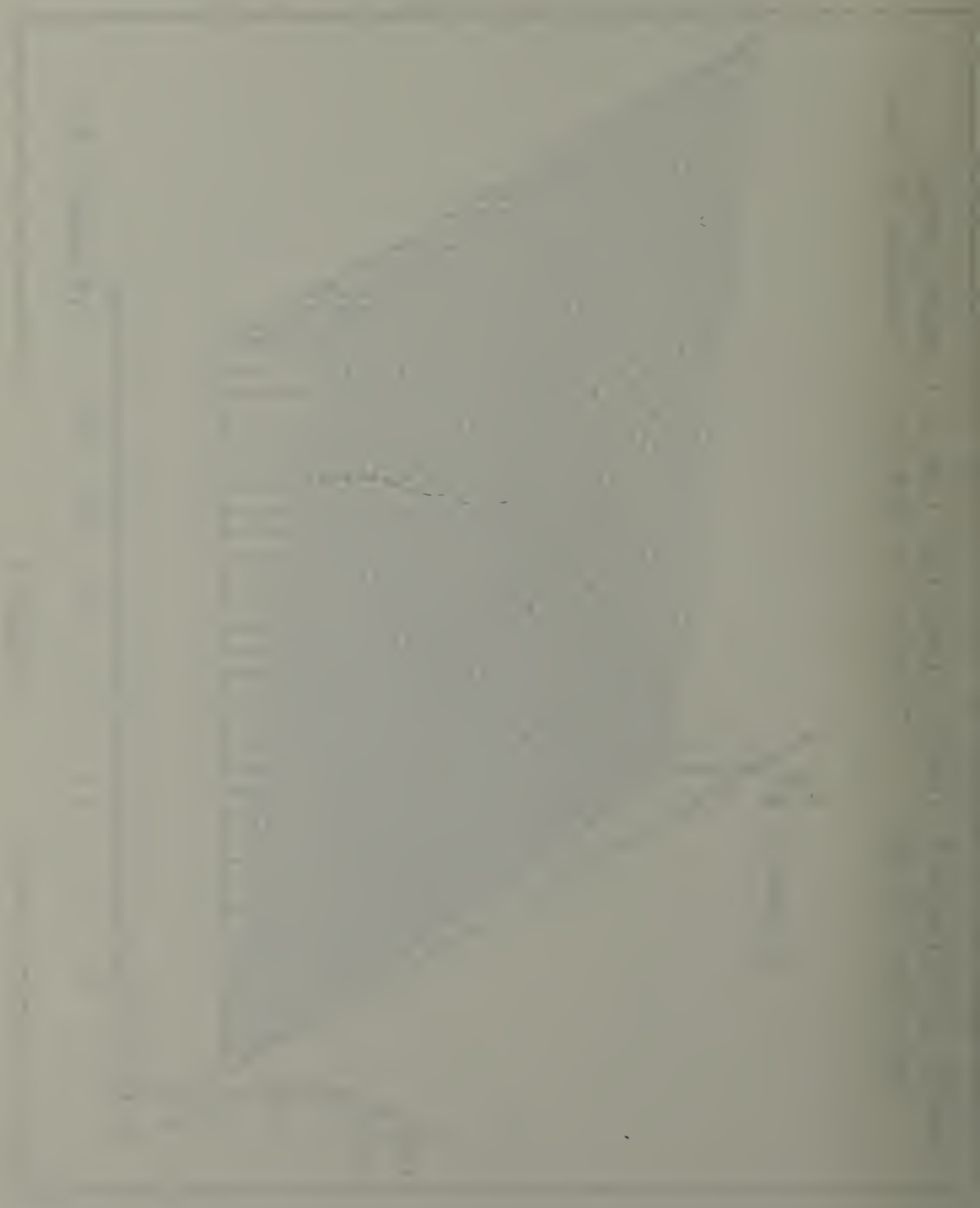

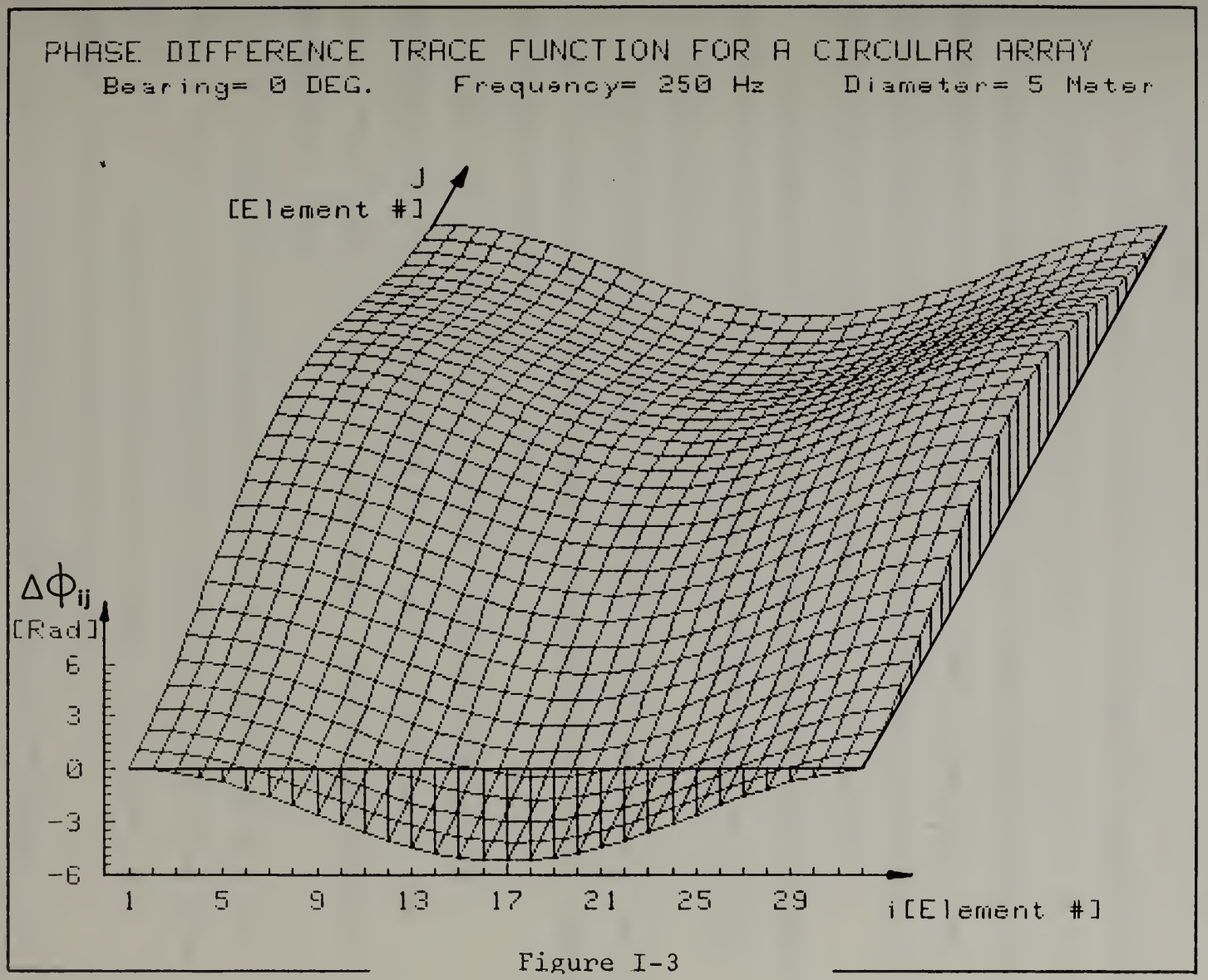
PHASE DIFFERENCE TRACE FUNCTION FOR A CIRCULAR ARRAY
Bearing= 0 DEG.
Frequency= 250 Hz
Diameter= 5 Meter
J
[Element #]
Δφij
[Rad]
6
3
0
-3
-6
1
5
9
13
17
21
25
29
i[Element #]

Figure I-3

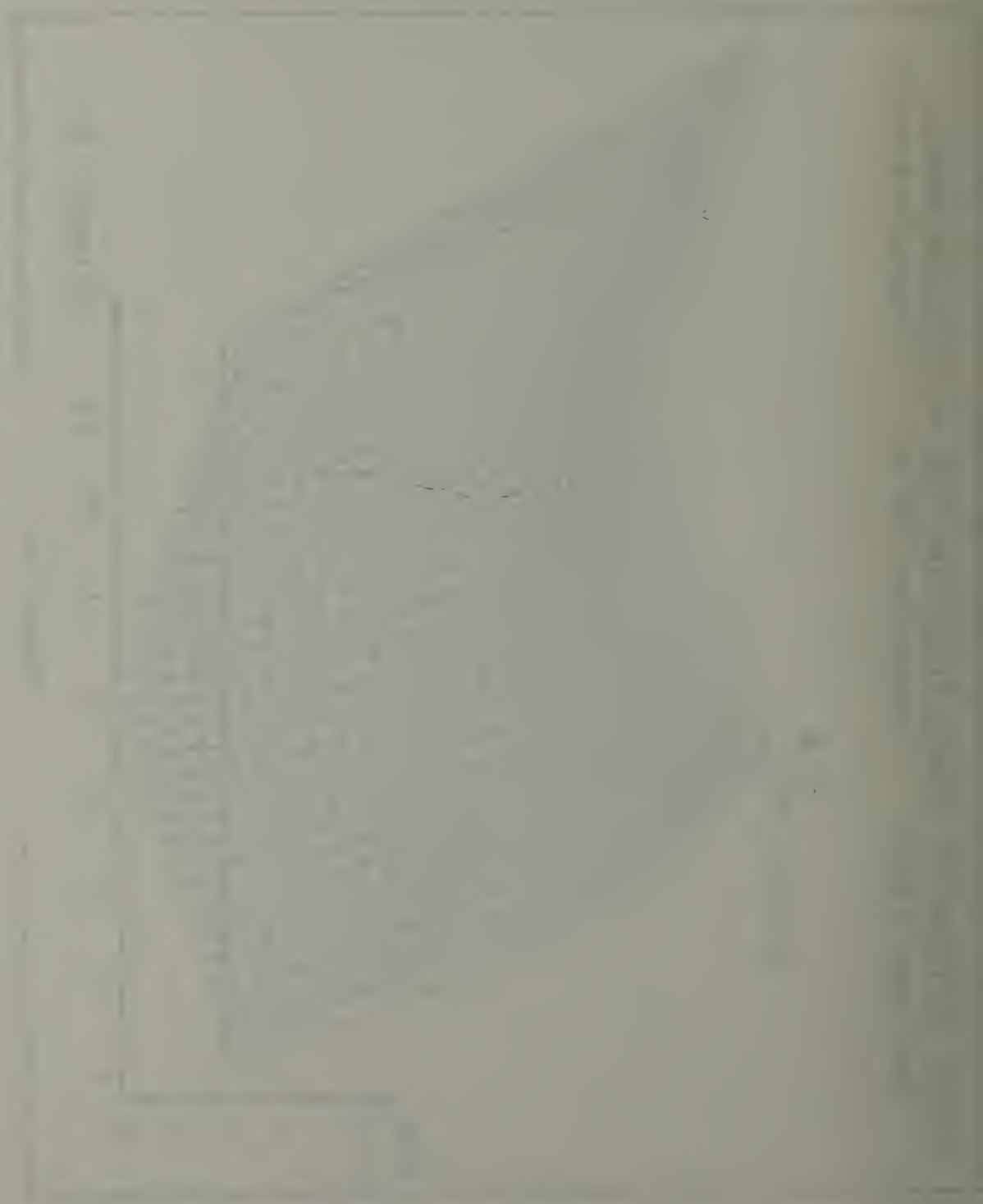

Two main features can be readily observed for any trace function:

- the elements on the diagonal are always zero ($\Delta\tau_{ii} \equiv 0$ and $\Delta\phi_{ii} \equiv 0$).
- the trace function is always antisymmetric across the diagonal ($\Delta\tau_{ij} \equiv -\Delta\tau_{ji}$ and $\Delta\phi_{ij} \equiv -\Delta\phi_{ji}$).

For the noise free conditions the trace function can be derived easily for a given geometry. Trace functions are defined separately for each look direction and for each frequency resolution cell (or for wide band time delay).

In Chapter II of this dissertation the subject of definition and construction of the trace function will be treated in great detail.

For the received signal in a noisy environment the above trace functions must be estimated for each narrow band signal present and for the wide band data.

Once the trace function of the received signals is estimated it can be "matched" to a stored replica of the noise-free trace function of the array (either in discrete or analytic form).

The task of estimating the trace function from the received data is not trivial mainly because it has to be done in the very difficult conditions of small array size and highly correlated noise between sensors.

All optimal processors use some scheme to "whiten" the noise in spatial domain and/or temporal domain before it is further processed. This approach has to be considered in

this case too. However, the trace function concept poses a heavy demand on that type of preprocessing because the preservation of relative phase within the array is required. Present prewhitening schemes are not readily applicable and ways have to be found to perform the above task. Suggestions about relative phase preserving spatial decorrelation methods are made in Chapter V (System Considerations) which use a compensation scheme to preserve phase, and are based on the knowledge (a priori or estimated) of the ambient noise spectrum and covariance functions.

The estimation of phase differences can be done by established cross spectral estimation methods, especially the "short modified periodogram" method [40, 25, 26] which was adopted in this work and is reviewed in Chapter V for this application.

For the time delay estimation several approaches are possible and this subject is treated extensively in the current literature [6, 9, 14, 15].

Of the above methods, the one which was the most applicable is reviewed in Chapter V and some adaptations to this work are suggested.

The match of the estimated and stored trace function was done by a minimum mean square error (MMSE) estimator which was fully derived in this work. The derivation of the estimation is given in Chapter III and its performance is detailed in Chapter IV. The performance of the estimator was checked by computer simulations and the results are presented and compared

to a classical benchmark, the Cramer-Rao Lower Bound (CRLB).

A block diagram for a possible implementation scheme is given in Chapter V.

Chapter VI presents a concise summary of this work. In addition it is suggested that the trace function concept and the estimators derived in this work are not limited in their application to sonar. They can be applied to related areas like seismic, and ocean wave analysis. The chapter concludes with some proposed topics for future work which were opened up by the introduction of the trace function principle.

## D. RELATED WORK

As the concept is new, very little related work can be mentioned as applying strictly to the basic idea of the trace function. Only two works [3, 22] can be defined as such. The rest of the references used in this dissertation could be more correctly described as supporting works.

Two previous papers published by the author (with G. L. Sackman) [30, 31] on the subject of the dissertation are also cited.

The two paper's which are related to the subject [3, 22, op.cit.] were brought to the attention of the author recently after the trace function concept had already been developed. The relationship is restricted to the general concept of "matching" some function of the cross spectral matrix to an incoming plane wave. Those two papers were analyzed in order

to contrast with and emphasize the present work.

The first paper by Munk et al [22] is the basic one in which the authors address the problem of estimation of the direction of ocean waves arising from distant storms using a relatively small array of three sensors. The problem is somewhat similar to the present one, however it is in a totally different discipline and the methods used for solution are also significantly different. The solution which was shown in that paper is a MSEE fitting of a full, measured cross spectral matrix (complex in general) of an array, to an assumed form of such a matrix for a plane wave. Their method used an "educated" search technique to minimize the error in the fitting process.

Very good results were achieved, however the computational complexity was tremendous.

The second paper by Bennett [ 3 ] is a tutorial report published almost ten years after the first one. In this report the author formalizes and reviews the methods of the paper by Munk et al adding some alternatives and demonstrating the theory by the results of processing real data. However, no departure was made from the basic approach of Munk et al.

It is worthwhile to mention that Bennett concluded that this method of least square fitting was the best available at that time for bearing estimation. In contrast to the above the present work uses only certain relevant parts of the cross spectral matrix - the phase differences - as a measure to be fitted and introduces the notion of the trace

function as a replica which is only dependent on array geometry. This simplification leads to an explicit MMSE estimator equation for some well defined array geometries.

The option of "educated" search remained open, but for a much simpler set of data. All this is done without degrading performance; in fact it is demonstrated by simulation that the present estimator is asymptotically efficient (achieves C. R. Lower Bound).

Another fact which should be mentioned is that the derivation of the trace function concept was initiated from the end product, the bearing, and how it effects the various measurable parameters in the array and not from the mathematical structure of the cross spectral matrix as in the previous works.

Nevertheless, the merit of these related works remains valid and both the previous and the author's methods complement each other, opening perhaps a whole new way of processing array data. The supporting works will not be considered in this section mainly because they cover a wide variety of subjects and do not affect the heart of the problem. They are mentioned and referenced elsewhere in this work, each along with its applicable subject.

## E. CONTRIBUTIONS

The principal contributions of this dissertation can be summarized as follows:

1. The first introduction and derivations of the phase-difference/time-delay trace function concept for arrays of

sensors, its applicability and limitations.

2. Derivation of a MMSE bearing estimator which implements the trace function concept for circular and linear arrays, and its performance.

3. Definition of a system which applies the new concepts along with suggestions for solution of some specific problems which arose from the special demands of phase preserving preprocessing for the trace function concept.

## II. PHASE DIFFERENCE/TIME DELAY TRACE FUNCTION OF ARRAYS - THE CONCEPT

### A. INTRODUCTION

The basic concept of the trace function of an array is the basis for the bearing estimation method developed in this dissertation.

In order to give the reader a good understanding of the subject, the concept of the trace function is defined and developed for a general three dimensional array first and then for some typical two dimensional geometries of arrays. Finally the advantages of this concept will be pointed out for symmetrical arrays, especially the circular array.

Shown in Fig. II-1 is an arbitrary three-dimensional array of N receiving elements. The location of the i-th element with respect to a fixed (x,y,z) cartesian coordinate system is defined by the vector $\bar{r}_i$ specifying both distance and direction from the center of the coordinate system.

A uniform plane wave propagates with speed c in a direction $\bar{\alpha}$ with respect to the coordinate system. The vector $\bar{\alpha}$ has a unit length.

The plane wave is assumed to contain a wide band random signal, $S_{wb}$ and a set of M line (sinusoidal) components with random initial amplitude and phase, $S_{nb}$. Then, if we assume that the same plane wave arrives at each element, we can specify vector signal to be:

$$\bar{x}(t) = \begin{bmatrix} S_{wb}(t-\tau_0) + S_{nb}(t-\tau_0) \\ S_{wb}(t-\tau_1) + S_{nb}(t-\tau_1) \\ \vdots \\ S_{wb}(t-\tau_{N-1}) + S_{nb}(t-\tau_{N-1}) \end{bmatrix} \qquad \text{(II-1)}$$

$$\text{where } \tau_i = \frac{\bar{\alpha} \cdot \bar{r}_i}{c} \qquad \text{(II-2)}$$

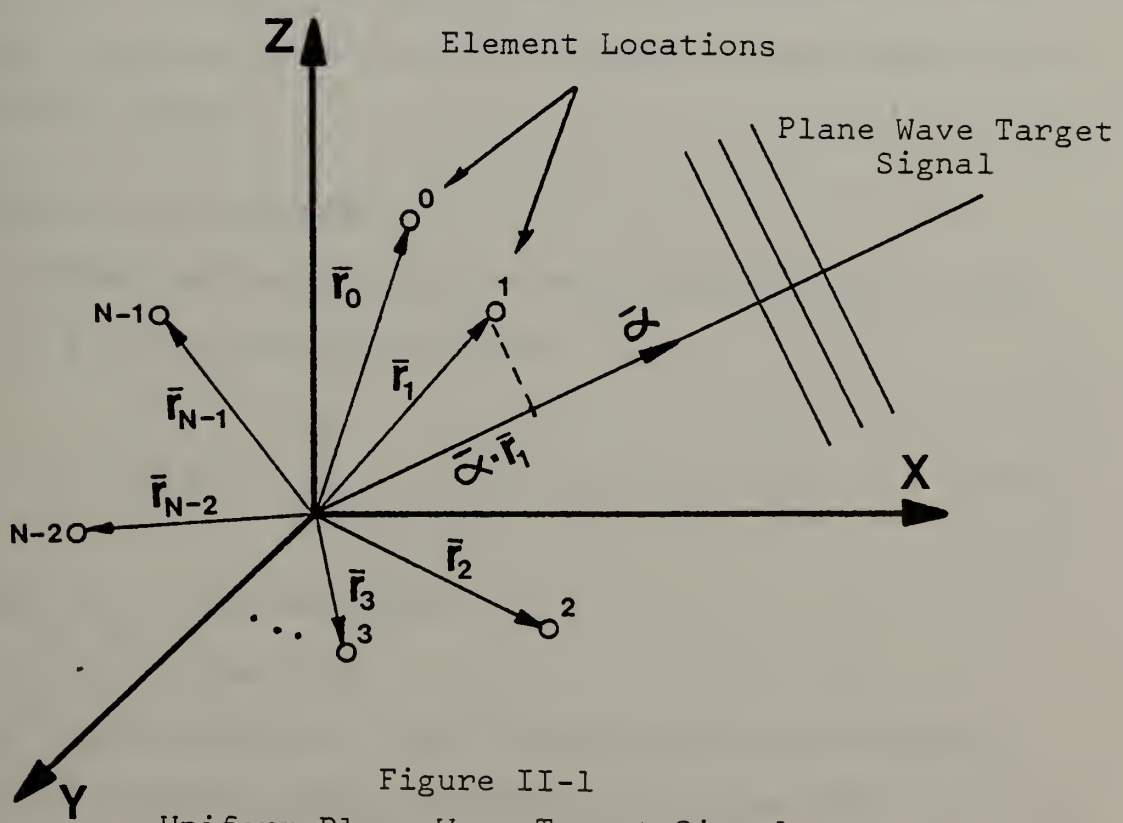


Figure II-1
Uniform Plane Wave Target Signal
Impinging On An Arbitrary
Three Dimensional Array Of Elements

The above definition of a uniform plane wave target signal shows that the signal component at each element is identical except for a delay. This is under the assumption that attenuation is negligible and no change in the speed of sound occurs within the array dimensions

From a total system point of view we have to include also the additive noise component at each element; however, for the conceptual demonstration of the trace function the noise free condition is adequate. Under the above stated conditions it is suggested that these delays ($\tau_i$) are the parameters which contain the directional information of the plane wave.

It is convenient to consider the wide band portion of the signal and the line components separately, although it will be shown that the trace function concept is applicable to both in a similar manner.

B. NARROW BAND COMPONENT

As stated before, the narrow band component $S_{nb}$ is composed of a set of sinusoidal lines:

$$S_{nb}(t,i) = \sum_{\ell=1}^{M} A_\ell \cos [\omega_\ell(t-\tau_i) + \phi_\ell] \qquad \text{(II-3)}$$

where $A_\ell$ - line amplitude

$\phi_\ell$ - line phase

The phase difference trace function is constructed by taking all possible pairs of elements and observing that the phase difference between <u>any pair</u> of elements' signals $S_{nb}(i,\ell)$ and $S_{nb}(j,\ell)$ is:

$$\Delta\phi_{ij,\ell} = \omega_\ell (\tau_i - \tau_j) \qquad \text{(II-4)}$$

Using (II-2) and (II-4):

$$\Delta\phi_{ij,\ell} = \omega_\ell(\tau_i - \tau_j) = \omega_\ell \frac{\bar{\alpha} \cdot (\bar{r}_i - \bar{r}_j)}{c} \qquad \text{(II-5)}$$

where "i" and "j" are equivalent indices of the array elements and denote the pairs which are considered for phase difference or time delays.

Definition: A phase difference trace function is defined as the plot of $\Delta\phi$ (phase difference as a discrete function of "i" and "j" (element numbers in the array) for "$\ell$" (frequency) constant.

An example of such a trace function is shown in Figure II-2 for a random array.

Observations:

a. Each $\Delta\phi$ is a constant for a given look direction $\bar{\alpha}$ so that for a fixed geometry (fixed $\bar{r}_i$) and frequency $\omega_\ell$ the trace function in invariant in time.

b. For various frequencies $\omega_\ell$=1,2..M we get a family of such invariant trace functions which are linearly related.

c. For various look directions we get a set of such families, one for each look direction $\bar{\alpha}$.

From the above observations we can conclude that if we know such a set of families of trace functions which are invariant for a given array geometry we can "match" a received and estimated trace function to the precomputed members

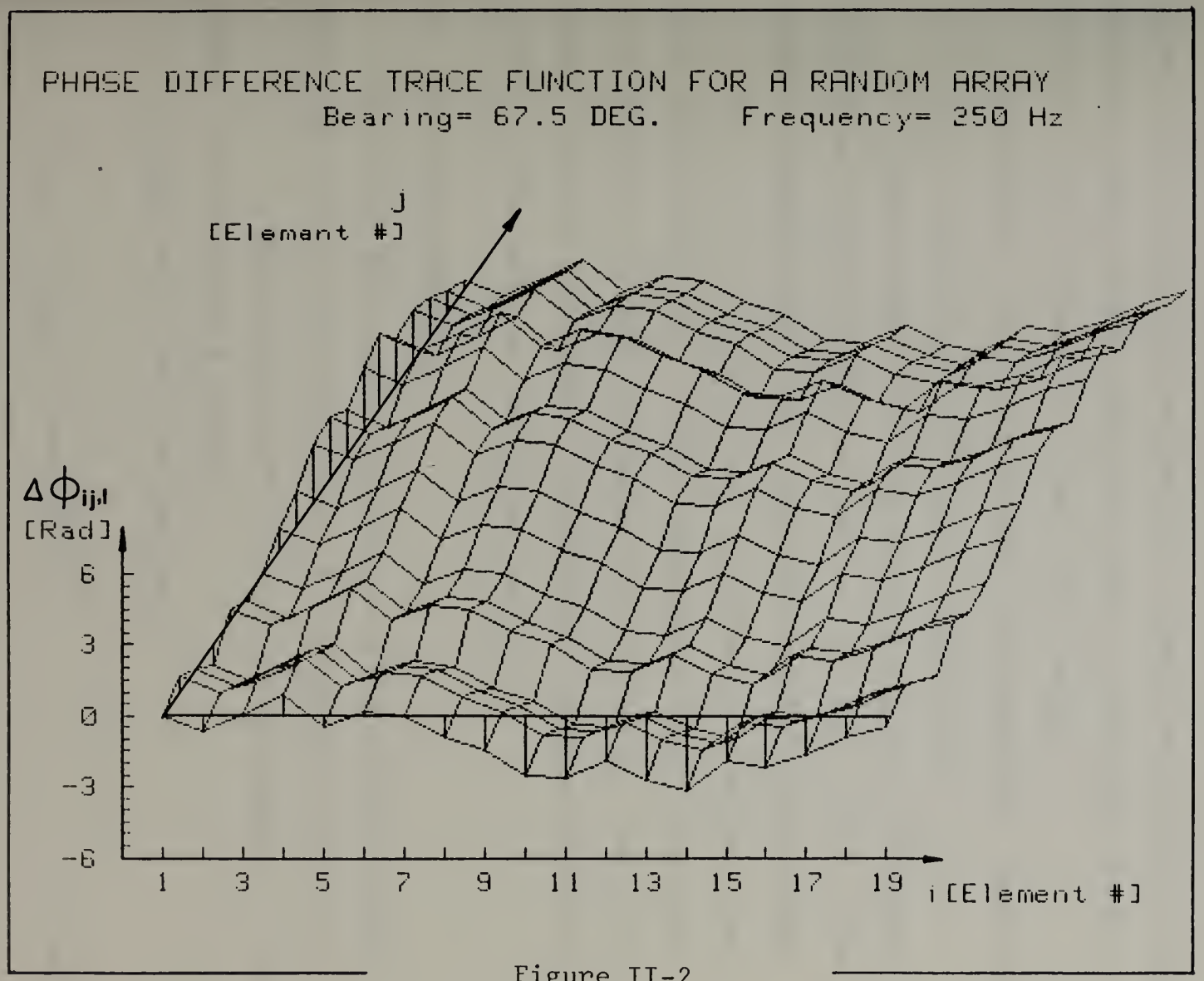
PHASE DIFFERENCE TRACE FUNCTION FOR A RANDOM ARRAY
Bearing= 67.5 DEG.
Frequency= 250 Hz
j
[Element #]
Δφij,l
[Rad]
6
3
0
-3
-6
1
3
5
7
9
11
13
15
17
19
i [Element #]

Figure II-2

of the sets/families and find the look direction for each frequency resolution element.

The task of performing the above match can be quite formidable for a practical situation, unless some regularity and symmetry can be found within the sets. It may even be prohibitive to be processed in real time systems.

Fortunately, for some practical and symmetrical geometries of arrays, this task of matching is facilitated.

It is easy to see that this concept applies to multiple targets as well if we assume that we can always find a fine enough frequency resolution such that two different targets will have their line components in different frequency analysis resolution cells. (This condition is easily achieved in practice.) If they are coming from different look directions they will be members of different families as defined above and they will be recognized as such.

C. WIDE BAND COMPONENT

For a wide band random process the phase is not defined, hence we will use the time delay as a measure for the trace function. As mentioned before the wide band component of the signal is defined as $S_{wb}(t-\tau_i)$.

In analogy with the line components

$$\Delta\tau_{ij} = (\tau_i-\tau_j) = \frac{\bar{\alpha} \cdot (\bar{r}_i-\bar{r}_j)}{c} \qquad \text{(II-6)}$$

Definition: A time delay trace function is defined as the plot of $\Delta\tau_{ij}$ (time delay) as a discrete function of "i" and "j" (element numbers in the array).

Figure II-3 shows such a time delay trace function for a random array.

The observations for the narrow band components are readily applicable to the wide band components as well with one exception: the frequency domain collapses into only one trace function, such that it results in a single set of trace functions, one for each look direction $\bar{\alpha}$.

The same conclusions as for the narrow band components apply, however the multiple target distinction based on frequency resolution cannot be done any more. Some suggestions to overcome this problem will be made in Chapter V.

## D. TRACE FUNCTION CALCULATION

### 1. Analytic Trace Functions

The trace functions of arrays which have a geometry such that they can be expressed in a closed form equation are defined here as "analytic". The calculation of these trace functions is simple and is based on geometry only. In this work only two dimensional arrays were treated, however the extension to three dimensions is straightforward.

The calculations are derived from equations (II-5) and (II-6) for phase difference and time delay trace functions respectively.

These derivations are shown in Appendix A for circular and linear arrays.

#### a. Circular Array

The configuration of this array is shown in Figure II-4. From Appendix A:

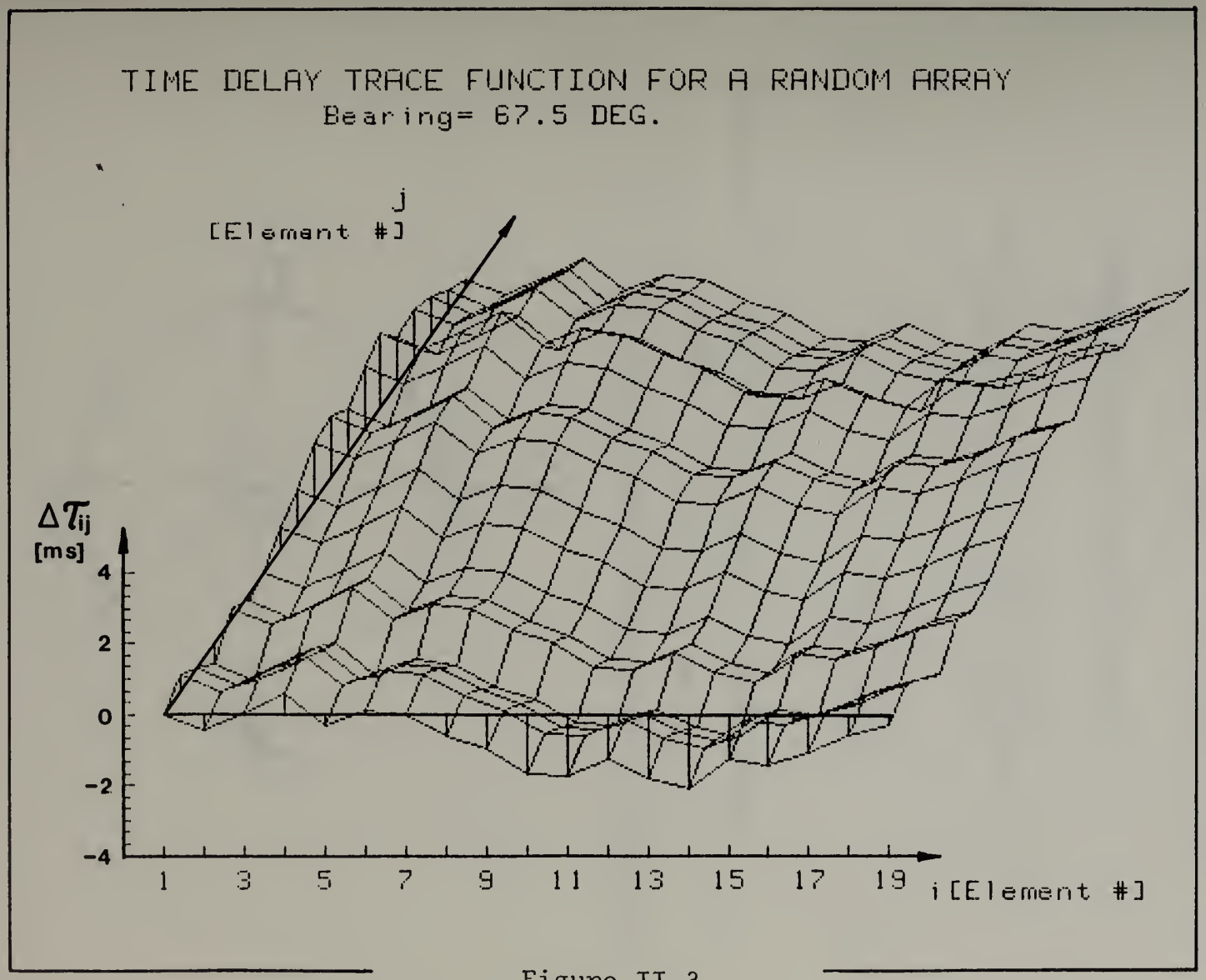
TIME DELAY TRACE FUNCTION FOR A RANDOM ARRAY
Bearing= 67.5 DEG.
j
[Element #]
Δτij
[ms]
4
2
0
-2
-4
1
3
5
7
9
11
13
15
17
19
i[Element #]

Figure II-3

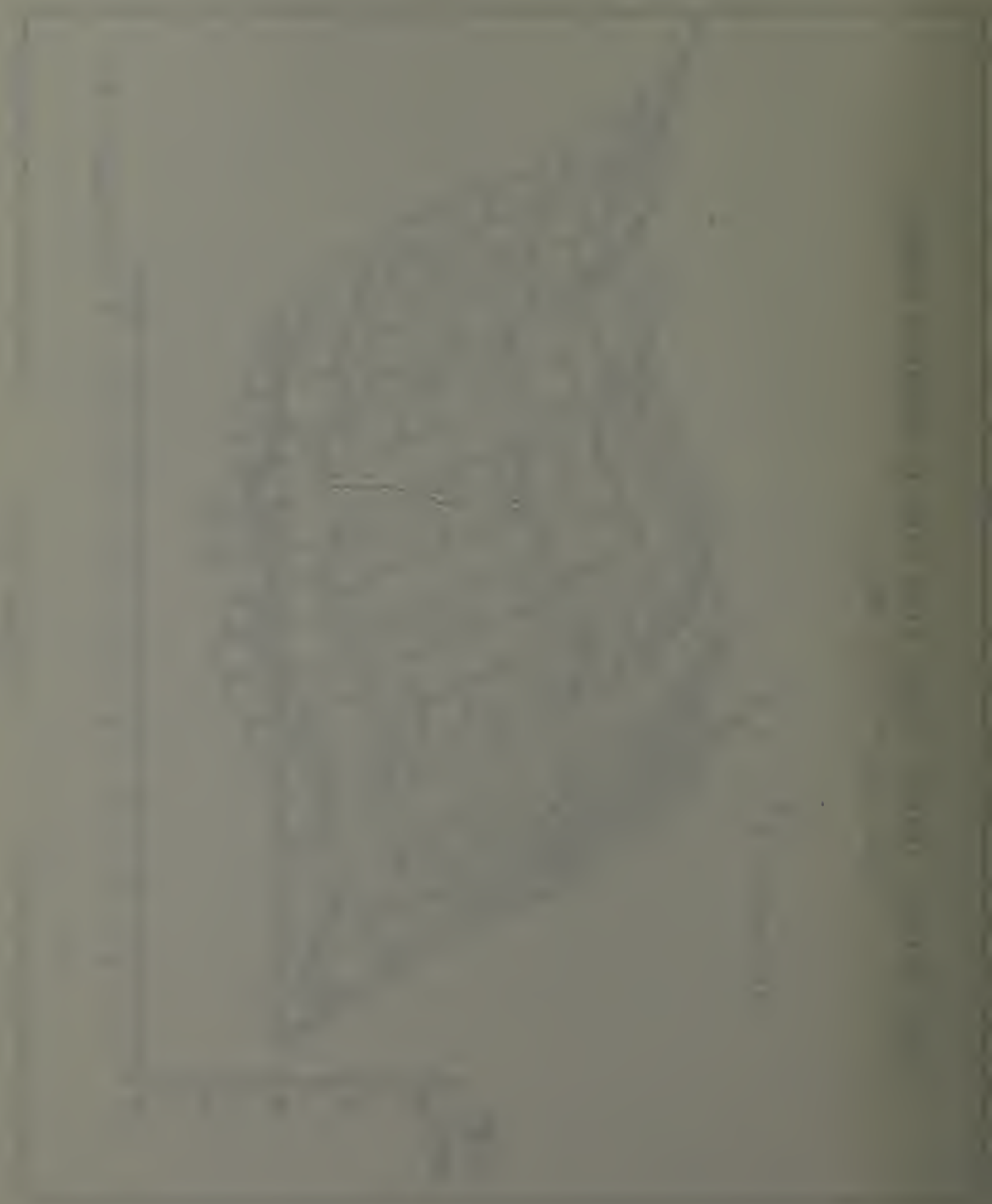

- Time delay trace function

$$\Delta\tau_{ij} = -2\frac{R}{c} \sin\left[\frac{\pi}{N}(i+j)-\theta\right]\sin\left[\frac{\pi}{N}(i-j)\right] \quad \text{(II-7)}$$

- Phase difference trace function

$$\Delta\phi_{ij,\ell} = \Delta\tau_{ij}\omega_{\ell} = -\frac{2\pi D}{\lambda_{\ell}} \sin\left[\frac{\pi}{N}(i+j) - \theta\right]$$

$$\times \quad \sin\left[\frac{\pi}{N}(i-j)\right] \quad \text{(II-8)}$$

where R,D - radius and diameter respectively

N - number of elements in the array

$\theta$ - incoming signal bearing (look direction)

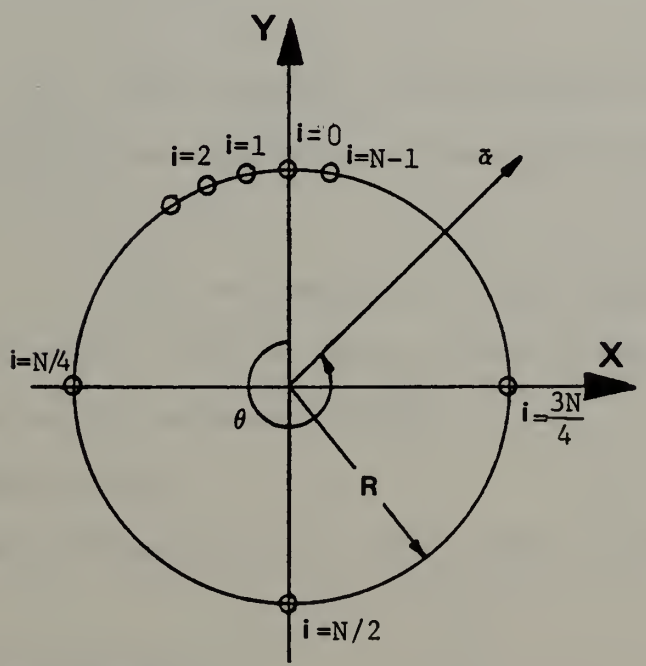


Figure II-4
Circular Array Configuration

In Figure II-5 through II-13 are shown the three dimensional plots of the phase difference trace functions - $\Delta\phi_{ij,\ell}$ for a circular array of 32 elements (Equation II-8) at various look directions (bearings). The effect of frequency change can be seen by comparing Figures II-5 and II-14. This effect is only on the "amplitude" of the trace function but not on its basic form (similar effects are caused by changes in diameter-D or sound velocity-C). The computer program for ploting these trace functions on a Hewlett-Packard 9845T computer is presented in Appendix B-1.

Observations:

(1) The trace functions of circular arrays are always a sampled two dimensional combined cosine and sine surface of exactly one period ($360^{\circ}$) in each dimension ("i" and "j").

(2) The "phase" of the above two dimensional wave is identically the direction of arrival of the incoming signal.

(3) The estimation of the "phase" can be done relatively easily for the noisy trace function by minimum mean square error surface fitting.

b. Linear Array

The configuration of this array is shown in Figure II-15.

From Appendix A:

- Time delay trace function

$$\Delta\tau_{ij} = \frac{d}{c}(i-j)\sin\theta \qquad \text{(II-9)}$$

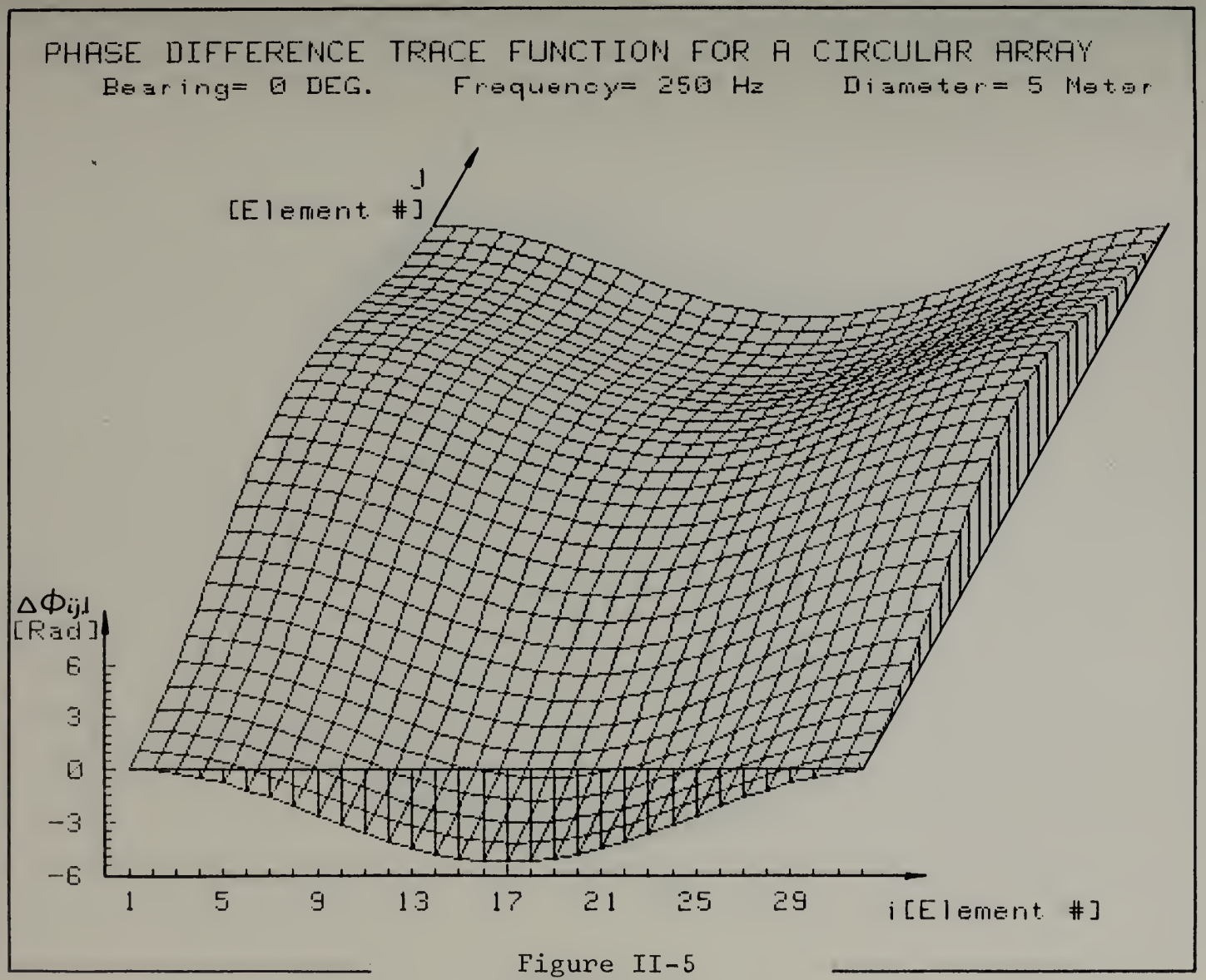
PHASE DIFFERENCE TRACE FUNCTION FOR A CIRCULAR ARRAY
Bearing= 0 DEG.
Frequency= 250 Hz
Diameter= 5 Meter
J
[Element #]
ΔΦijl
[Rad]
6
3
0
-3
-6
1
5
9
13
17
21
25
29
i[Element #]

Figure II-5

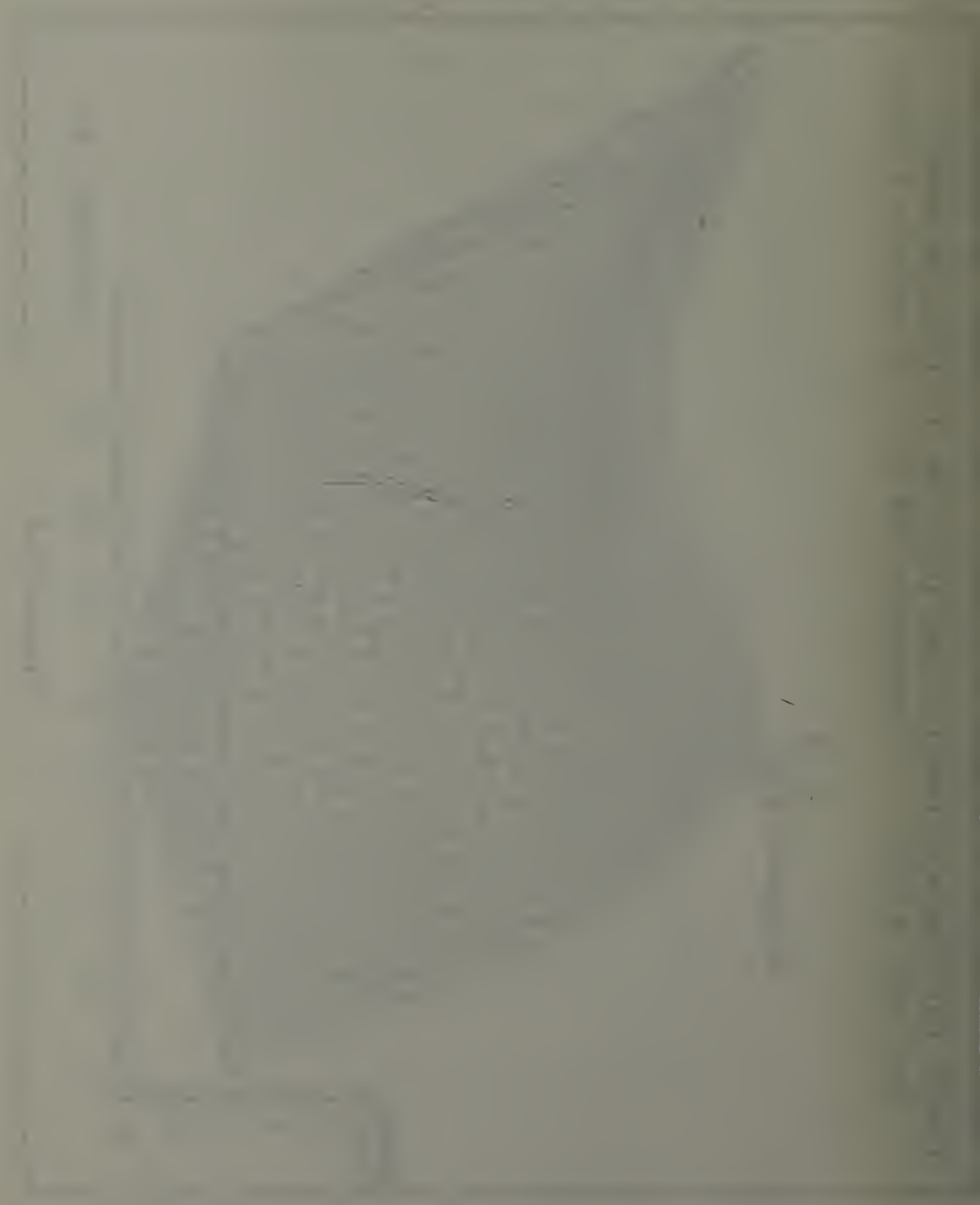

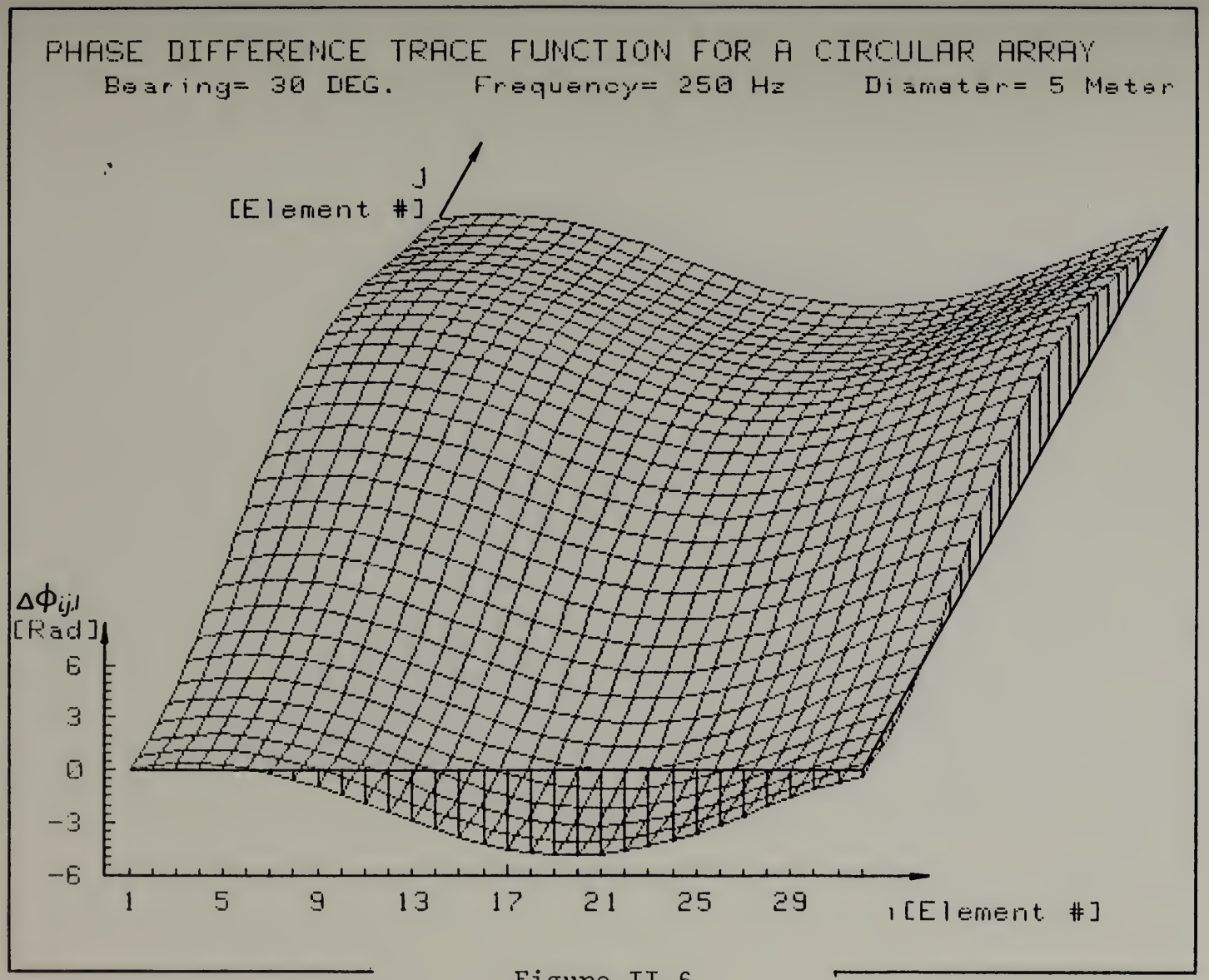
PHASE DIFFERENCE TRACE FUNCTION FOR A CIRCULAR ARRAY
Bearing= 30 DEG.
Frequency= 250 Hz
Diameter= 5 Meter
J
[Element #]
Δφij,l
[Rad]
6
3
0
-3
-6
1
5
9
13
17
21
25
29
I [Element #]

Figure II-6

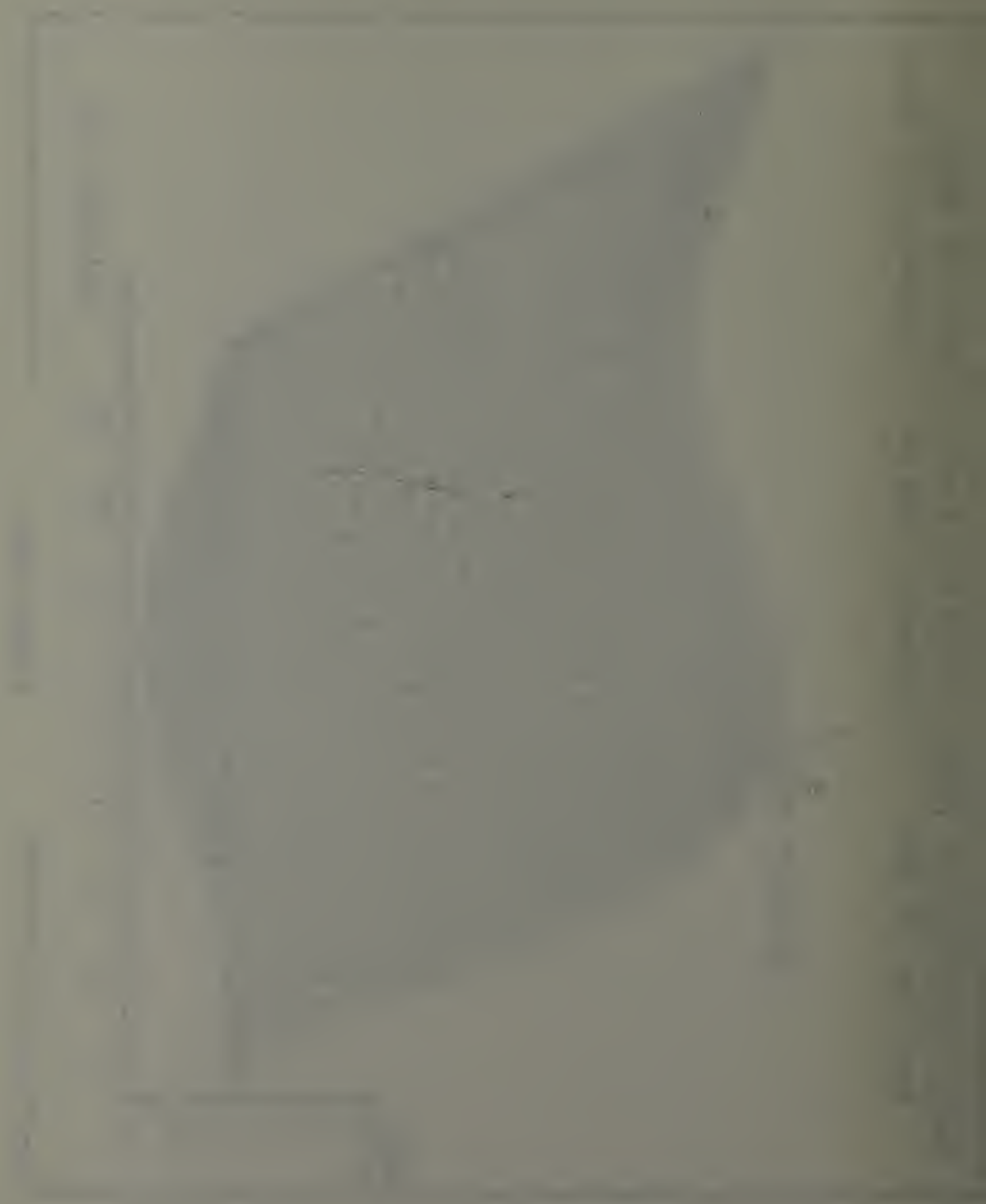

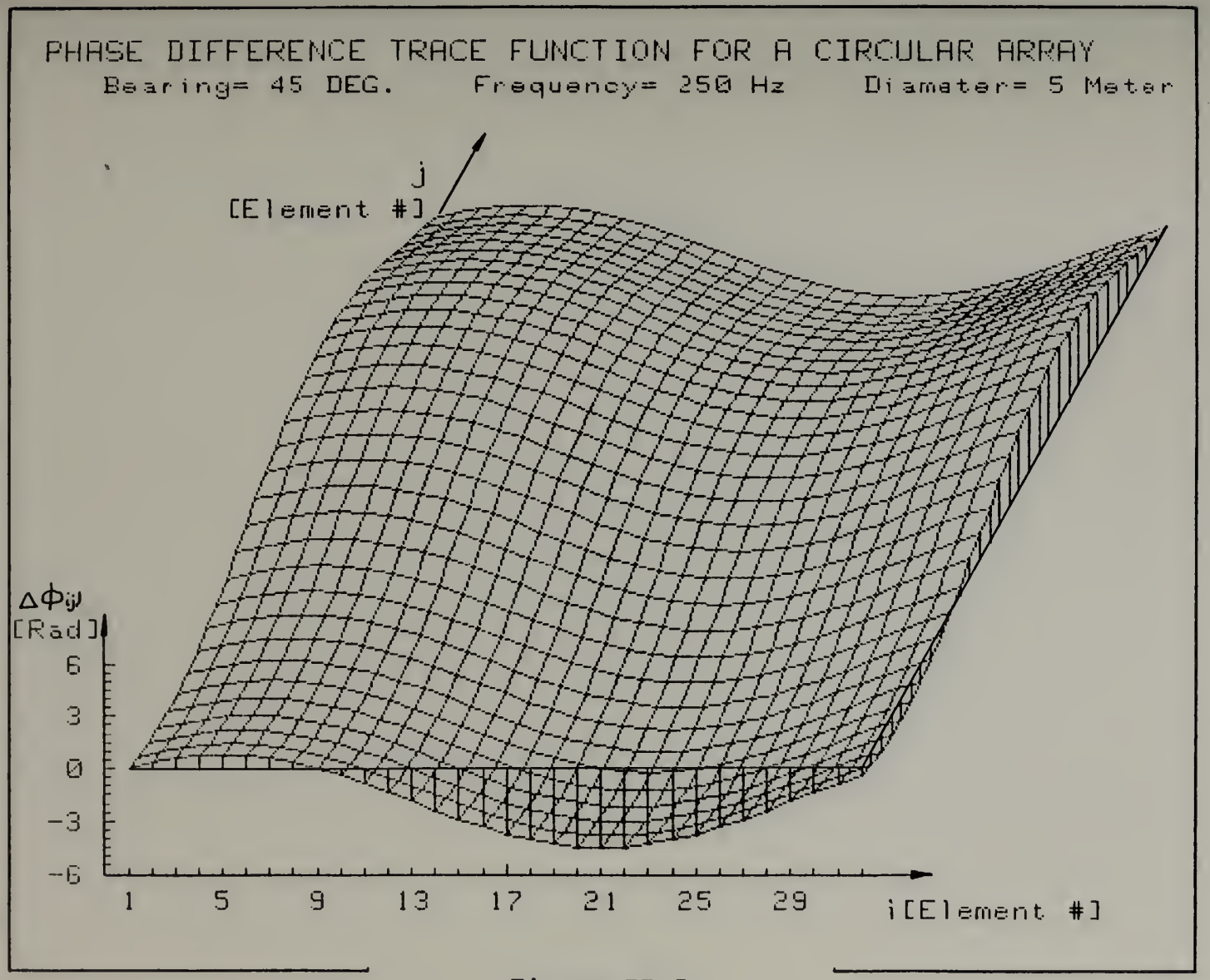
PHASE DIFFERENCE TRACE FUNCTION FOR A CIRCULAR ARRAY
Bearing= 45 DEG.
Frequency= 250 Hz
Diameter= 5 Meter
j
[Element #]
Δφij
[Rad]
6
3
0
-3
-6
1
5
9
13
17
21
25
29
i[Element #]

Figure II-7

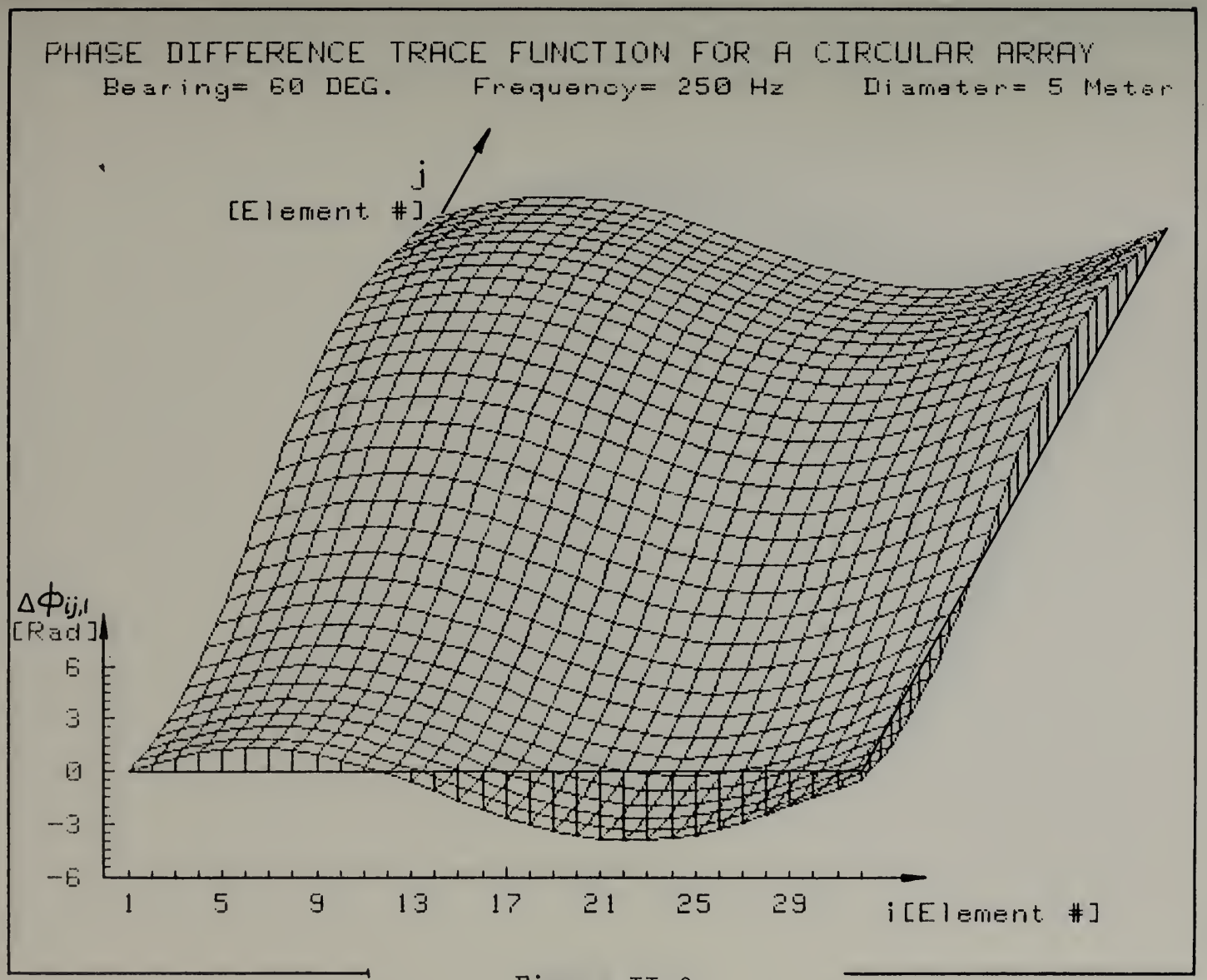
PHASE DIFFERENCE TRACE FUNCTION FOR A CIRCULAR ARRAY
Bearing= 60 DEG.
Frequency= 250 Hz
Diameter= 5 Meter
j
[Element #]
ΔΦij,l
[Rad]
6
3
0
-3
-6
1
5
9
13
17
21
25
29
i[Element #]

Figure II-8

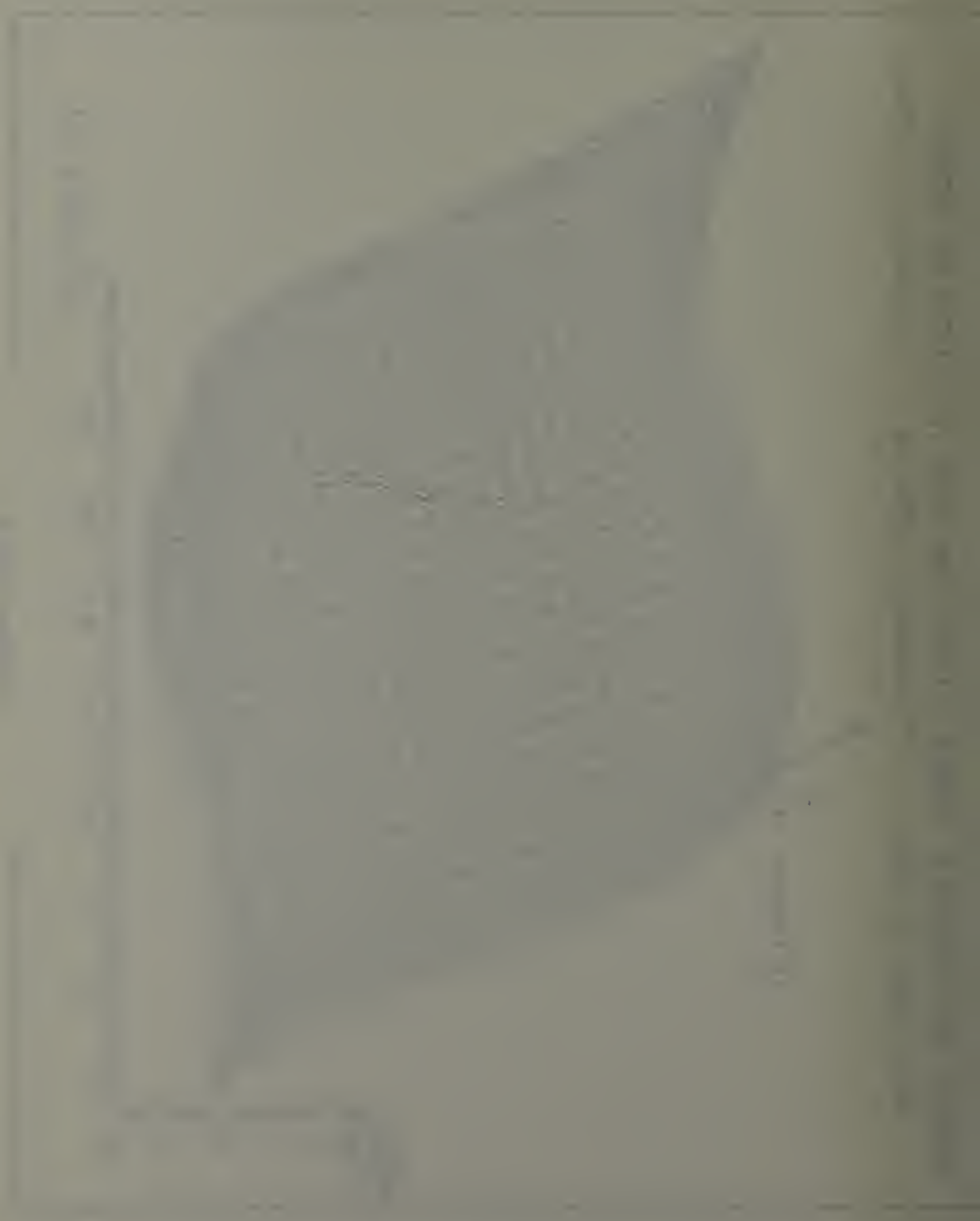

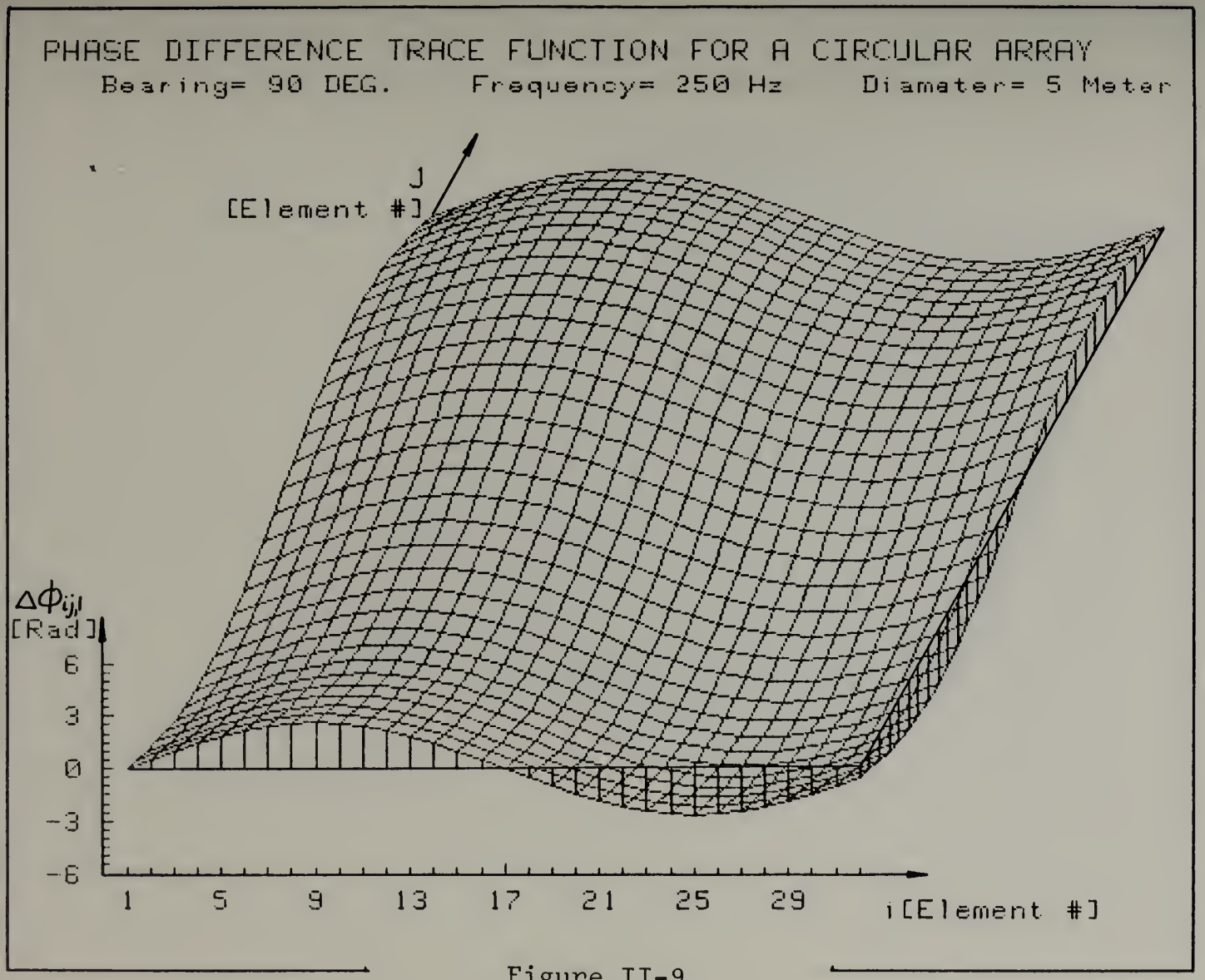
PHASE DIFFERENCE TRACE FUNCTION FOR A CIRCULAR ARRAY
Bearing= 90 DEG.
Frequency= 250 Hz
Diamater= 5 Meter
J
[Element #]
$\Delta\Phi_{ij,l}$
[Rad]
6
3
0
-3
-6
1
5
9
13
17
21
25
29
i[Element #]

Figure II-9

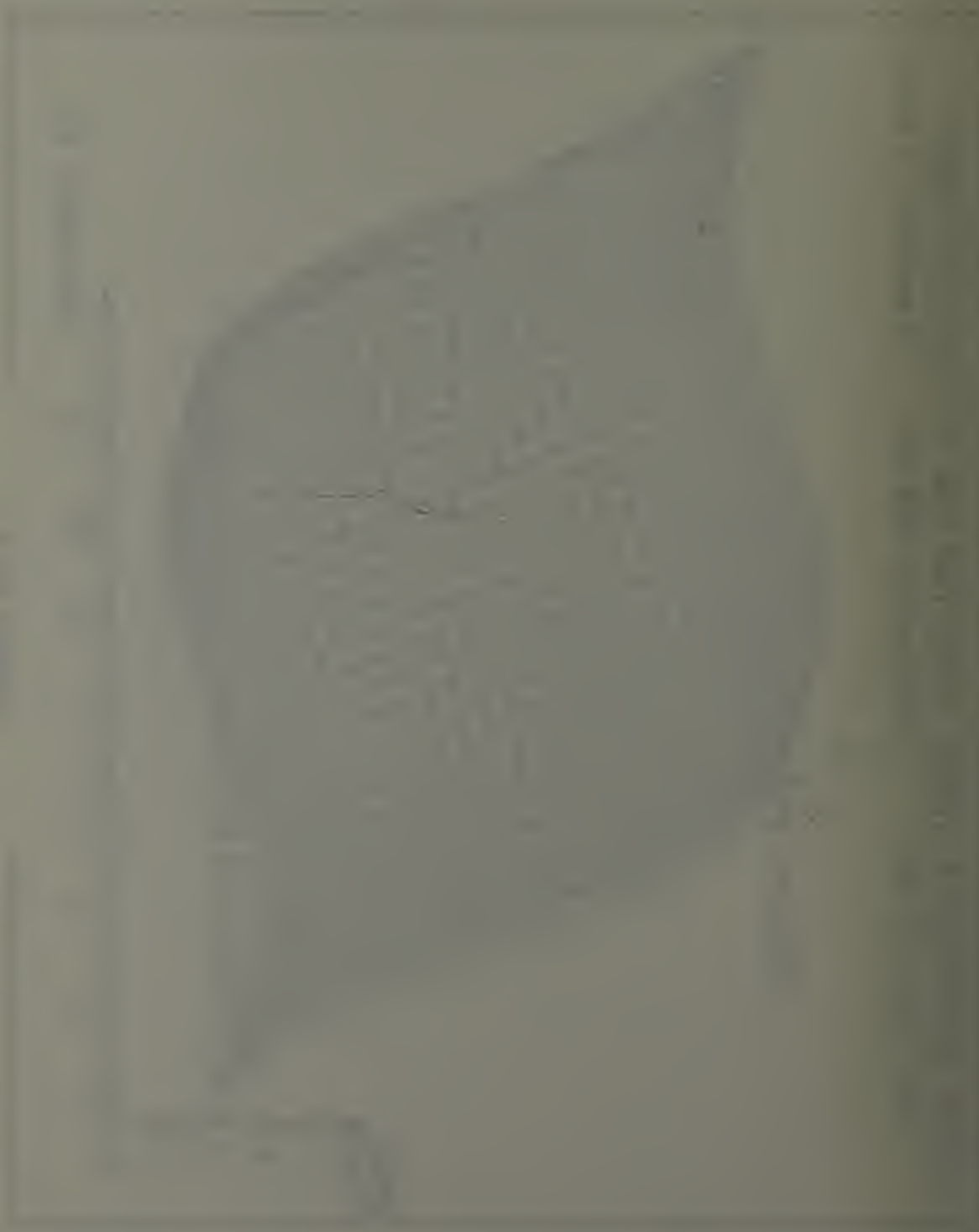

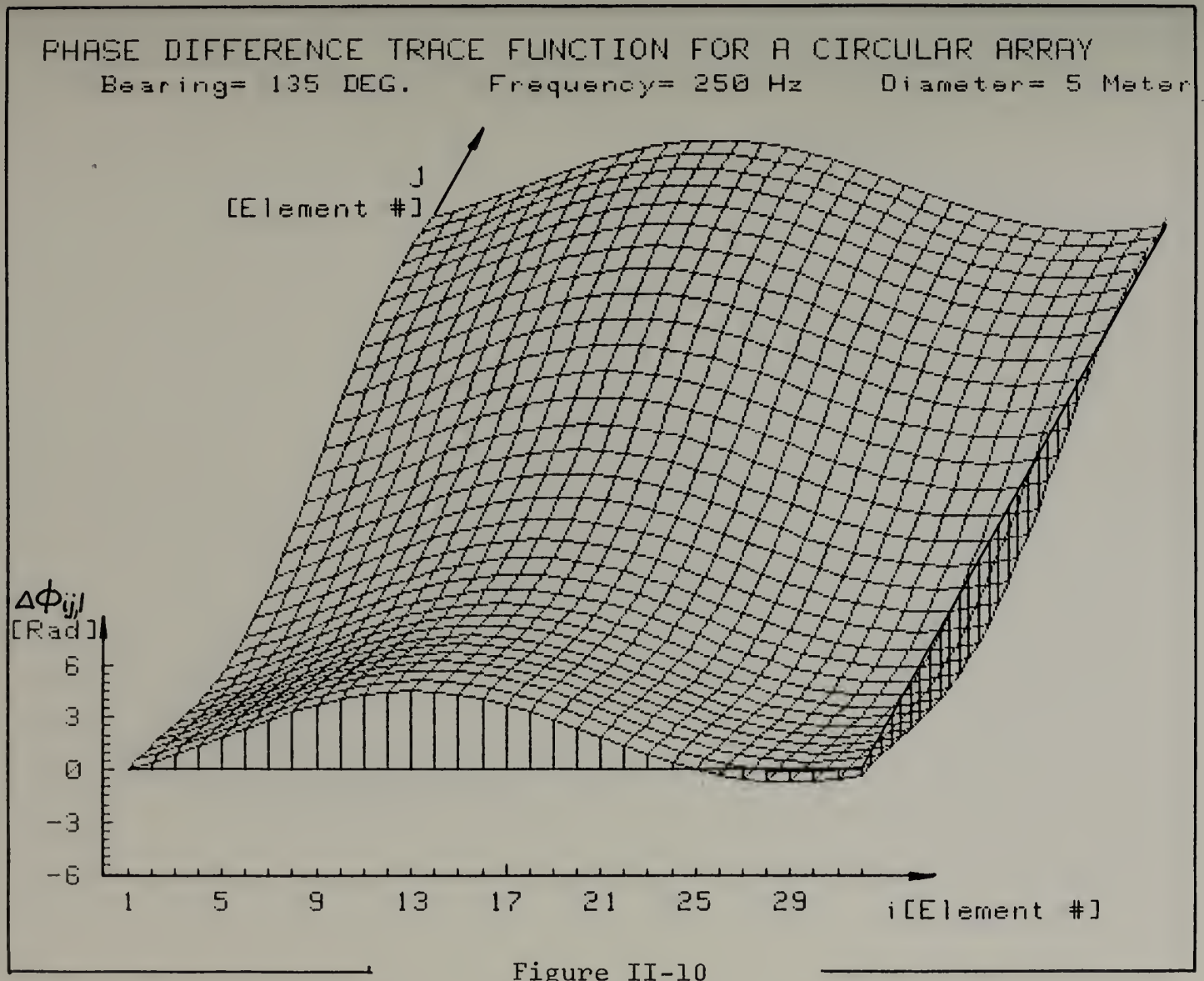
PHASE DIFFERENCE TRACE FUNCTION FOR A CIRCULAR ARRAY
Bearing= 135 DEG.
Frequency= 250 Hz
Diameter= 5 Meter
J
[Element #]
Δφij,l
[Rad]
6
3
0
-3
-6
1
5
9
13
17
21
25
29
i[Element #]

Figure II-10

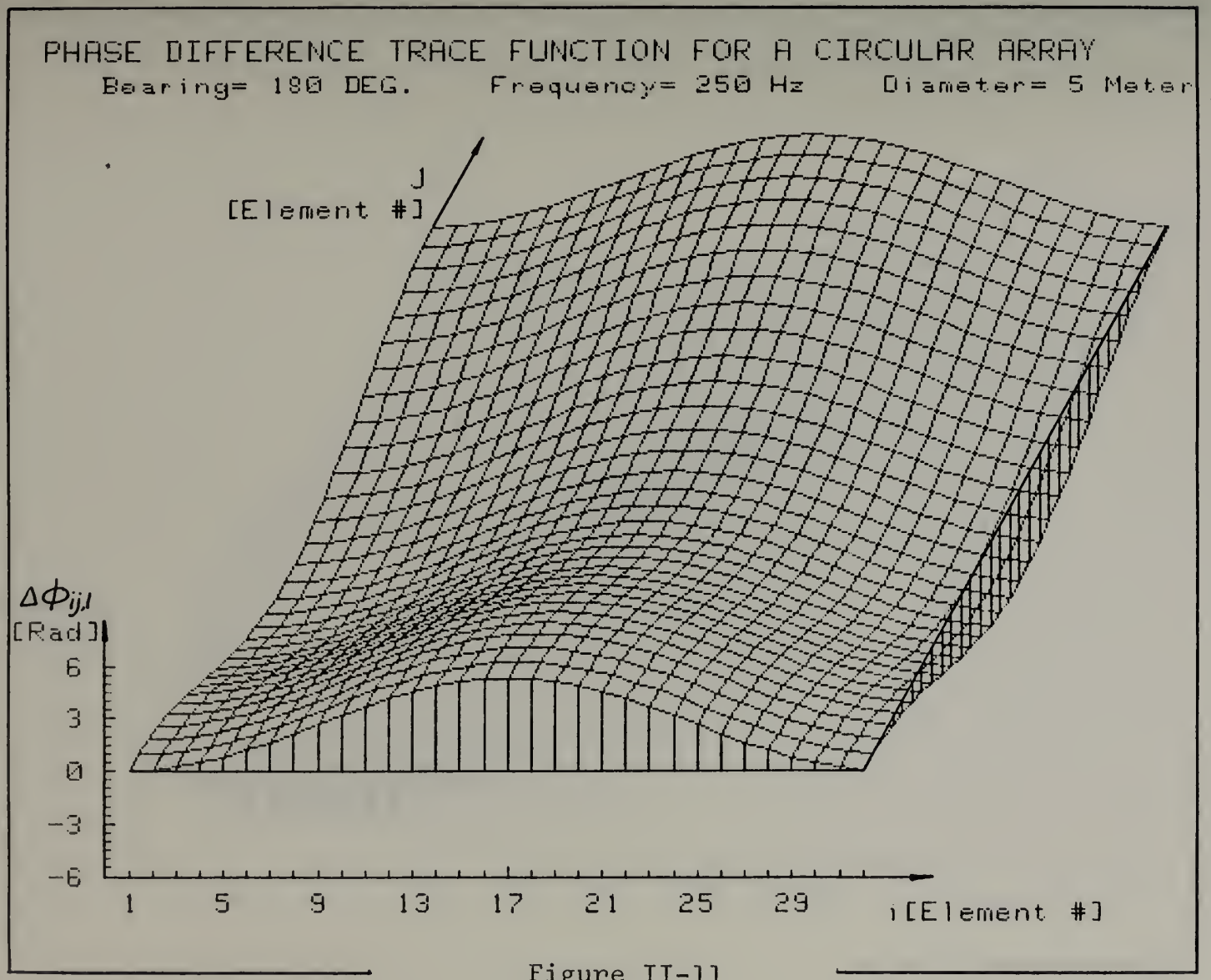
PHASE DIFFERENCE TRACE FUNCTION FOR A CIRCULAR ARRAY
Bearing= 180 DEG.
Frequency= 250 Hz
Diameter= 5 Meter
J
[Element #]
Δφij,l
[Rad]
6
3
0
-3
-6
1
5
9
13
17
21
25
29
i [Element #]

Figure II-11

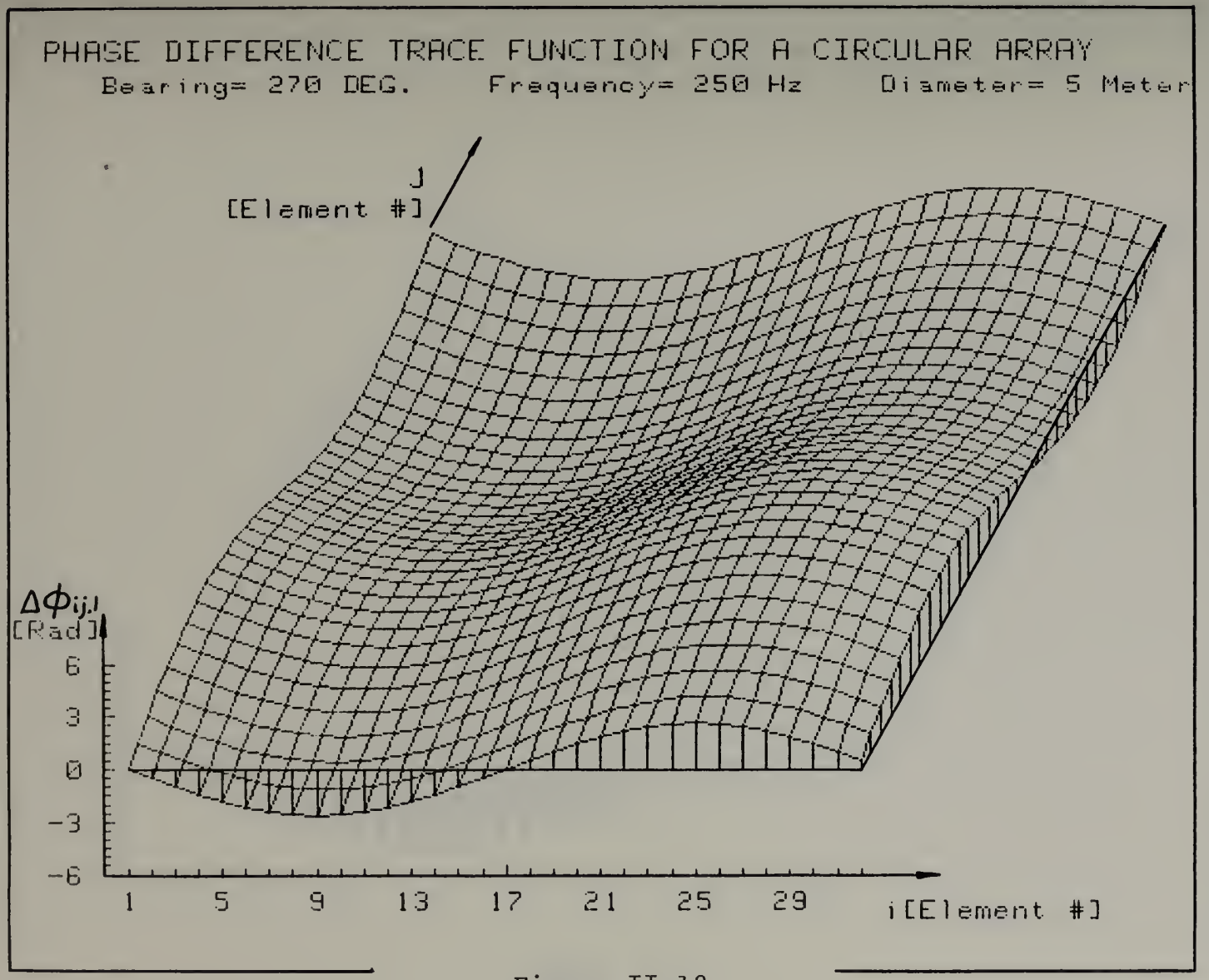
PHASE DIFFERENCE TRACE FUNCTION FOR A CIRCULAR ARRAY
Bearing= 270 DEG.
Frequency= 250 Hz
Diameter= 5 Meter
J
[Element #]
Δφij,l
[Rad]
6
3
0
-3
-6
1
5
9
13
17
21
25
29
i[Element #]

Figure II-12

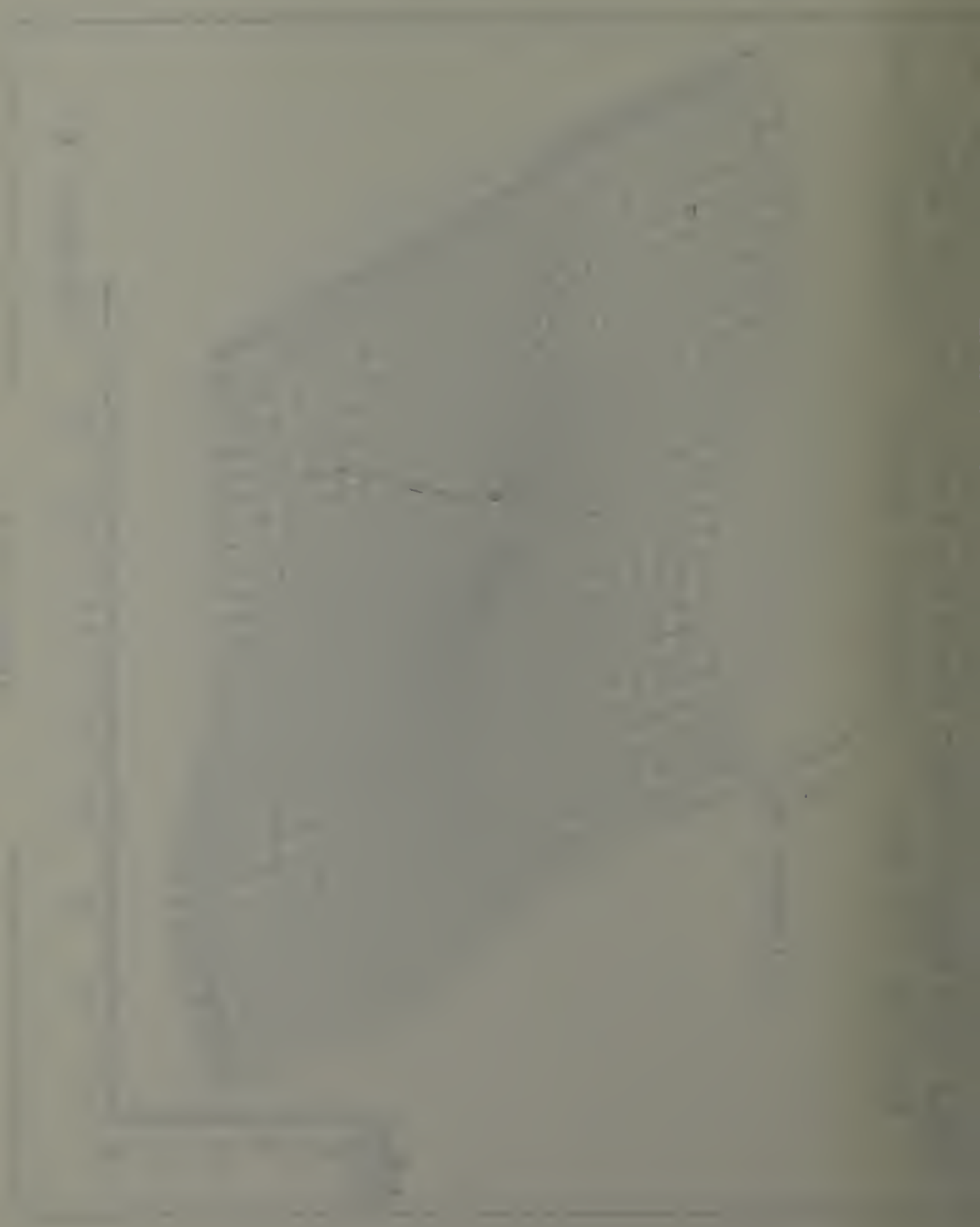

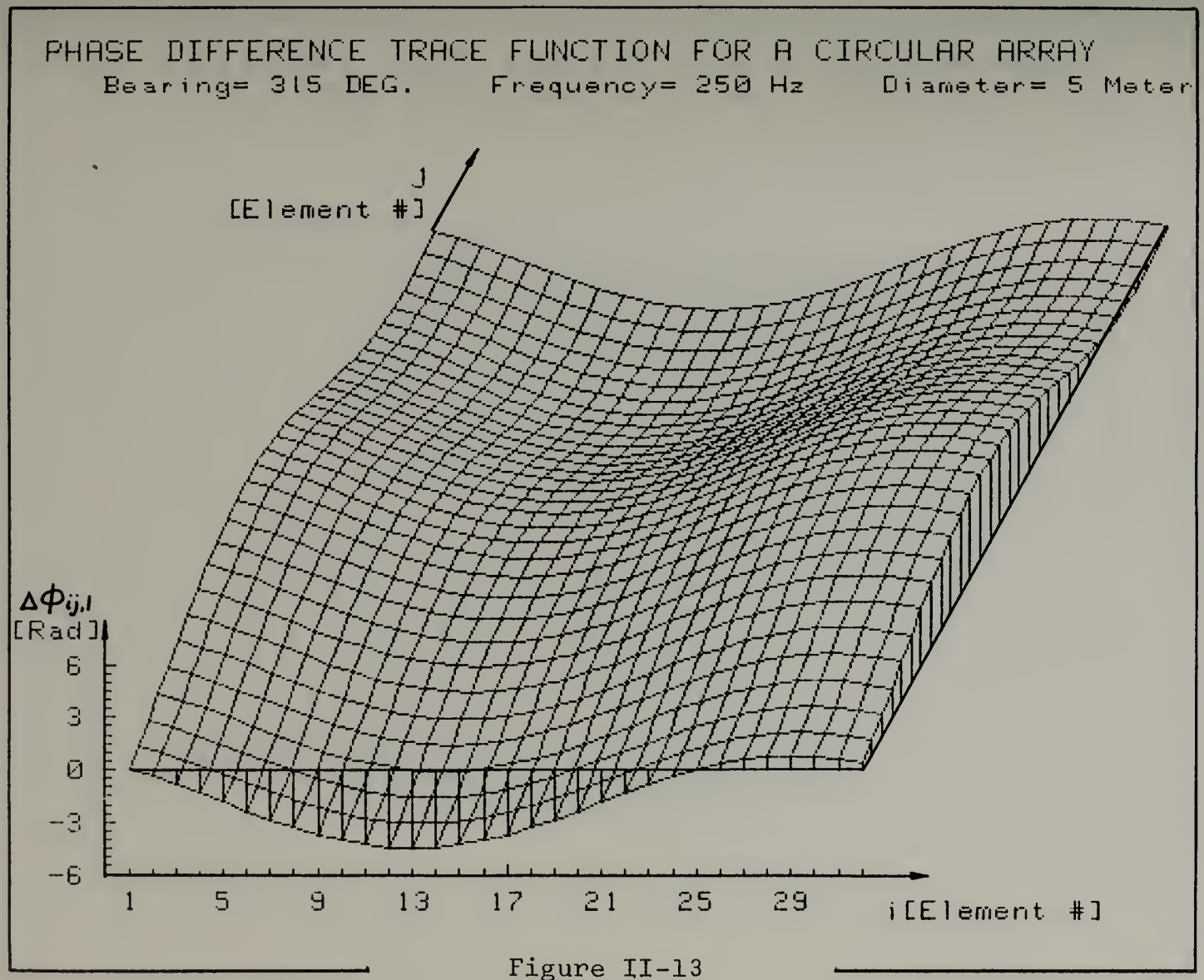
PHASE DIFFERENCE TRACE FUNCTION FOR A CIRCULAR ARRAY
Bearing= 315 DEG. Frequency= 250 Hz Diameter= 5 Meter
j
[Element #]
Δφij,l
[Rad]
6
3
0
-3
-6
1
5
9
13
17
21
25
29
i[Element #]

Figure II-13

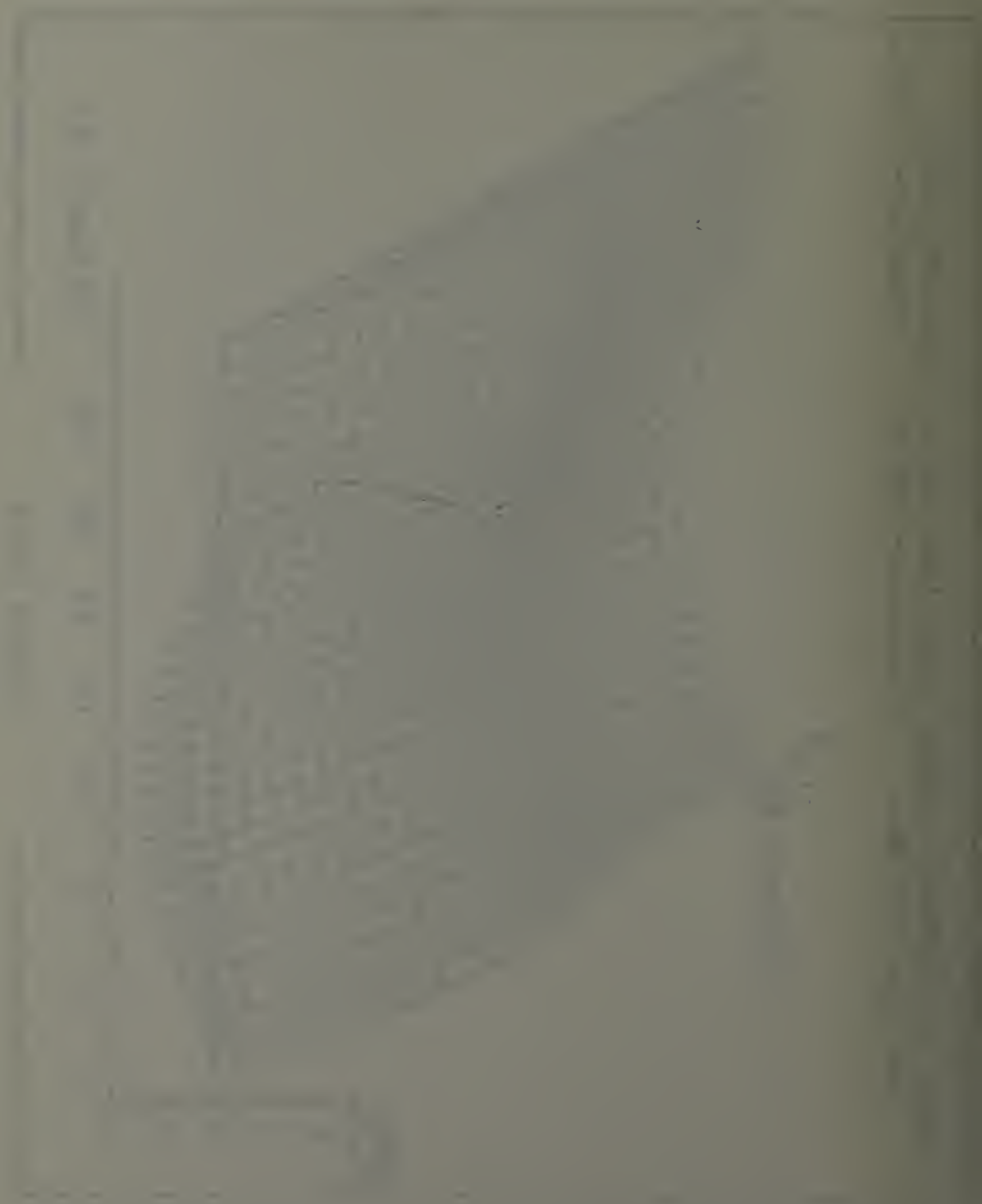

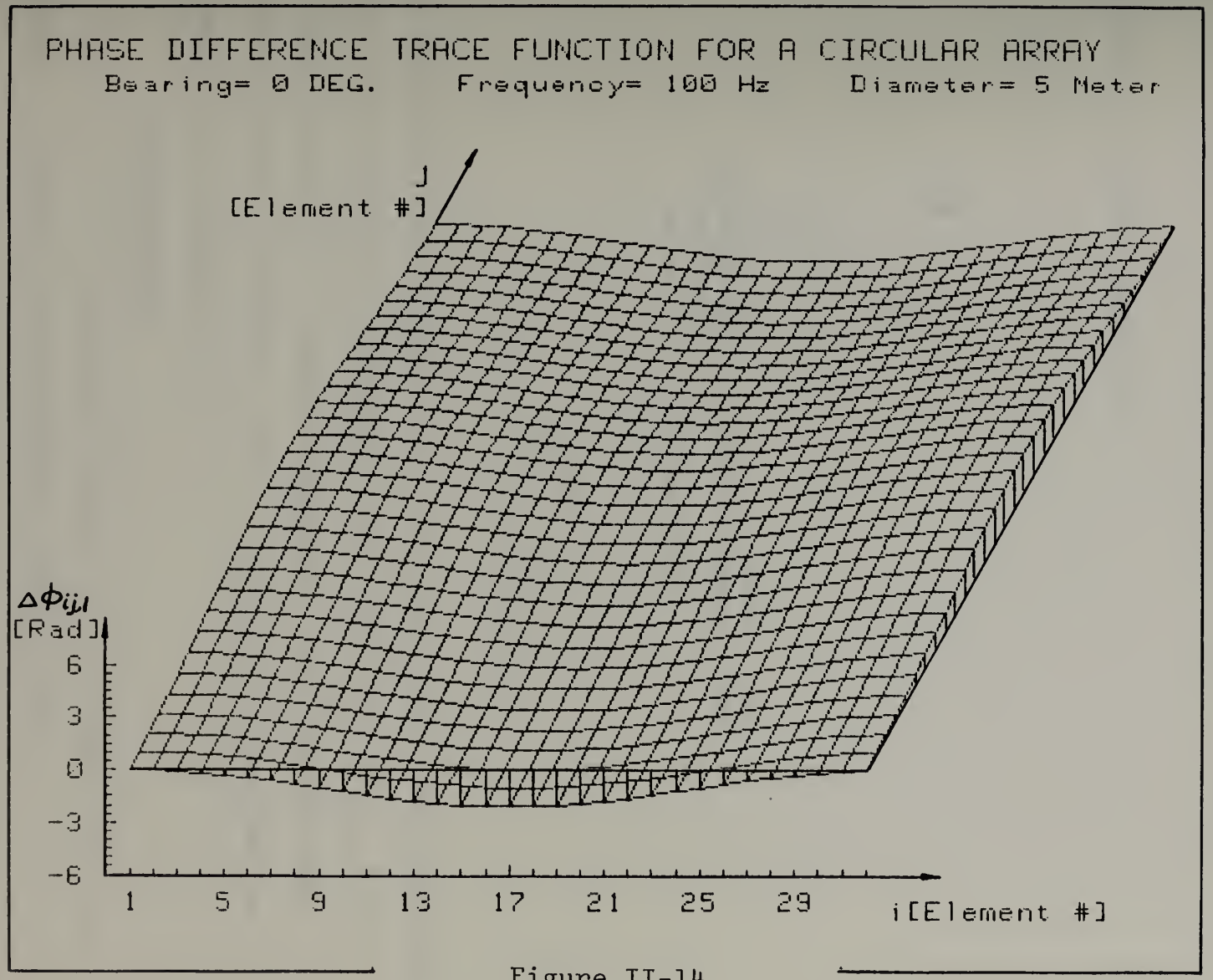
PHASE DIFFERENCE TRACE FUNCTION FOR A CIRCULAR ARRAY
Bearing= 0 DEG.
Frequency= 100 Hz
Diameter= 5 Meter
J
[Element #]
Δφij
[Rad]
6
3
0
-3
-6
1
5
9
13
17
21
25
29
i[Element #]

Figure II-14

- Phase difference trace function

$$\Delta\phi_{ij,\ell} = \Delta\tau_{ij}\ \omega_\ell = \frac{2\pi d}{\lambda_\ell}(i-j)\sin\theta \qquad \text{(II-10)}$$

where d - element spacing.

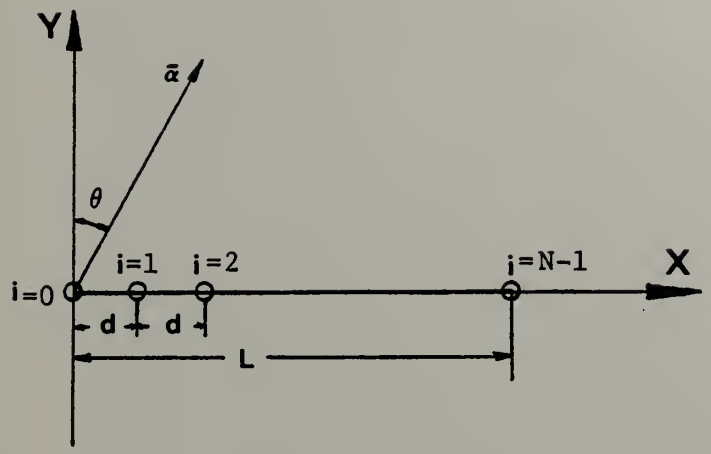


Figure II-15
Linear Array Configuration

In Figures II-16 through II-20 are shown the three dimensional plots of the phase difference trace functions $\Delta\phi_{ij,\ell}$ for a linear array of 32 elements (Equation II-10) of the same aperture as the circular array. The computer program is presented in Appendix B-2.

Observations:

(1) The trace functions of a linear array are always a sampled two dimensional plane surface.

(2) The "slope" of this plane is indicative of the direction of arrival of the incoming signal.

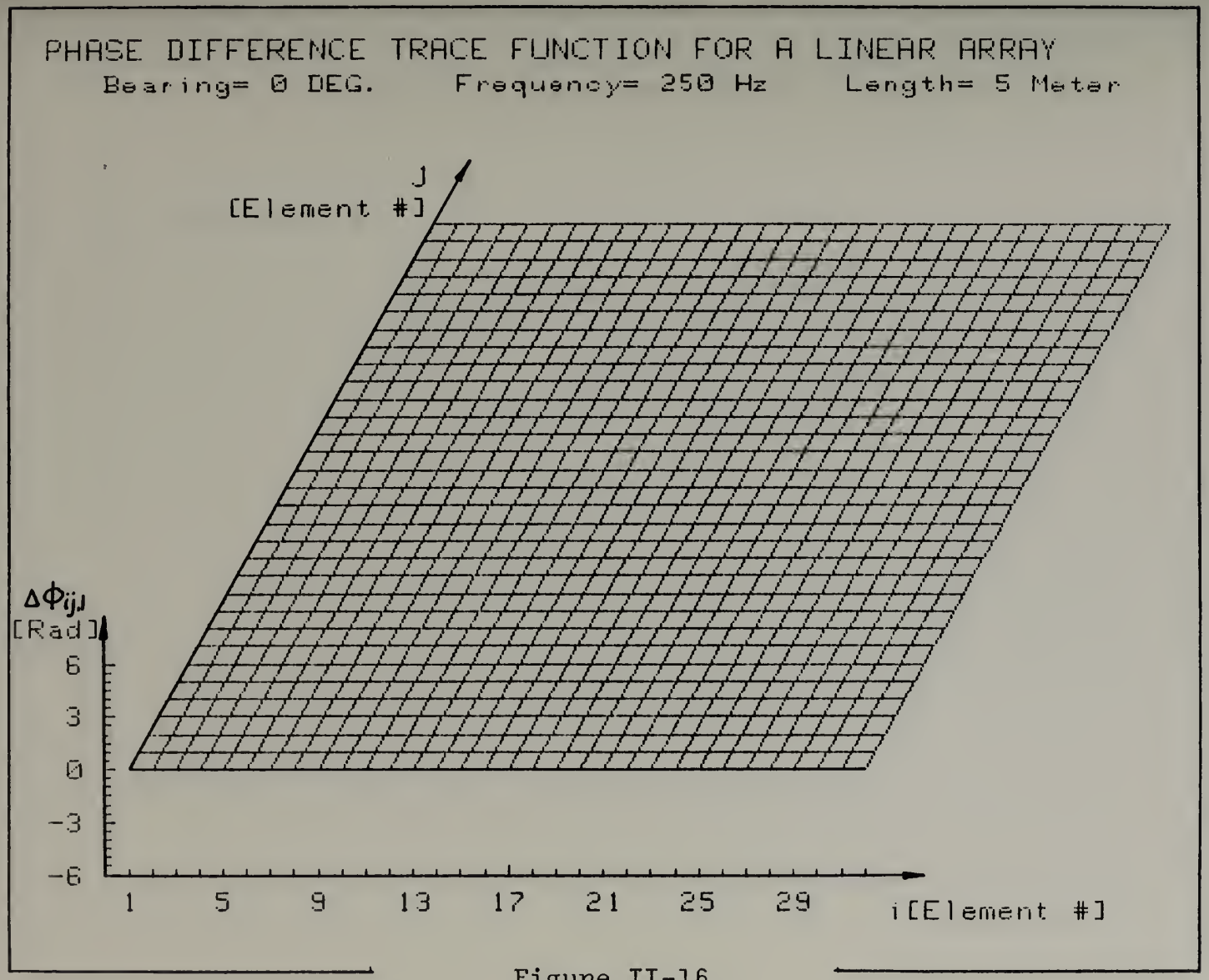
PHASE DIFFERENCE TRACE FUNCTION FOR A LINEAR ARRAY
Bearing= 0 DEG.
Frequency= 250 Hz
Length= 5 Meter
J
[Element #]
Δφij,l
[Rad]
6
3
0
-3
-6
1
5
9
13
17
21
25
29
i[Element #]

Figure II-16

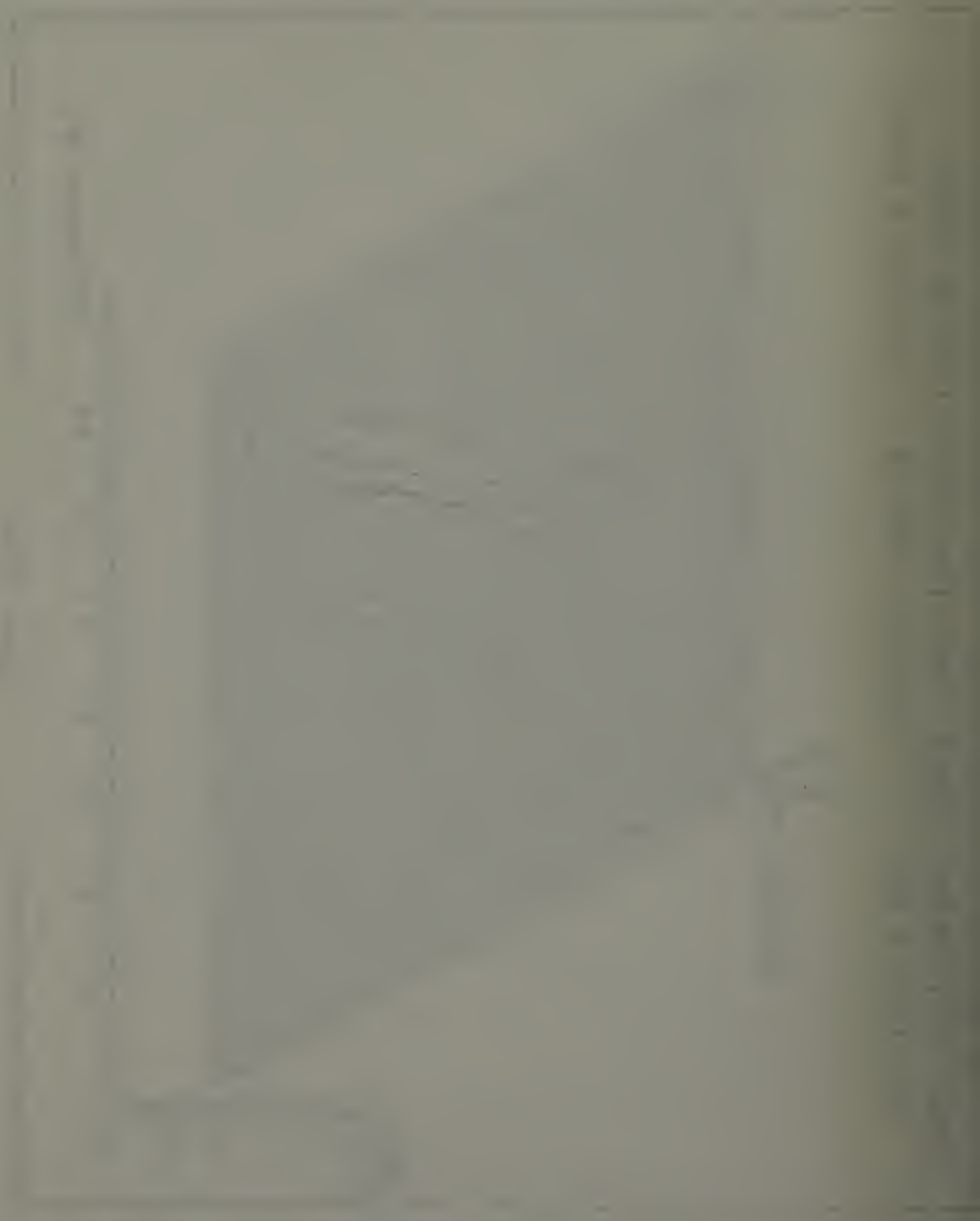

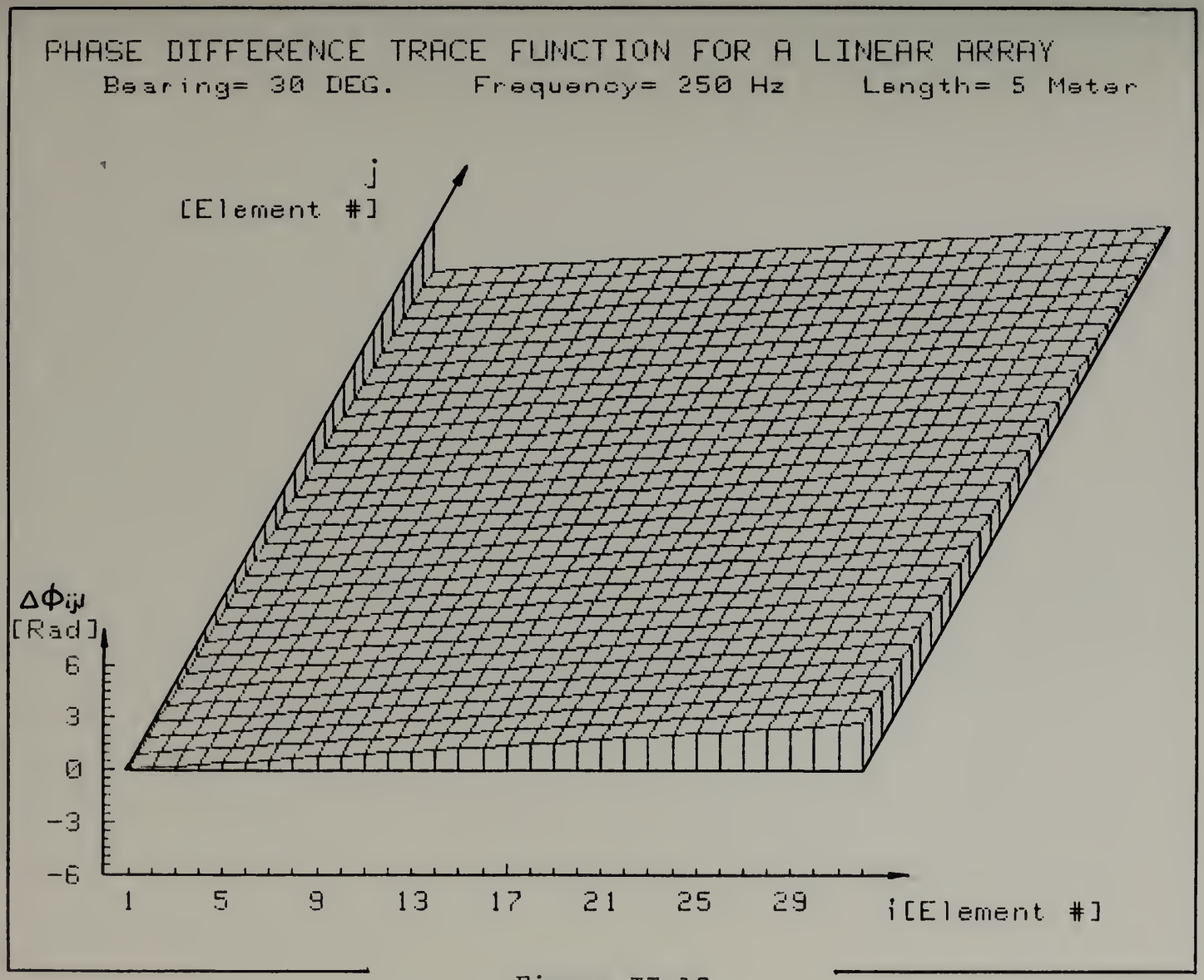
PHASE DIFFERENCE TRACE FUNCTION FOR A LINEAR ARRAY
Bearing= 30 DEG.
Frequency= 250 Hz
Length= 5 Meter
j
[Element #]
Δφij
[Rad]
6
3
0
-3
-6
1
5
9
13
17
21
25
29
i[Element #]

Figure II-17

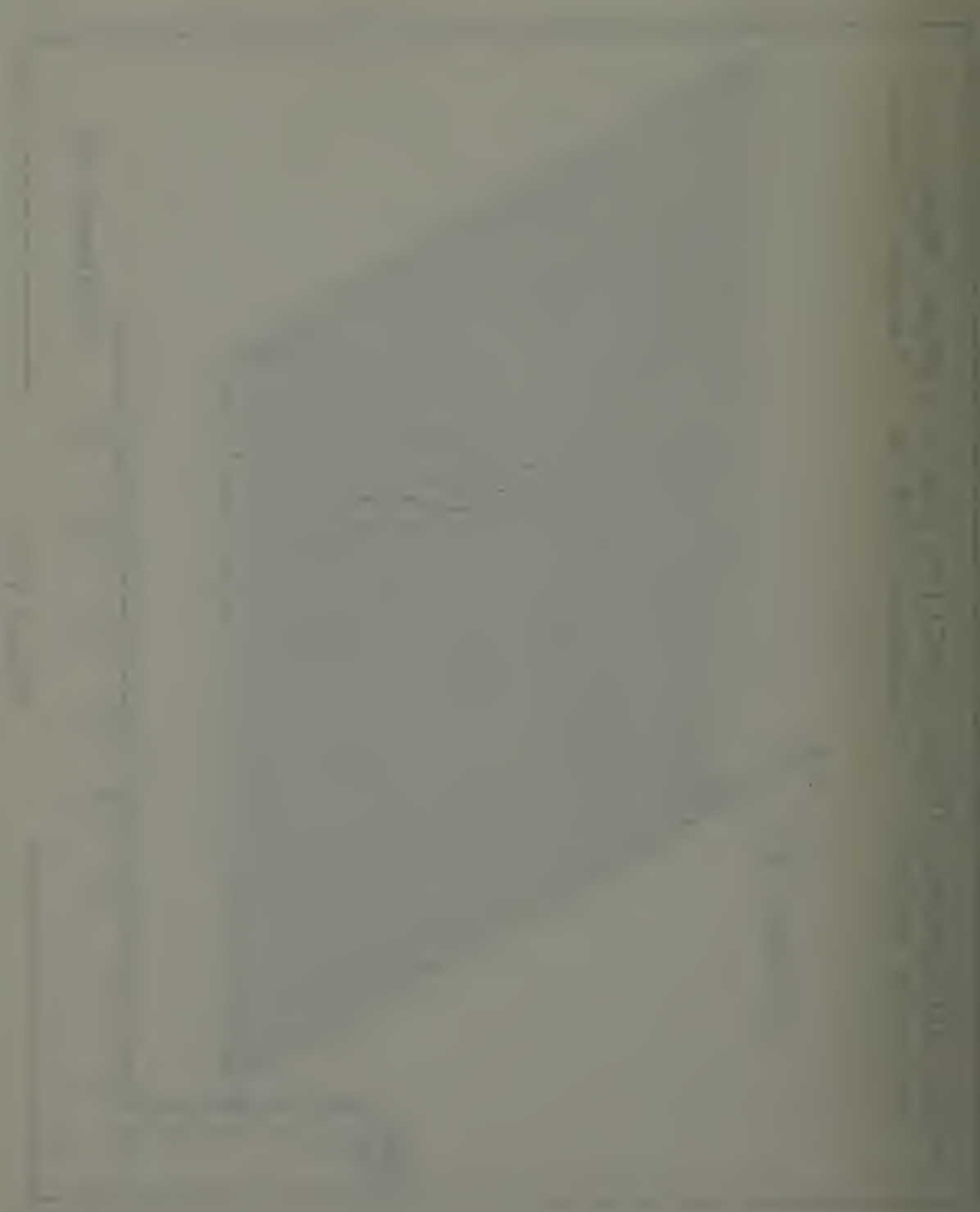

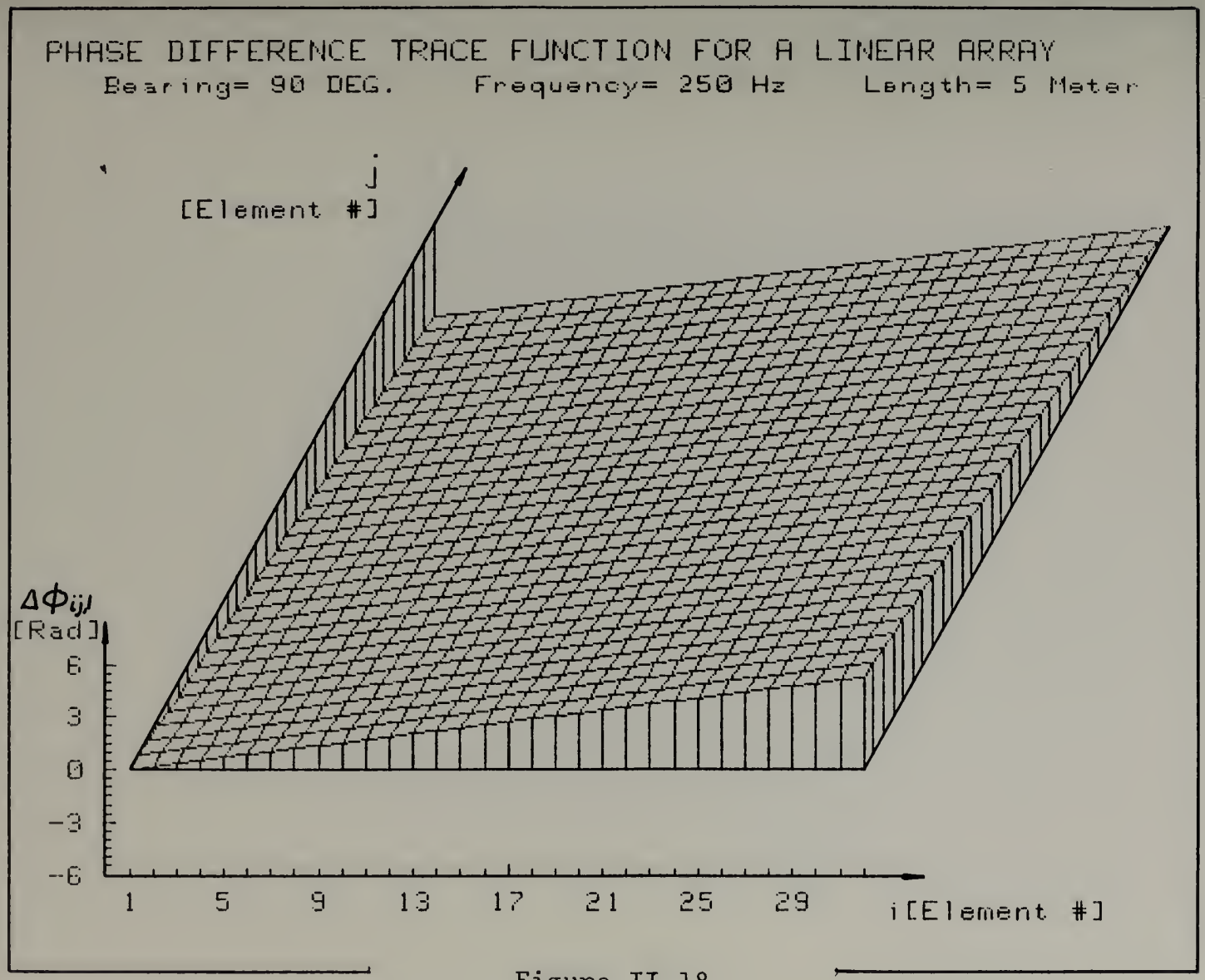
PHASE DIFFERENCE TRACE FUNCTION FOR A LINEAR ARRAY
Bearing= 90 DEG.
Frequency= 250 Hz
Length= 5 Meter
j
[Element #]
Δφij
[Rad]
6
3
0
-3
-6
1
5
9
13
17
21
25
29
i[Element #]

Figure II-18

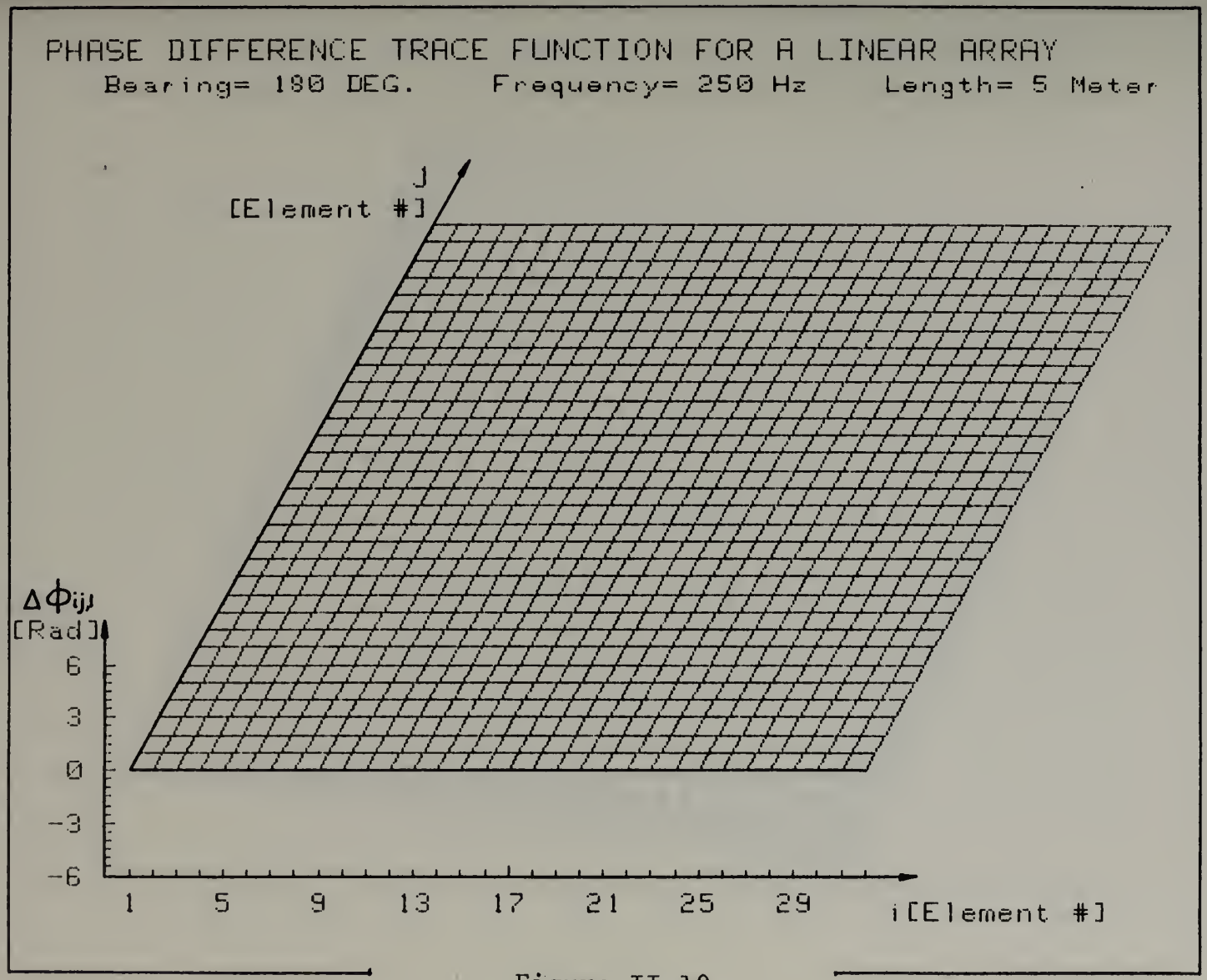
PHASE DIFFERENCE TRACE FUNCTION FOR A LINEAR ARRAY
Bearing= 180 DEG.
Frequency= 250 Hz
Length= 5 Meter
J
[Element #]
Δφij
[Rad]
6
3
0
-3
-6
1
5
9
13
17
21
25
29
i[Element #]

Figure II-19

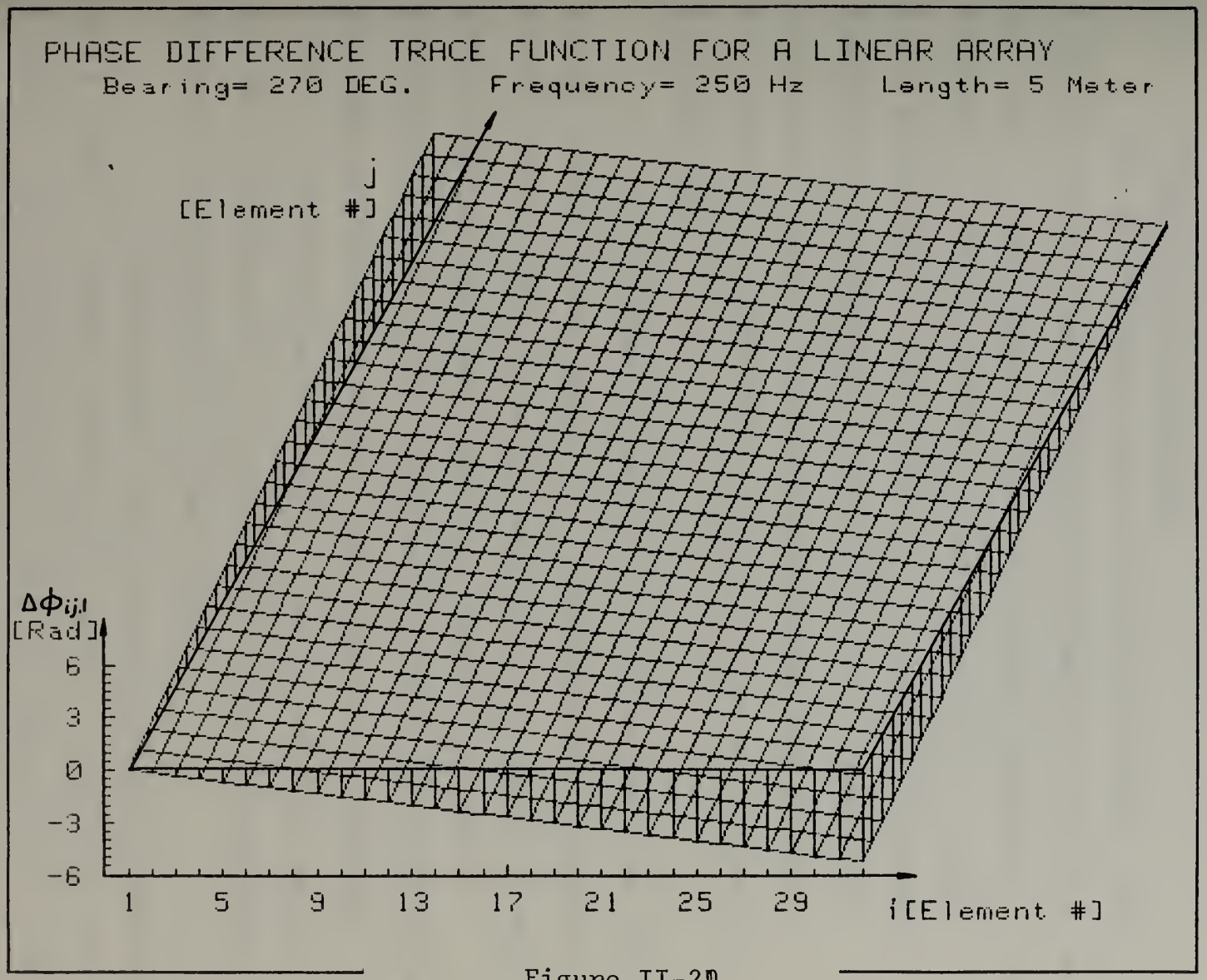
PHASE DIFFERENCE TRACE FUNCTION FOR A LINEAR ARRAY
Bearing= 270 DEG.
Frequency= 250 Hz
Length= 5 Meter
j
[Element #]
Δφij
[Rad]
6
3
0
-3
-6
1
5
9
13
17
21
25
29
i[Element #]

Figure II-20

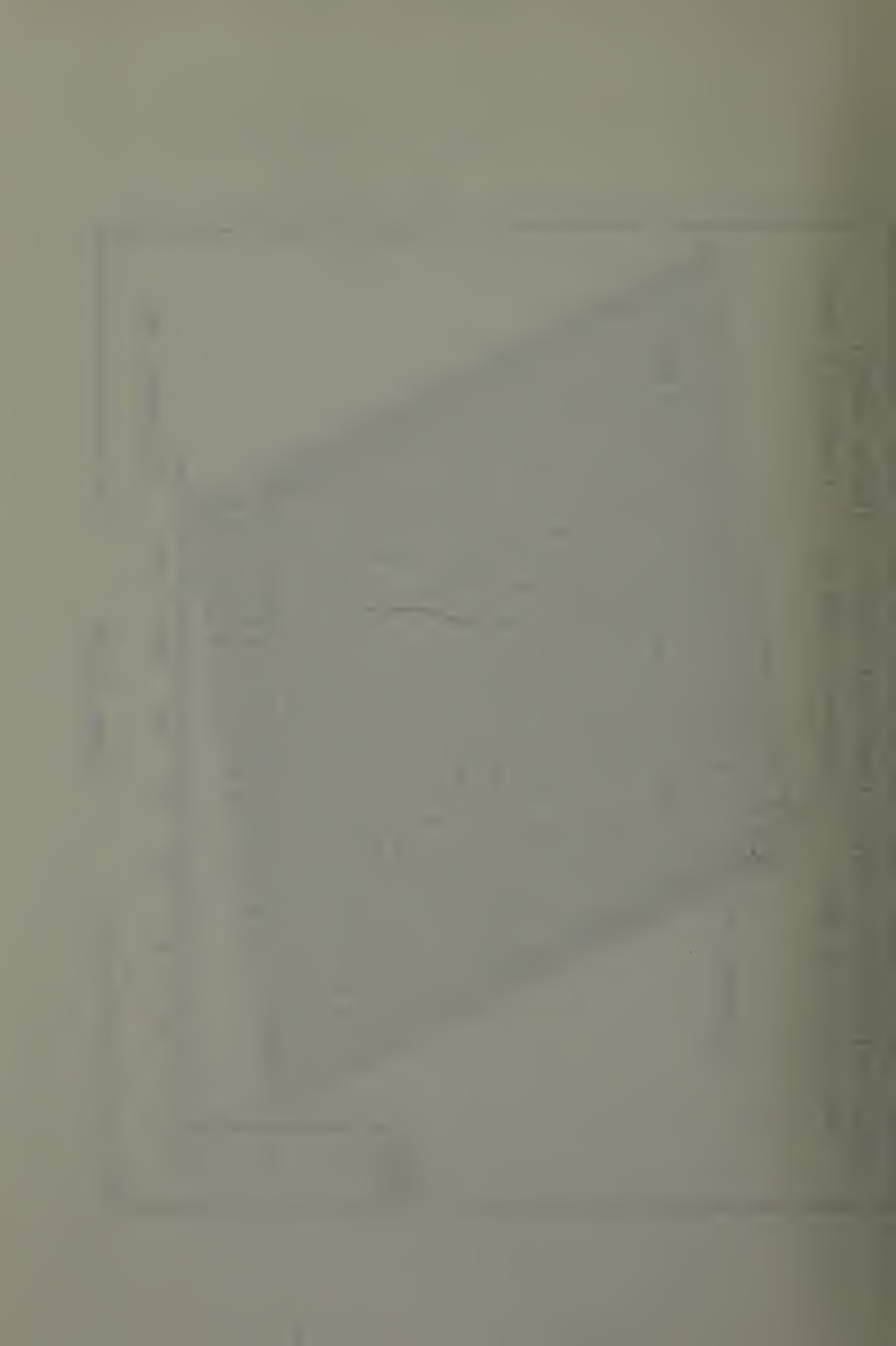

(3) The estimation of this slope can be done easily for the noisy trace function by minimum mean square error surface fitting.

2. General Trace Functions

For those arrays which do not have analytic trace functions the approach is slightly different. In this case in order to use equations (II-5) and (II-6) the value of the vectors $\bar{r}_i$ is needed either in cartesian (x,y) or polar (r,θ) coordinates. Then each $\tau_i$ (Eq. II-2) is calculated separately as referenced to the origin of the coordinate system, and the differences are calculated and plotted. In this section two geometrical configurations were chosen for demonstration:

a. A "Conformal array" which is composed of a half circle and two linear parts. The configuration is shown in Figure II-21. For this array, although it is built of well defined geometrical forms its trace function cannot be expressed in closed form. Figures II-22 through II-28 present the trace function for various look directions (bearings). It can be observed that it still preserves symmetry around the zero bearing and it is built up of pieces of the trace functions of circular and linear arrays.

b. A "Random array" is illustrated which is composed of 19 elements randomly distributed within a circle of about 5 meters. The configuration is shown in Figure II-29. The trace functions for various look directions (bearings) are shown in Figures II-30 through II-34. These trace functions

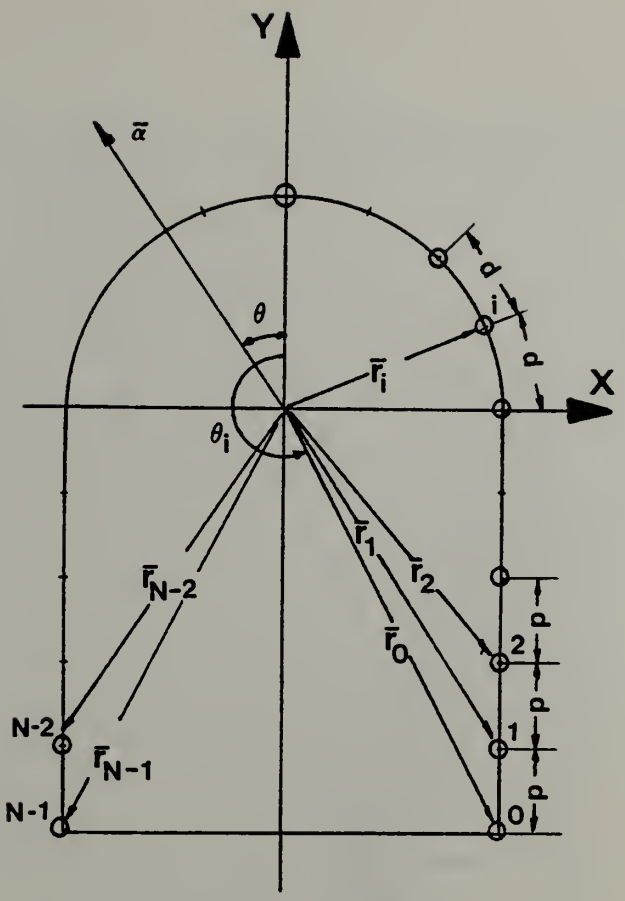


Figure II-21
Conformal Array Configuration

are totally random and only two obvious types of symmetries are preserved:

- $\Delta\phi_{ij} = -\Delta\phi_{ji}$
- the whole trace function is antisymmetric for bearings of 180 degrees apart (this second characteristic is a result of the first one).

The computer program which generates both the "conformal" and "random" trace can be found in Appendix B-3.

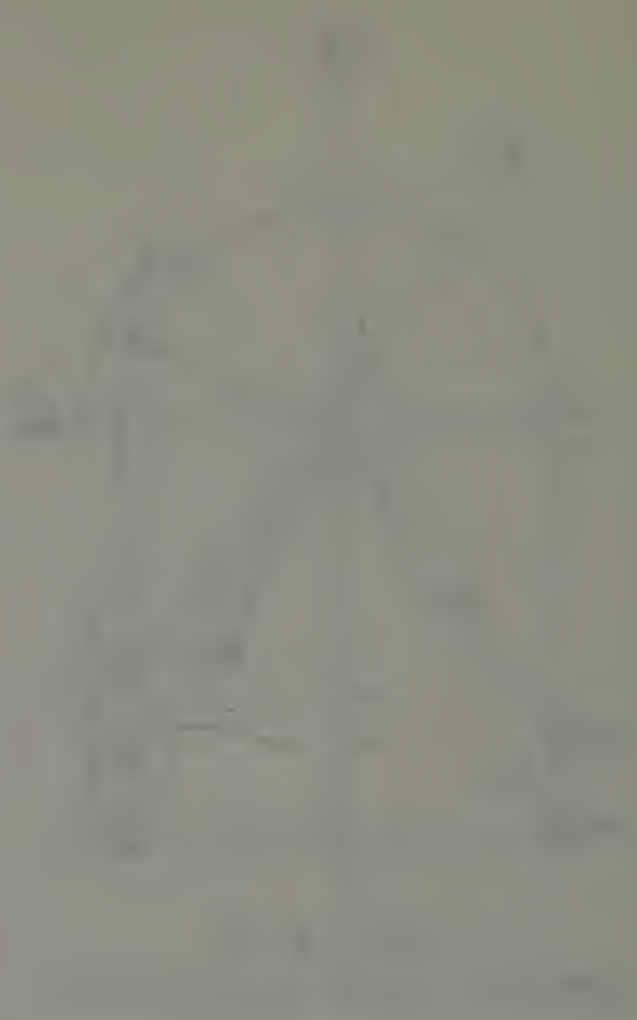

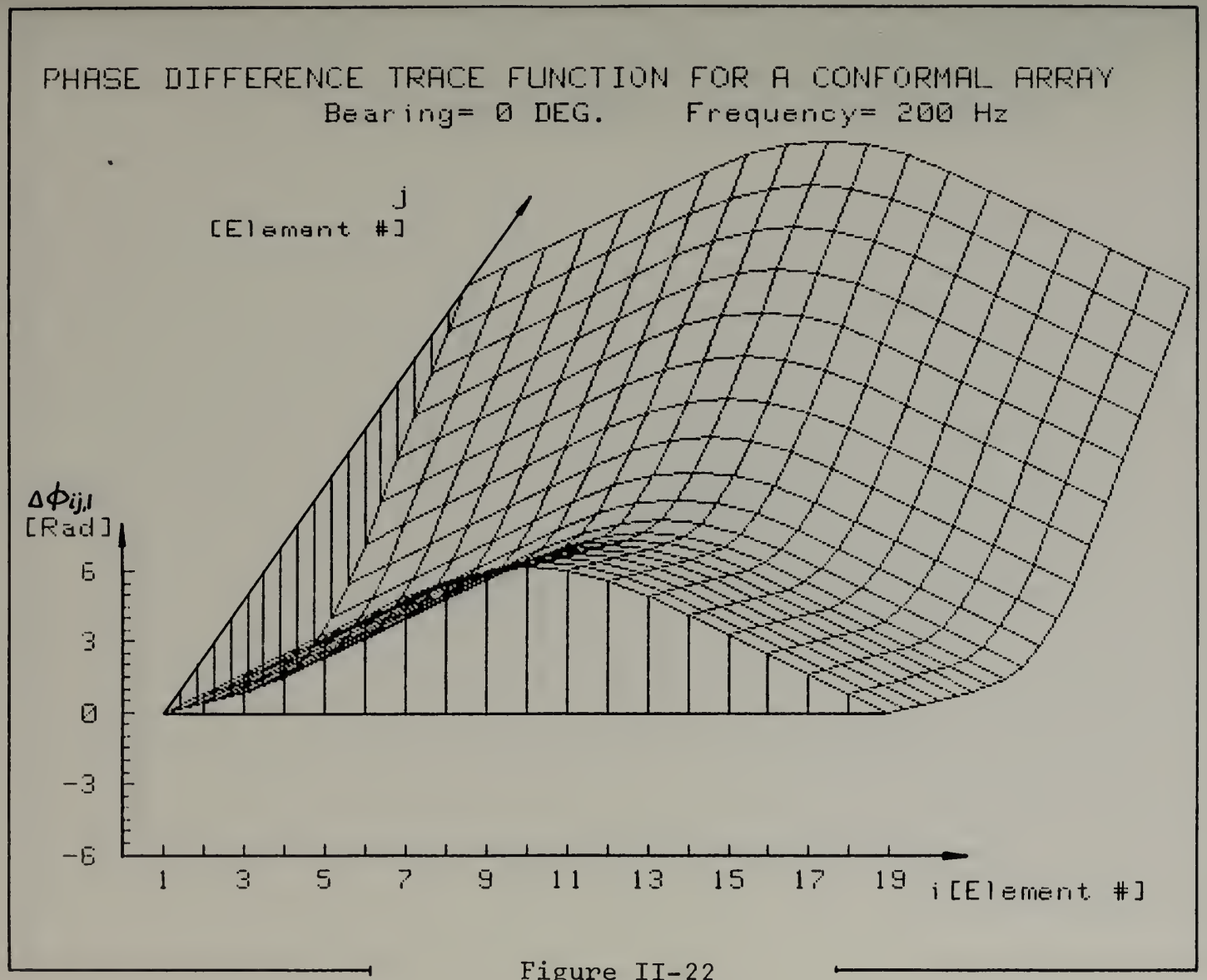
PHASE DIFFERENCE TRACE FUNCTION FOR A CONFORMAL ARRAY
Bearing= 0 DEG. Frequency= 200 Hz
j
[Element #]
Δφij,l
[Rad]
6
3
0
-3
-6
1
3
5
7
9
11
13
15
17
19
i [Element #]

Figure II-22

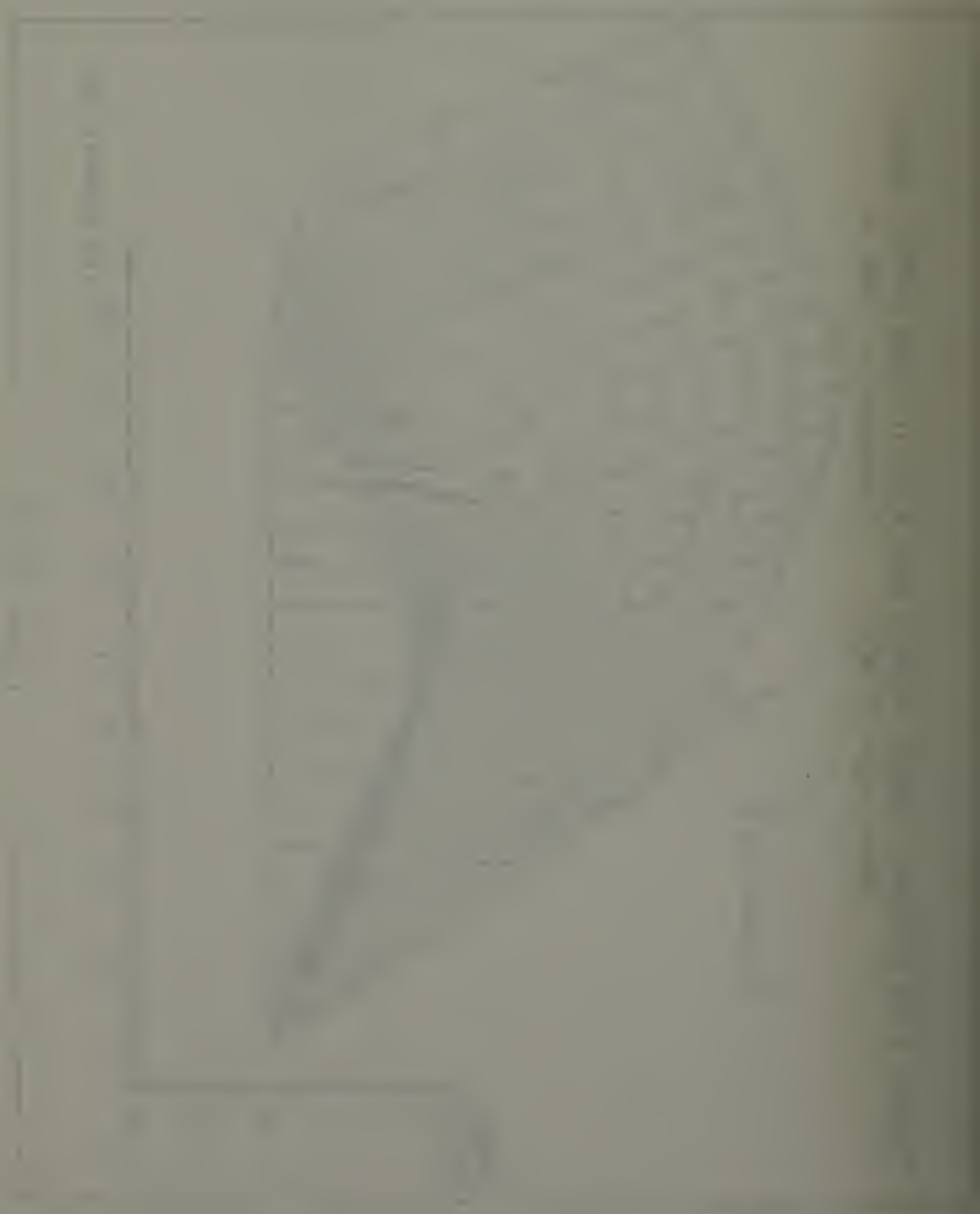

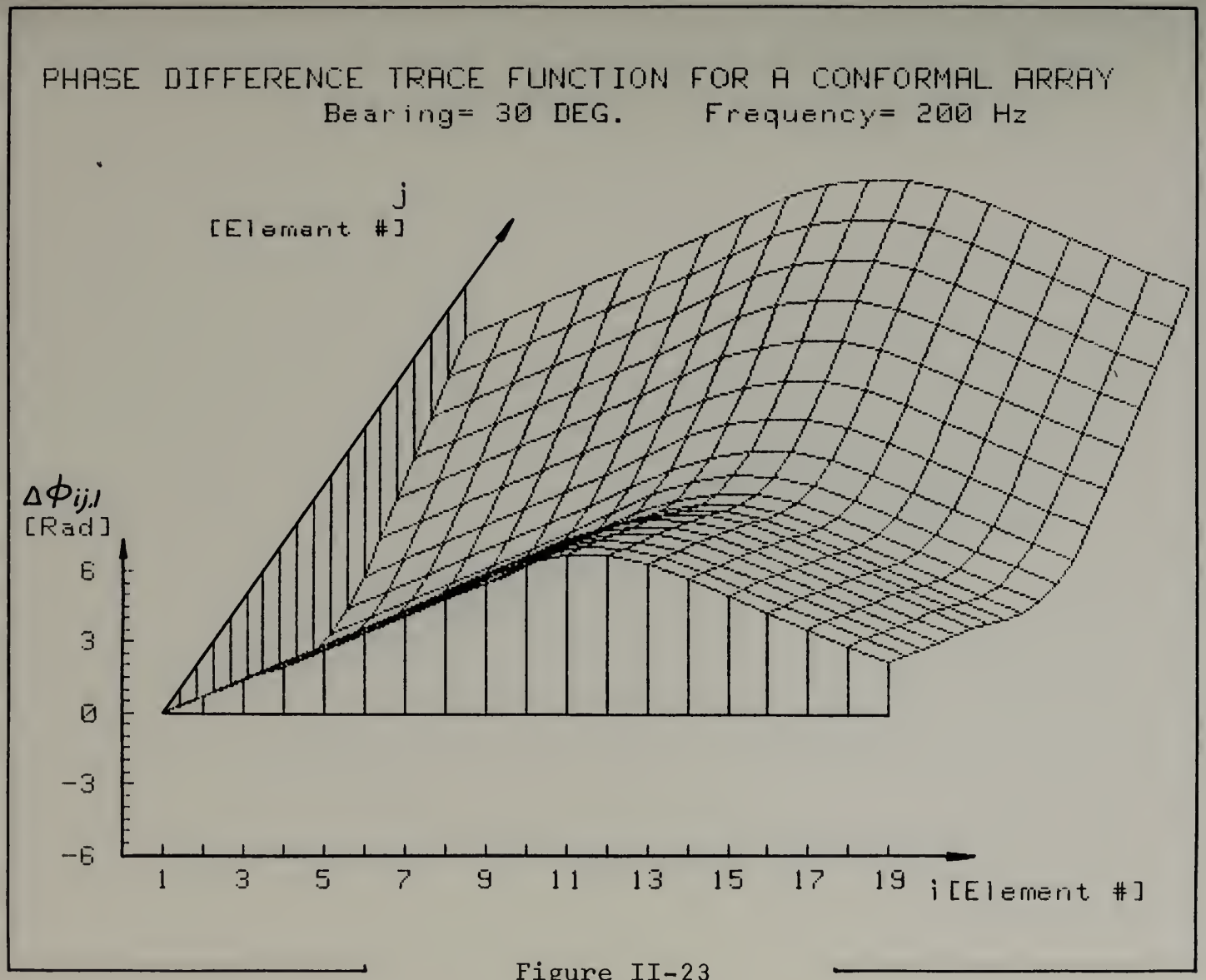
PHASE DIFFERENCE TRACE FUNCTION FOR A CONFORMAL ARRAY
Bearing= 30 DEG. Frequency= 200 Hz
j
[Elemant #]
$\Delta\phi_{ij,l}$
[Rad]
6
3
0
-3
-6
1
3
5
7
9
11
13
15
17
19
i[Element #]

Figure II-23

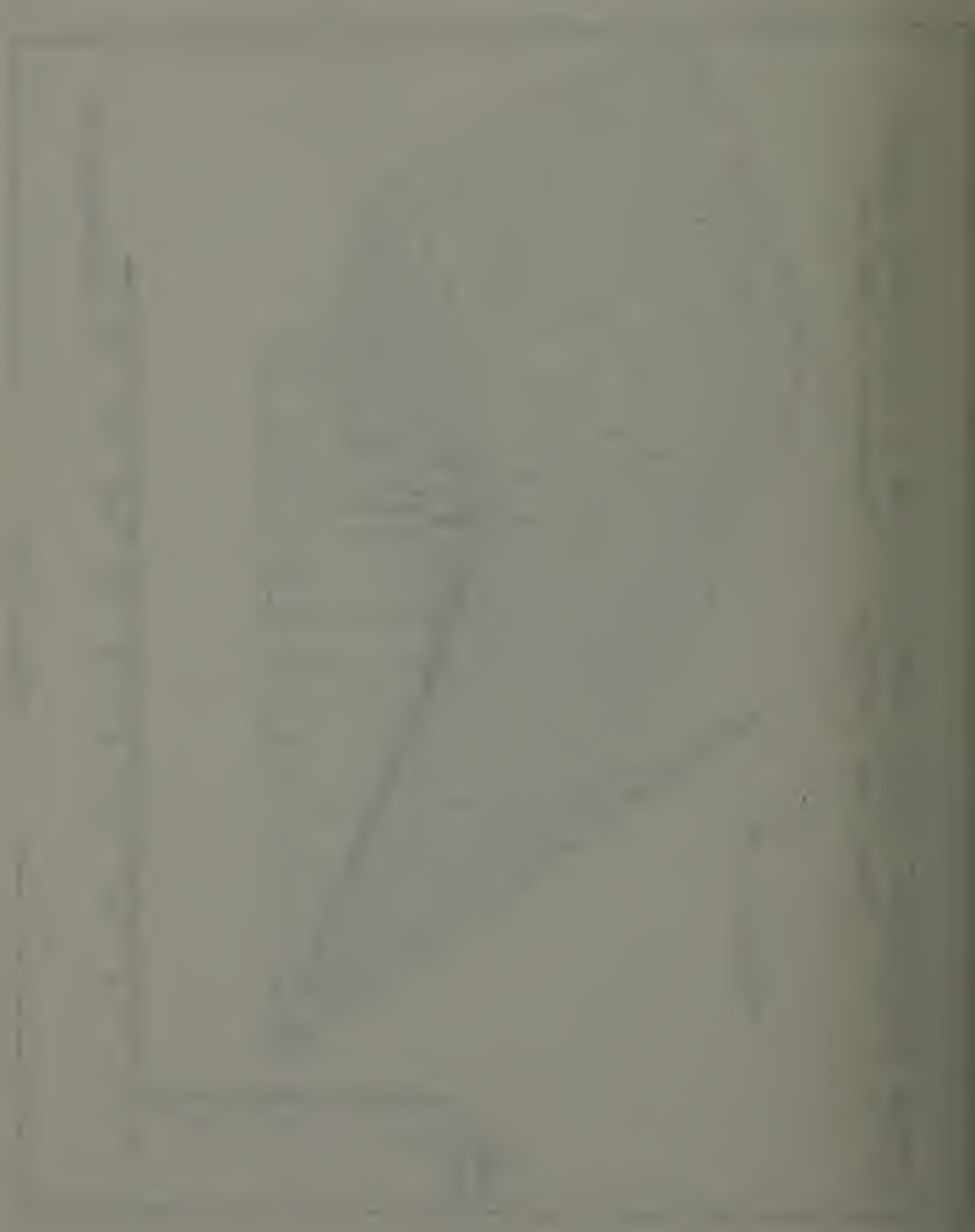

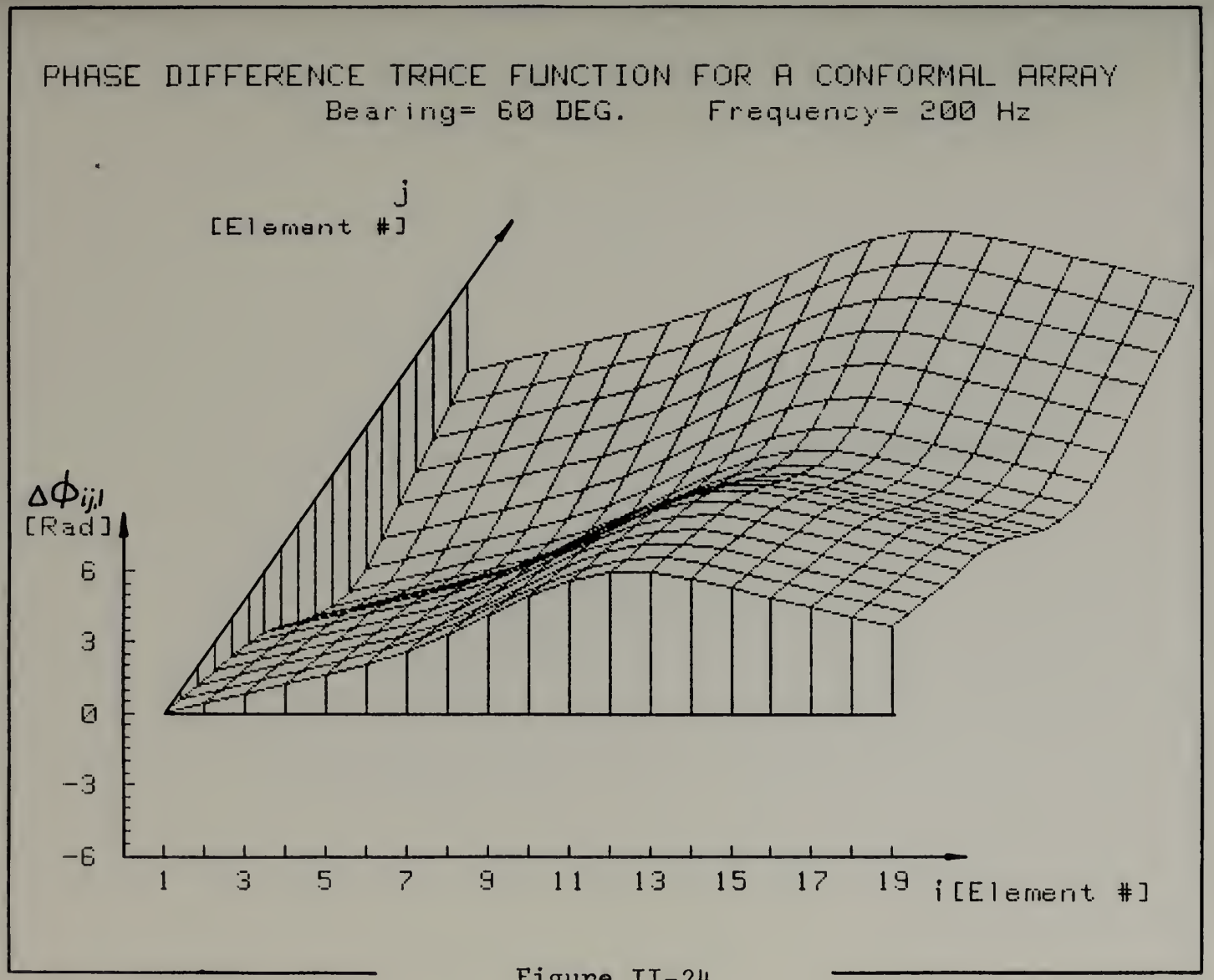
PHASE DIFFERENCE TRACE FUNCTION FOR A CONFORMAL ARRAY
Bearing= 60 DEG. Frequency= 200 Hz
j
[Element #]
Δφij,l
[Rad]
6
3
0
-3
-6
1
3
5
7
9
11
13
15
17
19
i[Element #]

Figure II-24

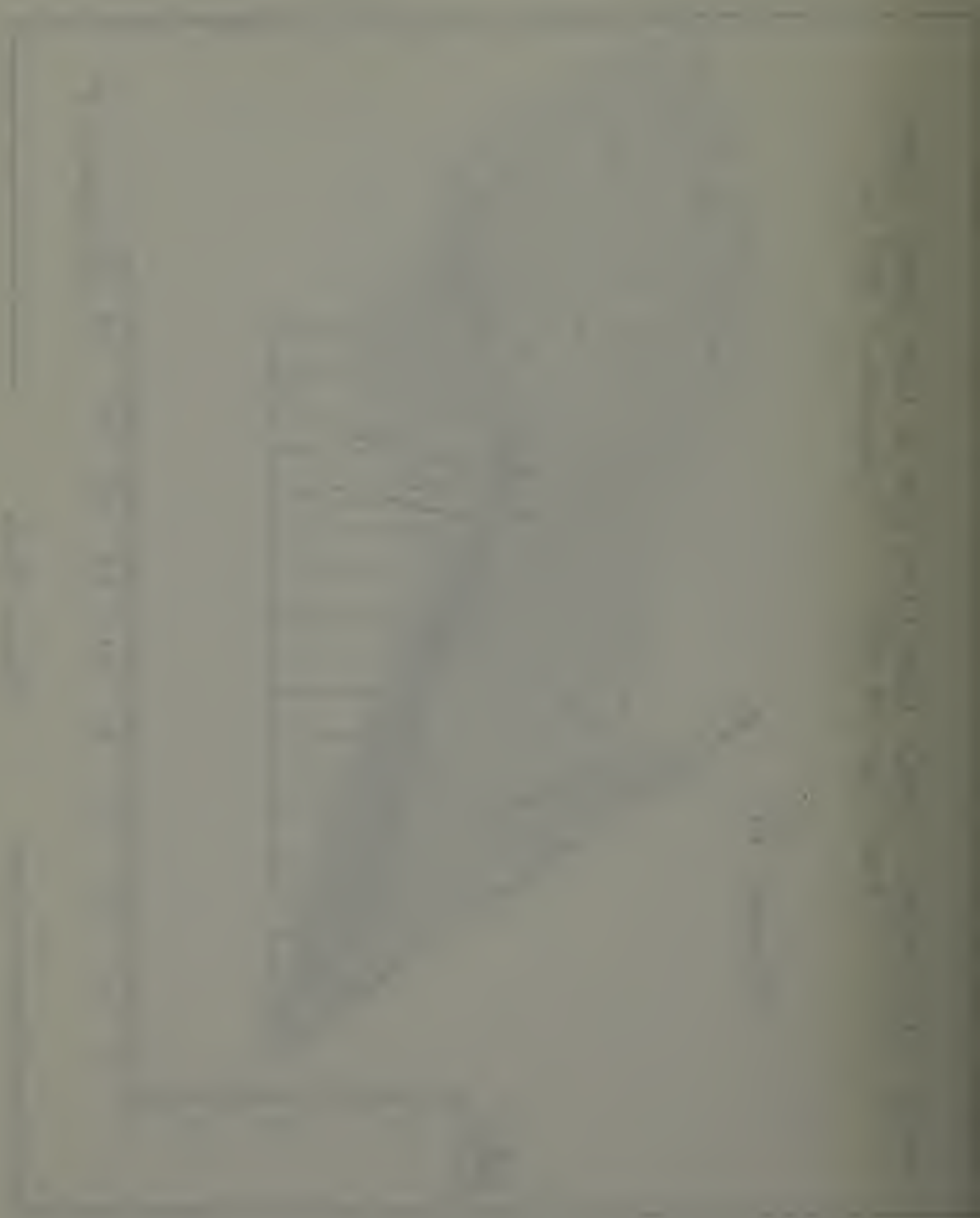

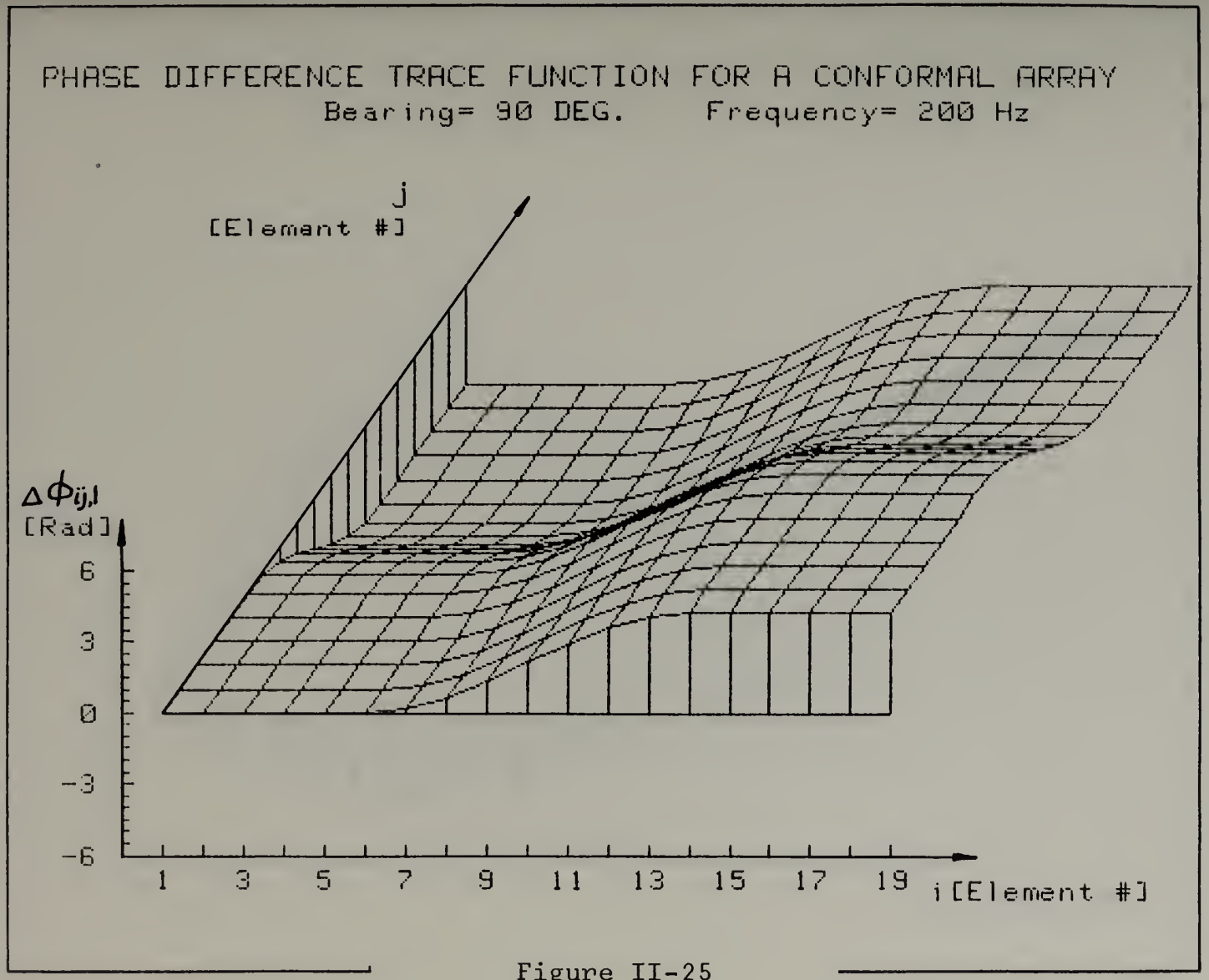
PHASE DIFFERENCE TRACE FUNCTION FOR A CONFORMAL ARRAY
Bearing= 90 DEG. Frequency= 200 Hz
j
[Element #]
Δφij,l
[Rad]
6
3
0
-3
-6
1
3
5
7
9
11
13
15
17
19
i[Element #]

Figure II-25

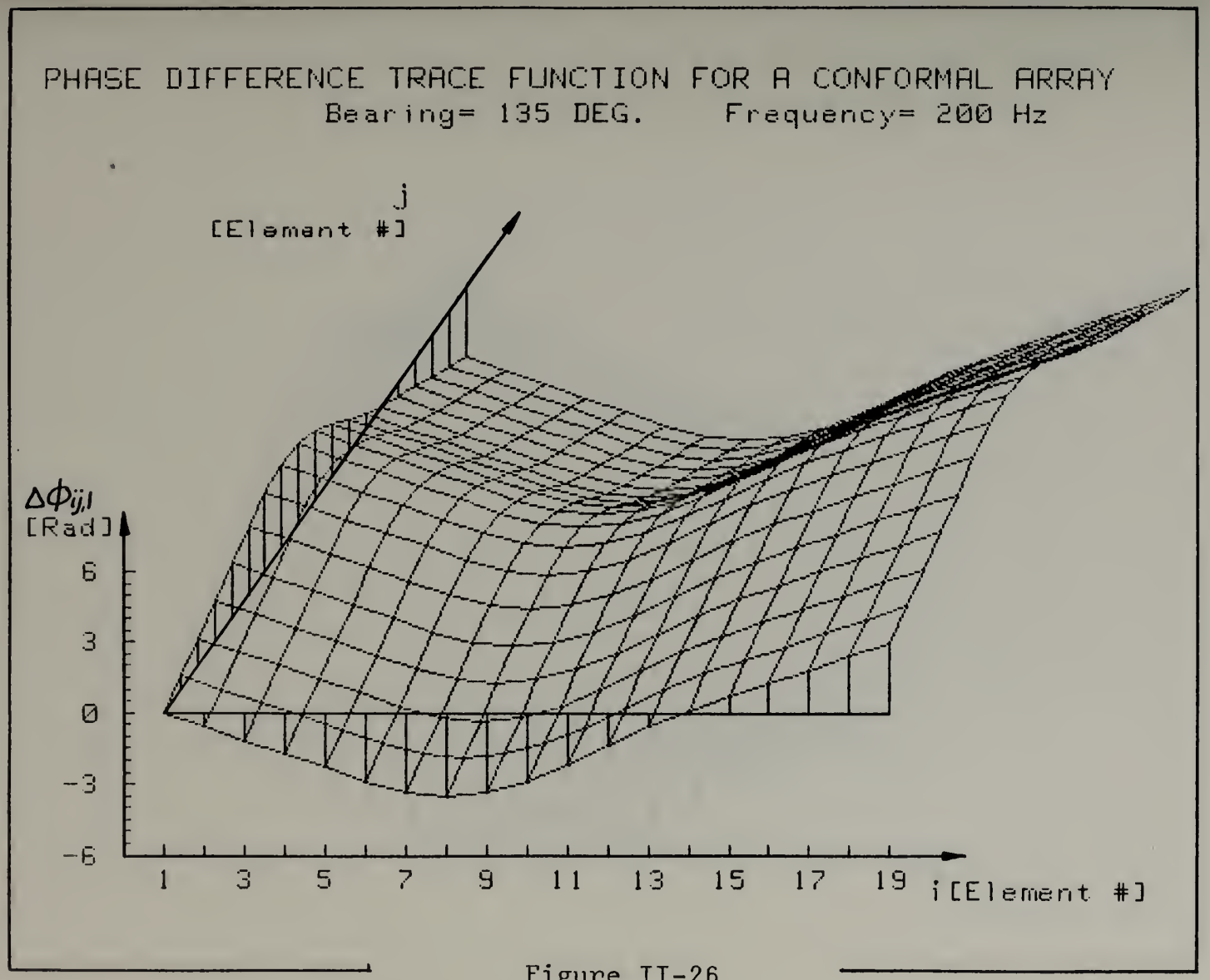
PHASE DIFFERENCE TRACE FUNCTION FOR A CONFORMAL ARRAY
Bearing= 135 DEG.
Frequency= 200 Hz
j
[Elemant #]
Δφij,l
[Rad]
6
3
0
-3
-6
1
3
5
7
9
11
13
15
17
19
i[Element #]

Figure II-26

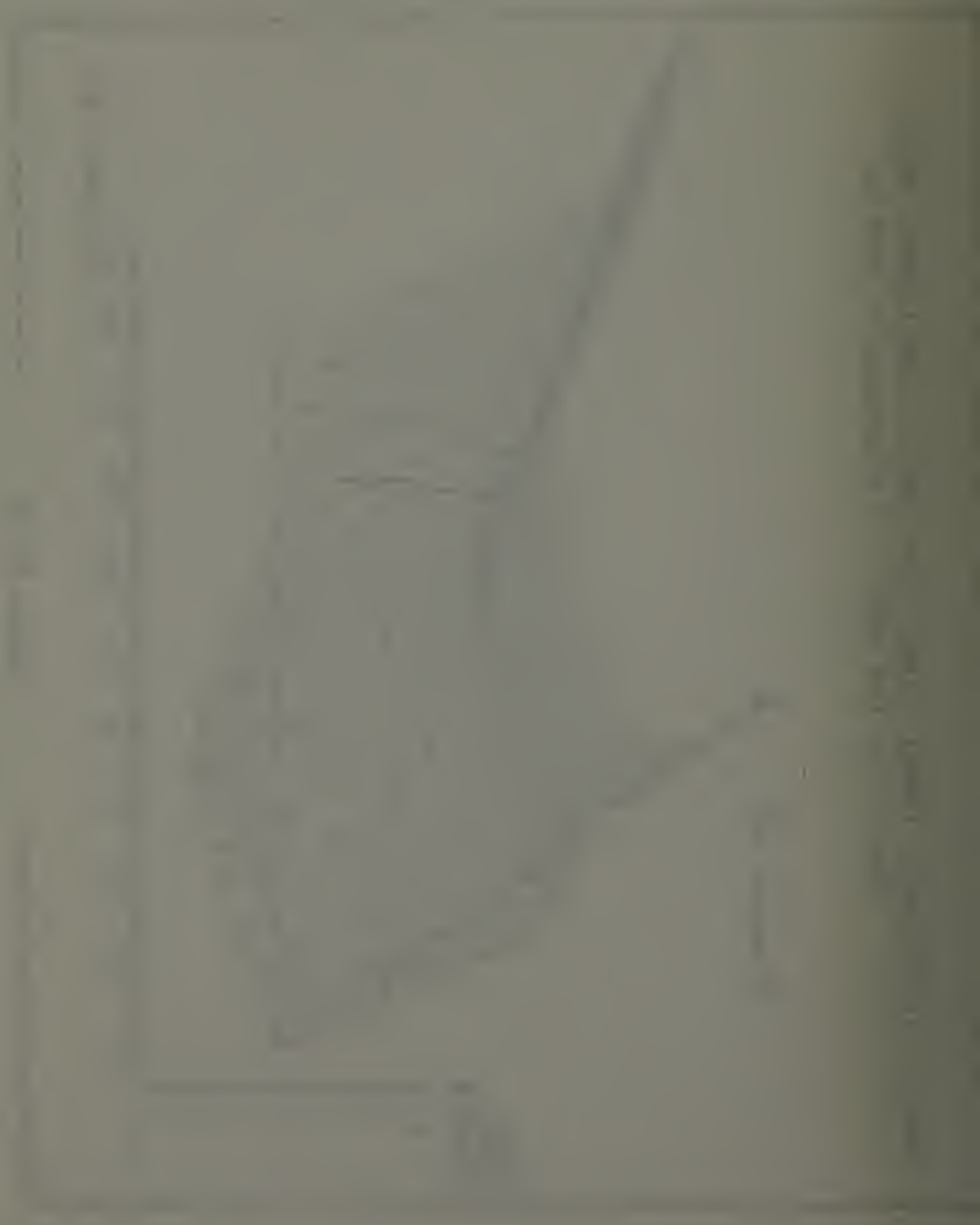

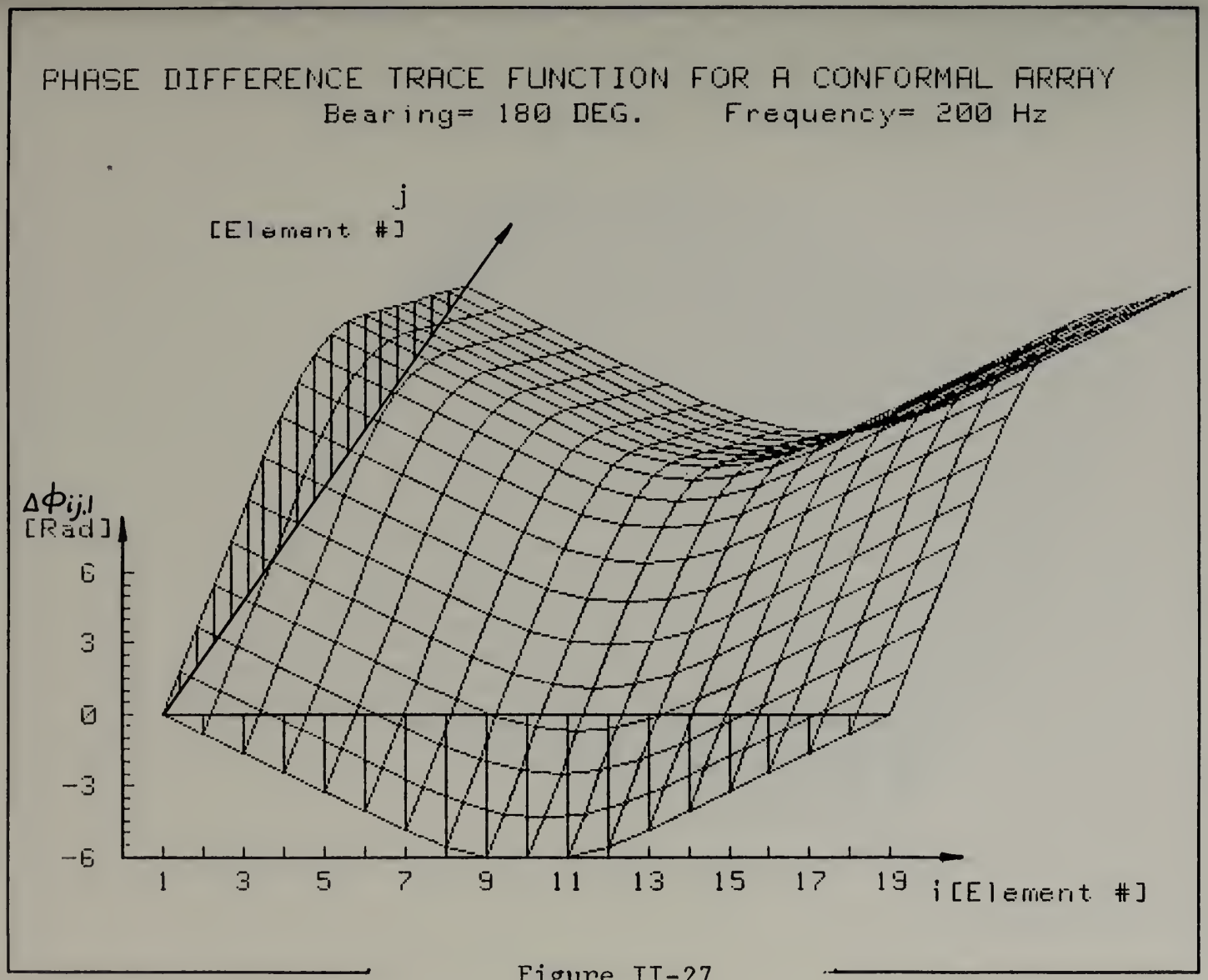
PHASE DIFFERENCE TRACE FUNCTION FOR A CONFORMAL ARRAY
Bearing= 180 DEG.
Frequency= 200 Hz
j
[Element #]
Δφij,l
[Rad]
6
3
0
-3
-6
1
3
5
7
9
11
13
15
17
19
i [Element #]

Figure II-27

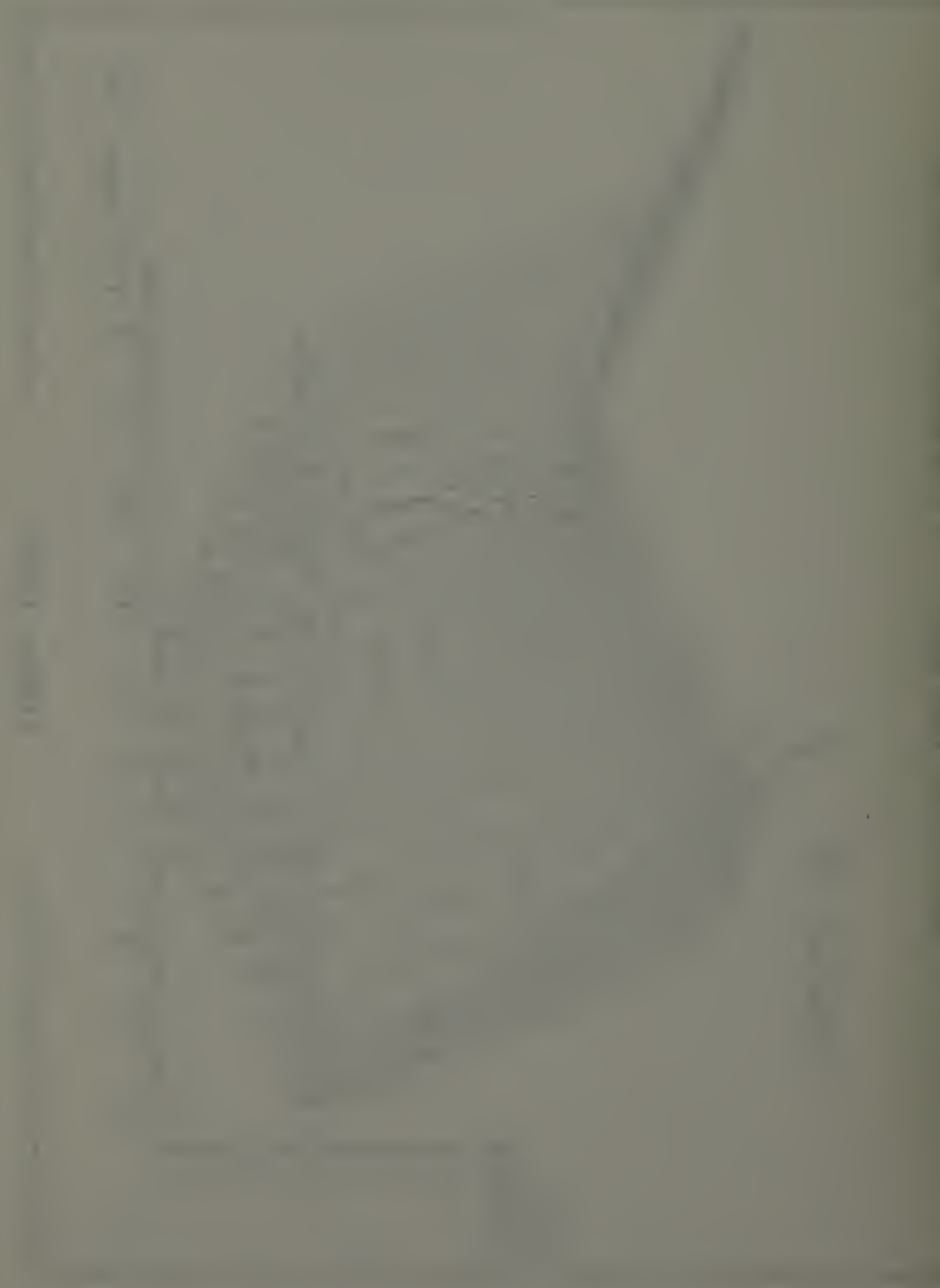

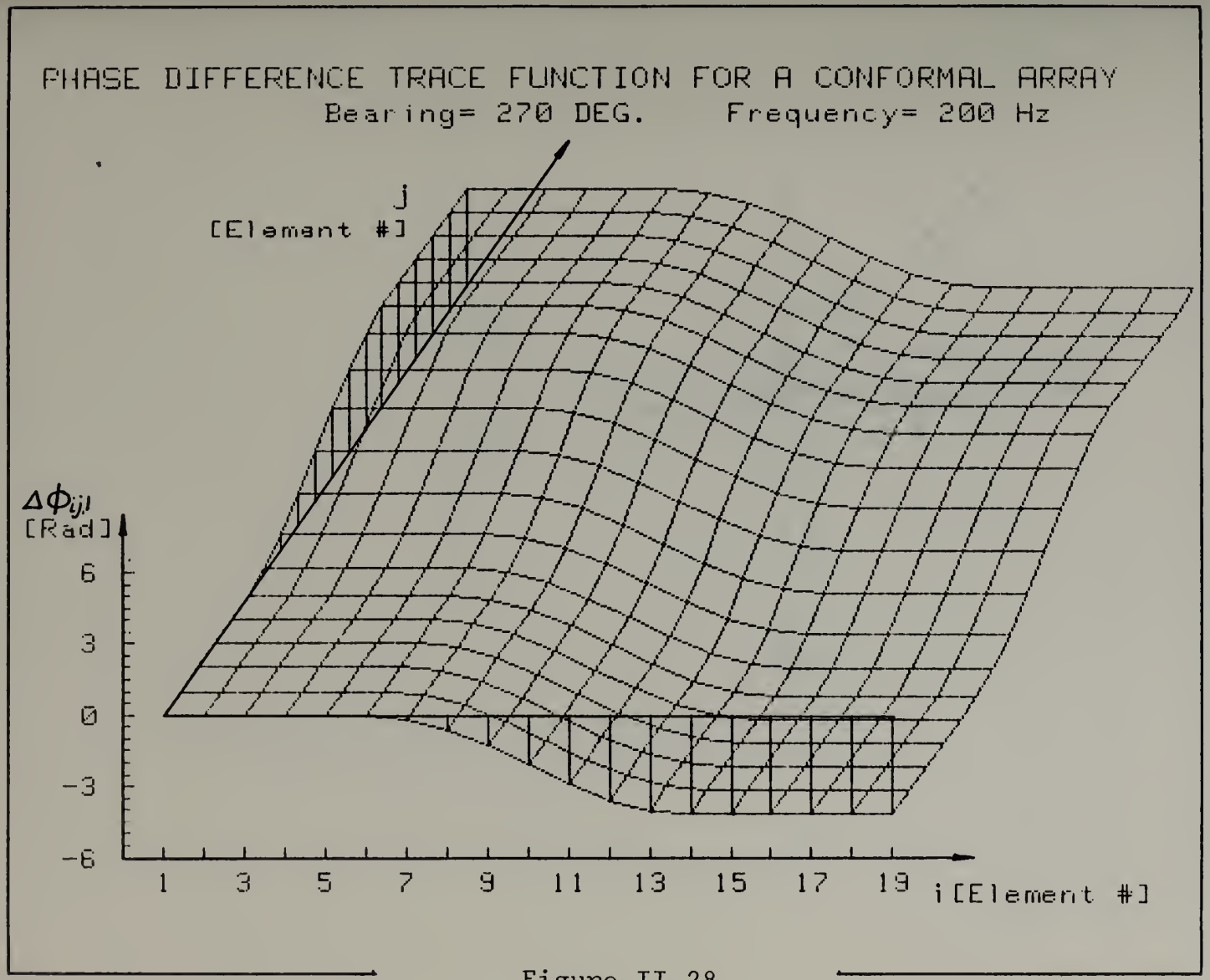
PHASE DIFFERENCE TRACE FUNCTION FOR A CONFORMAL ARRAY
Bearing= 270 DEG.
Frequency= 200 Hz
j
[Element #]
Δφij
[Rad]
6
3
0
-3
-6
1
3
5
7
9
11
13
15
17
19
i[Element #]

Figure II-28

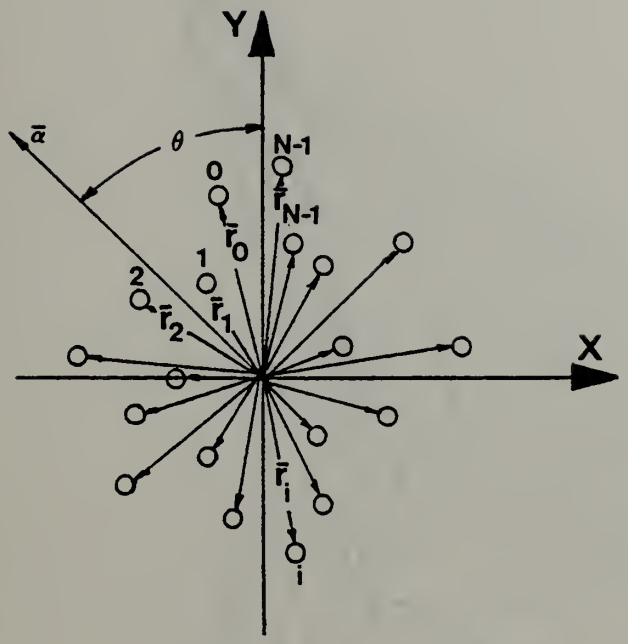


Figure II-29
Random Array Configuration

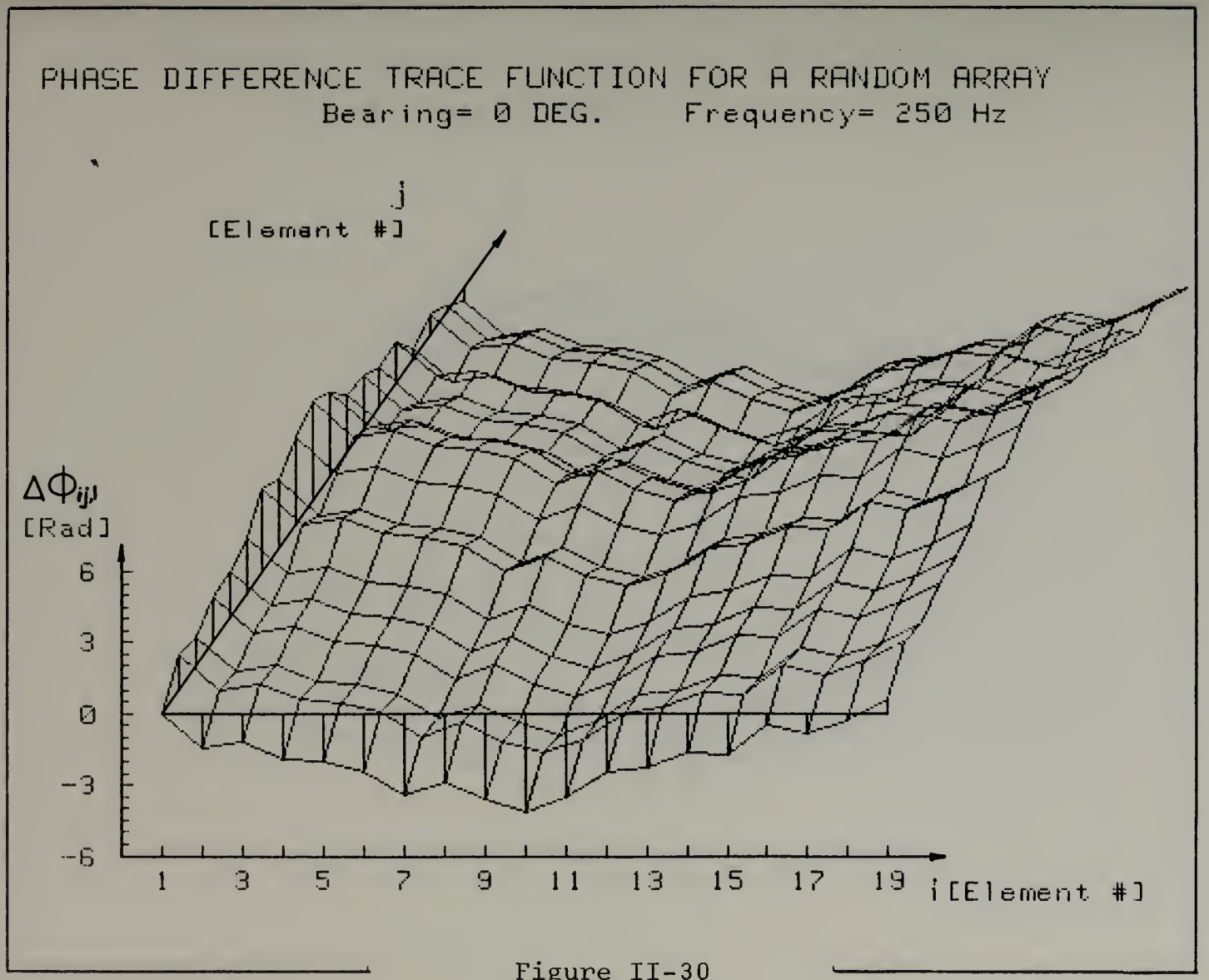
PHASE DIFFERENCE TRACE FUNCTION FOR A RANDOM ARRAY
Bearing= 0 DEG. Frequency= 250 Hz
j
[Element #]
$\Delta\Phi_{ij,l}$
[Rad]
6
3
0
-3
-6
1
3
5
7
9
11
13
15
17
19
i [Element #]

Figure II-30

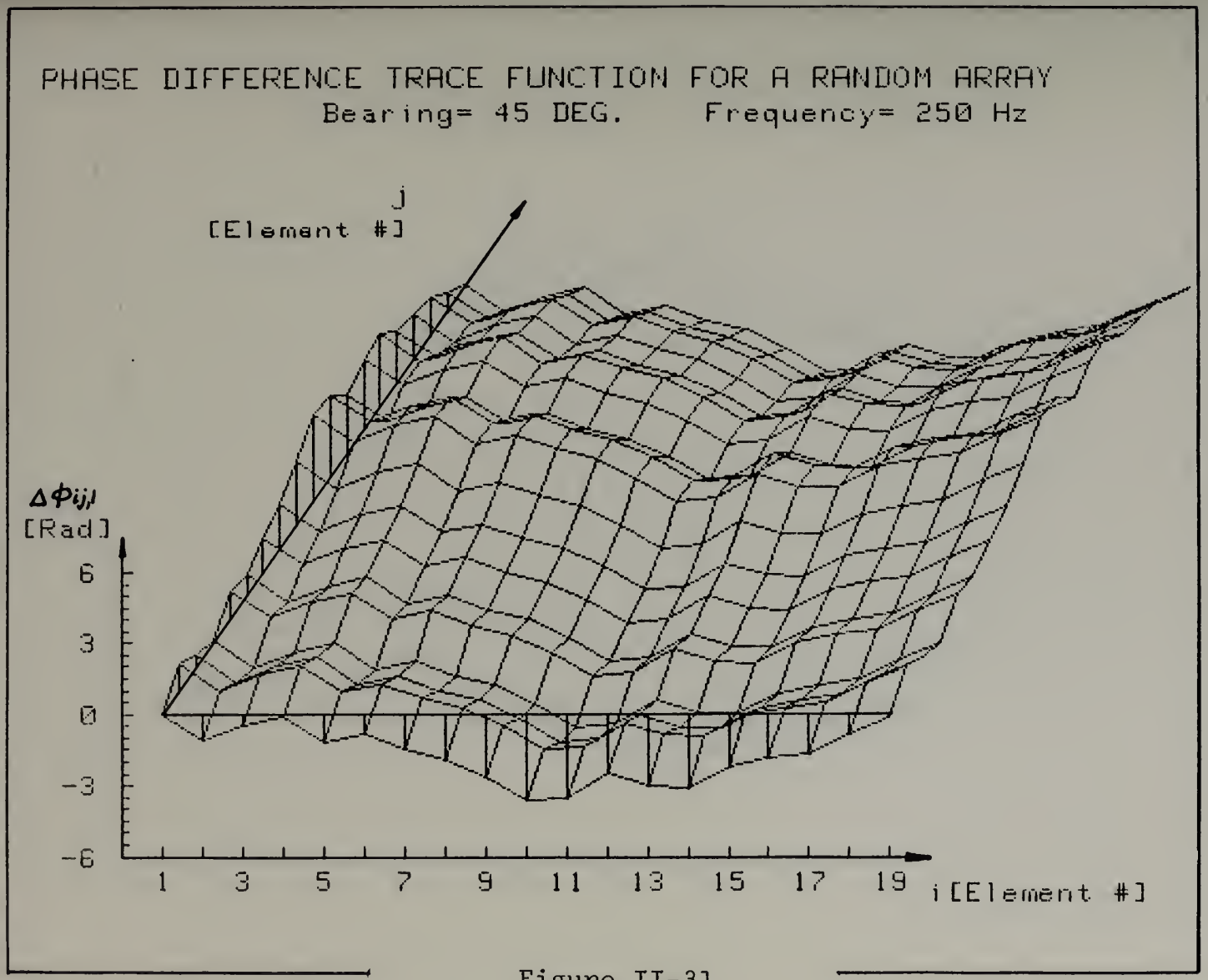
PHASE DIFFERENCE TRACE FUNCTION FOR A RANDOM ARRAY
Bearing= 45 DEG. Frequency= 250 Hz
j
[Element #]
Δφij,l
[Rad]
6
3
0
-3
-6
1
3
5
7
9
11
13
15
17
19
i[Element #]

Figure II-31

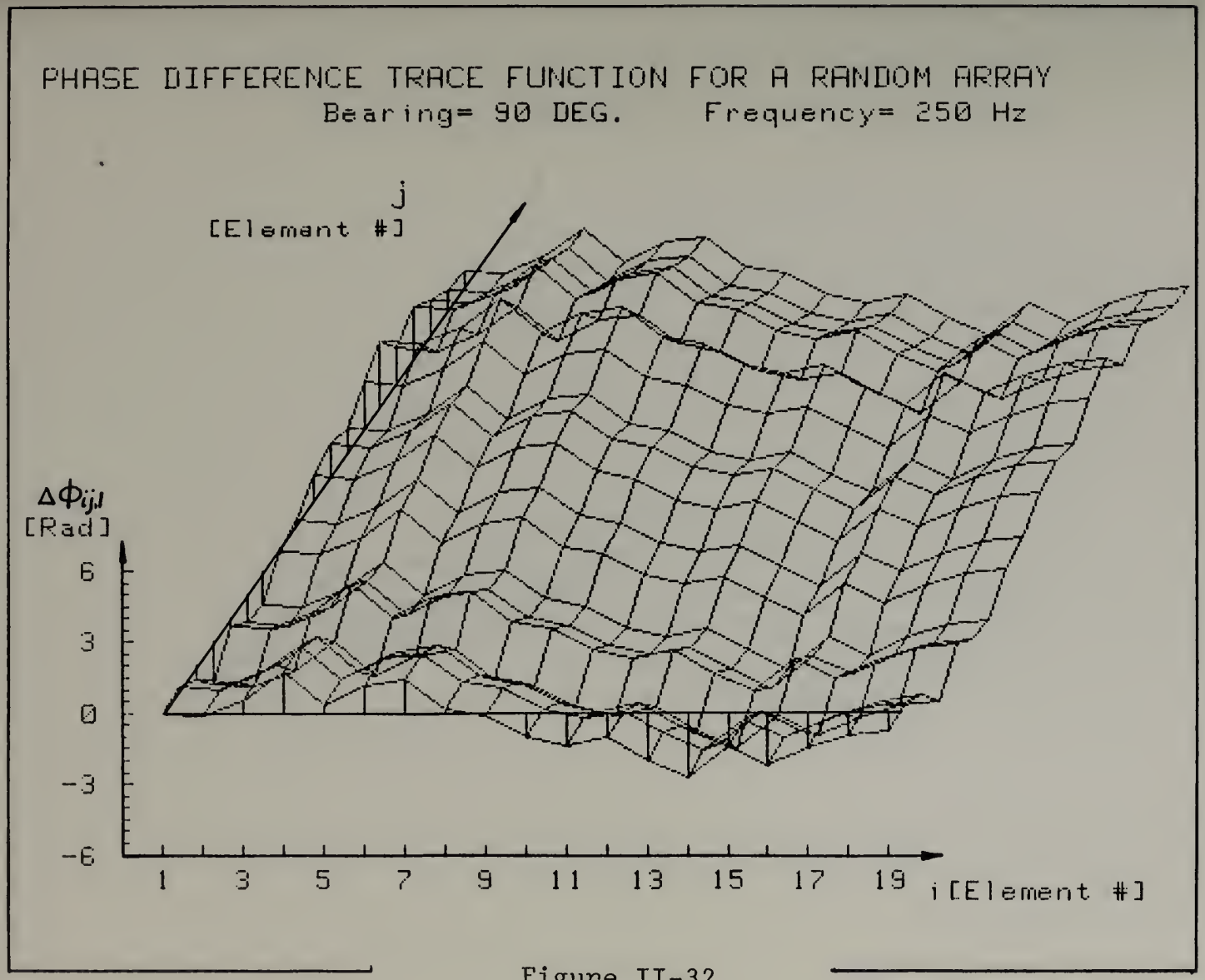
PHASE DIFFERENCE TRACE FUNCTION FOR A RANDOM ARRAY
Bearing= 90 DEG. Frequency= 250 Hz
j
[Elemant #]
Δφij,l
[Rad]
6
3
0
-3
-6
1
3
5
7
9
11
13
15
17
19
i[Element #]

Figure II-32

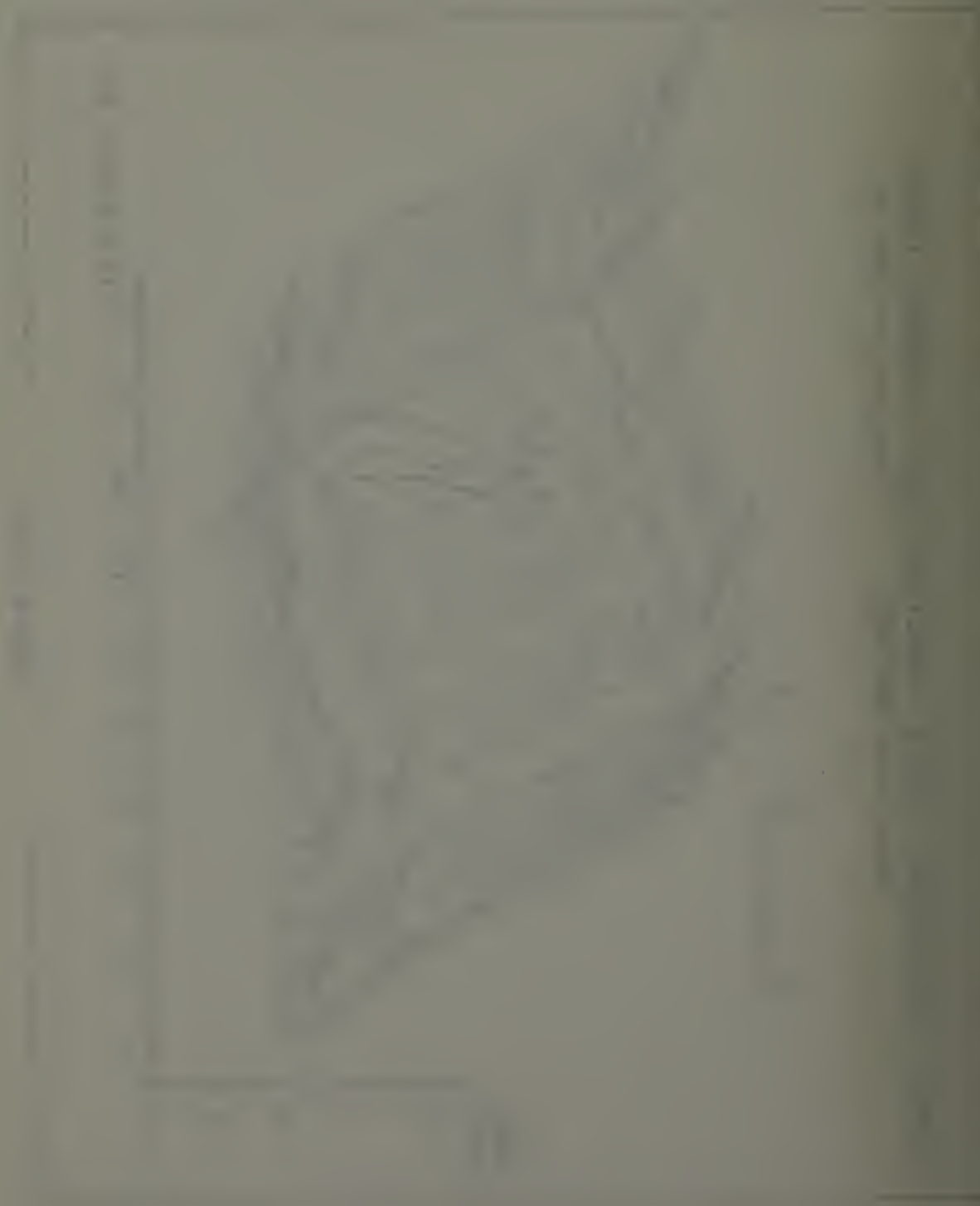

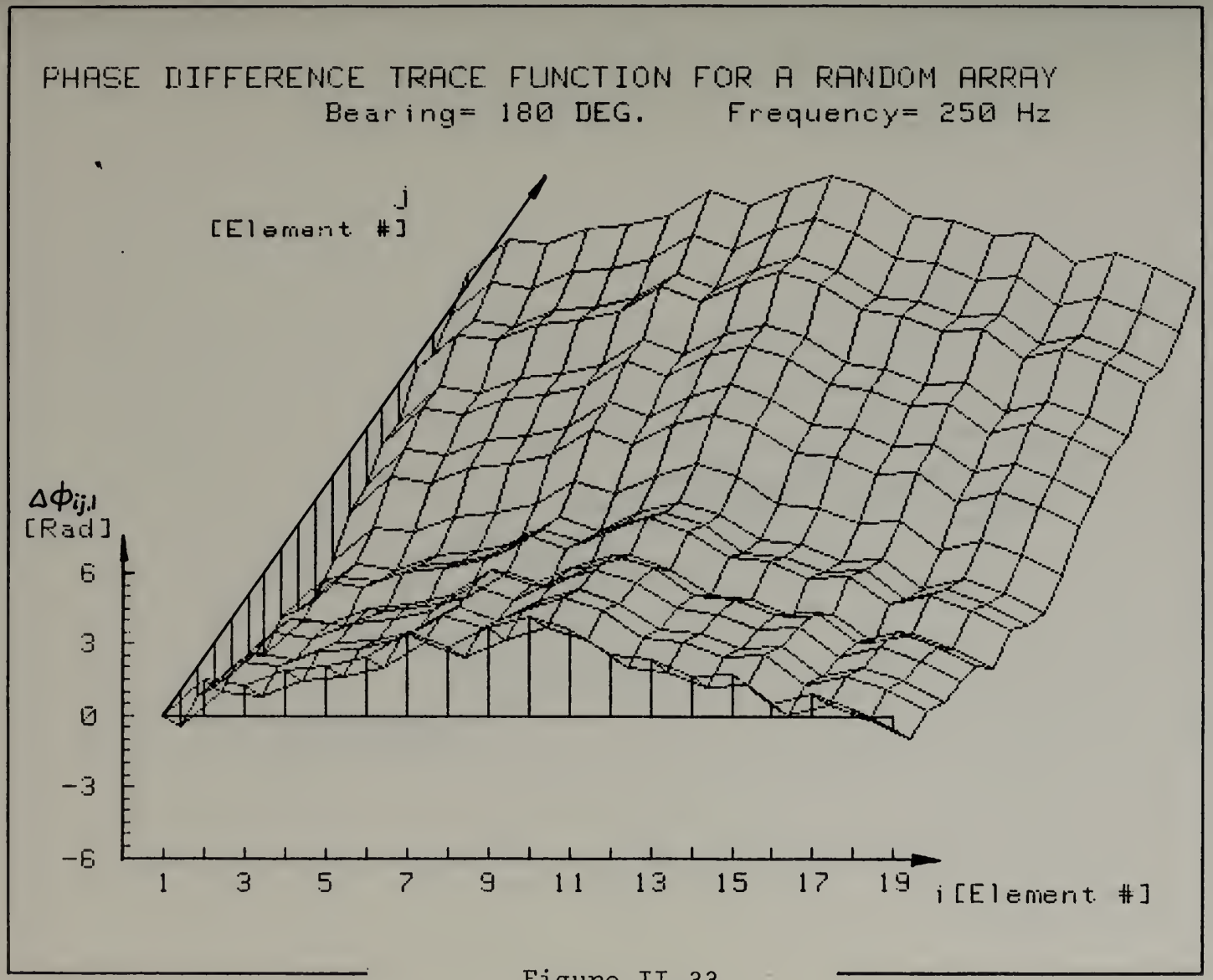
PHASE DIFFERENCE TRACE FUNCTION FOR A RANDOM ARRAY
Bearing= 180 DEG.
Frequency= 250 Hz
j
[Element #]
Δφij,l
[Rad]
6
3
0
-3
-6
1
3
5
7
9
11
13
15
17
19
i [Element #]

Figure II-33

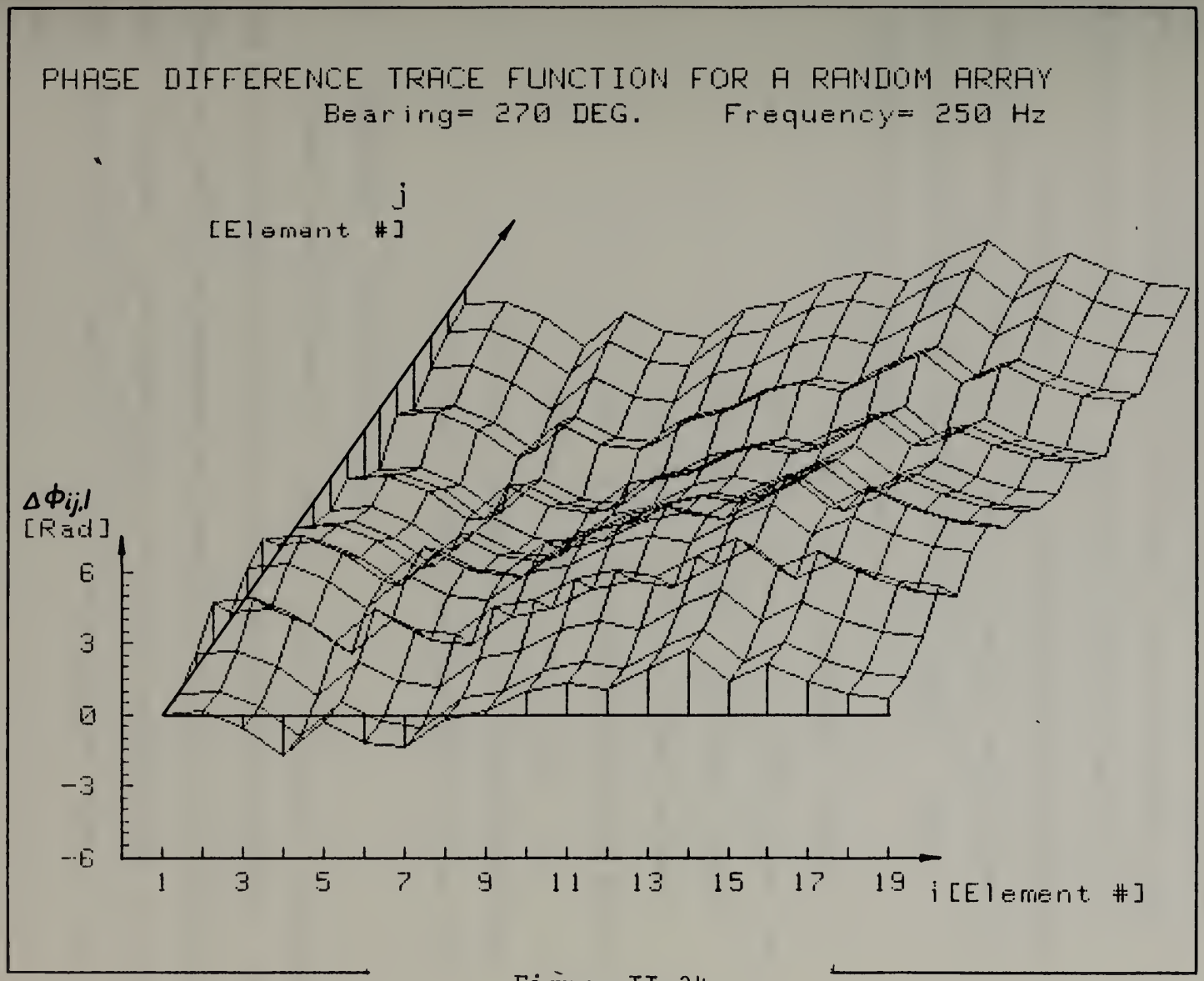
PHASE DIFFERENCE TRACE FUNCTION FOR A RANDOM ARRAY
Bearing= 270 DEG.
Frequency= 250 Hz
j
[Element #]
Δφij,l
[Rad]
6
3
0
-3
-6
1
3
5
7
9
11
13
15
17
19
i[Element #]

Figure II-34

Common characteristics of the non-analytic trace functions are:

- They do not have a distinct single parameter which is indicative of the bearing of the incoming signal; however, they still have a distinct form for each bearing.

- As a result of (a) the minimum mean square error surface fitting still can be used; however, each trace function must be fitted on a point-by-point basis. Some "educated" search procedures may be used.

NOTE: 1. All the trace functions plotted in this part were phase difference trace functions. The time delay trace functions were not given because they are only scaled versions with the same functional form.

2. Each intersection in the trace function plots corresponds to a data point.

## E. DEGENERATE TRACE FUNCTIONS

In some applications the task of generating and processing the full trace function may not be necessary or possible. For those situations a degenerate version of the trace functions can be applied. The degenerate versions are derived by taking only some distinct pairs from all the possible pairs of elements.

For example for a circular array a logical choice of pairs will be on opposite sides of diameters such that:

$$j = (i + \frac{N}{2}) \bmod N \qquad \text{(II-11)}$$

Then, by substitution in (II-7)

$$\Delta\tau_{ij} = \frac{2R}{c} \cos\left(\frac{2\pi i}{N} - \theta\right) \qquad \text{(II-12)}$$

and in (II-8)

$$\Delta\phi_{ij,\ell} = \Delta\tau_{ij}\omega_{\ell} = \frac{2\pi D}{\lambda} \cos\left(\frac{2\pi i}{N} - \theta\right) \qquad \text{(II-13)}$$

which is a simple cosine wave whose phase is identically the bearing of the incoming signal. It can be shown that the performance of the degenerate trace function is not as good as that of the full trace function but may be adequate for some applications.

## F. CHAPTER SUMMARY

In this chapter the concept of the trace function was developed and demonstrated. From the few examples shown it can be concluded that the concept is well adapted to be used in a generalized spatial replica correlation scheme. In addition, for highly symmetrical arrays the amount of processing requires is significantly reduced.

As such the circular array is a natural one to be treated this way. In subsequent chapters the bearing estimator for

a circular array will be developed based on trace function concepts. In addition to the circular array the linear array will be also treated mainly for comparison purposes.

# III. MINIMUM MEAN SQUARE ERROR SURFACE FITTING AS APPLIED TO BEARING ESTIMATION BY TRACE FUNCTIONS

## A. INTRODUCTION

In the previous chapter it was shown that the trace function can be represented by a three dimensional surface (function) whose shape is dependent on the bearing $\theta$. For a given array the trace functions are known either analytically or in the form of a data matrix at any bearing $\theta$. For the received data from an array of sensors the trace functions are estimated via a cross spectral estimation procedure, and are always in a data matrix form. In order to estimate the bearing by means of the trace function one has to "match" the estimated trace function to the known (stored or analytic) trace function. There are several ways to perform the above "match", some of them require the knowledge of the noise statistics and others do not require it. As the noise statistics, especially the cross noise statistics, may be inaccessible, the methods which will be followed in this analysis will not require this knowledge.

The best known method of this class is the minimum mean square error (MMSE). In this method the sum of squared errors between the estimated (measured) value of the trace function and the "known" value of it at all coordinates "i,j" will be minimized with respect to the parameter "$\theta$" (the bearing). The value of $\theta$ which will give the minimum is the expected one.

In order to give the reader a better intuitive feeling about the estimation problem Figures III-1 through III-10

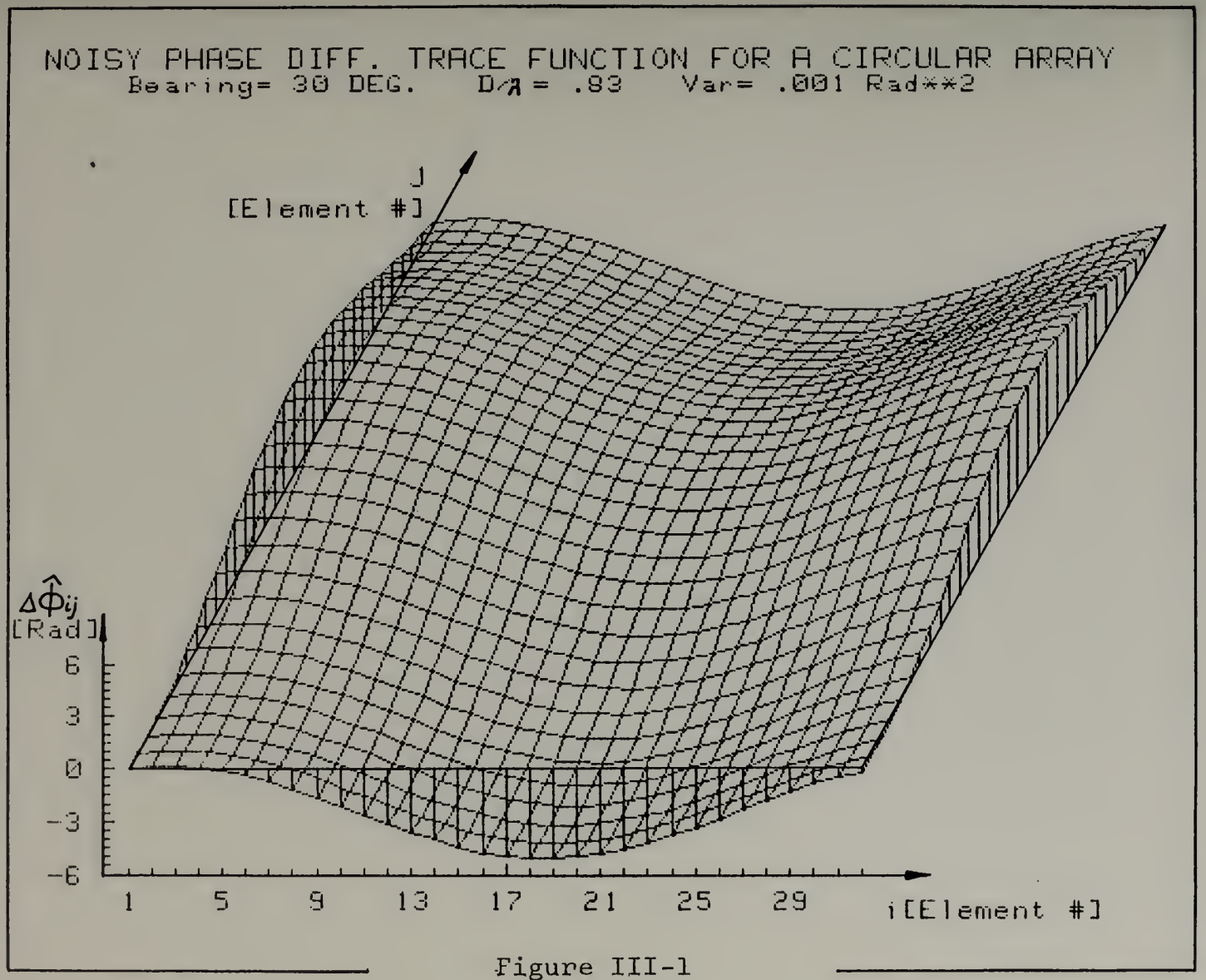
NOISY PHASE DIFF. TRACE FUNCTION FOR A CIRCULAR ARRAY
Bearing= 30 DEG. D/λ = .83 Var= .001 Rad**2
J
[Element #]
Δ$\hat{\Phi}_{ij}$
[Rad]
6
3
0
-3
-6
1
5
9
13
17
21
25
29
i[Element #]

Figure III-1

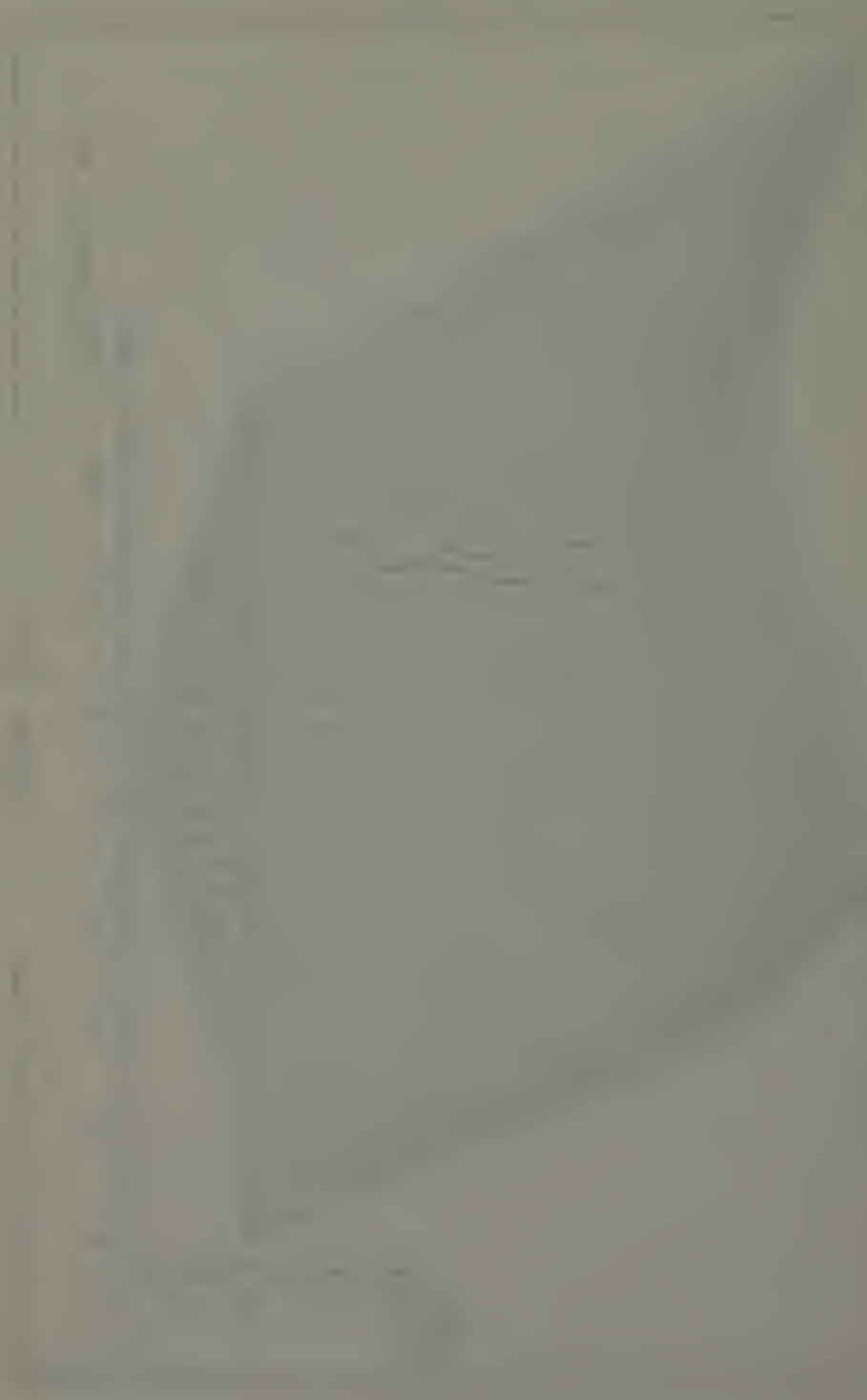

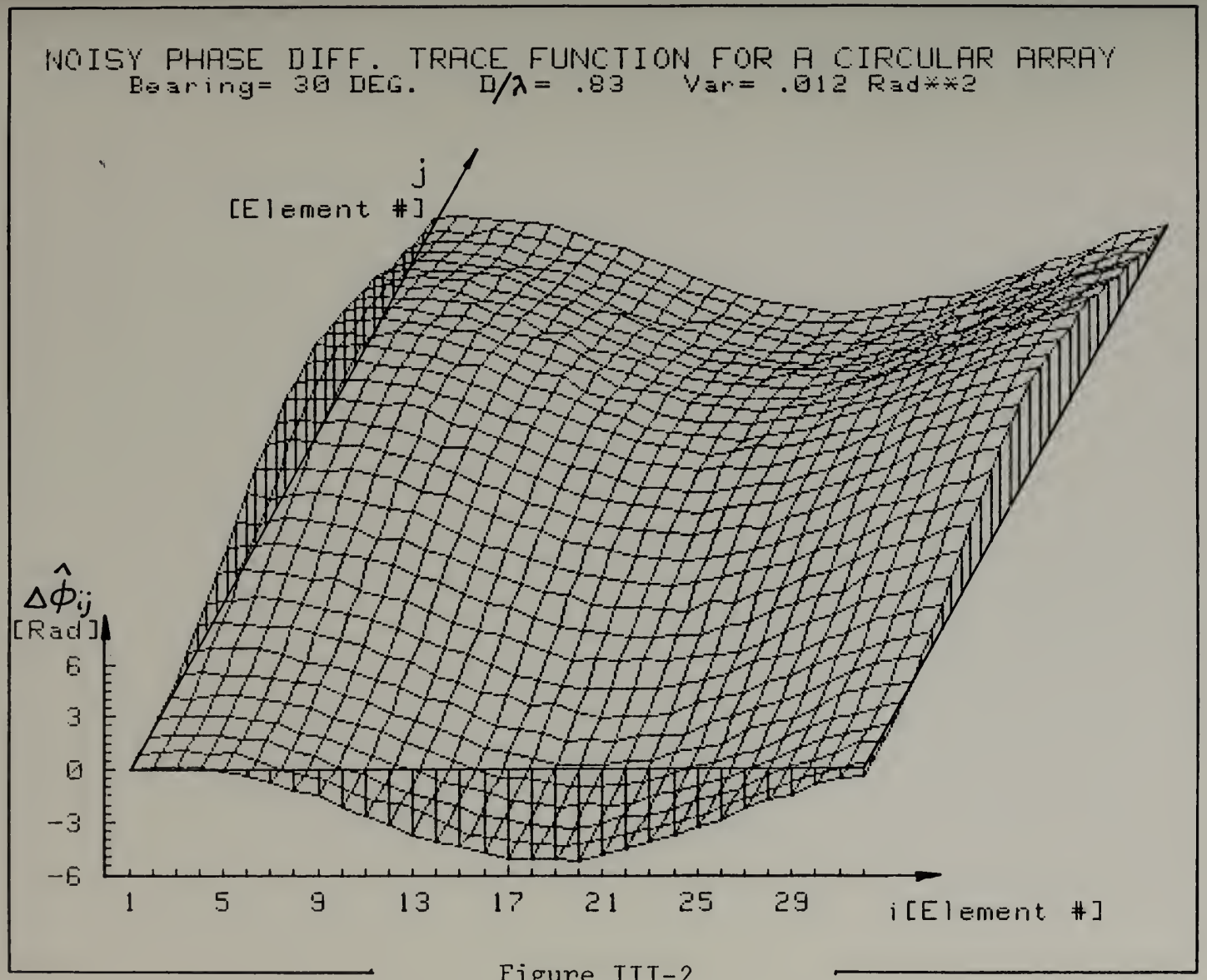
NOISY PHASE DIFF. TRACE FUNCTION FOR A CIRCULAR ARRAY
Bearing= 30 DEG. D/λ= .83 Var= .012 Rad**2
j
[Element #]
$\Delta\hat{\phi}_{ij}$
[Rad]
6
3
0
-3
-6
1
5
9
13
17
21
25
29
i[Element #]

Figure III-2

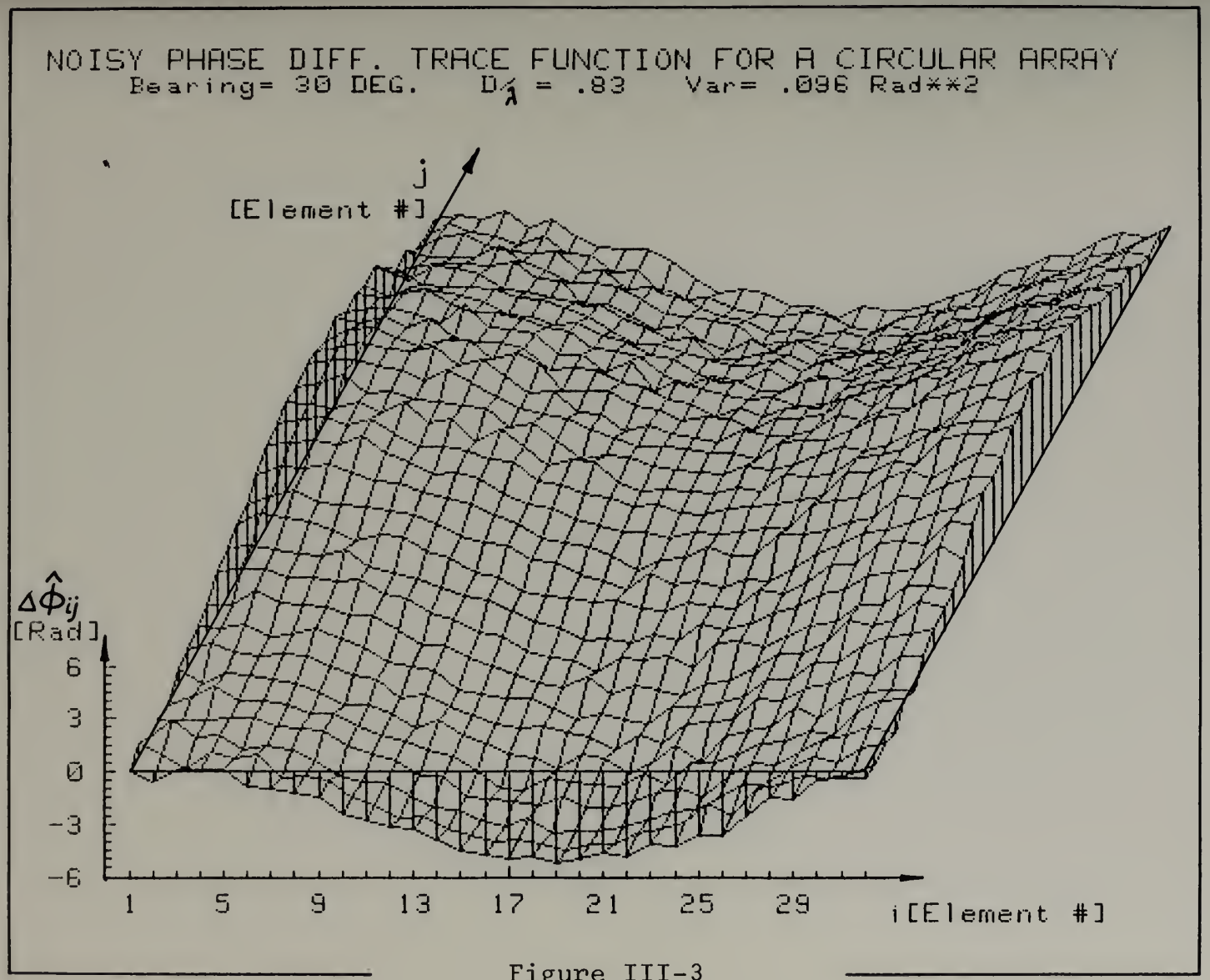
NOISY PHASE DIFF. TRACE FUNCTION FOR A CIRCULAR ARRAY
Bearing= 30 DEG. D/λ = .83 Var= .096 Rad**2
j
[Element #]
Δφ̂ij
[Rad]
6
3
0
-3
-6
1
5
9
13
17
21
25
29
i[Element #]

Figure III-3

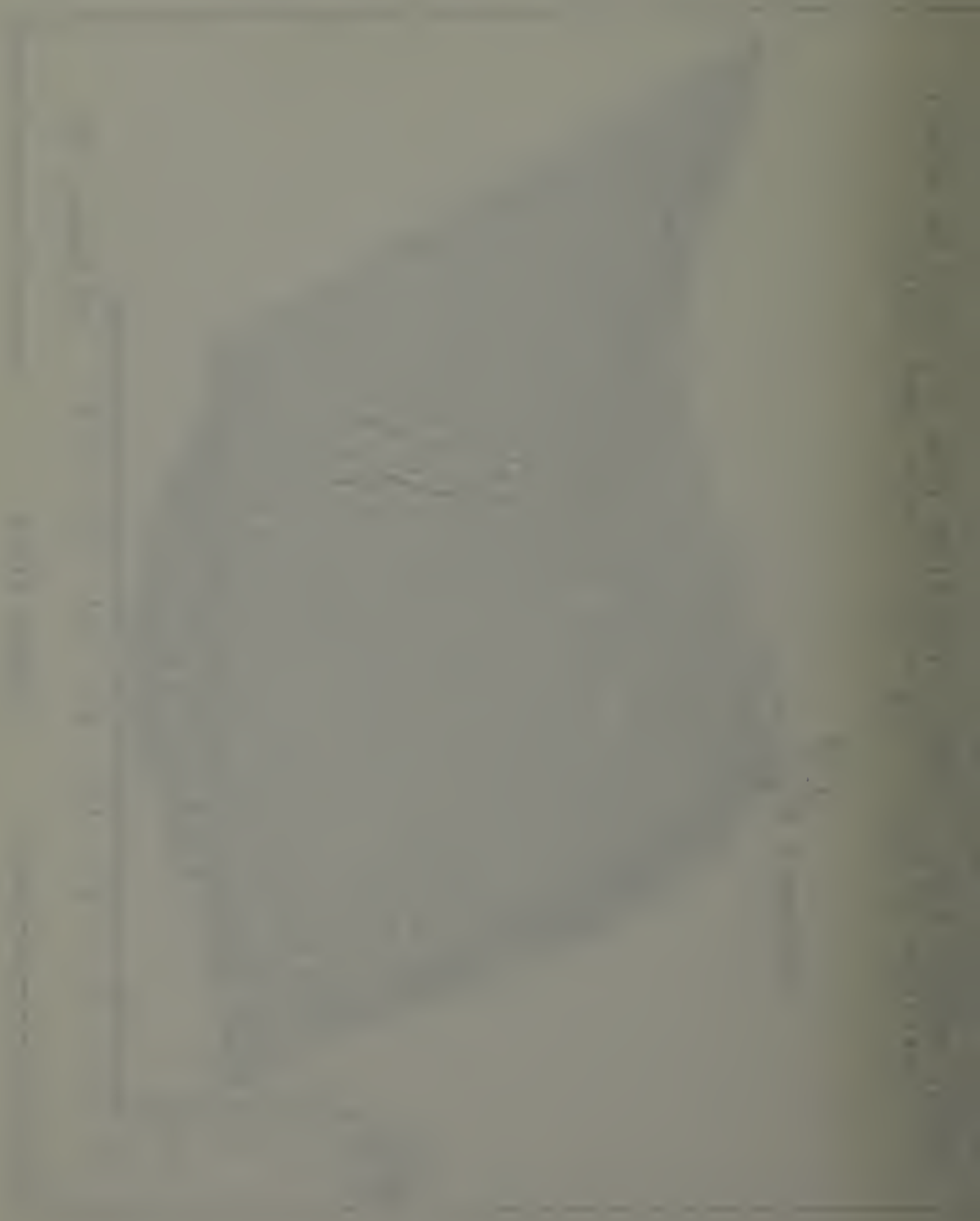

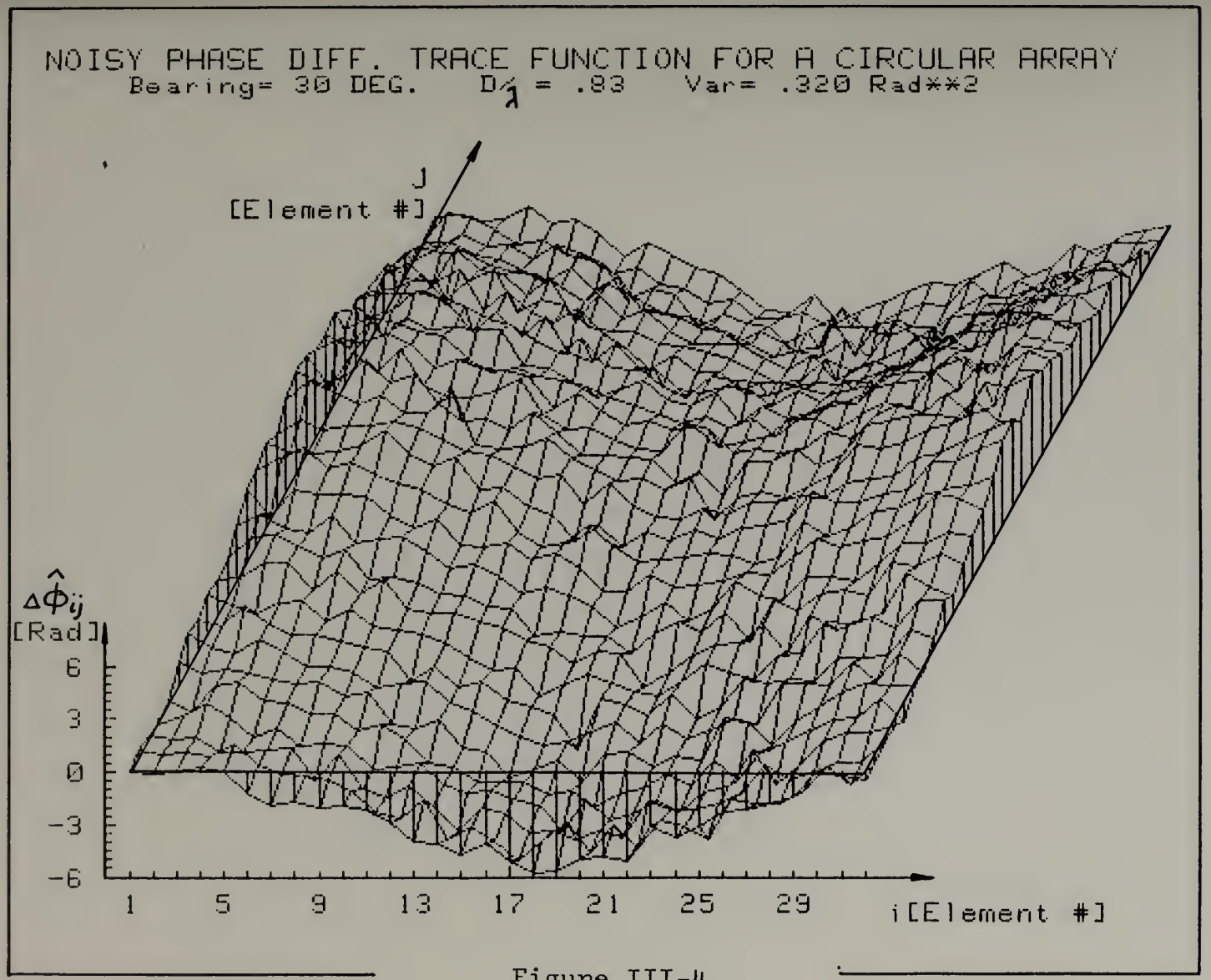
NOISY PHASE DIFF. TRACE FUNCTION FOR A CIRCULAR ARRAY
Bearing= 30 DEG. D/λ = .83 Var= .320 Rad**2
J
[Element #]
Δφ̂ij
[Rad]
6
3
0
-3
-6
1
5
9
13
17
21
25
29
i[Element #]

Figure III-4

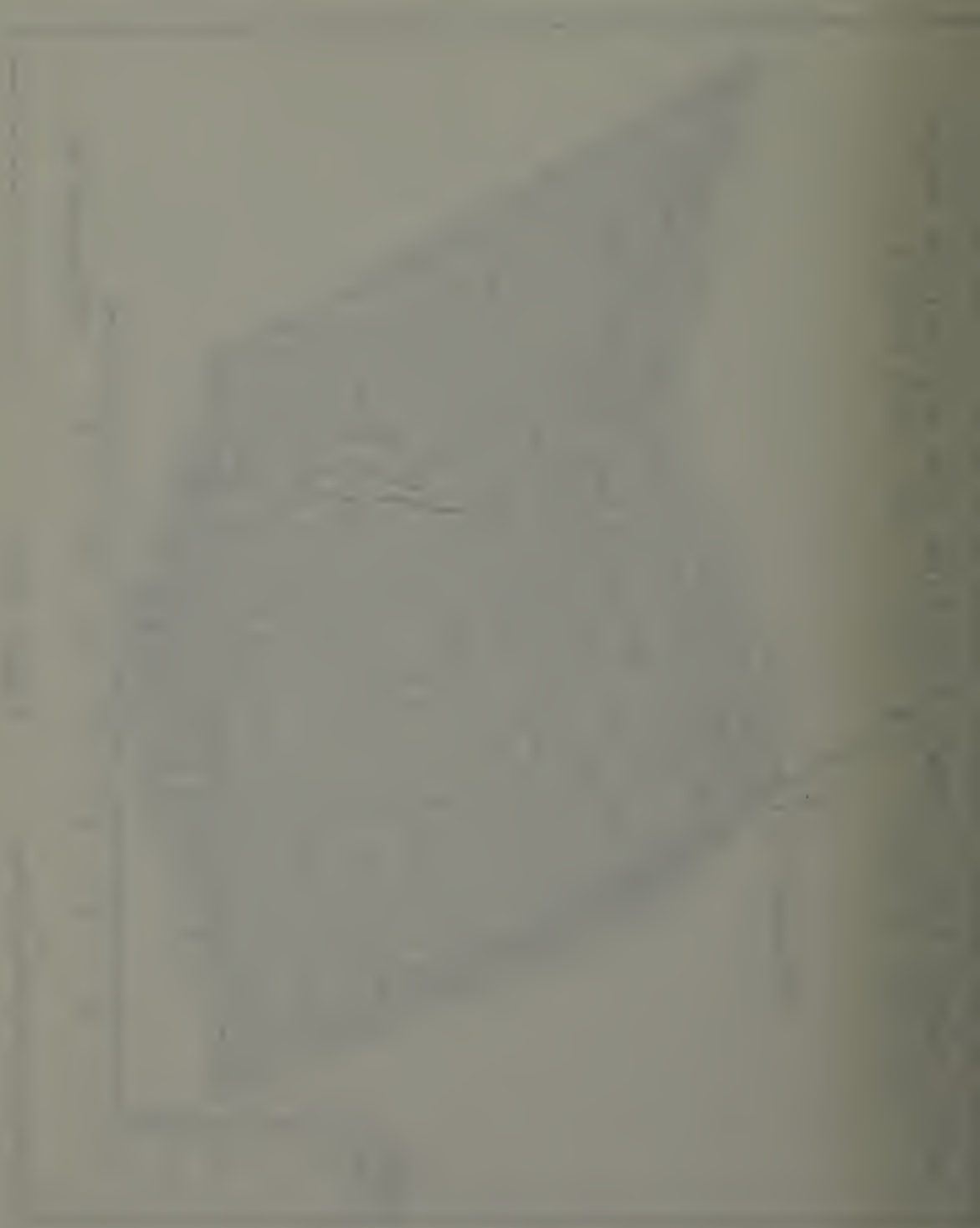

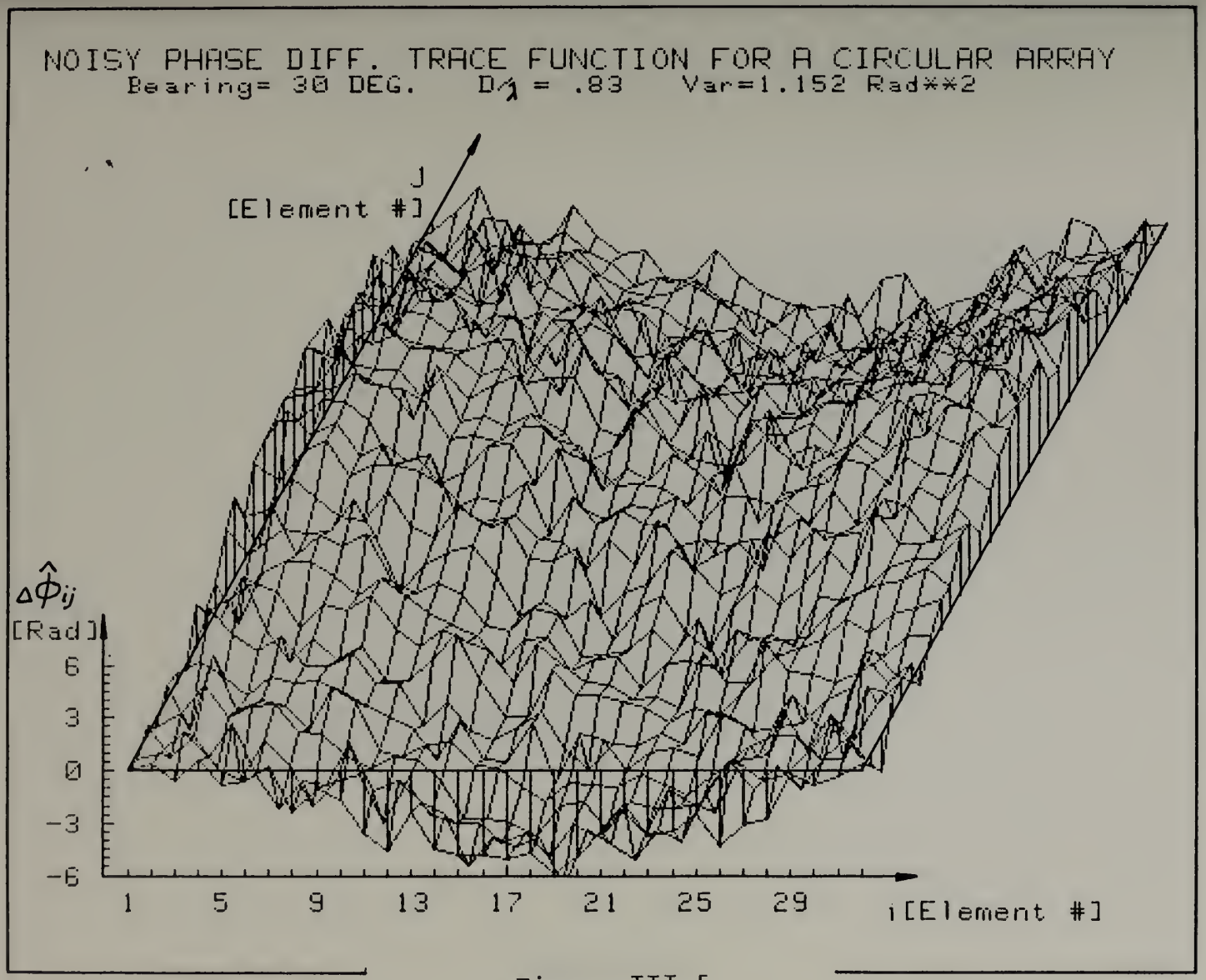
NOISY PHASE DIFF. TRACE FUNCTION FOR A CIRCULAR ARRAY
Bearing= 30 DEG. D/λ = .83 Var=1.152 Rad**2
J
[Element #]
$\Delta\hat{\phi}_{ij}$
[Rad]
6
3
0
-3
-6
1
5
9
13
17
21
25
29
i[Element #]

Figure III-5

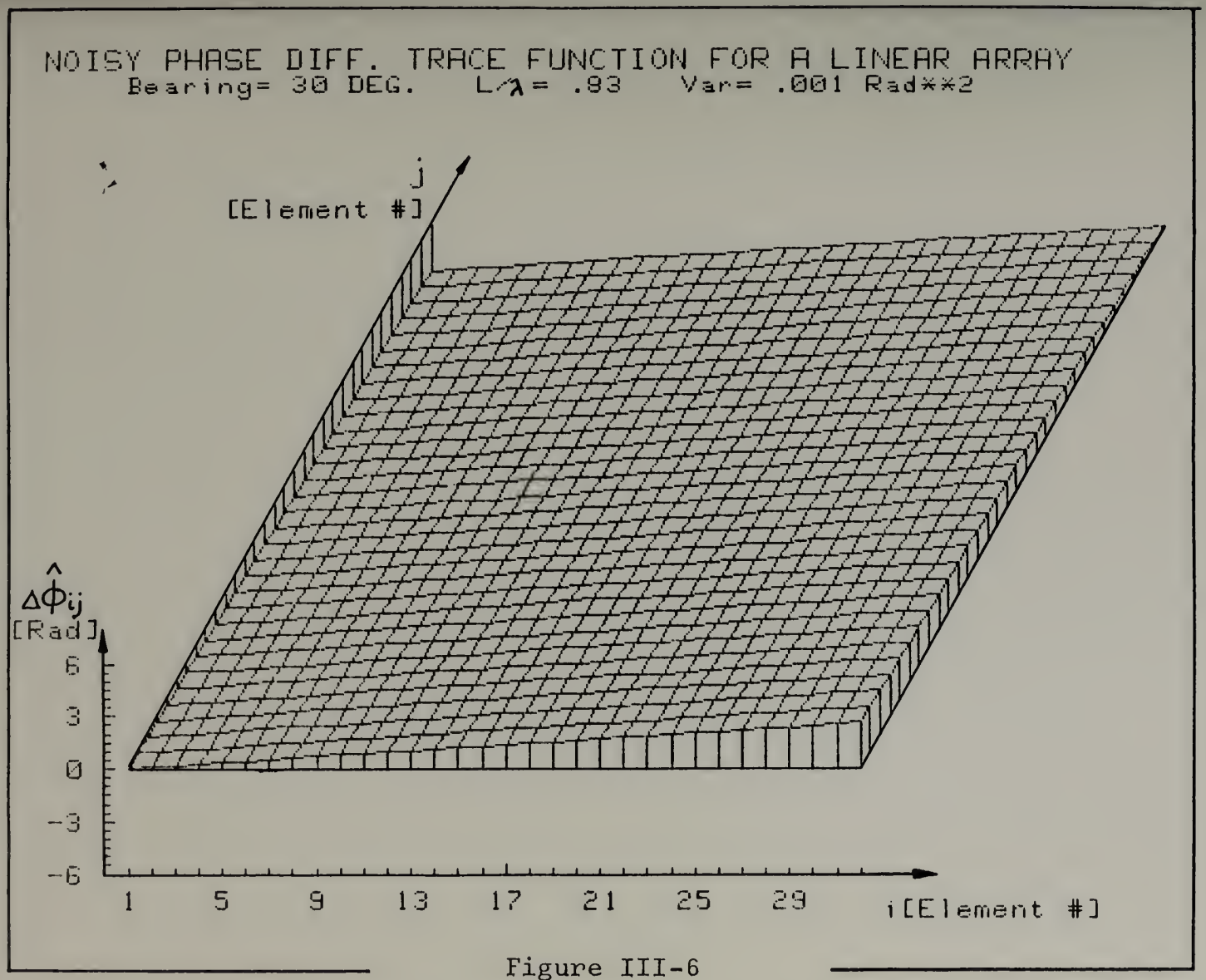
NOISY PHASE DIFF. TRACE FUNCTION FOR A LINEAR ARRAY
Bearing= 30 DEG. L/λ= .93 Var= .001 Rad**2
j
[Element #]
Δφ̂ij
[Rad]
6
3
0
-3
-6
1
5
9
13
17
21
25
29
i[Element #]

Figure III-6

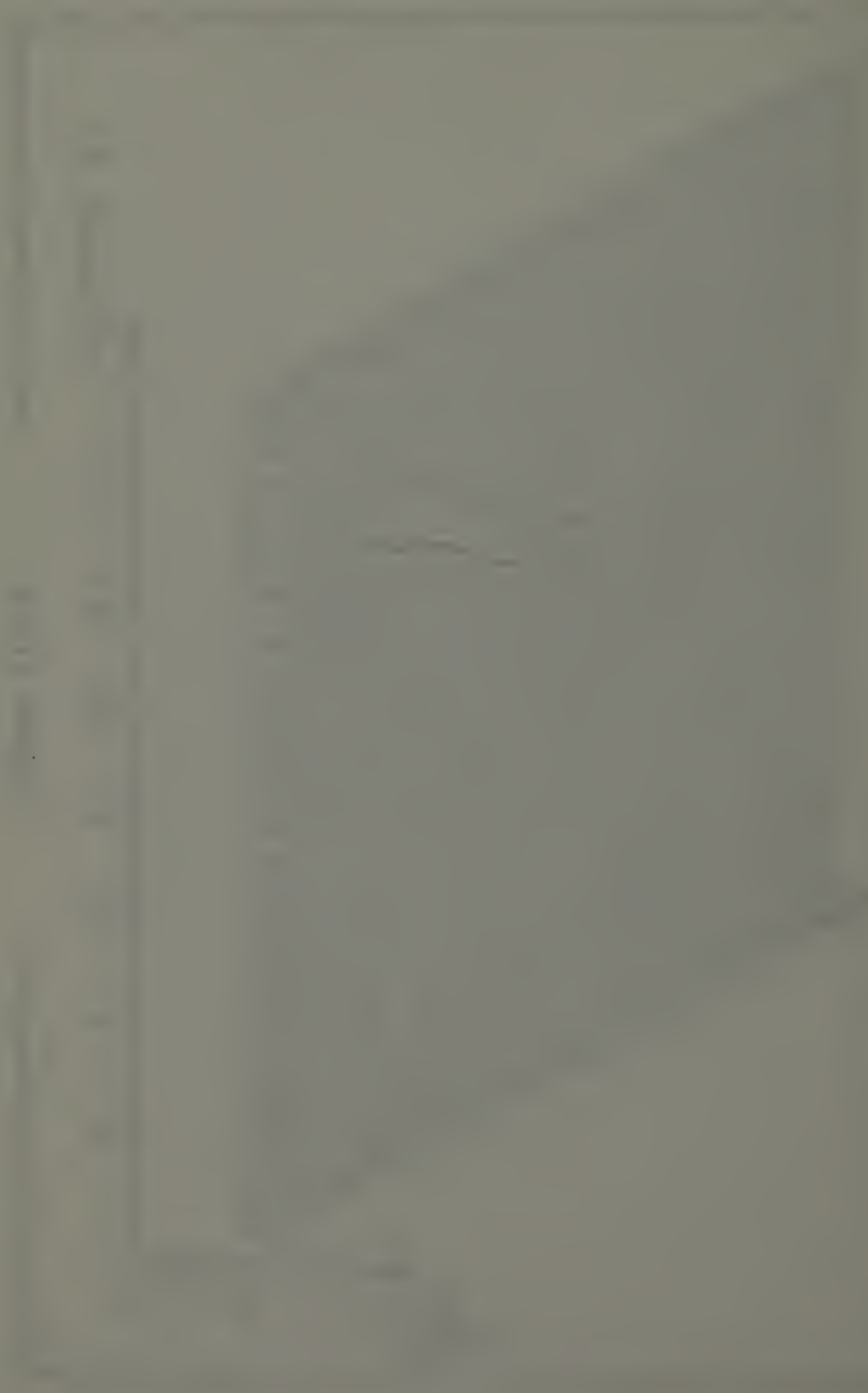

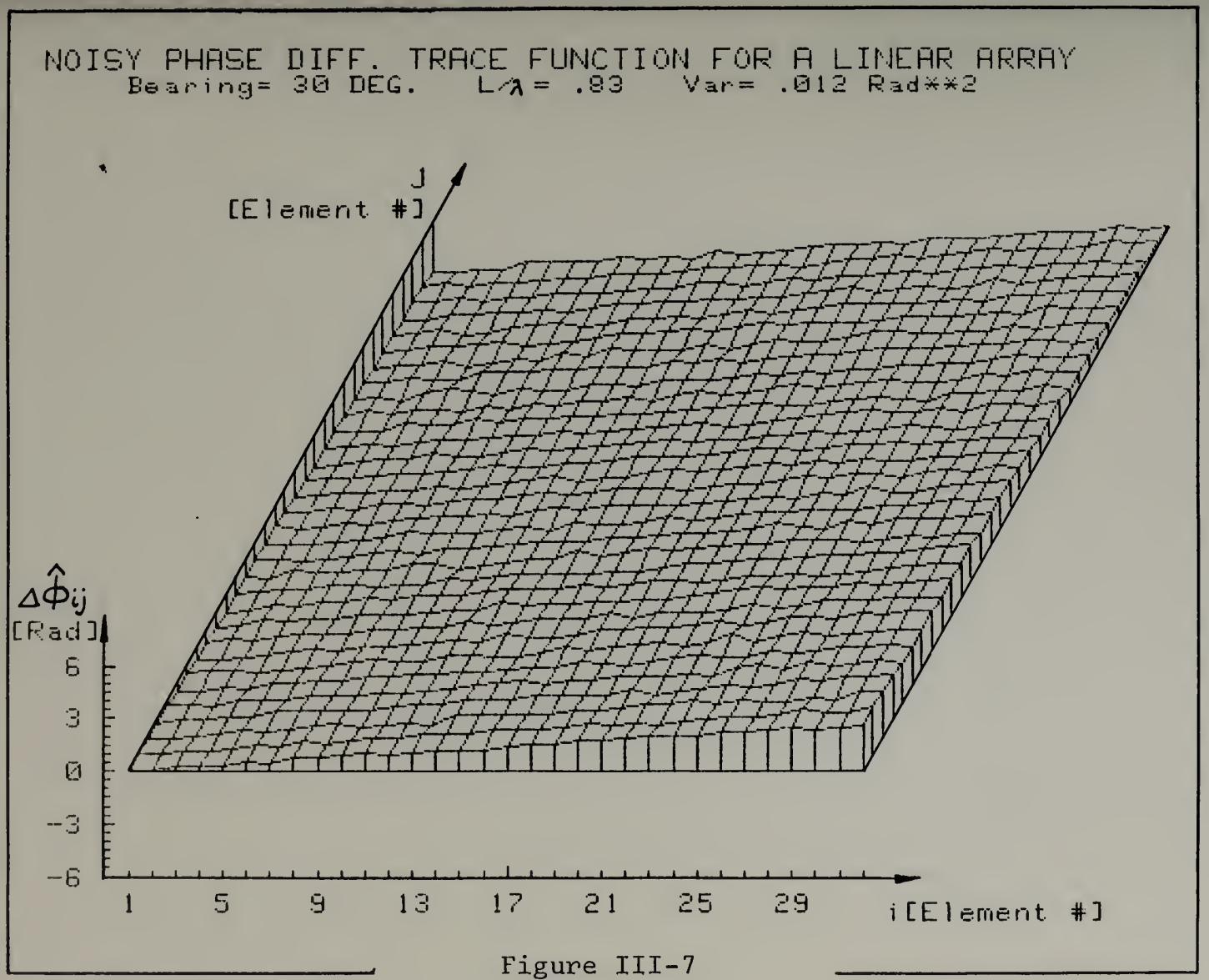
NOISY PHASE DIFF. TRACE FUNCTION FOR A LINEAR ARRAY
Bearing= 30 DEG. L/λ = .83 Var= .012 Rad**2
J
[Element #]
$\Delta\hat{\Phi}_{ij}$
[Rad]
6
3
0
-3
-6
1
5
9
13
17
21
25
29
i[Element #]

Figure III-7

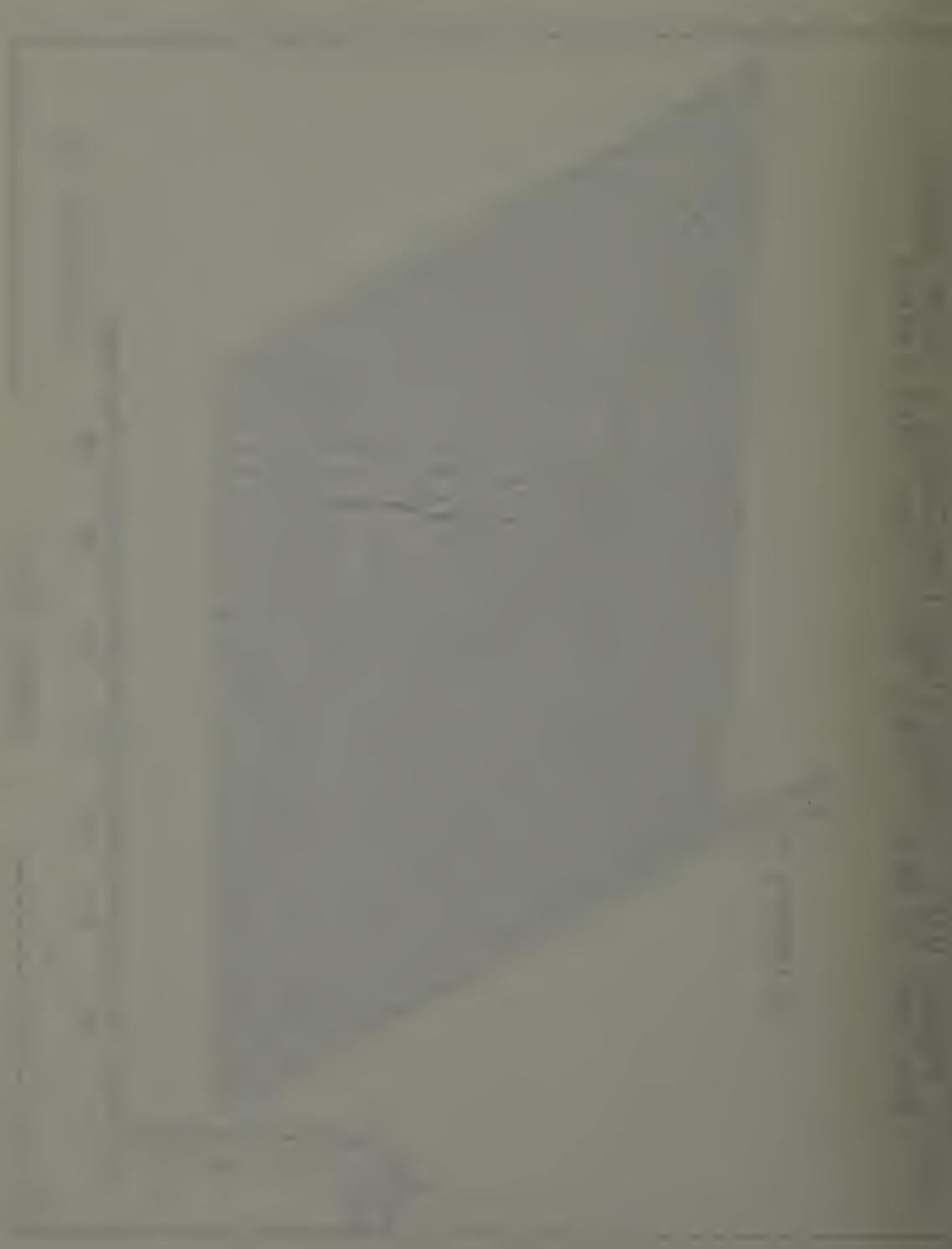

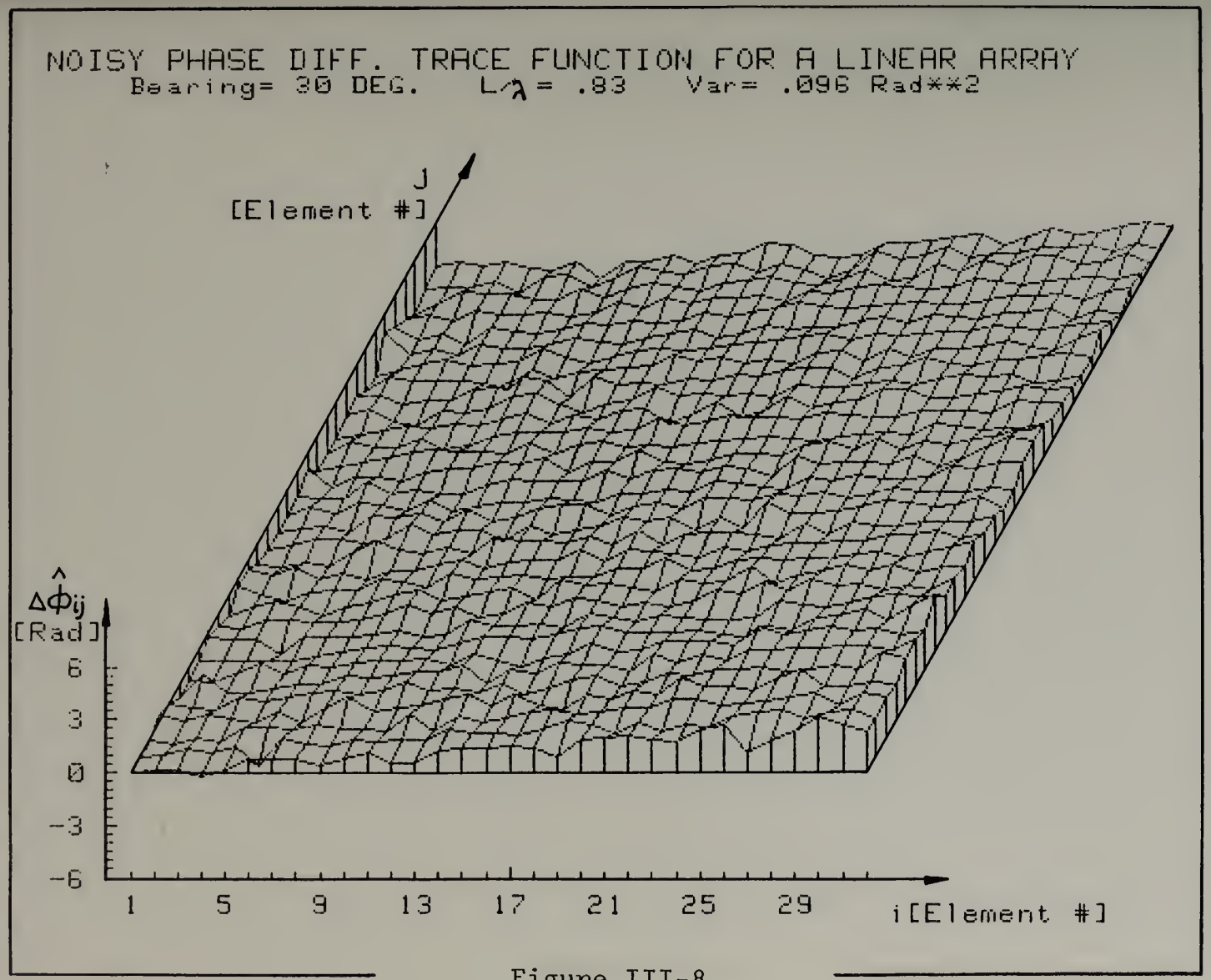
NOISY PHASE DIFF. TRACE FUNCTION FOR A LINEAR ARRAY
Bearing= 30 DEG. L/λ = .83 Var= .096 Rad**2
J
[Element #]
Δφ̂ij
[Rad]
6
3
0
-3
-6
1
5
9
13
17
21
25
29
i[Element #]

Figure III-8

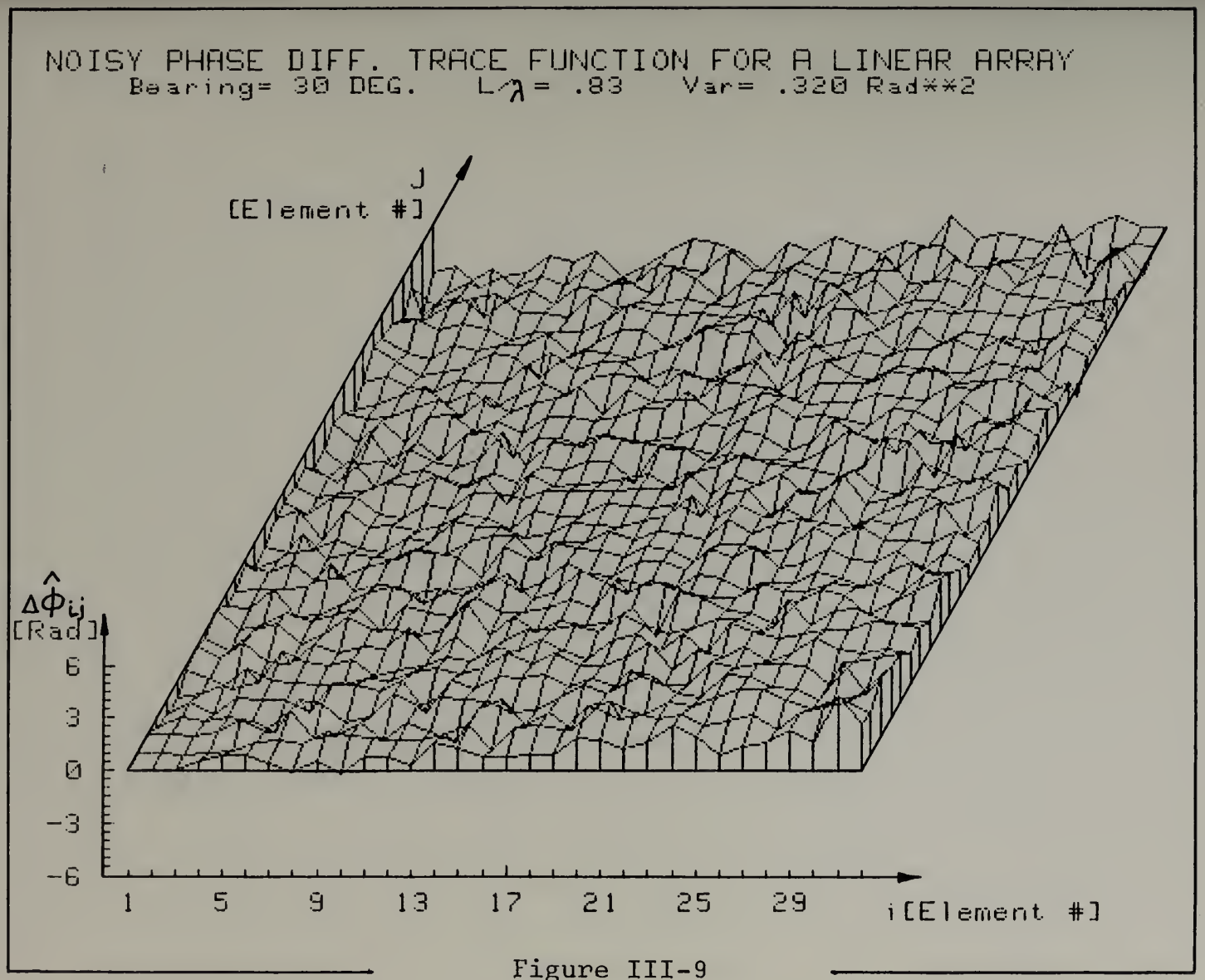
NOISY PHASE DIFF. TRACE FUNCTION FOR A LINEAR ARRAY
Bearing= 30 DEG. L/λ = .83 Var= .320 Rad**2
J
[Element #]
Δφ̂ij
[Rad]
6
3
0
-3
-6
1
5
9
13
17
21
25
29
i[Element #]

Figure III-9

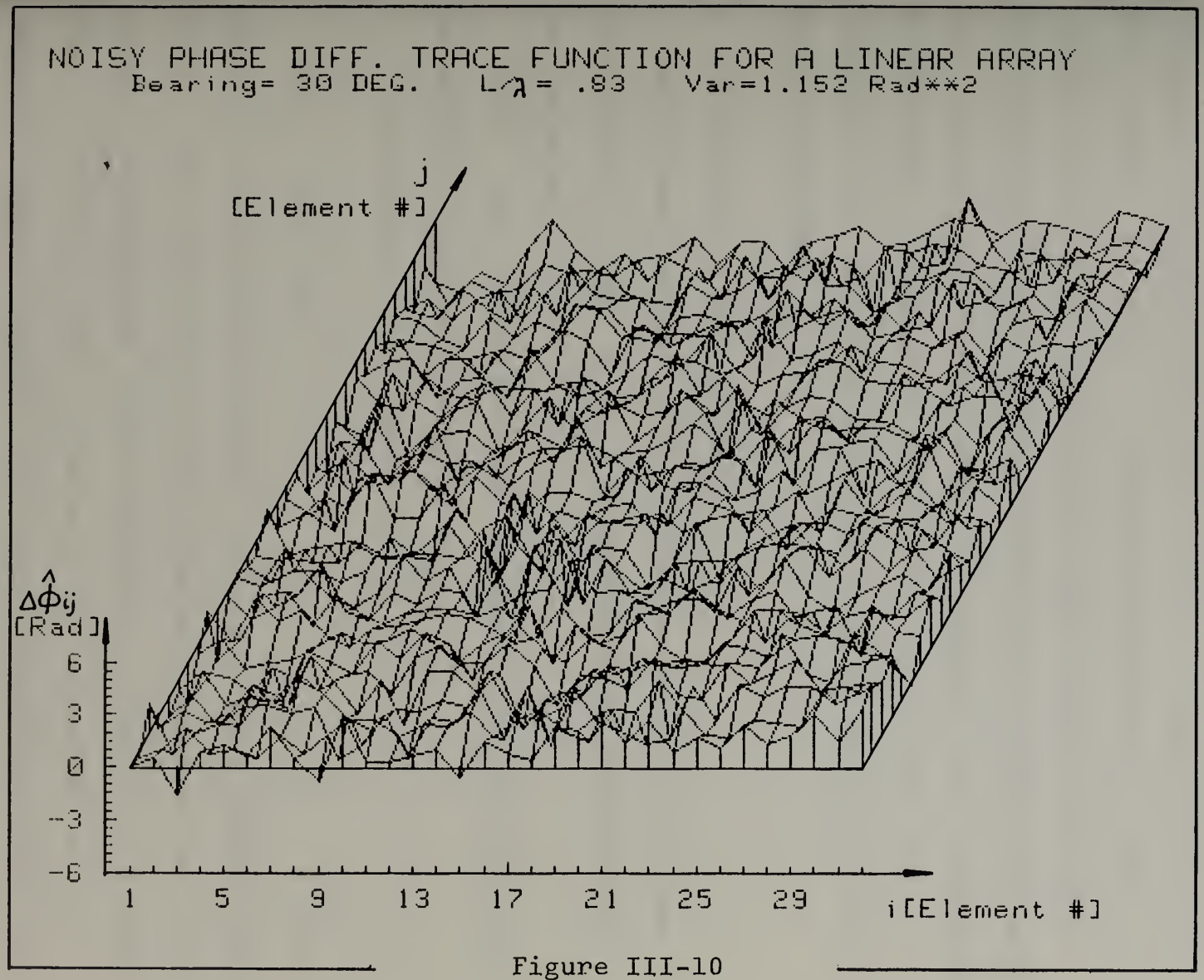


Figure III-10

show noisy trace functions one would get after the cross spectral estimation process. The above figures show trace functions for circular and linear arrays for various noise variance levels from .001 $Rad^2$ (St.dev. 1.86deg.) to 1.152 $Rad^2$ (St.dev. 61.5deg.). It can be seen that even for the highest noise level shown one can still visually perceive the form of the trace function while for a single data point this noise may be overwhelming. The cause of this perception is the visual integration over the surface of the trace function. The very same characteristic is used by an estimation processor.

## B. DERIVATION OF THE ESTIMATOR

As it was shown the phase difference/time delay trace function ($\Delta\phi_{ij,\theta}$ and $\Delta\tau_{ij,\theta}$) is dependent on indices "i,j" and parameter $\theta$.

NOTE: $\Delta\phi_{ij,\theta}$ will be used throughout the derivation but the analysis applies as well to $\Delta\tau_{ij,\theta}$.

The estimated trace function will be:

$$\hat{\Delta\phi}_{ij} = f_{Tr}(i,j,\theta) + v(i,j) \qquad \text{(III-1)}$$

where $f_{Tr}$ is the trace function and v(i,j) is a random estimation error which will be approximately gaussian for long enough averaging time in the estimation process. As it was shown in [26] the error variance is not dependent on the estimated value. However v(i,j) has a covariance matrix of order ($N^2 x N^2$) which is complicated and its knowledge is not

assumed in the forthcoming derivation. Its effect on the estimator however will be checked by simulation.

The general "weighted" least squared cost function is defined as:

$$J = \sum_{i=0}^{N-1} \sum_{j=0}^{N-1} W_{ij} \; (\Delta\hat{\phi}_{ij} - \Delta\phi_{ij,\theta})^2 \qquad \text{(III-2)}$$

The weights $W_{ij}$ can be used to account for different quality of the measurements $\Delta\hat{\phi}_{ij}$, and must have two main features:

$$W_{ij} = W_{ji}$$

$$W_{ij} = 0 \text{ for } i=j$$

Minimizing the cost function J with respect to $\theta$ will give:

$$0 = \frac{\partial J}{\partial \theta} = \sum_{i=0}^{N-1} \sum_{j=0}^{N-1} W_{ij} \; (\Delta\hat{\phi}_{ij} - \Delta\phi_{ij,\theta})(-2\frac{\partial \Delta\phi_{ij,\theta}}{\partial \theta}) \qquad \text{(III-3)}$$

This is as far as one can go without specifying the trace function explicitly.

To solve the minimization problem two approaches are possible:

- For "analytic" trace functions, to derive an explicit estimator.

- For "random" trace function to conduct an exhaustive or "educated" search (which is not efficient), or use some form of gradient search algorithm to achieve minimization.

In this dissertation the first approach will be followed due to the fact that the circular and linear arrays have "analytic" trace functions.

1. Circular Arrays

The trace function for circular array is (Eq. II-8):

$$\Delta\phi_{ij,\theta} = \frac{2\pi FD}{C} \sin\left[\frac{\pi}{N}(i+j)-\theta\right] \sin\left[\frac{\pi}{N}(i-j)\right]$$

$$= K \sin\left[\frac{\pi}{N}(i+j)-\theta\right] \sin\left[\frac{\pi}{N}(i-j)\right] \qquad \text{(III-4)}$$

where K is a constant for a given trace function. Inserting the above equation in (III-2) and (III-3) gives:

$$J = \sum_{i=0}^{N-1} \sum_{i=0}^{N-1} W_{ij} \{\Delta\hat{\phi}_{ij} - K \sin[\tfrac{\pi}{N}(i+j)-\theta] \sin[\tfrac{\pi}{N}(i-j)]\}^2 \qquad \text{(III-5)}$$

and

$$0 = \frac{\partial J}{\partial \theta} = 2K \sum_{i=0}^{N-1} \sum_{j=0}^{N-1} W_{ij} \{\Delta\hat{\phi}_{ij} - K \sin[\tfrac{\pi}{N}(i+j)-\theta] \sin[\tfrac{\pi}{N}(i-j)]\}$$

$$\times \sin[\tfrac{\pi}{N}(i-j)] \cos[\tfrac{\pi}{N}(i+j)-\theta] \qquad \text{(III-6)}$$

$$0 = 2K \sum_{i=0}^{N-1} \sum_{j=0}^{N-1} W_{ij}\Delta\hat{\phi}_{ij} \sin\left[\frac{\pi}{N}(i-j)\right]\cos\left[\frac{\pi}{N}(i+j) - \theta\right]$$

$$- KW_{ij}\sin\left[\frac{\pi}{N}(i+j)-\theta\right]\cos\left[\frac{\pi}{N}(i+j)-\theta\right]\sin^2\left[\frac{\pi}{N}(i-j)\right]$$

$$0 = \sum_{i=0}^{N-1} \sum_{j=0}^{N-1} W_{ij}\Delta\hat{\phi}_{ij}\left(\sin\frac{2\pi}{N}i - \sin\frac{2\pi}{N}j\right)\cos\theta$$

$$- \sum_{i=0}^{N-1} \sum_{j=0}^{N-1} W_{ij}\Delta\hat{\phi}_{ij}\left(\cos\frac{2\pi}{N}i - \cos\frac{2\pi}{N}j\right)\sin\theta$$

$$- \frac{K}{4} \sum_{i=0}^{N-1} \sum_{j=0}^{N-1} W_{ij}\left(\sin\frac{4\pi}{N}i + \sin\frac{4\pi}{N}j - 2\sin\frac{2\pi}{N}i \cos\frac{2\pi}{N}j\right.$$

$$\left. -2\cos\frac{2\pi}{N}i \sin\frac{2\pi}{N}j\right)\cos 2\theta$$

$$+ \frac{K}{4} \sum_{i=0}^{N-1} \sum_{j=0}^{N-1} W_{ij}\left(\cos\frac{4\pi}{N}i + \cos\frac{4\pi}{N}j - 2\cos\frac{2\pi}{N}i \cos\frac{2\pi}{N}j\right.$$

$$\left. +2\sin\frac{2\pi}{N}i \sin\frac{2\pi}{N}j\right)\sin 2\theta \qquad \text{(III-7)}$$

In general the last two terms of the equation are non-zero; however, for some important and practical choices of $W_{ij}$ they are zero.

Two cases for which the last two terms are zero are:

-for $W_{ij} = 1$ for all $i \neq j$

-for $W_{ij}$ being equal in groups such that each pair which has the same value for $\cos[\frac{2\pi}{N}(i-j)]$ will have the same $W_{ij}$.

The importance of the second case is due to the fact that pairs which are at equal distance in physical space will have the same weights.

For the cases when the last two terms of equation (III-7) are zero the estimator will have a particularly simple form:

$$\hat{\theta}_C = tg^{-1} \frac{\sum_{i=0}^{N-1} \sum_{j=0}^{N-1} W_{ij} \Delta\hat{\phi}_{ij} (\sin\frac{2\pi}{N} i - \sin\frac{2\pi}{N} j)}{\sum_{i=0}^{N-1} \sum_{j=0}^{N-1} W_{ij} \Delta\hat{\phi}_{ij} (\cos\frac{2\pi}{N} i - \cos\frac{2\pi}{N} j)} \qquad \text{(III-8)}$$

In the general case however, when the last two terms are not zero, the derivation is different. One can write the following equation from (III-7):

$$0 = K_1 \cos\theta - K_2 \sin\theta - K_3 \cos 2\theta + K_4 \sin 2\theta \qquad \text{(III-9)}$$

where $K_1$, $K_2$, $K_3$, $K_4$ are expressions which can be easily calculated for a given estimated trace function.

After some manipulations one obtains:

$$0 = K_1\sqrt{1+tg^2} - K_2 tg\theta \sqrt{1+tg^2\theta} - K_3(1-tg^2\theta) + 2K_4 tg\theta \qquad \text{(III-10)}$$

Which is an equation in one variable and can be written as:

$$0 = K_1\sqrt{1+x^2} - K_2 x\sqrt{1+x^2} - K_3(1-x^2) + 2K_4 x \qquad \text{(III-11)}$$

and

$$\hat{\theta}_C = tg^{-1}\, x \qquad \text{(III-12)}$$

The above equation can be solved by numerical methods. As mentioned before this procedure is required only if the weights are almost arbitrary.

An additional feature of the estimator in (III-8) is that it does not require the knowledge of the constant K, which contains the frequency F, diameter D and speed of sound C.

$$K = 2\pi FD/C$$

In fact it is important to realize that after estimating $\hat{\theta}$, K can be estimated and as a result the speed of sound C, can be calculated when the frequency F and the diameter D are known. This feature is important for some applications such as seismic signal processing where there exists the problem of dispersive propagation in which the speed of sound is varying with frequency. The estimation of K will be done as follows:

using the same cost function (Eq. III-5) but minimizing with respect to K when $\hat{\theta}$ is known:

$$\frac{\partial J}{\partial K} = -2 \sum_{i=0}^{N-1} \sum_{j=0}^{N-1} W_{ij} \{\Delta\hat{\phi}_{ij} - K \sin[\tfrac{\pi}{N}(i+j)-\hat{\theta}]\sin[\tfrac{\pi}{N}(i-j)]\}$$

$$\times \sin[\tfrac{\pi}{N}(i+j)-\hat{\theta}]\sin[\tfrac{\pi}{N}(i-j)] \qquad \text{(III-13)}$$

and the estimator is:

$$\hat{K} = \frac{\sum_{i=0}^{N-1} \sum_{j=0}^{N-1} W_{ij} \Delta\hat{\phi}_{ij} \sin[\tfrac{\pi}{N}(i+j)-\hat{\theta}] \sin[\tfrac{\pi}{N}(i-j)]}{\sum_{i=0}^{N-1} \sum_{j=0}^{N-1} W_{ij} \sin^2[\tfrac{\pi}{N}(i+j)-\hat{\theta}]\sin^2[\tfrac{\pi}{N}(i-j)]} \qquad \text{(III-14)}$$

knowing $\hat{K}$:

$$\hat{C} = \frac{2\pi FD}{\hat{K}} \qquad \text{(III-15)}$$

2. Linear Arrays

Following the same development as used for the circular array, the trace function is (Eq. II-10):

$$\Delta\phi_{ij,\theta} = \frac{2\pi FD}{C} (i-j) \sin\theta$$

$$= K_L(i-j)\sin\theta \qquad \text{(III-16)}$$

$$J = \sum_{i=0}^{N-1} \sum_{j=0}^{N-i} W_{ij} \left[\Delta\hat{\phi}_{ij} - K_L(i-j)\sin\theta\right]^2 \qquad \text{(III-17)}$$

and

$$0 = \frac{\partial J}{\partial \theta} = 2K_L \sum_{i=0}^{N-1} \sum_{j=0}^{N-1} W_{ij}\left[\Delta\hat{\phi}_{ij} - K_L(i-j)\sin\theta\right](i-j)\cos\theta \qquad \text{(III-18)}$$

and

$$\hat{\theta}_L = \sin^{-1} \frac{\sum_{i=0}^{N-1} \sum_{j=0}^{N-1} W_{ij}\Delta\hat{\phi}_{ij}(i-j)}{K_L \sum_{i=0}^{N-1} \sum_{j=0}^{N-1} W_{ij}(i-j)^2} \qquad \text{(III-19)}$$

3. The Degenerate Trace Function Estimator

The degenerate trace function for circular arrays is (Eq. II-13):

$$\Delta\phi'_{ij,\theta} = \frac{2\pi FD}{C} \cos\left(\frac{2\pi}{N}i - \theta\right) \qquad \text{(III-20)}$$

where it was assumed

$$j = (i + N/2) \bmod N \qquad \text{(III-21)}$$

Inserting this equation to the estimator (Eq. III-8) and assuming all $W_{ij}$ equal to unity:

$$\hat{\theta}_{C.D.} = tg^{-1} \frac{\sum_{i=0}^{N-1} \Delta\hat{\phi}_i \sin\frac{2\pi}{N}i}{\sum_{i=0}^{N-1} \Delta\hat{\phi}_i \cos\frac{2\pi}{N}i} \qquad \text{(III-22)}$$

which is the phase of the first harmonic of the discrete fourier transform of $\Delta\hat{\phi}_i$.

## C. CHAPTER SUMMARY

In this chapter the MMSE estimator of the bearing was developed for circular and linear arrays based on the trace function principle. Two general remarks should be mentioned:

1. The MMSE estimator is equivalent to the Maximum Likelihood estimator when the noise is gaussian and independent among the data points. This case can be considered the "best" case and it will be used to develop the Cramer-Rao Lower Bound for the estimator. This CRLB will serve as a benchmark to the performance of the estimator which was derived by simulations.

2. If all the data points in a trace function are estimated from the same time frame/s the two halves of the trace function are totally dependent, because $\Delta\hat{\phi}_{ij}=-\Delta\hat{\phi}_{ji}$ result from the same "measurement". In addition the terms $\Delta\hat{\phi}_{ii}$ are not contributing to the bearing estimation process.

As a result of these the number of contributing terms in the trace function data matrix is:

$$(N^2 - N)/2.$$

The summation limits in the estimators must be changed accordingly:

Equation (III-8) becomes:

$$\hat{\theta}_C = tg^{-1} \frac{\sum_{i=0}^{N-2} \sum_{j=i+1}^{N-1} W_{ij} \Delta\hat{\phi}_{ij} (\sin\frac{2\pi}{N} i - \sin\frac{2\pi}{N} j)}{\sum_{i=0}^{N-2} \sum_{j=i+1}^{N-1} W_{ij} \Delta\hat{\phi}_{ij} (\sin\frac{2\pi}{N} i - \sin\frac{2\pi}{N} j)} \qquad \text{(III-23)}$$

Equation (III-19) becomes

$$\hat{\theta}_L = \sin^{-1} \frac{\sum_{i=0}^{N-2} \sum_{j=i+1}^{N-1} W_{ij} \Delta\hat{\phi}_{ij} (i-j)}{\sum_{i=0}^{N-2} \sum_{j=i+1}^{N-1} W_{ij} \quad (i-j)^2} \qquad \text{(III-24)}$$

Equation (III-22) becomes

$$\hat{\theta}_{C.D.} = tg^{-1} \frac{\sum_{i=0}^{N/2-1} \Delta\hat{\phi}_i \sin\frac{2\pi}{N} i}{\sum_{i=0}^{N/2-1} \Delta\hat{\phi}_i \cos\frac{2\pi}{N} i} \qquad \text{(III-25)}$$

However, if the measurements for $\Delta\phi_{ij}$ an $\Delta\phi_{ji}$ are done from independent data blocks the equations should remain in the original form.

The exact structure of the weights $W_{ij}$ was not treated here and it will not be pursued in this work, however, it should be emphasized that this is a subject for future work. Especially it is recommended to check the derivation of the weights with respect to their connection to the coherence of the two channels participating in each pair.

In the next chapter the performance of the estimators which have been derived in this chapter will be checked by simulation to demonstrate the effect of changes in various significant parameters on the estimator performance.

# IV. ESTIMATOR PERFORMANCE

## A. INTRODUCTION

In the previous chapter bearing estimators for circular and linear arrays were developed using trace function principles.

In this chapter the performance of the estimators will be checked by simulations. The two main measures of performance are:

- Bias
- "Beamwidth" which here is defined as twice the standard deviation of the bearing estimate ($2\sigma$)

In addition to the above a phenomenon called threshold effect was observed which is expected to be present in most nonlinear phase estimating processors [38, p. 287]. This threshold was also checked for various parameters, and it was defined arbitrarily as the input phase difference variance level for which the output "beamwidth" is less than five degrees.

The input to the estimator was the "estimated" phase difference trace function (Eq. III-1):

$$\Delta\hat{\phi}_{ij} = f_{Tr}(i,j,\theta) + v(i,j) \qquad \text{(IV-1)}$$

Two noise models were used for v(i,j):

- independent gaussian noise from pair to pair
- correlated gaussian noise from pair to pair

The model of the correlated noise is defined in Appendix C along with the simulation method and computer program. The intent of including the correlated noise was to give a feeling about its effects on the performance and not so much on its accurate modeling.

The simulation runs were performed mainly for circular arrays, however some performance measures were checked for linear arrays as well as for comparison purposes.

For each parameter change 48 computer runs were done in order to get reasonable statistics. The mean and the variance of the results of the 48 runs were calculated and they served as the estimated bearing and bearing variance.

## B. CRAMER-RAO LOWER BOUND FOR THE IDEALIZED ESTIMATOR

As a benchmark for the performance of the estimators the Cramer-Rao Lower Bound (CRLB) was used. It was calculated for the maximum likelihood estimator which is equivalent to the MMSE estimator for uncorrelated gaussian noise [23, p. 198]. This case can be considered as "best case" and it can be used as a lower bound for any realizable estimator. The CRLB for a maximum likelihood estimation of a parameter "$\alpha$" is (38, p. 275, 41, p. 335).

$$\sigma_{\hat{\alpha}}^2 \geq \frac{No}{2 \int_o^T \left[\frac{\partial s(t,\alpha)}{\partial \alpha}\right]^2 dt} \qquad \text{(IV-2)}$$

where No - the input noise level (variance)

$s(t,\alpha)$ - the "clean" signal

$\alpha$ - the parameter to be estimated

Adaptation of the above to the present case will be:

- No = $\sigma^2_{\Delta\hat{\phi}_{ij}}$ - variance of the estimated phase difference

- $S(t,\alpha)$ is the discrete trace function $f_{Tr}(i,j,\theta)$

- The integration becomes double summation

and for a circular array:

$$\sigma^2_{\hat{\theta}_C} \geq \frac{\sigma^2_{\Delta\hat{\phi}_{ij}}}{2\sum_{i=0}^{N-2}\sum_{J=i+1}^{N-1}\left\{\frac{\partial}{\partial\theta}\left\{K\sin\left[\frac{\pi}{N}(i+j)-\theta\right]\sin\left[\frac{\pi}{N}(i-j)\right]\right\}\right\}^2}$$

$$= \frac{\sigma^2_{\Delta\hat{\phi}_{ij}}}{2K^2\sum_{i=0}^{N-2}\sum_{j-i+1}^{N-1}\cos^2\left[\frac{\pi}{N}(i+j)-\theta\right]\sin^2\left[\frac{\pi}{N}(i+j)\right]} \qquad \text{(IV-3)}$$

for a linear array:

$$\sigma^2_{\hat{\theta}_L} \geq \frac{\sigma^2_{\Delta\hat{\phi}_{ij}}}{2\sum_{i=0}^{N-2}\sum_{j=i+1}^{N-1}\left\{\frac{\partial}{\partial\theta}\left[K_L\sin\theta(i-j)\right]\right\}^2}$$

$$= \frac{\sigma^2_{\Delta\hat{\phi}_{ij}}}{2K_L\cos^2\theta\sum_{i=0}^{N-2}\sum_{j=i+1}^{N-1}(i-j)^2} \qquad \text{(IV-4)}$$

The above bounds were plotted along with the simulation results for comparison purposes and, as it will be shown the simulation results achieve this bound asymptotically.

C. BIAS

1. Circular Array

For this performance test the simulation was run for 4, 8 and 16 element 5 meter diameter circular arrays at 100 Hz and target bearing $30^{\circ}$. For each element number change, the input phase difference variance was changed between $4.35 Rad^2$ ($120^{\circ}$St.Dev.) down to $6x10^{-5}$ $Rad^2$ ($.45^{\circ}$St.Dev.) in 25 steps. The bias was calculated for each run by the equation:

$$\hat{B} = \hat{\theta} - \theta$$

where $\hat{B}$ - bias

$\hat{\theta}$ - estimated bearing

$\theta$ - real bearing $= 30^{\circ}$

The results are plotted in Figure IV-1.

The "lock-on" range was marked on the plots and although the bias was not the criterion for the "lock-on" range definition, it is clearly shown that the bias fluctuation becomes very small within the "lock-on" range.

Observations:

a. Within the "lock-on" range the bias is very small and is bipolar, a fact which suggests that the apparent bias is due to an insufficient number of runs for ensemble averaging

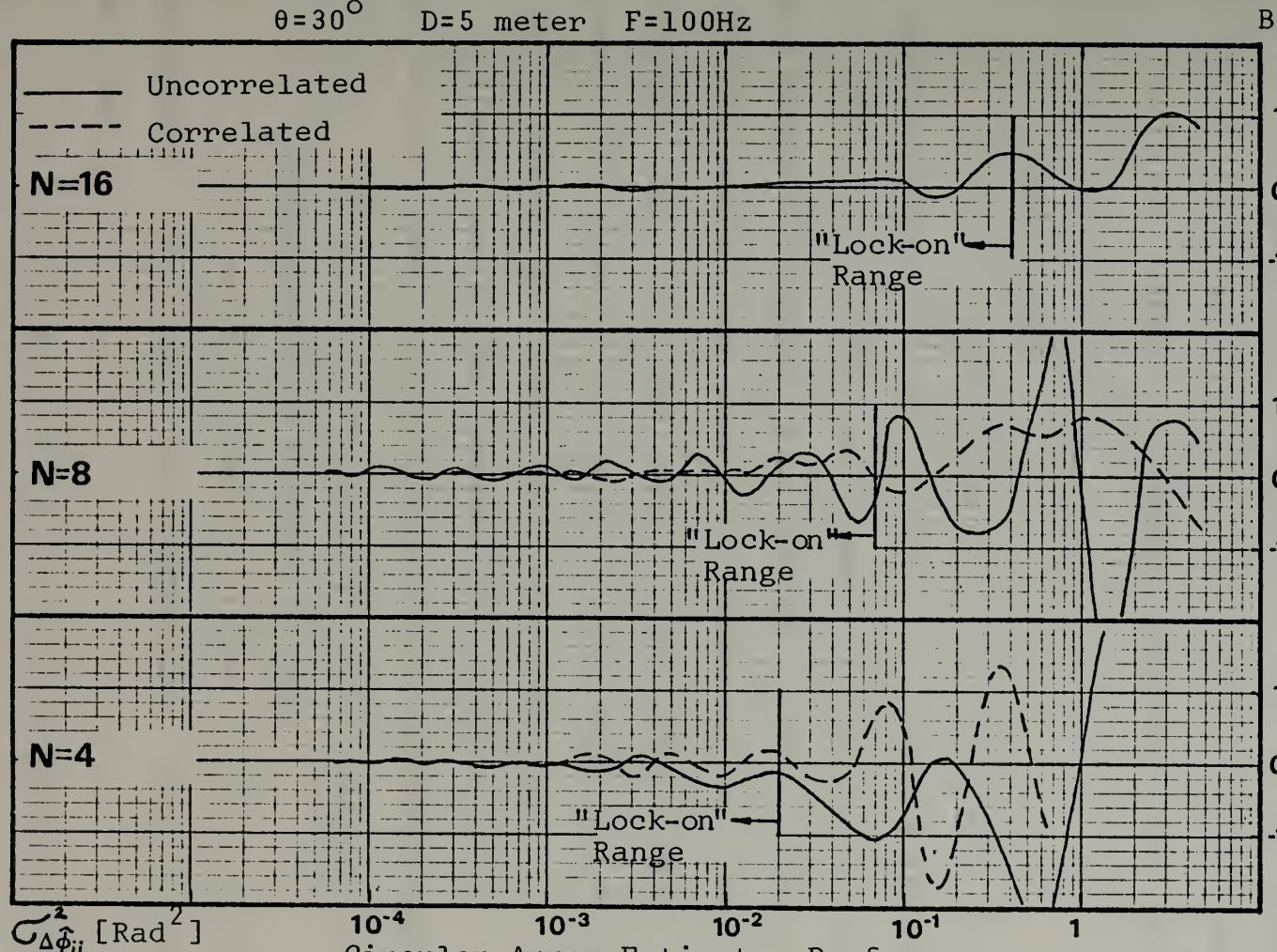


Circular Array-Estimator Performance
Bias vs input variance for various number of elements

Figure IV-1

and that the estimator itself is really unbiased.

b. Even if "a" is not true the estimator is at least asymptotically unbiased.

c. The correlated measurement noise has no apparent effect on the bias compared to the uncorrelated noise.

d. As the number of elements increases the fluctuations in the bias are smaller.

2. Linear Array

For this performance test the simulation was run for a linear array of 8 elements with 1.91 meter element-spacing at 100Hz (taking a 5 meter diameter circular array with the same number of elements and opening it up). However, this time the bearing was varied as a parameter because unlike the circular array the linear array is not symmetric in the x-y plane. The range of the input was the same as for circular array. Figure IV-2 shows the resultant plots.

In addition to the observations of the circular array, it can be seen that the bias fluctuations increase toward end-fire but even at those bearings the bias is asymptotically zero.

3. Conclusions With Respect To Bias

a. It can be assumed that the MMSE estimators developed in this work are unbiased or at least asymptotically unbiased.

b. The lock-on range is a good measure for the region where the bias fluctuations settle down.

c. Increasing the number of elements reduces the bias fluctuations.

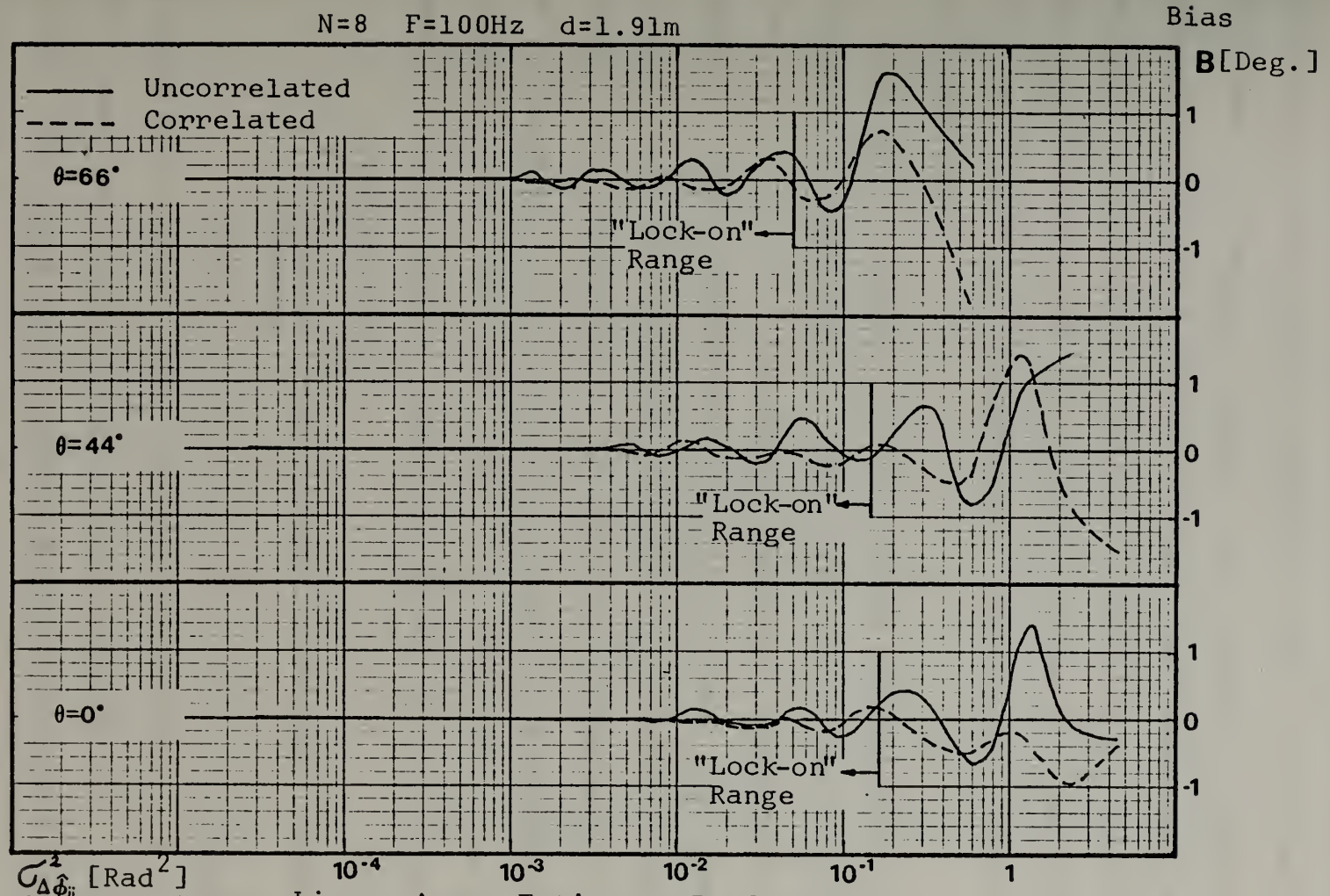


Linear Array-Estimator Performance
Bias vs input variance for various look directions

Figure IV-2

D. BEAMWIDTH

The beamwidth, which was defined as twice the standard deviation of the bearing estimates ($2\sigma_{\hat{\theta}}$), is by far the most important performance measure. As a result it was most extensively checked both by varying the various parameters which effect the performance and comparing to the CRLB. In this section most of the simulation runs were performed for both correlated and uncorrelated "measurement" noise along with the CRLB.

The model used for the correlated measurement noise is presented in Appendix C. This case of correlated noise is the actual one when the phase difference estimation for all pairs is done simultaneously (from the same time frame). However, if the estimation will be done from different time frames for various groups of pairs the measurement noise can be accounted as uncorrelated and then the uncorrelated measurement noise case will apply. The effects on the performance of both cases is shown throughout this section.

1. Circular Arrays

a. Beamwidth Versus Phase Difference Estimation Noise Variance

Figures IV-3 through IV-6 show the results of the simulation runs for this performance measure for 4, 8, 12 and 16 element circular arrays of equal diameter of 5 meters at 100Hz. For the 4 and 8 element arrays both correlated and uncorrelated measurement noise is given. For all the plots the CRLB is shown along with the simulation results as a benchmark to performance.

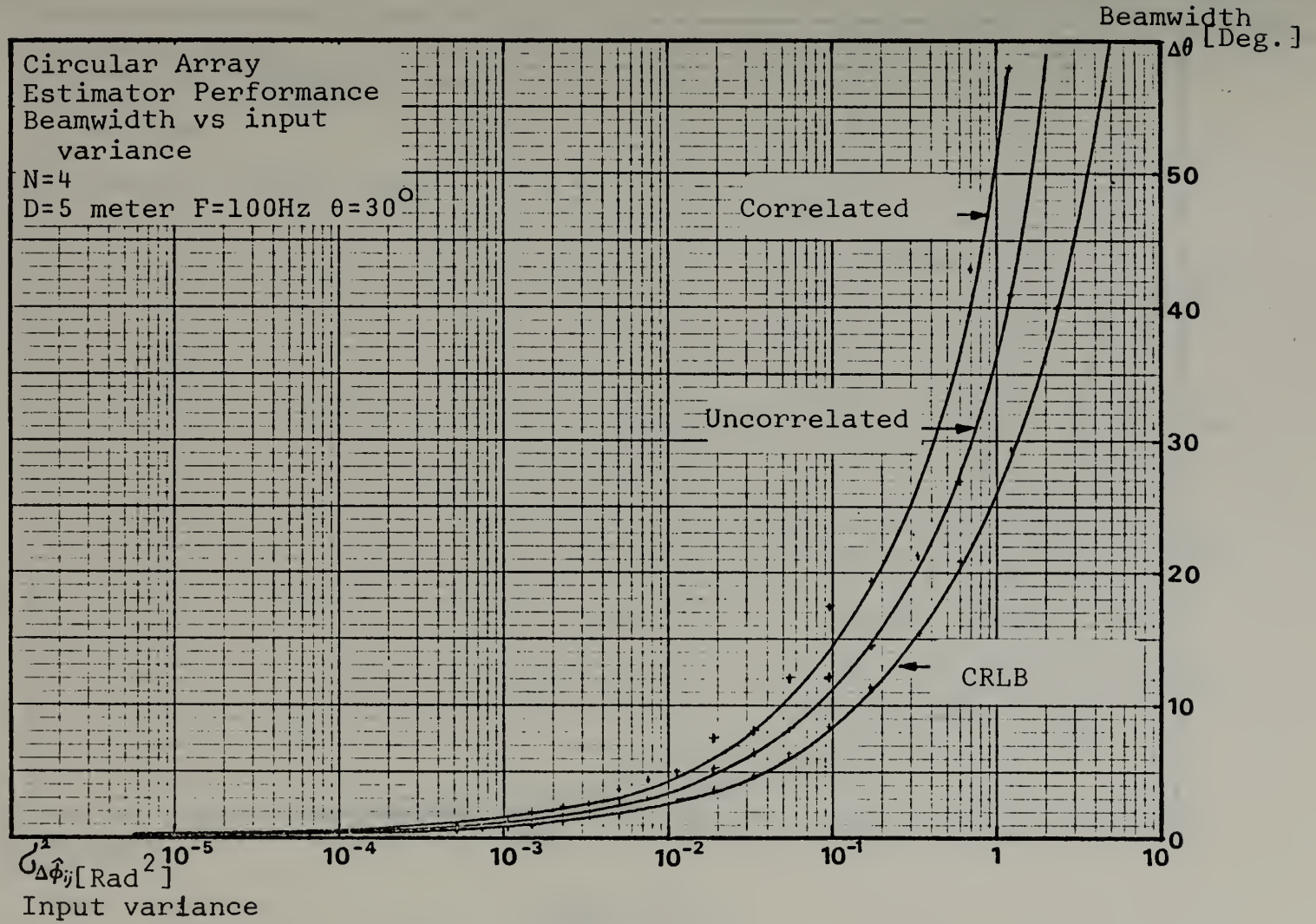
Circular Array
Estimator Performance
Beamwidth vs input
variance
N=4
D=5 meter F=100Hz θ=30°
Correlated
Uncorrelated
CRLB
Beamwidth
Δθ [Deg.]
50
40
30
20
10
0
10^-5
10^-4
10^-3
10^-2
10^-1
1
10
σ²Δφ̂ij[Rad²]
Input variance

Figure IV-3

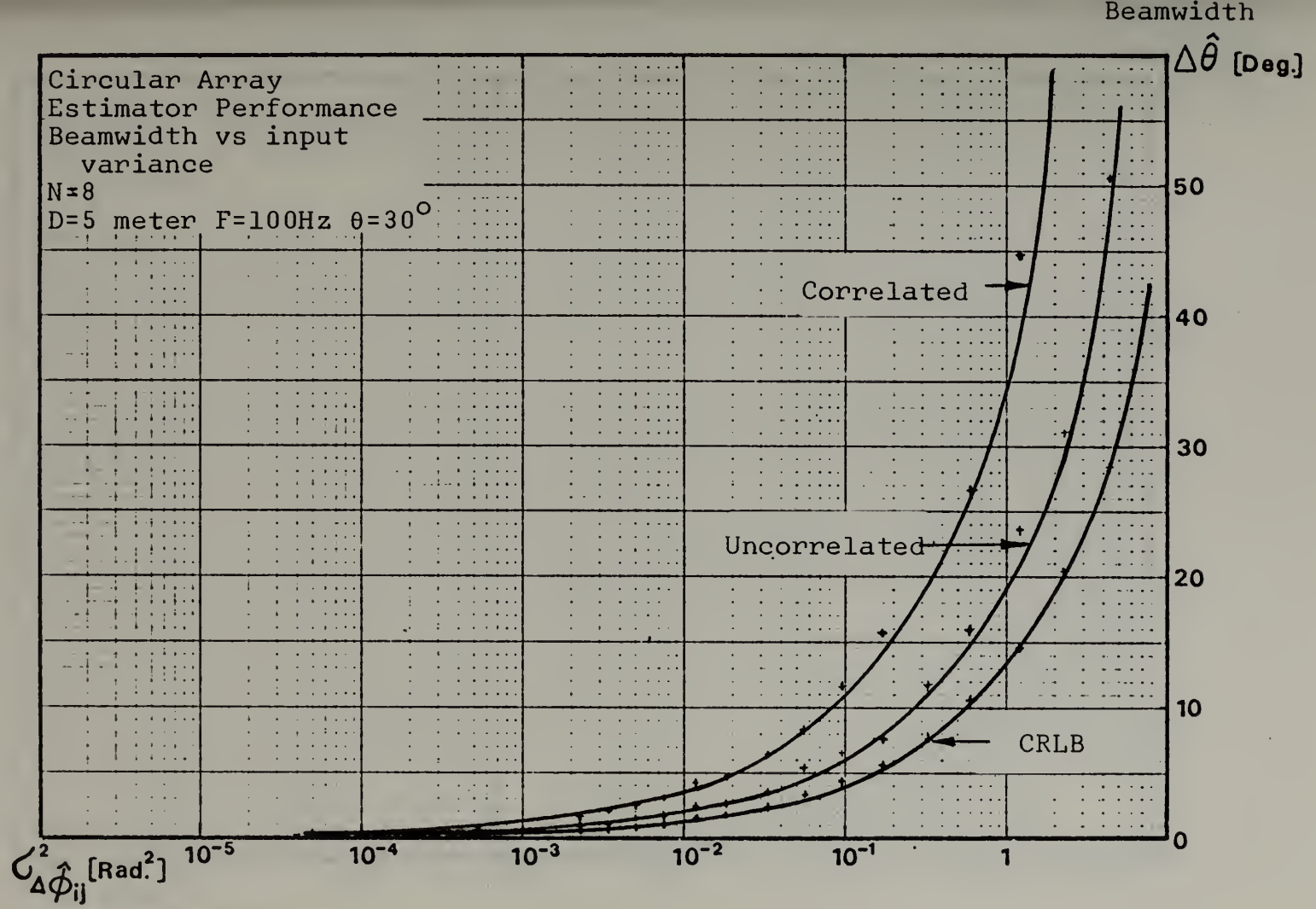


Input variance

Figure IV-4

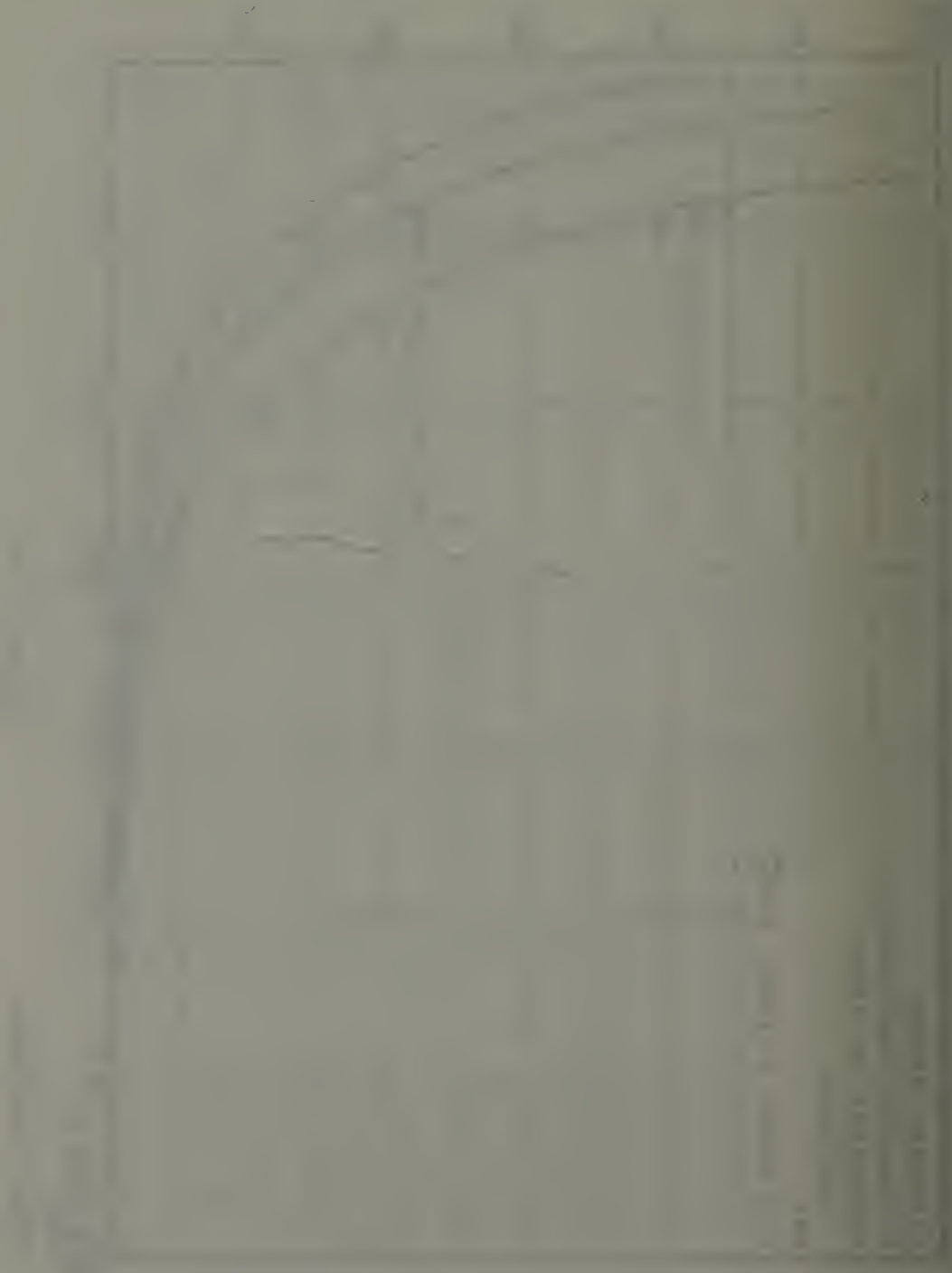

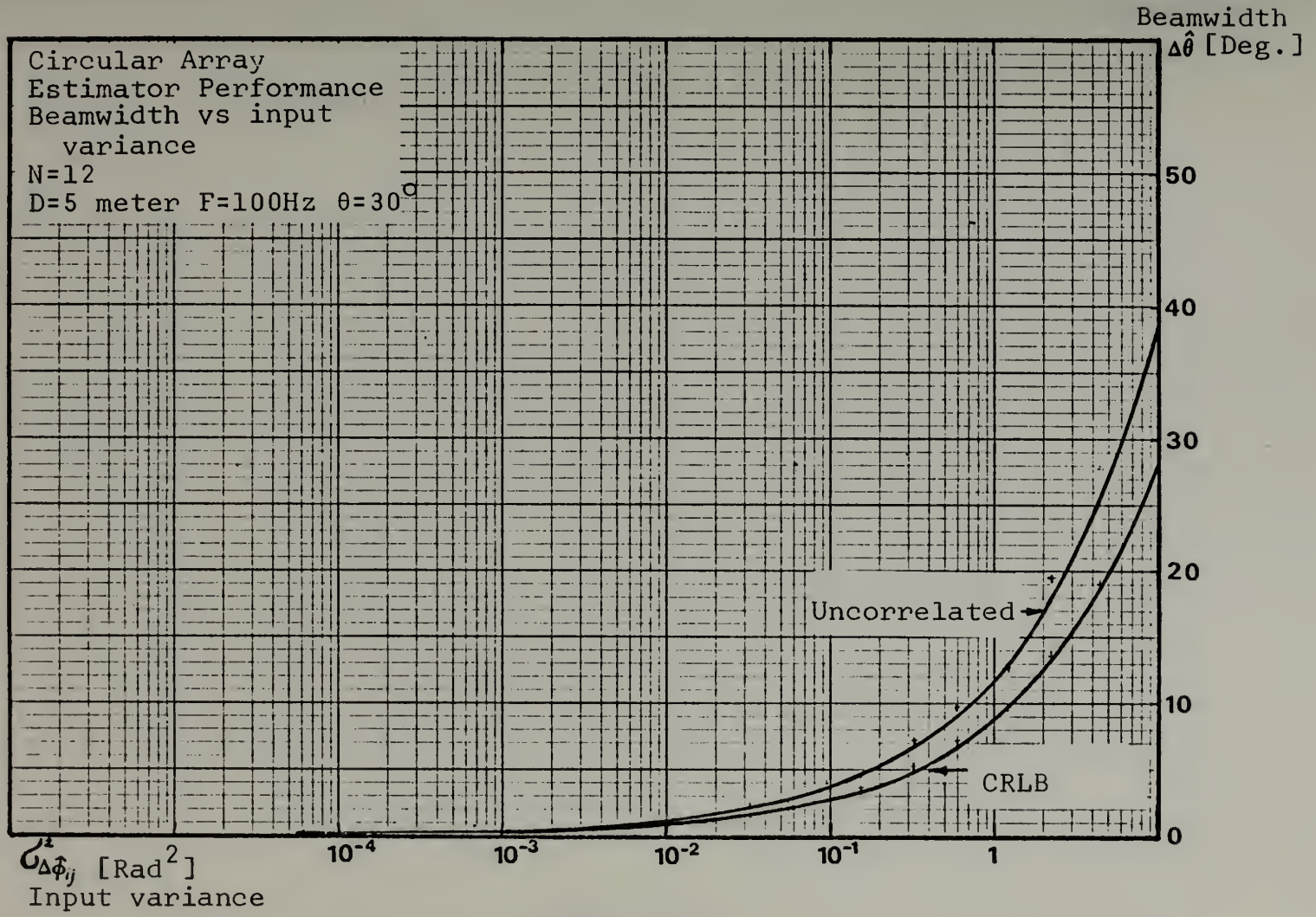
Circular Array
Estimator Performance
Beamwidth vs input
variance
N=12
D=5 meter F=100Hz θ=30°
Beamwidth
$\Delta\hat{\theta}$ [Deg.]
50
40
30
20
10
0
Uncorrelated
CRLB
$10^{-4}$
$10^{-3}$
$10^{-2}$
$10^{-1}$
1
$\sigma^2_{\Delta\hat{\phi}_{ij}}$ [Rad$^2$]
Input variance

Figure IV-5

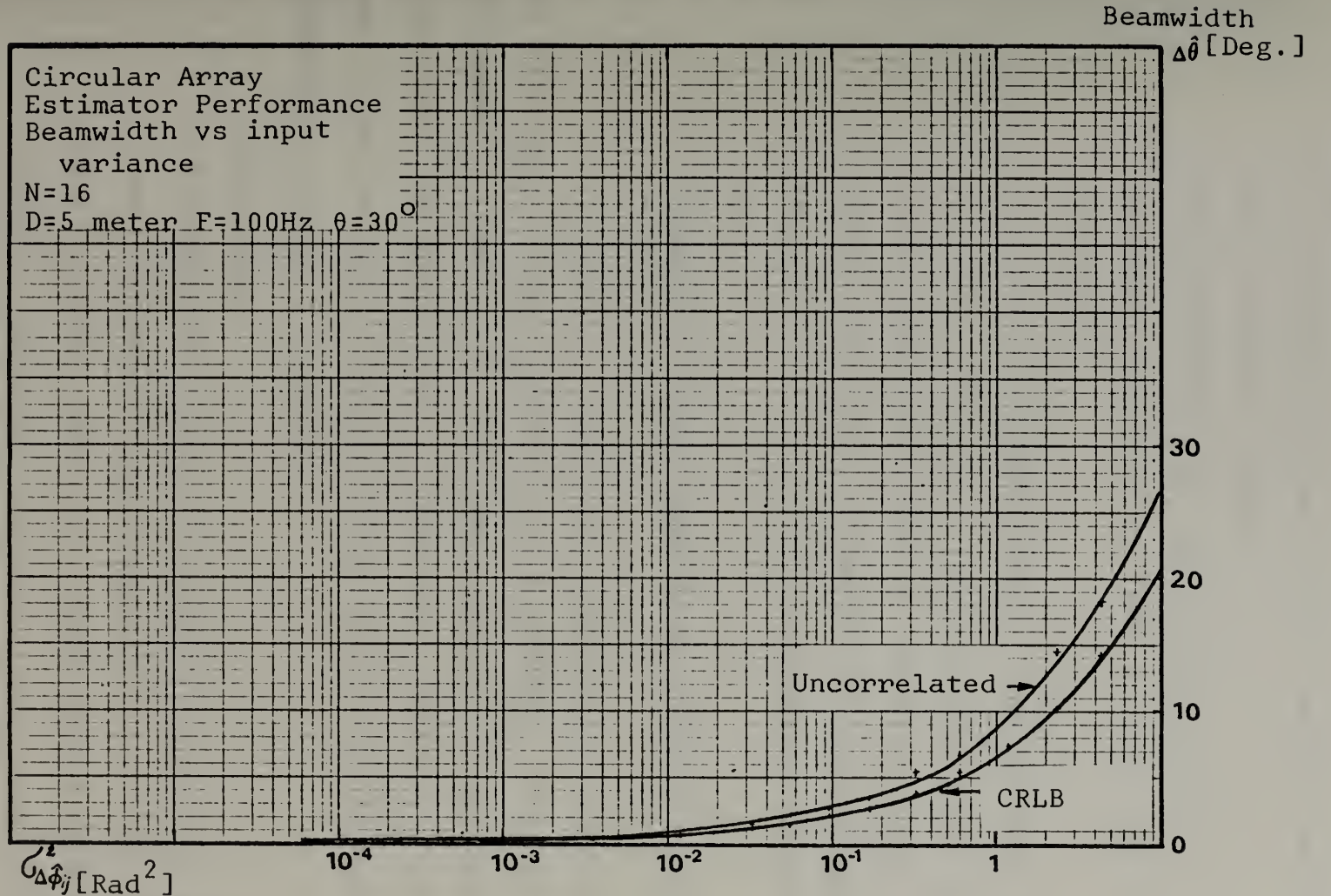
Beamwidth
$\Delta\hat{\theta}$ [Deg.]
Circular Array
Estimator Performance
Beamwidth vs input
variance
N=16
D=5 meter F=100Hz θ=30°
30
20
10
0
Uncorrelated
CRLB
$10^{-4}$
$10^{-3}$
$10^{-2}$
$10^{-1}$
1
$\sigma^2_{\Delta\hat{\phi}_{ij}}$ [Rad$^2$]
Input variance

Figure IV-6

Observations:

- In all plots the results and the CRLB exhibit a clear threshold effect.
- The correlated noise assumption (which is the realistic one) does not have a major effect on the performance.
- Under both correlated and the uncorrelated measurement noise assumption the estimator achieves asymptotically the CRLB at low level input noise variance, thus the estimator is asymptotically efficient [38, p. 276] for decreasing input noise level.

b. Beamwidth Versus Numbers Of Elements At Constant Diameter

Figure IV-7 shows the dependence of the beamwidth on the number of the elements for a circular array of 5 meter diameter at 100Hz. The plots were done for three representative input variance levels. Only the uncorrelated measurements along with the CRLB are shown which are adequate to represent the basic behavior.

Observations:

- A saturation effect is clear for all three variance levels shown; at each noise level at a given diameter and frequency there is a limit on the number of elements required, increasing the number of elements above this "saturation number" will improve performance only marginally. For example for the lowest curves ($\sigma_{\Delta\hat{\phi}_{ij}} = 2.25 \times 10^{-3}$ Rad$^2$) this number is

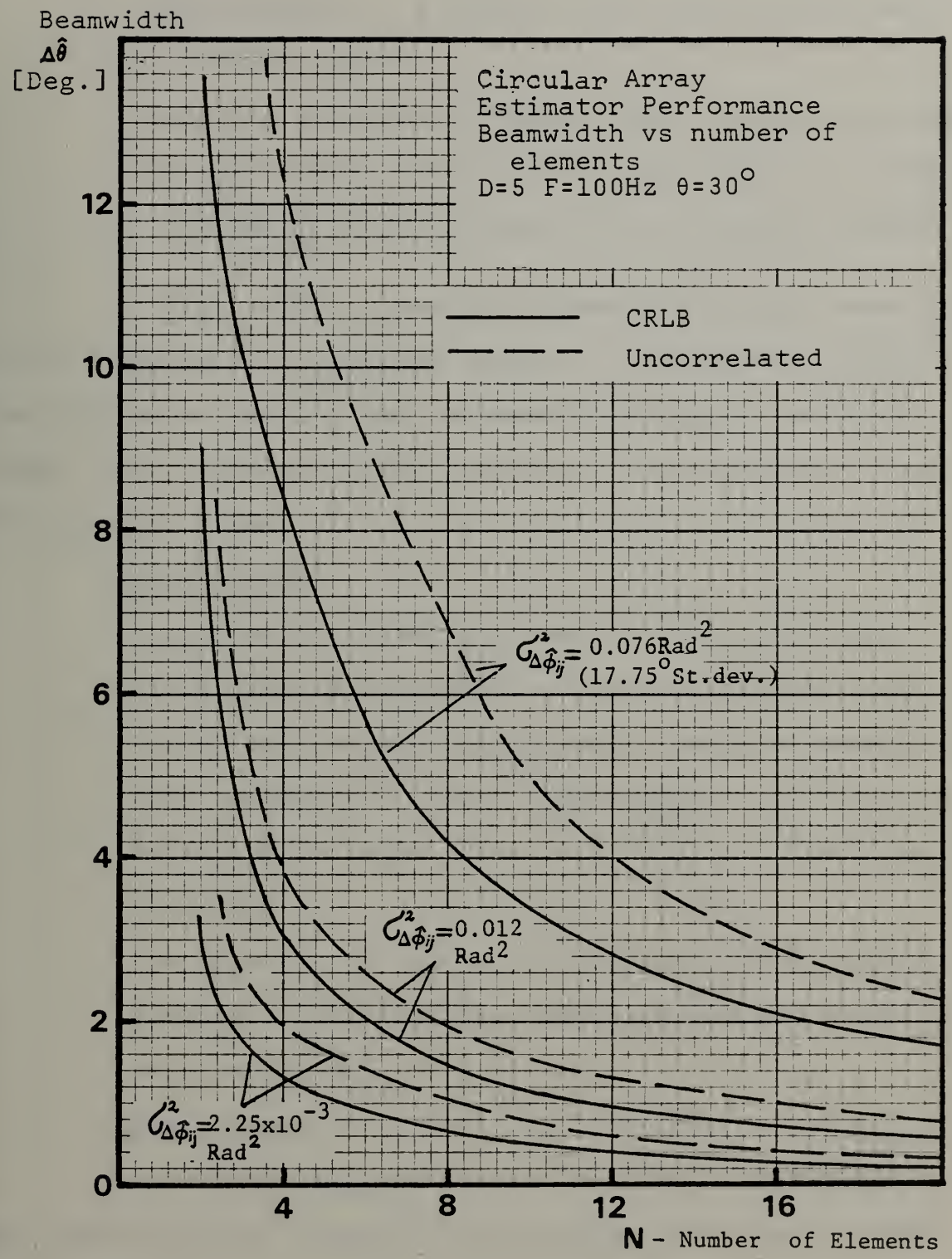
Beamwidth
$\Delta\hat{\theta}$
[Deg.]
Circular Array
Estimator Performance
Beamwidth vs number of
elements
D=5 F=100Hz θ=30°
CRLB
Uncorrelated
$\sigma^2_{\Delta\hat{\phi}_{ij}}$= 0.076Rad$^2$
(17.75° St.dev.)
$\sigma^2_{\Delta\hat{\phi}_{ij}}$=0.012
Rad$^2$
$\sigma^2_{\Delta\hat{\phi}_{ij}}$=2.25x10$^{-3}$
Rad$^2$
0
2
4
6
8
10
12
4
8
12
16
N - Number of Elements

Figure IV-7

approximately 16 elements, for higher noise levels it will be higher.

- Again the simulated estimator performance approaches the CRLB asymptotically for large number of elements.

c. Beamwidth Versus Diameter For A Constant Number Of Elements

Figure IV-8 shows the dependence of the beamwidth on the diameter of a circular array of 8 elements at 100Hz. The plots were done for two representative input variance levels. The correlated and uncorrelated measurements along with CRLB are shown.

Observations:

- A saturation effect is clear in this case too; increasing the diameter of the array above certain limits will improve performance (smaller beamwidth) only marginally. This limit appears to be approximately at 15 meter diameter which is one wavelength at 100Hz.
- The behavior of the simulation resultant curves is similar to the CRLB and they approach the CRLB asymptotically.

2. Linear Arrays

The analysis of performance for the linear array is much less extensive than for the circular array and its aim is two fold:

- It is the most standard geometrical configuration treated in literature and a reader of this work can readily compare it with other results.

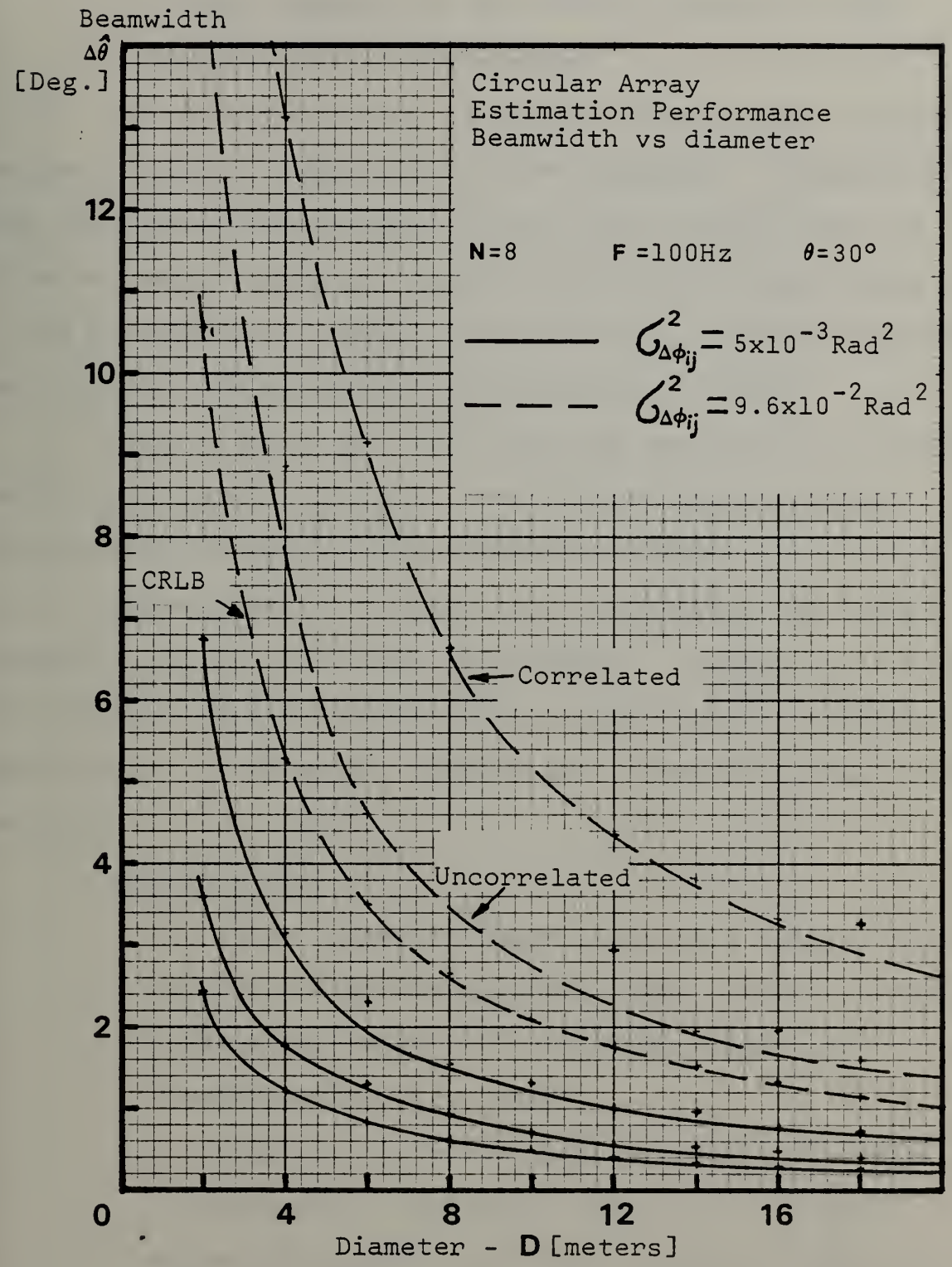
Beamwidth
$\Delta\hat{\theta}$
[Deg.]
Circular Array
Estimation Performance
Beamwidth vs diameter
N=8
F =100Hz
$\theta$=30°
$\sigma^2_{\Delta\phi_{ij}} = 5\times10^{-3}\,Rad^2$
$\sigma^2_{\Delta\phi_{ij}} = 9.6\times10^{-2}\,Rad^2$
CRLB
Correlated
Uncorrelated
12
10
8
6
4
2
0
4
8
12
16
Diameter - D [meters]

Figure IV-8

- It was compared to the circular array in some aspects of its performance.

In this section only beamwidth versus phase difference estimation noise variance plots are presented. Figures IV-9 and IV-10 show the resultant curves for a linear array of 5 meter length (same aperture as the circular array) with 4 and 8 elements at 100Hz. The plots are for both correlated and uncorrelated measurements along with the CRLB.

Figure IV-11 and IV-12 show the results for a linear array of 8 elements and 1.91 meter interelement spacing. This configuration is equivalent to an "opened up" version of a 5 meter diameter circular array preserving the inter-element distance and number of elements. Figures IV-11 and IV-12 differ in the look direction which causes a different performance, as expected, because the asymmetry of the linear array in the x-y plane.

Observations:

- The linear array estimates present a similar behavior as the circular array with respect to their performance relative to the CRLB - they are asymptotically efficient.
- A linear array with the same aperture and number of elements as a circular array has a slightly worse performance, the reason being the trend to concentration of elements at the ends for the circular array, a characteristic which improves bearing estimation.

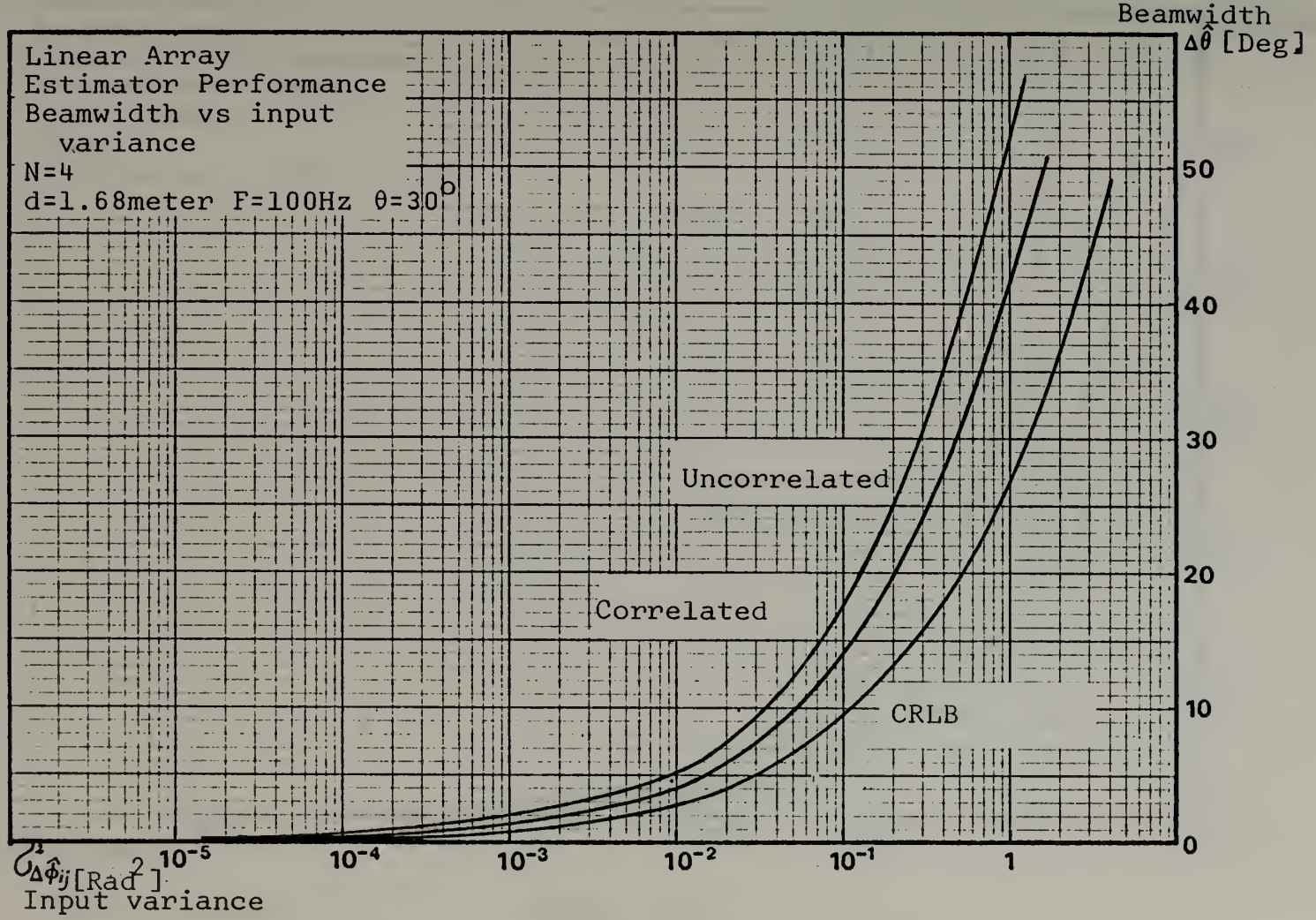
Linear Array
Estimator Performance
Beamwidth vs input
variance
N=4
d=1.68meter F=100Hz θ=30°
Beamwidth
Δθ̂ [Deg]
50
40
30
20
10
0
Uncorrelated
Correlated
CRLB
10⁻⁵
10⁻⁴
10⁻³
10⁻²
10⁻¹
1
σ²Δφ̂ij [Rad²]
Input variance

Figure IV-9

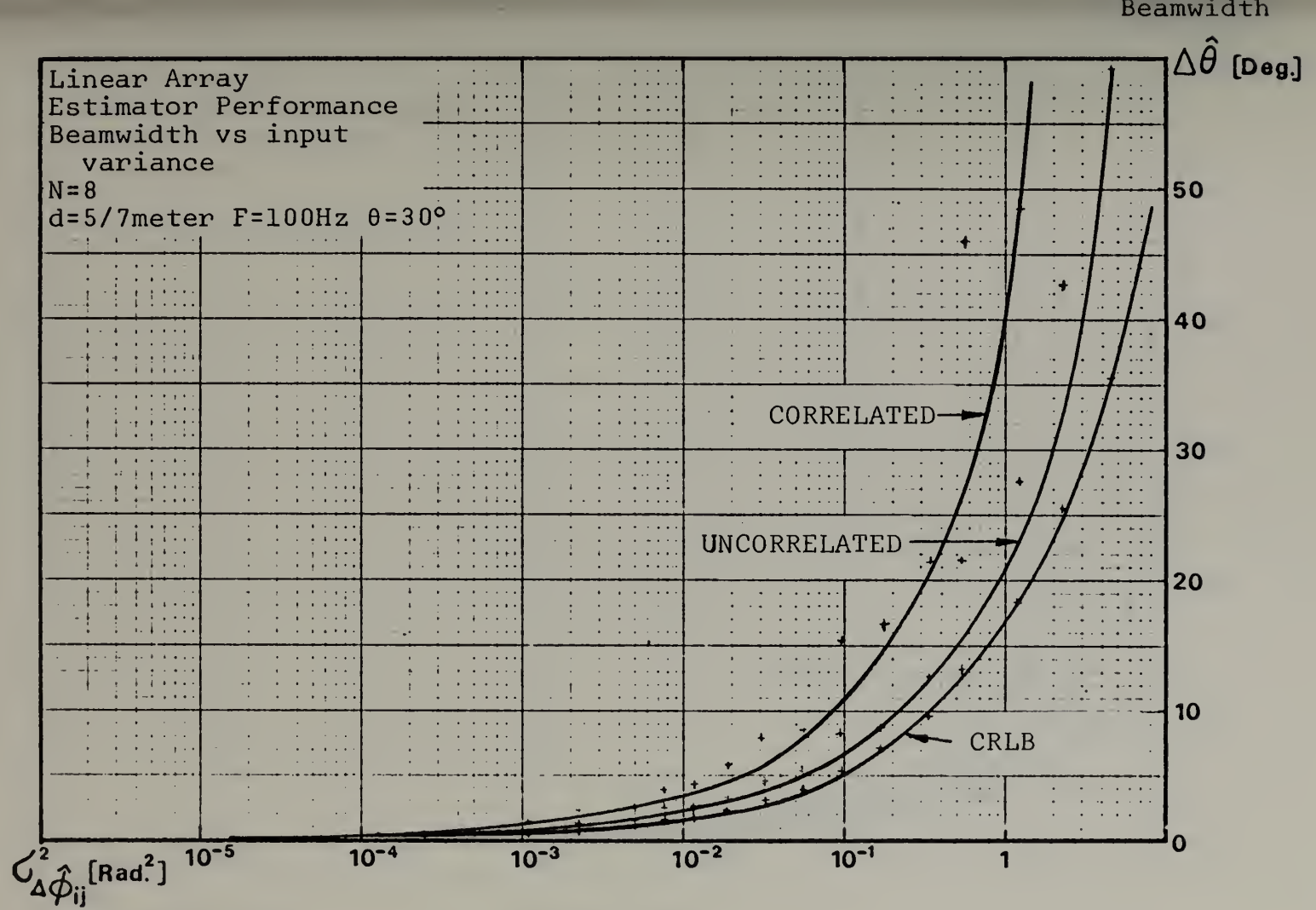
Linear Array
Estimator Performance
Beamwidth vs input
variance
N=8
d=5/7meter F=100Hz θ=30°
Beamwidth
$\Delta\hat{\theta}$ [Deg.]
50
40
30
20
10
0
CORRELATED
UNCORRELATED
CRLB
$10^{-5}$
$10^{-4}$
$10^{-3}$
$10^{-2}$
$10^{-1}$
1
$\sigma^2_{\Delta\hat{\phi}_{ij}}$ [Rad.$^2$]
Input variance

Figure IV-10

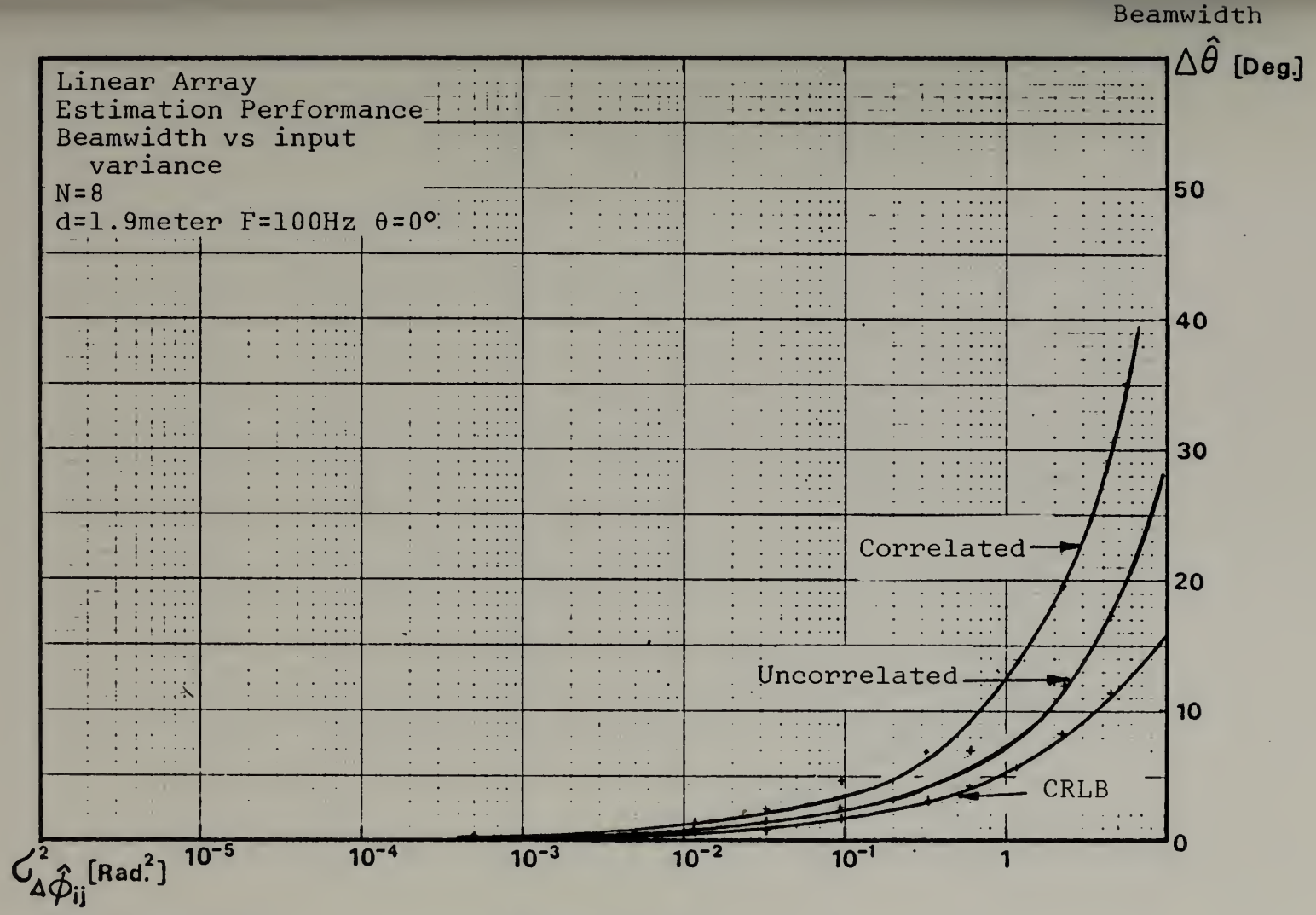
Linear Array
Estimation Performance
Beamwidth vs input variance
N=8
d=1.9meter F=100Hz θ=0°
Beamwidth
$\Delta\hat{\theta}$ [Deg.]
50
40
30
20
10
0
Correlated
Uncorrelated
CRLB
$10^{-5}$
$10^{-4}$
$10^{-3}$
$10^{-2}$
$10^{-1}$
1
$\sigma^2_{\Delta\hat{\phi}_{ij}}$ [Rad.$^2$]
Input variance

Figure IV-11

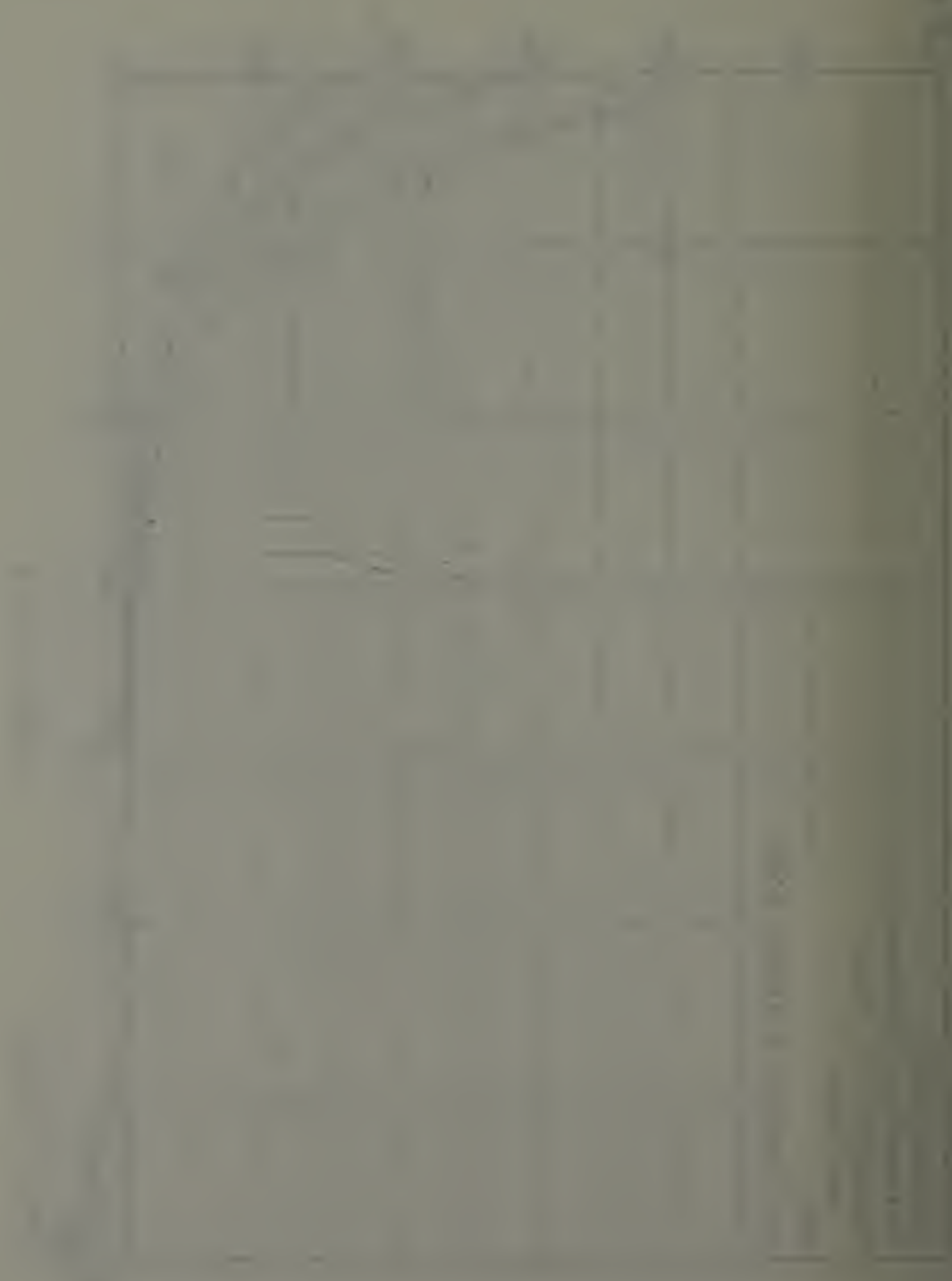

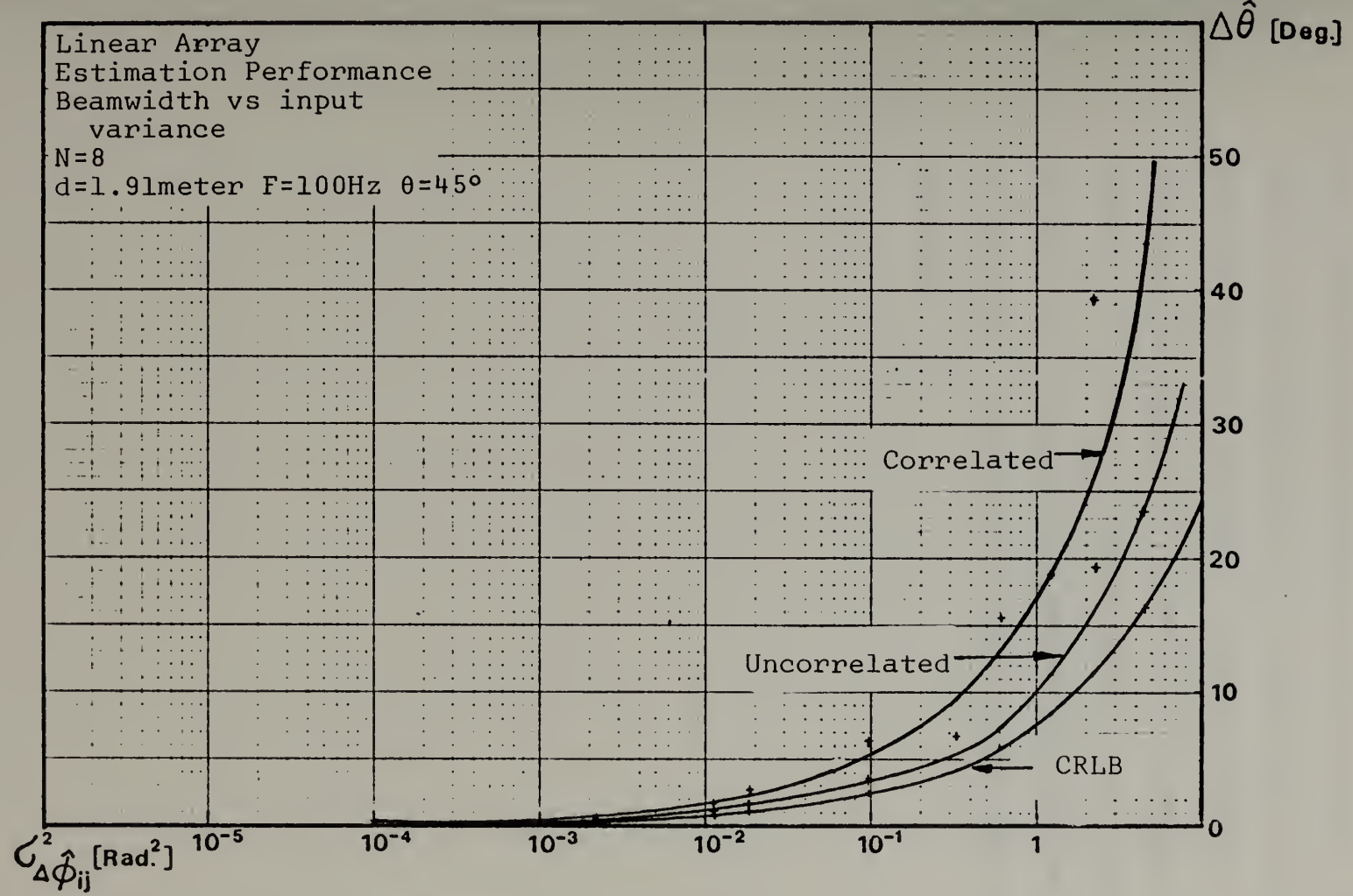


Input variance

Figure IV-12

- A linear array with the same number of elements and linear-element distance has however a much better performance than the equivalent circular array because of the much bigger aperture.
- For a linear array the beamwidth increases toward endfire, a fact which is expected from the equation of CRLB (Eq. IV-4) where the dependence on $1/\cos^2\theta$ is observed. The simulation results show the same behavior.

## E. THRESHOLD EFFECT AND ITS IMPORTANCE

As mentioned in the introduction to this chapter a threshold effect which can be expected in this kind of non-linear estimator was observed. In this work the threshold was defined as "lock-on point" and it is the value of the input variance for which the output beamwidth becomes less than five degrees. The number of five degrees was chosen arbitrarily and it can be any number in the vicinity of the knee of the performance curve (see for example Figures IV-3 through IV-6 for circular arrays and Figure IV-9 through IV-12 for linear arrays).

The range of input variances for which the beamwidth is less than the threshold value, in this case 5 degrees, is defined as "lock-on range".

The importance of this issue is due to the following:

- The lock-on point can be translated to a threshold on the coherence at a specific frequency and only those phase difference measurements for which this threshold is exceeded are processed by the trace function estimator. (This connection will be further explained in Chapter V.) This thresholding may ensure that only

those frequencies which will guarantee a certain beam-width will be processed. It should be mentioned that the threshold is frequency dependent exactly in the same manner as the diameter dependence which will be shown later in this section.

- As it can be seen from Figures IV-1 and IV-2 operating within the "lock-on range" ensures also that within the beam width there will be less variability of the resultant bearing estimate.

The dependence of the lock-on point for a circular array on number of elements and diameter is shown in Figures IV-13 and IV-14 respectively. The plots are for uncorrelated measurements and for the CRLB.

The frequency dependence of the lock-on point is exactly the same as for diameter and is not shown separately (both have an "$x^2$" effect).

The values of SNR shown on the plots are obtained from variance values related back to the system input and their aim is to give a feeling of the change in the noise tolerance of the system as the diameter (or frequency) and number of elements are changed.

Although the simulation results do not achieve CRLB within the range of values presented, nevertheless the trend shown suggest that it is eventually asymptotically achieved for higher number of element and larger diameter.

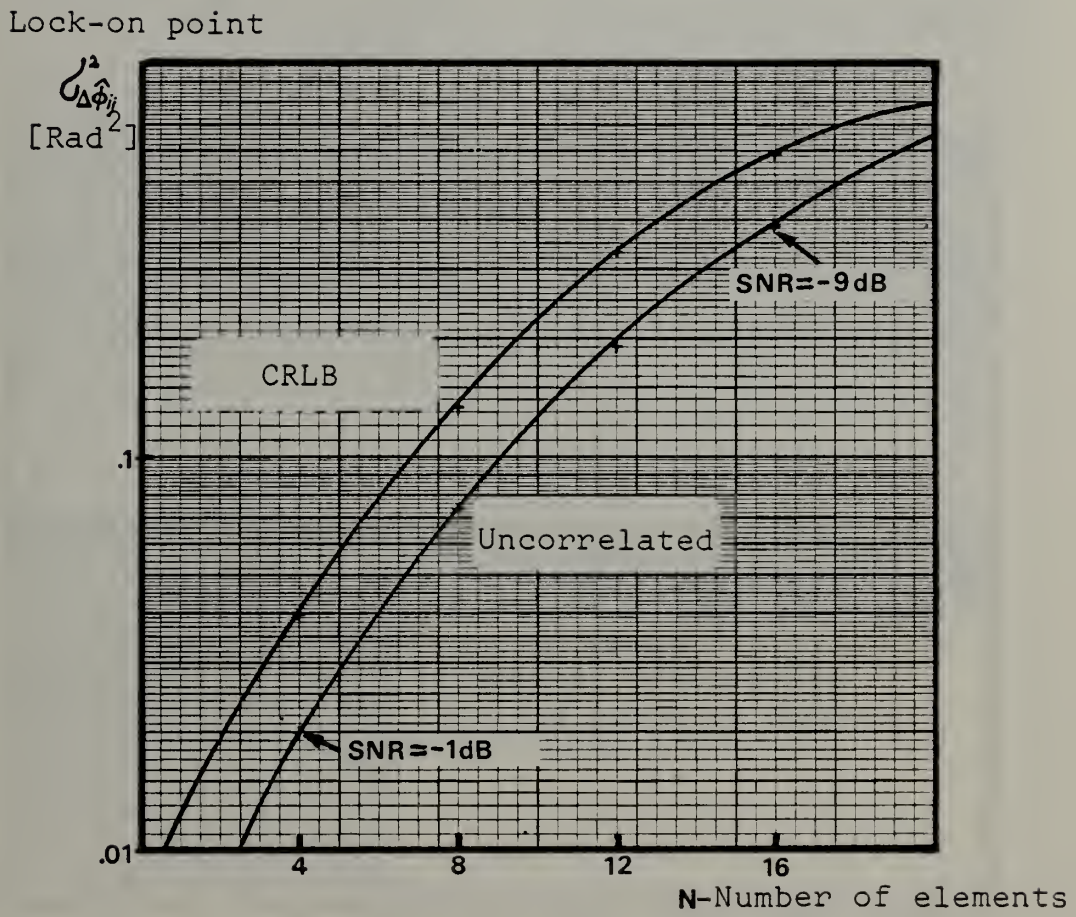


Circular Array
Estimation Performance
"Lock-on" point vs number of elements
D=5 meter F=100Hz $\theta=30^{\circ}$

Figure IV-13

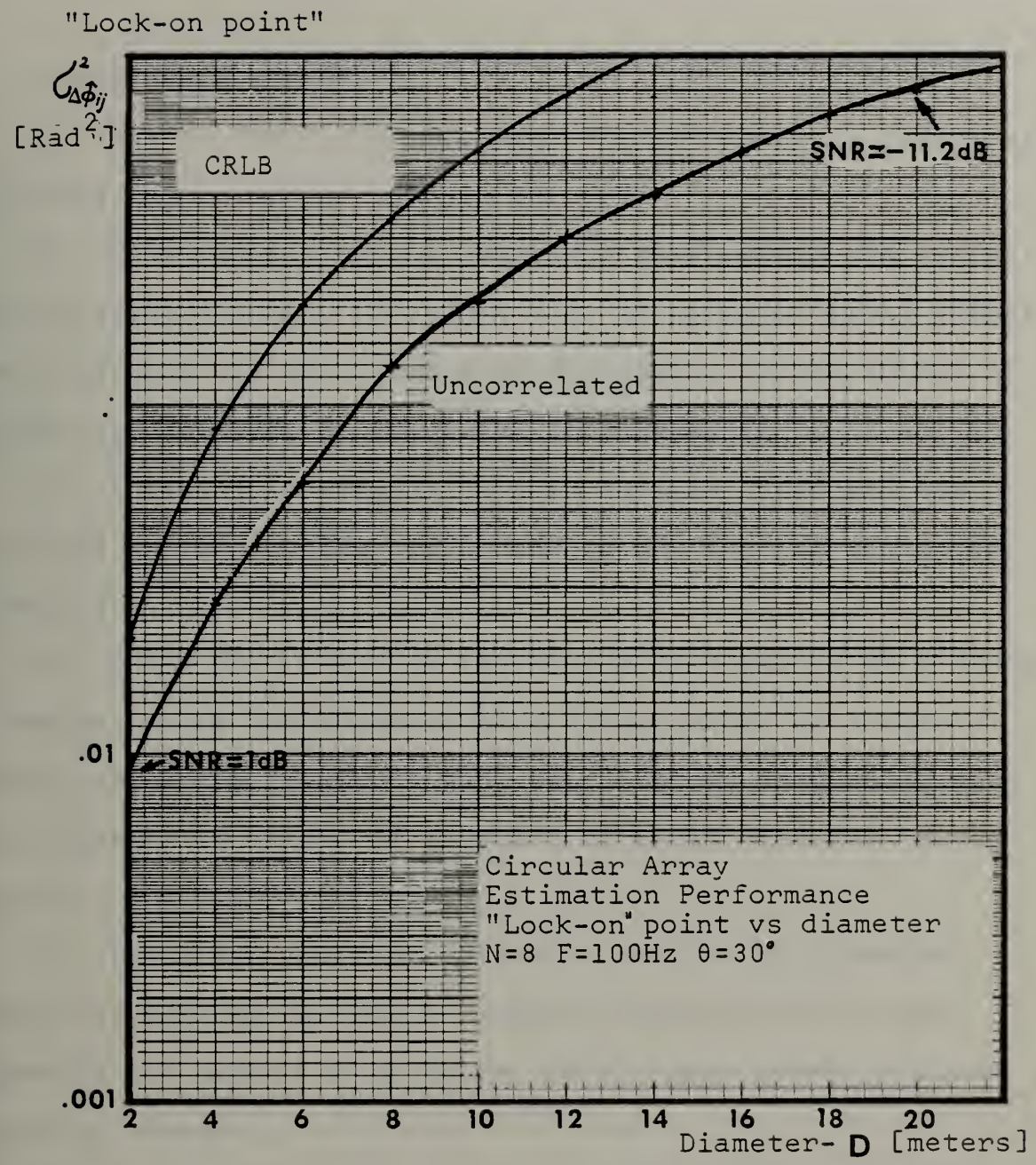
"Lock-on point"
$\sigma^2_{\Delta\hat{\phi}_{ij}}$ [Rad$^2$]
CRLB
SNR=-11.2dB
Uncorrelated
SNR=1dB
.01
.001
Circular Array
Estimation Performance
"Lock-on" point vs diameter
N=8 F=100Hz θ=30°
2
4
6
8
10
12
14
16
18
20
Diameter- D [meters]

Figure IV-14

## F. PERFORMANCE SUMMARY

1. Within the "lock-on range" the estimator is practically unbiased.

2. With respect to the beamwidth performance the estimator is asymptotically efficient i.e. it asymptotically achieves the CRLB when the input variance decreases, or the number of elements, diameter, or frequency increases.

3. A threshold effect, defined here as "lock-on" was observed and it enables one to tailor the desired system performance.

4. There is a limit on the number of elements at a fixed diameter (or on the diameter at a fixed number of elements) beyond which the beamwidth will only improve marginally with the increase of number of elements or array diameter respectively.

5. The trace function estimator applies to circular arrays as well as to linear arrays, however for the same aperture and number of elements the circular array performs slightly better.

In the next chapter on system considerations a system which uses the estimators developed here will be suggested. The problems involved in implementing such a system will be analyzed.

# V. SYSTEM CONSIDERATIONS

## A. INTRODUCTION

The motivation behind this work has been to find a solution to the practical problem of improved bearing estimation using a small array. The trace function concept offers a way to solve the problem but is not the solution itself. In order to solve the problem giving a meaningful and practical result the "pieces" must be connected together into a system concept which considers the signal from the sea to the display. In this chapter such a possible system will be suggested and outlined. It is not the intent to design a system but rather to highlight those points which are to be considered in a system using the trace function concept.

The main task would be to process the received data at the sensors (hydrophones) to bring it to a trace function format.

Once the data is in phase difference and/or time delay trace function format the estimation process developed in previous chapters can be applied and the bearing estimated for each frequency resolution cell of interest or for the wide band signal.

In the process of performing this task there is a major difficulty to be overcome; any processing scheme used must preserve the relative phase between the signals received the same as they were at the receiving sensors in order to result in a meaningful trace function.

Two process steps may be identified which pose this difficulty:

- The decorrelation (prewhitening) both in space and time.
- The phase unwrapping which is needed because of the inherent $2\pi$ ambiguity present in any phase measuring system.

Those and other points will be reviewed and analyzed briefly in this chapter. Some suggestions will be made to overcome the mentioned difficulties.

In Figure V-1 a conceptual system functional block diagram is presented. It applies the trace function principles as discussed in previous chapters. In the forthcoming sections the functions and problems associated with various blocks will be treated.

## B. SENSOR ARRAY

The sensor which will usually be a hydrophone is the first part of the system interacting with the signal. The major characteristics which have to be considered at the sensor array are:

- Accurate and known geometrical configuration.
- Equal phase response of the sensors across the frequency band of interest.

If the phase response characteristic cannot be satisfied because of practical problems, at least an accurate response chart at all frequencies of interest must be obtained and stored in a computer memory. This data can be used in turn to compensate for the different response characteristics of

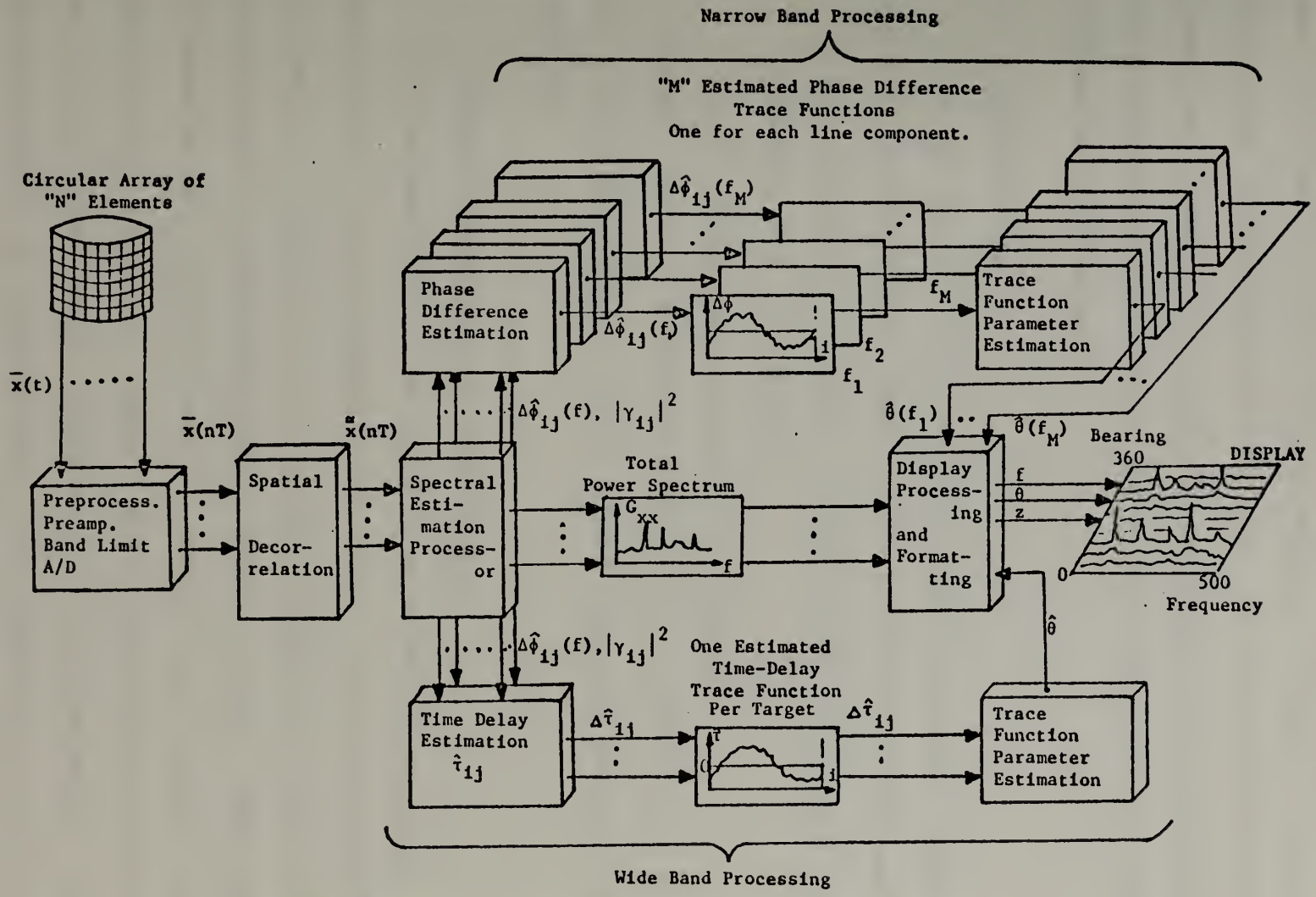


Conceptual system block diagram applying trace function principle.

Figure V-1

the various sensors when the phase difference calculations are performed for each pair of sensors. This way the relative phase differences at the input to the system can be preserved. Any other change in response of the sensors will be treated by the system as additional noise on the phase difference measurements.

C. PREPROCESSING

In this part of the system preamplification, bandlimiting and A to D conversion takes place. The only requirements are:

- zero phase or at least linear phase response at all frequencies of interest.
- Equal phase response for all channels.

After the A to D conversion digital methods will be used and the preservation of equal phase response becomes much simpler.

D. SPATIAL DECORRELATION (WHITENING)

The processing of the signals received by an array of sensors in a noisy background is based upon the relative coherency of the directional signal compared to the relative incoherency of the background (ambient) noise. When this difference is distinctive (i.e. the noise is almost uncorrelated from sensor to sensor) the processing is relatively easy and not very much dependent on the noise model. This characteristic is achieved when the separation between sensors is in the order of a half-wavelength for the frequencies of interest. The task is very much complicated where the separation

is small, because the high correlation of the background noise narrows the difference between the signal and noise in that domain.

In the problem defined in this dissertation the case is of small arrays where the whole array aperture is much smaller than a wavelength at the lowest frequencies of interest and as such the noise will be highly correlated.

The conventional way to decorrelate the noise among the sensors is by multiplication with the inverse noise covariance matrix or the inverse signal and noise covariance matrix. This operation is prescribed by every "optimal array processor" ( 2, 5, 39) and it can be performed based on a priori knowledge, "estimate and plug", or adaptive calculation of the inverse matrix.

This operation is inherentely not phase preserving and this fact will be shown in the forthcoming simple example:

Assume two sensors with the signal part of the input being:

$$\bar{x} = \begin{bmatrix} x_1 \\ \\ x_2 \end{bmatrix} = \begin{bmatrix} e^{i\omega t} \\ \\ e^{i(\omega t+\Delta\phi)} \end{bmatrix} \qquad \text{(V-1)}$$

clearly the phase difference is $\Delta\phi$.

A typical covariance matrix has the form:

$$Q = \begin{bmatrix} 1 & \rho \\ \\ \rho & 1 \end{bmatrix} \qquad \text{(V-2)}$$

then

$$Q^{-1} = \frac{1}{1-\rho^2}\begin{bmatrix} 1 & -\rho \\ -\rho & 1 \end{bmatrix} \quad \text{and} \quad Q^{-\frac{1}{2}} = \frac{1}{b}\begin{bmatrix} 1 & -a \\ -a & 1 \end{bmatrix} \qquad \text{(V-3)}$$

where

$$a = \frac{1-\sqrt{1-\rho^2}}{\rho} \qquad \text{and} \quad \frac{1}{b} = \frac{\rho}{\sqrt{2(1-\rho^2)(1-\sqrt{1-\rho^2})}}$$

The prewhitening process is defined as $Q^{-\frac{1}{2}}\bar{x}$ as it can be seen from:

$$E\{Q^{-\frac{1}{2}}\bar{x}\ \bar{x}^t\ Q^{-\frac{1}{2}}\} = Q^{-\frac{1}{2}}\ E\{\bar{x}\ \bar{x}^t\}\ Q^{-\frac{1}{2}} = Q^{-\frac{1}{2}}\ Q\ Q^{-\frac{1}{2}} = I$$

and

$$Q^{-\frac{1}{2}}\bar{x} = \frac{1}{b}\begin{bmatrix} 1 & -a \\ -a & 1 \end{bmatrix}\begin{bmatrix} e^{i\omega t} \\ e^{i(\omega t+\Delta\phi)} \end{bmatrix} = \frac{1}{b}\begin{bmatrix} e^{i\omega t}-ae^{i(\omega t+\Delta\phi)} \\ -ae^{i\omega t}+e^{i(\omega t+\Delta\phi)} \end{bmatrix} \qquad \text{(V-4)}$$

$$\tilde{x}_1 = \frac{e^{i\omega t}}{b}(1 - ae^{i\Delta\phi}) \qquad \tilde{x}_2 = \frac{e^{i\omega t}}{b}(e^{i\Delta\phi}-a) \qquad \text{(V-5)}$$

After some manipulations the phase difference between $\tilde{x}_2$ and $\tilde{x}_1$ is:

$$\Delta\tilde{\phi}_{\tilde{x}_2\tilde{x}_1} = tg^{-1}\frac{\sin\Delta\phi(1-a^2)}{\cos\Delta\phi(1+a^2)-2a} = tg^{-1}\frac{\sin\Delta\phi(\rho^2-1+\sqrt{1-\rho^2})}{(\cos\Delta\phi-\rho)(1-\sqrt{1-\rho^2})} \qquad \text{(V-6)}$$

which clearly cannot be equal to $\Delta\phi$ for any value of $\rho$ except $\rho\to 0$ which the trivial uncorrelated case.

In order to preserve phase from the total system point of view one must correct for the above phase distortion.

A new method called "phase preserving spatial decorrelation (or prewhitenning)" by the author is proposed and outlined here. The notion is that the phase distortion caused by the decorralation process can be calculated and compensated for, after the cross spectral estimation process, provided that one knows exactly the inverse covariance matrix.

To demonstrate the above, the previous example is continued:

the original phase difference was $\Delta\phi_{x_1x_2}$

the resultant phase difference after decorrelation was

$$\Delta\tilde{\phi}_{\tilde{x}_1\tilde{x}_2} = tg^{-1}\ \frac{\sin\Delta\phi(1-a^2)}{\cos\Delta\phi(1+a^2)-2a}$$

The difference between the two is the compensation term:

$$\Delta\phi-\Delta\tilde{\phi} = tg^{-1}\ \frac{2a\sin\Delta\phi(1-a\cos\Delta\phi)}{1-a^2\cos2\Delta\phi-2a\cos\Delta\phi} \qquad \text{(V-7)}$$

The above compensation term is impractical to calculate because it is dependent on the real phase difference which is unknown. As a result no simple compensation can be used. Equation (V-6) can be solved numerically however for $\Delta\phi_{x_1x_2}$ once $\Delta\tilde{\phi}_{\tilde{x}_1\tilde{x}_2}$ is measured provided $\rho$ is known.

As shown by this simple example this approach is very complicated even for simple arrays (2 elements) because it has to be calculated for each frequency bin and each sensor

pair. For practical number of elements in an array this kind of operation becomes prohibitive. To solve the problem a different approach has to be found.

As the ambient noise is a wideband process its cross covariance function has a limited time width

$$\rho_{ij}(\tau) < \varepsilon \text{ for } \tau > \tau_o \qquad \text{(V-8)}$$

i.e. it can be made arbitrarily small if long enough delay between the elements is applied.

Figure V-2 shows such a covariance function for a bandwidth of 50 to 250 Hz a power spectrum of -6dB/octave for 2.5 and 5 meter distance between sensors.

The graph clearly shows the decay of the covariance "ρ" as function of delay time "τ". This characteristic can be used for the decorrelation process. One can introduce successive and known delays between the elements of an array such that the smallest delay is enough to decorrelate the noise down to a desired level for the closest pair in the array.

After this process the signal is:

$$\tilde{\bar{x}}(t) = \begin{bmatrix} x_o(t) \\ x_1(t-\Delta) \\ \vdots \\ x_{N-1}(t-(N-1)\Delta) \end{bmatrix} \qquad \text{(V-9)}$$

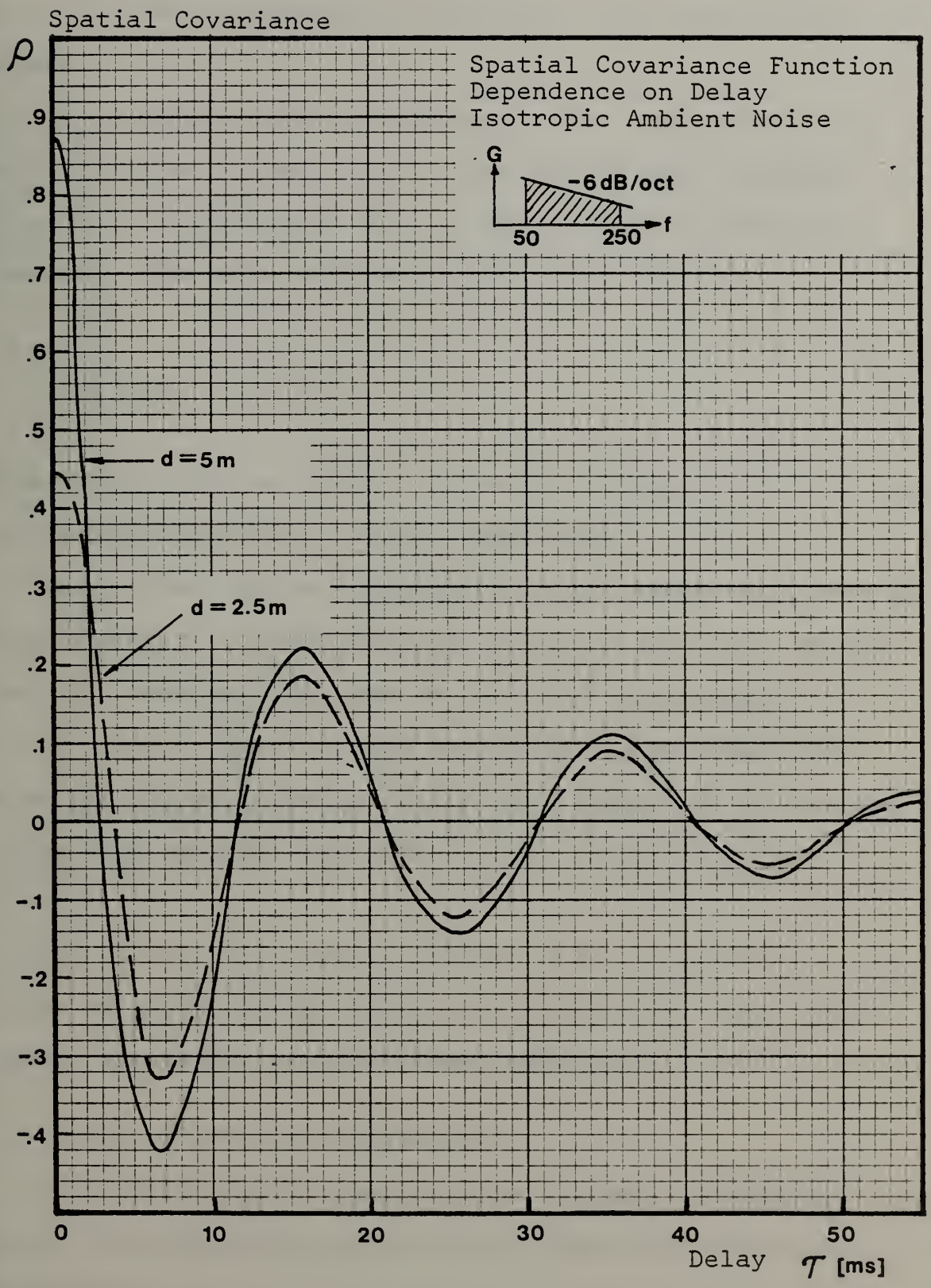
Spatial Covariance
ρ
Spatial Covariance Function
Dependence on Delay
Isotropic Ambient Noise
G
-6 dB/oct
f
50
250
.9
.8
.7
.6
.5
.4
.3
.2
.1
0
-.1
-.2
-.3
-.4
d = 5 m
d = 2.5 m
0
10
20
30
40
50
Delay τ [ms]

Figure V-2

where $\Delta$ is the incremental time delay introduced between the elements.

It is obvious that to compensate for this process the only operation to be done is to re-add at each frequency $\omega_\ell$ a phase compensation term to the calculated phase difference. This term will be for the pair "i,j":

$$\Delta\phi_{ij\ comp.} = \Delta(i-j)\omega_\ell \qquad \text{(V-10)}$$

This method will not affect narrow band signals but may also decorrelate partially the wide band signal.

This effect can be minimized if $\Delta$ is chosen such that is large enough to decorrelate the noise but $(N-1)\Delta$ is smaller than the decorrelation time of the wide band signal.

In order to perform this operation one must have the noise and signal correlation function which can be obtained either from apriori knowledge or from estimations made in situ.

The above method should be viewed as a suggestion and not a firm solution mainly because it is based on theory only without simulation or measurement back-up.

## E. REVIEW OF SPECTRAL ESTIMATION

This section will summarize the spectral estimation tools needed for subsequent estimation of time delay and phase difference.

As it will be shown later if one has infinitely long data record he can get both stable estimates and infinitely good resolution of the power spectra, and phase spectra of a stationary random process. The main factor which limits achieving the desired performance is the limited length of data available. The reasons are many, but one of the most important ones is the time limit on the stationarity of the environment. In the case of data in the ocean, a few minutes can be considered as a good measure for stationary environment.

The analysis which will follow reproduces the main results in Ref. [25, 26, 27] which deal with the limited time record auto and cross spectral estimations.

The two basic parameters which control the performance of spectral estimation are the available record length, T, over which the sample of the random process is assumed stationary and the desired frequency resolution, B, of the spectral analysis. Large values of BT give good performance but small values are often encountered because of short T available or requirement for fine resolution B.

In order to take advantage as much as possible of the available data a method was developed [40] to obtain good reduction of variance by overlapped processing of the data. This method is less efficient than the same number of segments non-overlapped but it is much better than using the available data in non-overlapped form.

Several questions arise when one attacks the problem: what percentage of overlap to use?, which windows?, how big

the FFTs have to be? Those questions and others were answered in Ref. [25, 26] and the results follow.

The stationary random process x and y are observed for a time T seconds, thus x(t), y(t) are available for $0<t<T$. One wishes to estimate the cross spectrum $G_{xy}(f)$ with a resolution of B Hz over a bandwidth of Ω Hz.

The method of segmenting the available data is shown in Figure V-3.

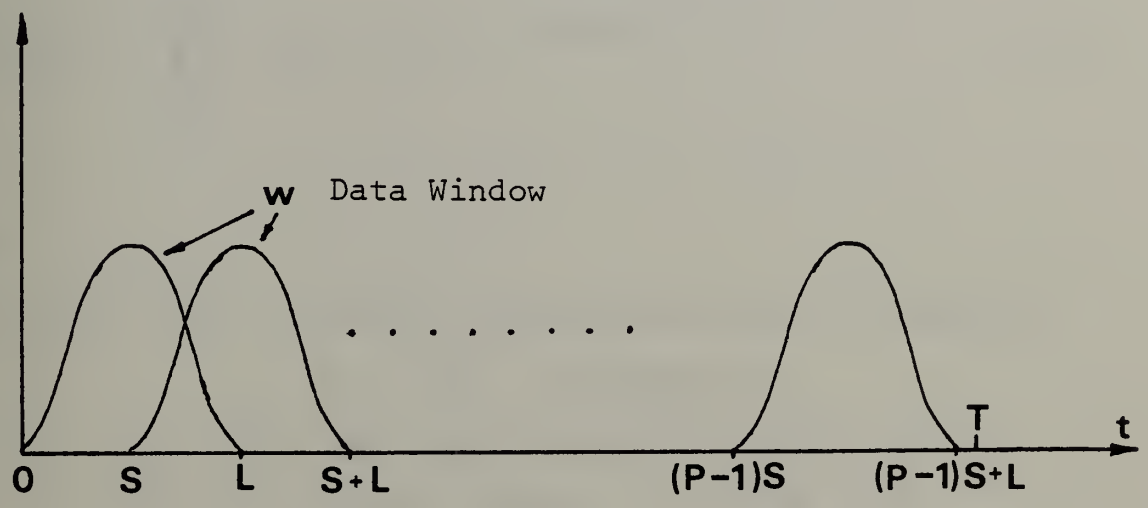


Figure V-3
Segmenting Data With Overlapp

The connection between the various terms in Figure V-3 is:

$$(P-1)S+L \leq T \qquad \text{(V-11)}$$

where P - number of segments

S - shift of each adjacent window

L - data window length

T - total available data length (time)

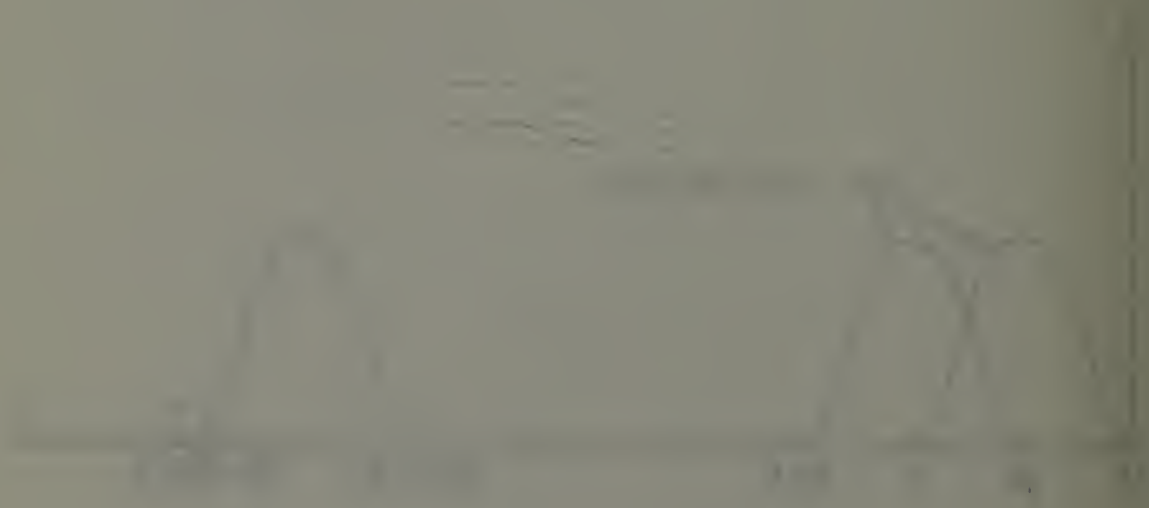

1. Estimation Procedure

The estimation of the auto and cross spectrum is done in the following way:

a. DFT the segmented and windowed data x and y:

$$X_k(f_n) = \sum_{j=0}^{L-1} X_k(j)\, w_k(j)\, e^{-i2\pi jn/L} \qquad \text{(V-12)}$$

$$Y_k(f_n) = \sum_{j=0}^{L-1} Y_k(j)\, w_k(j)\, e^{-i2\pi jn/L} \qquad \text{(V-13)}$$

where

$X_k(f_n)$, $Y_k(f_n)$ - Fourier transformed data at frequency $f_n = \frac{nF_s}{L}$ of segment k

j - time index (discrete) 0,1,2...L-1

k - segment index 1,2....P

n - frequency index 0,1,2,L/2

$F_s$ - sampling frequency

NOTE: The index j begins from zero at each segment k.

b. Estimate of auto power spectra

$$\hat{G}_{xx}(f_n) = \frac{1}{PF_sL} \sum_{k=1}^{P} |X_k(f_n)|^2 \qquad \text{(V-14)}$$

$$\hat{G}_{yy}(f_n) = \frac{1}{PF_sL} \sum_{k=1}^{P} |Y_k(f_n)|^2 \qquad \text{(V-15)}$$

c. Estimate of cross spectra

$$\hat{G}_{xy}(f_n) = \frac{1}{PF_s L} \sum_{k=1}^{P} X_k(f_n)\, Y_k^*(f_n) = A_{xy}(f_n) e^{i\hat{Ph}_{xy}(f_n)} \qquad \text{(V-16)}$$

$$\text{Phase} \quad Ph_{xy}(f_n) = tg^{-1}\left\{\frac{Im[\hat{G}_{xy}(f_n)]}{Re[\hat{G}_{xy}(f_n)]}\right\} = \Delta\hat{\phi}_{xy}(f_n) \qquad \text{(V-17)}$$

$$\text{Amplitude} \quad \hat{A}_{xy}(f_n) = \sqrt{Re[\hat{G}_{xy}(f_n)])^2 + (Im[\hat{G}_{xy}(f_n)])^2} \qquad \text{(V-18)}$$

d. Estimate of magnitude squared coherence

$$|\hat{\gamma}_{xy}(f_n)|^2 = \frac{|\hat{G}_{xy}(f_n)|^2}{\hat{G}_{xx}(f_n)\hat{G}_{yy}(f_n)} \qquad \text{(V-19)}$$

NOTE: The magnitude squared coherence function whose role will be discussed later, is given here because of its connection to the other estimation processes.

2. Statistics Of The Estimates

The spectral estimates presented are random variables. Their means and variances will be stated under the assumptions that x and y are Gaussian random processes and the frequency resolution of the spectral window $|W|^2$ is narrower than the finest detail in spectrum G.

where

$$W(f_n) = \sum_{j=0}^{L-1} w(j)\, e^{-i2\pi jn/L} \qquad \text{(V-20)}$$

a. Means

$$E\{\hat{G}_{xx}(f_n)\} \cong G_{xx}(f_n) \int |W(\nu)|^2 d\nu \qquad \text{(V-21)}$$

$$E\{\hat{G}_{xy}(f_n)\} \cong G_{xy}(f_n) \int |W(\nu)|^2 d\nu \qquad \text{(V-22)}$$

One can assume without loss of generality that the windows are normalized i.e. $\int |W|^2 = 1$ then:

$$E\{\hat{G}_{xx}(f_n)\} \approx G_{xx}(f_n) \qquad \text{(V-23)}$$

$$E\{\hat{G}_{xy}(f_n)\} \approx G_{xy}(f_n) \qquad \text{(V-24)}$$

Thus the estimators are unbiased

$$E\{\Delta\hat{\phi}_{xy}(f_n)\} = \Delta\hat{\phi}_{xy}(f_n) \qquad \text{(V-25)}$$

$$E\{\hat{A}_{xy}(f_n)\} = A_{xy} = |G_{xy}| \qquad \text{(V-26)}$$

$$E\{|\hat{\gamma}_{xy}|^2\} = |\gamma|^2 + \frac{1}{P}(1-|\gamma|^2)^2\left(1+\frac{2|\gamma|^2}{P}\right) \qquad \text{(V-27)}$$

(after [28])

The estimate is biased by the second term of the equation. A note about the above bias is given below.

It is calculated for <u>nonoverlapping</u> segments. However, when overlap occurs this bias is substantially reduced to a value of about 50% of the above figure at 50% overlap.

b. Equivalent number of degrees of freedom

The convenient way to describe the stability of any positive estimate is its equivalent number of degrees of freedom (EDF) [18]. The definition of this stability constant is:

$$EDF = K = \frac{2[\text{average}]^2}{\text{variance}} = \frac{2[E\{\hat{G}(f)\}]^2}{Var\{\hat{G}(f)\}} \qquad (V\text{-}28)$$

Basically using tables as in Ref. [18] one can estimate his confidence in the measurements.

For example for K=500 90% of the measurements will be in the range of 0.92 to 1.081 of the average. Maximizing those K's will be one of the important criteria for the overlap and window choice.

c. Variances

$$Var\{\hat{G}_{xx}(f_n)\} \cong G_{xx}^2(f_n) \frac{1}{P} \sum_{k=-(P-1)}^{(P-1)} (1-\frac{|k|}{P}) |\Phi_w(kS)|^2 \qquad (V\text{-}29)$$

where

$$\Phi_w(\tau) = \int w(t)w^*(t-\tau)dt \qquad (V\text{-}30)$$

$$Var\{\hat{G}_{xy}(f_n)\} \cong G_{xy}^2(f_n) \frac{1}{P} \sum_{k=-(P-1)}^{(P-1)} (1-\frac{|k|}{P}) |\Phi_w(kS)|^2 \qquad (V\text{-}31)$$

At this point we can define EDF (k) for both auto and cross spectra [25, 26].

$$K_A = \frac{2P}{\sum_{k=-(P-1)}^{(P-1)} (1-\frac{|k|}{P}) \left|\frac{\Phi_w(kS)}{\Phi_w(0)}\right|^2} \quad \text{for auto spectra} \qquad (V-32)$$

and

$$K_c = |\gamma_{xy}|^2 K_P \qquad \text{for cross spectra} \qquad (V-33)$$

$$\text{Var}\{\hat{A}_{xy}(f_n)\} = G_{xx}(f_n)G_{yy}(f_n)[1+|\gamma_{xy}(f_n)|^2]/K_A \qquad (V-34)$$

$$\text{Var}\{\Delta\hat{\phi}_{xy}(f_n)\} = \frac{1-|\gamma_{xy}(f_n)|^2}{|\gamma_{xy}(f_n)|^2 K_A} \qquad (V-35)$$

Those are based on the assumption that $K_c = K_A|\gamma_{xy}|^2 >> 1$. It should be noted that neither of the two cross variances depend on the actual phase and the phase variance is not dependent on actual data values at all, but only on the coherence between the two sequences and the processing scheme.

$$\text{Var}\{|\hat{\gamma}_{xy}(f_n)|^2\} \cong \frac{2}{P}|\gamma_{xy}(f_n)|^2(1-|\gamma_{xy}(f_n)|^2)^2 \text{ for } \gamma_{xy} \neq 0 \qquad (V-36)$$

3. Design Tradeoffs

As one can see from all the above statistics, k and P are playing major roles in the variance reduction.

In order to improve performance one has to maximize k and P (which are connected) for a given amount of available data.

In Ref. [25] this subject was thoroughly investigated for various window functions.

Following is a summary of important results:

a. The EDF(k) has a maximum as related to P for a given amount of data T.

b. This maximum was proven to be almost independent of the window employed for large BT products

$$\max \text{EDF} \approx 3(BT-1) \qquad \text{(V-37)}$$

c. The required fractional overlap which is defined as

$$FO = \frac{L-S}{L} = \frac{P-T/L}{P-1} \qquad \text{(V-38)}$$

is significantly increased for max EDF compared to 0.99 max EDF so it is not recommended to design for max EDF, but 1% or 2% less.

As an example using cosine window (Hanning) and BT=64 for max EDF P=146 segments are needed but for 0.99 max EDF only 112 segments are needed. Clearly the additional 30% of processing is not worth the one percent increase in EDF.

The optimal FO comes out to be in general not a convenient number to use, e.g.. 0.61 for cosine window. One will probably choose the closest convenient value like FO=0.5 which will give for cosine window EDF=92% of max EDF which is a reasonable figure.

d. As the max EDF is practically independent of the window employed no tradeoffs had to be made to realize better side lobe response of the more sophisticated windows. This issue is effecting the size of the particular FFT's to be performed.

$$N_s = \frac{C_w}{B\Delta t} \qquad \text{(V-39)}$$

where

$N_s$ = number of samples in one FFT

$C_w$ = half power bandwidth constant of a window

$\Delta t$ = sampling interval

Clearly for a "better" window $C_w$ is bigger in general and $N_s$ will be bigger. Thus the side lobe performance for a given B can be improved by paying with bigger FFT's and not affecting stability of the estimates.

4. Effect Of Pure Tones (Lines) In The Spectrum

The results shown so far were true under the assumption that the B of the spectral window $|W(f_n)|^2$ is narrower than the finest detail of the spectrum. For tonal signals this will not be the case and a change in the statistics will occur but the processing method will not change. In

Ref. [27] those changes were made and the following statistics derived:

a. Mean

$$E\{G(f_n)\} = G(f_n)_{wide} + G(f_n)_{line} \qquad \text{(V-40)}$$

where

$G(f_n)_{wide}$ = The previous wide band power spectrum

$$G(f_n)_{line} = A^2|W(f_n-f_o)|^2 \qquad \text{(V-41)}$$

A - line amplitude

$f_o$ - line frequency

$$E\{\hat{G}_{xy}(f_n)\} = G_{xy}(f_n)_{wide}+A_xA_y|W(f_n-f_o)|^2 \qquad \text{(V-42)}$$

b. Variance

$$Var\{\hat{G}(f_n)\} = Var\{\hat{G}(f_n)\}_{wide}+2G(f_n)_{wide}G(f_n)_{narrow} \times \frac{1}{P}\sum_{k=1-P}^{P-1}(1-\frac{|k|}{P})\Phi_w(kS)e^{i2\pi k(f_n-f_o)S} \qquad \text{(V-43)}$$

from which a bigger absolute value of the variance can be expected when a tonal is present. However, if the EDF (K) is calculated for $G(f_n)_{wide} \ll G(f_n)$ line which is the case in general when lines are present, one can see that this relative measure is increased which means a more stable estimation.

For $G(f_n)_{narrow} >> G(f_n)_{wide}$:

$$EDF = K_{tonal} = \frac{PG(f_n)_{narrow}}{G(f_n)_{wide} \sum_{k=1-P}^{P-1} (1-\frac{|k|}{P})\Phi_w(kS)e^{i2\pi k(f_n-f_o)S}} \quad (V-44)$$

this $K_{tonal}$ is bigger than the one for wide band alone by a factor of approximately

$$\tfrac{1}{2}G(f_n)_{narrow}/G(f_n)_{wide} >> 1 \quad (V-45)$$

All the other equations for cross spectral estimation statistics will still hold with the new $K_{tonal}$.

It is worthwhile to note the $|\gamma_{xy}|^2$ will be much bigger in this case (very close to unity) and its bias and variance will be very small because of the increased "S/N".

## F. PHASE DIFFERENCE ESTIMATION AND THE UNWRAPPING PROBLEM

The basic phase difference estimation is done entirely by the cross spectral estimation process as reviewed in the previous section. However there are some additional steps to be performed in order to construct the phase difference trace function or estimate the wide band time delay [32, 36]:

- The frequency bins for which further processing will be done must be detected.
- The phase difference estimated value must be recompensated for the decorrelation process as stated in Eq. (V-10).

- The resultant phase difference has to be unwrapped because it is measured only in the range $\pm\pi$ while it can have any $\pm n2\pi$ ambiguity.

1. Detection Problem

The detection of the frequency bins which are candidates for further processing is important for the following reasons:

- To reduce the false alarms in the system.
- To reduce the computation load in subsequent stages of processing.

Probably the most representative parameter of the phase difference integrity at a specific frequency is the magnitude squared coherence $|\gamma_{xy}|^2$. This fact can be seen from Eq. (V-35). While $K_A$ is a fixed system parameter $|\gamma_{xy}(f_n)|^2$ is the data dependent term, or more precisely dependent on the ratio of the coherent to uncoherent signals between the two sensors considered. Moreover it can be related to the input SNR under certain assumptions of equal and uncorrelated noise between the sensors and linear processing up to the estimation stage, by the equation [6]:

$$SNR_i = \frac{|\gamma_{xy}(f_n)|}{1-|\gamma_{xy}(f_n)|} \qquad \text{(V-46)}$$

As such the magnitude squared coherence $|\gamma_{xy}|^2$ can be a good measure for detection [7]. There are two different processing paths, each with slightly different requirements from the detection process:

a. Time Delay Estimation Path

This path will require probably a lower threshold on the coherence because it is estimating the time delay from a large number of frequency bins, as it will be shown in the next section, and it further reduces the noise level, before the trace function processing.

b. Phase Difference Path

This path will have a higher threshold because it is intended to process mainly line or narrow band components which if they are present exhibit a fairly high coherence.

To preserve the integrity of the trace function which includes all the pairs in the array it is not enough to detect a potential frequency bin on a "per pair" basis. This operation has to be done across the whole array (all the pairs). Two possible ways to perform this task are:

- At each frequency bin each pair is thresholded for its magnitude squared coherence. Then the number of pairs which pass the threshold are counted and if this figure exceeds a predetermined number this frequency bin is qualified for further processing.
- At each frequency bin the sum of the magnitude square coherence of all the pairs is calculated and if this sum exceeds a threshold this frequency bin is qualified.

It should be noted that this detection process based on the coherence is a data adaptive process. It qualifies the various frequency bins based on its estimated magnitude square coherence in real time.

2. Compensation

This operation is straight forward as explained in Section V-D.

One has only to add the compensation term Eq. (V-10) to each "qualified" phase difference measurement according to its frequency and the participating sensors in the pair.

3. Unwrapping Problem

This problem is well explained in Ref. [32]. There are several solutions treated in the literature [32, 36] however in the case of the circular array or similar two dimensional arrays the problem can be eased by taking in consideration the following:

a. For small arrays no ambiguities will occur at low frequencies. Ambiguities occur when $|\tau|\omega > \pi$ for the largest aperture (diameter in circular array). However, for a small array when $D/\lambda << 1$, we get $|\tau|\omega = \frac{2\pi D}{\lambda} << \pi$ which is unambiguous.

b. The pairs of sensors have different orientation and one can find always (if there are enough sensors) a pair of sensors or more which have unambiguous phase difference measurement even at higher frequencies than the limit in a. Those will be the pairs which are in a line parallel to the incoming signal wavefront.

Using the above two facts the following procedure can be outlined to effectively unwrap the phase.

- Beginning at the low frequencies where there is no ambiguity find those pair/s which are perpendicular to the bearing of the target/s.

- At the higher frequency beginning from those unambiguous pairs, and knowing the geometry, i.e. knowing what is the biggest possible change of phase between adjacent (in orientation) pairs, one can readily detect any $2\pi$ jump in phase difference and thus effectively unwrap the phase.

This procedure will be valid only if the target will have spectral components under the ambiguity frequency for the given array. For example, for a 5 meter diameter array this ambiguity frequency is 150Hz and practically we can always find some line components below this limit (50 and 60Hz for instance).

## G. TIME DELAY ESTIMATION

The time delay estimation process is essential to the derivation of the time delay trace function. In some sense this process can be more powerful in a detection stage when the signals are relatively weak (low SNR per frequency bin) because unlike the phase difference trace function it "integrates" over all "qualified" frequencies.

This subject is extensively treated in the current literature and two basically different ways emerged:

- The Generalized Correlation method which was treated in depth by G. C. Carter [6], several works derived and extended from it [19] as well as other works on optimal and suboptimal versions of correlation schemes [8, 15].
- Minimization of some weighted cost function [9, 14].

Both the above methods are closely related to the spectral estimation which was reviewed in a previous section (V.E).

During this work both methods were analyzed, however, it seems that the second method is more applicable to the problem of small arrays mainly because its time delay resolution is not limited by the sampling interval as in the correlation method. (In the correlation method the problem can also be overcome by elaborated interpolation schemes.)

As a result the second method will be reviewed here, specifically the development done by Chan et. al. [9] which uses the weighted least square error criteria. This method was adopted and will be followed.

The model of the signal to be processed is represented by:

$$x(t) = s(t) + n_1(t)$$
$$y(t) = \alpha s(t-\tau) + n_2(t) \qquad \text{(V-47)}$$

The signal s(t) is uncorrelated with the corrupting noises $n_1$ and $n_2$ which are stationary random processes.

Assume that the two inputs x(t) and y(t) are passed through a cross spectral estimation process, as described before. The phase difference of the cross spectra and the magnitude squared coherence function are calculated. These two parameters will be used for this processor

$$\Delta\hat{\phi}_{xy}(f_n) = \tau\omega_n + \varepsilon_n \qquad n = 0,1,\ldots M+1 \qquad \text{(V-48)}$$
$$\omega_n = 0, \frac{\pi}{M+1} \ldots \pi$$

however the 0 and $\pi$ frequencies will not be used.

$\varepsilon_n$ is an error (noise) with the following statistics:

Without signal - $\varepsilon_n$ is uniformly distributed from $-\pi$ to $\pi$

$$E\{\varepsilon_n\} = 0 \qquad \text{Var}\{\varepsilon_n\} = \frac{\pi^2}{3} \tag{V-49}$$

With signal for practical cases of K (EDF $\geq$ 300) we can assume it is approximately gaussian and has a variance

$$\sigma_n^2 = \frac{1}{\psi_n K} \tag{V-50}$$

where

$$\psi_n = \frac{|\gamma_{xy}(f_n)|^2}{1-|\gamma_{xy}(f_n)|^2} \tag{V-51}$$

The errors for different frequencies are uncorrelated i.e. $E\{\varepsilon_j \varepsilon_i\}=0$ for $i \neq j$ and for $\Omega T > 8$ [16].

The weighted least squares cost function is:

$$J = \sum_{n=1}^{M} \psi_n \, (\Delta\hat{\phi}_n - \tau\omega_n)^2 \tag{V-52}$$

where the subscripts of $\Delta\hat{\phi}_{xy}(f_n)$ were dropped.

$$0 = \frac{\partial J}{\partial \tau} = 2 \sum_{n=1}^{M} -\psi_n (\Delta\hat{\phi}_n - \tau\omega_n)\omega_n \tag{V-53}$$

and

$$\hat{\tau} = \frac{\sum_{n=1}^{M} \psi_n \Delta\hat{\phi}_n \omega_n}{\sum_{n=1}^{M} \psi_n \omega_n^2} \qquad \text{(V-54)}$$

This estimator has two prominent features:

- It weighs those measurements which have less variance more heavily.
- It implicitly assumes that $\Delta\hat{\phi}_o = 0$ so it provides one fixed point on the straight line $\Delta\phi = \omega\tau$, a feature that intuitively should reduce the variance of the estimate.

The statistics of the estimate are:

$$E\{\hat{\tau}\} = \tau \quad \rightarrow \quad \text{unbiased}$$

$$E\{(\hat{\tau}-\tau)^2\} = \frac{\sum_{n=1}^{M} \psi_n^2 \, \omega_n^2 E\{\varepsilon_n^2\}}{\left[\sum_{n=1}^{M} \psi_n \, \omega_n\right]^2} = \frac{1}{K \sum_{n=1}^{M} \psi_n \, \omega_n^2} \qquad \text{(V-55)}$$

which for a reasonable $\psi$ is very small for practical values of K and M.

There are some points to be remembered:

- The factor $\psi$ is not given but calculated from

$$\hat{\psi} = \frac{|\hat{\gamma}_{xy}|^2}{1-|\hat{\gamma}_{xy}|^2} \qquad \text{(V-56)}$$

It can be defined by the detection (qualifying) process mentioned in the previous section and as such the performance of the estimator may be tailored as desired.

- The summation over the frequency ( $\sum_{n=1}^{M}$ ) does not necessarily include all frequencies, only those which are qualified by the detection process and for the others $\psi_n$ should be set to zero.

This section will not be complete without discussing the multiple target problem. For a multiple target environment the estimator as defined here will not function properly because it will not have one distinct line $\Delta\phi=\omega\tau$ to estimate.

In order to apply the estimator some preselection of the $\Delta\hat{\phi}_n$ measurements should be done.

A heuristic way to perform the preselection is suggested as follows:

- Beginning from the lowest "qualified" frequency assume a "target" line ($\tau_1$) which correponds to the $\Delta\hat{\phi}_n$ at this point and to the zero frequency point.
- Take the next valid $\Delta\hat{\phi}_n$ and test if

$$\tau_1-\xi<\omega_n\Delta\hat{\phi}_n<\tau_1+\xi \qquad \text{(V-57)}$$

where $\xi$ is chosen based on some knowledge of the variance of $\Delta\hat{\phi}_n$ i.e. the threshold on $|\gamma|^2$ in the qualifying process.

- If it passed the test it is attributed to the same "target", $\tau_1$.
- If the test is not passed a new "target" line is assumed ($\tau_2$) from $\Delta\hat{\phi}_n$ and the zero frequency.
- Take the next valid $\Delta\hat{\phi}_n$ and perform:

$$\tau_1-\xi < \omega_n\Delta\hat{\phi}_n < \tau_1+\xi$$

if passed attribute to $\tau_1$

if not test for $\tau_2$:

$$\tau_2-\xi < \omega_n\Delta\hat{\phi}_n < \tau_2+\xi$$

if passed attribute to $\tau_2$

if not assume a new target line $\tau_3$

.
.
.

- When this procedure is finished for all qualified frequency bins the data points attributed to each "target" line may be counted and for those targets which pass a certain limit of valid data points the estimator in Eq. (V-54) is applied.

This procedure must be done for all the pairs in the system in order to derive the time delay trace function.

It should be mentioned however that once some targets are detected the test will be performed relative to them first and if the "new" data does not fit within the limits then new "target" lines are assumed.

## H. SYSTEM LEVEL PERFORMANCE

Once the trace functions are derived the bearing estimators derived in Chapter III may be applied. The resultant bearing along with the frequency and power spectral estimate for that frequency can be displayed. In this section some system level performance curves will be presented. System level means that the output beamwidth as defined in Chapter IV is plotted versus the input SNR. The relations used to reflect the phase difference estimation variance back to the input $SNR_i$ are Equations (V-35) and (V-46) and their assumptions set forth:

Eq. (V-46)

$$SNR_i = \frac{|\gamma|}{1-|\gamma|}$$

$$|\gamma| = \frac{SNR_i}{SNR_i+1}$$

Eq. (V-35)

$$\sigma^2_{\Delta\phi ij} = \frac{1-|\gamma|^2}{|\gamma|^2 K_A} = \frac{1-\left(\frac{SNR_i}{SNR_i+1}\right)^2}{\frac{(SNR_i)^2}{(SNR_i+1)^2}} K_A$$

$$= \frac{SNR_i^2+2SNR_i+1-SNR_i^2}{SNR_i^2 K_A}$$

$$= \frac{1+2SNR_i}{SNR_i^2 K_A} \qquad (V-58)$$

$K_A$ was chosen at a value which will validate the gaussian assumption for v(i,j) as defined in Chapter IV, and it was set to 250.

Figures V-4 through V-12 show these performance curves for circular and linear arrays along with the same CRLB presented in Chapter IV but also related to the input SNR.

As expected these curves show the same basic behavior as the estimator level performance.

It should be remembered that the relations used, expecially Eq. (V-46) are somewhat restrictive in their application and as a result the system performance curves shown may not reflect accurately the real situation. Nevertheless they can give a good perspective on the expected performance.

NOTE: The $SNR_i$ is per analysis bandwidth and not total SNR at the input.

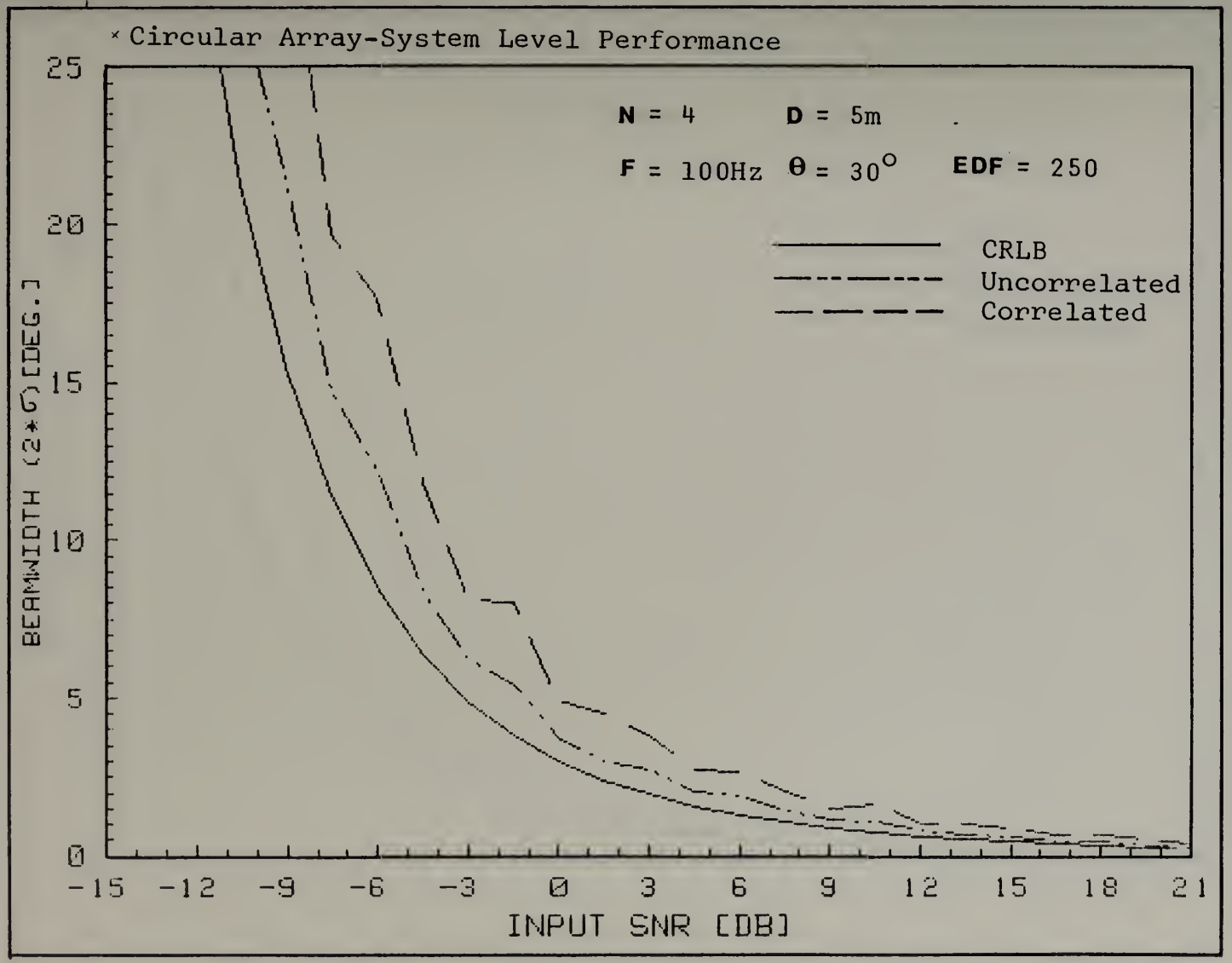
× Circular Array-System Level Performance
N = 4
D = 5m
F = 100Hz
θ = 30°
EDF = 250
CRLB
Uncorrelated
Correlated
BEAMWIDTH (2*σ)[DEG.]
INPUT SNR [DB]
25
20
15
10
5
0
-15
-12
-9
-6
-3
0
3
6
9
12
15
18
21

Figure V-4

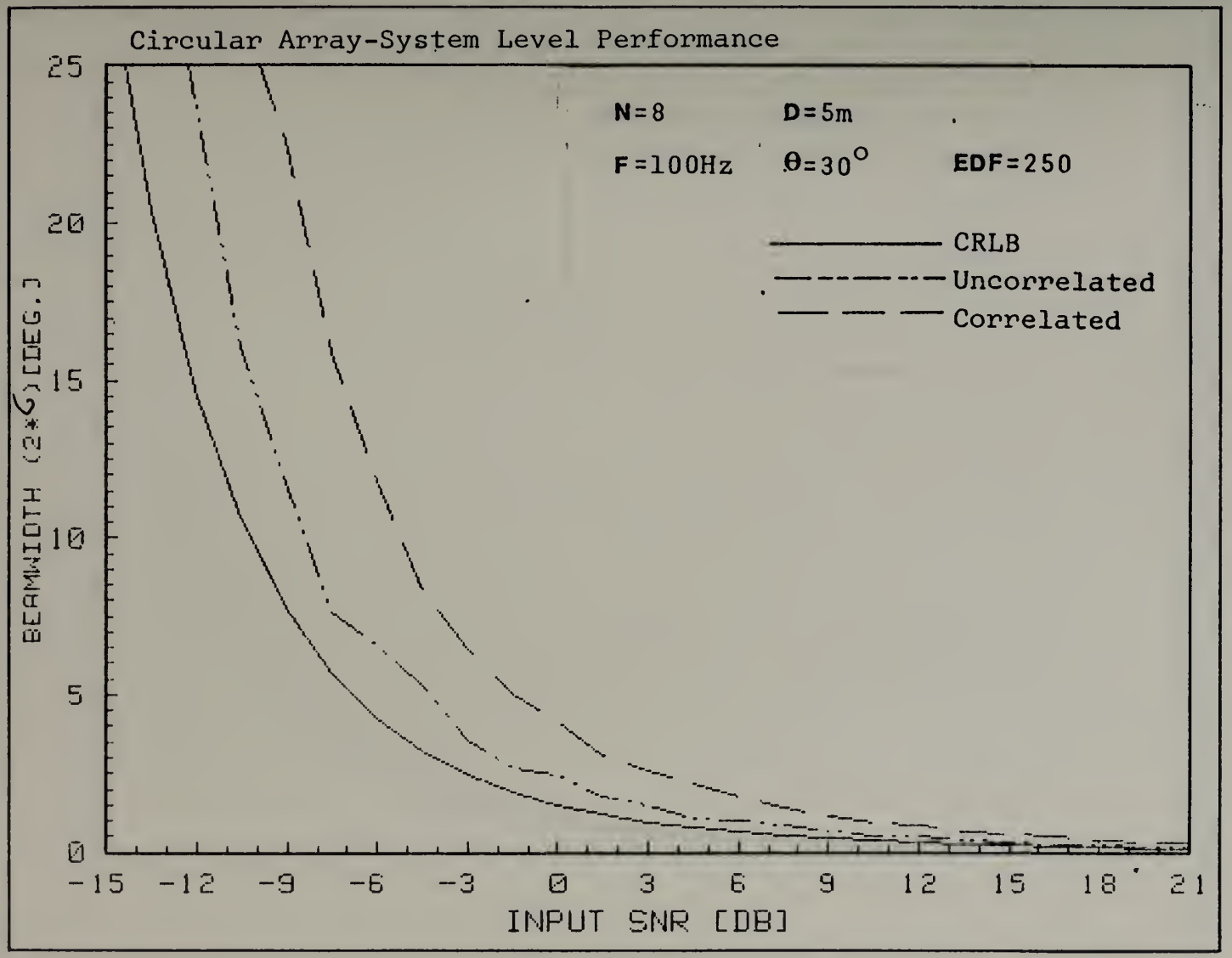
Circular Array-System Level Performance
N=8
D=5m
F=100Hz
θ=30°
EDF=250
CRLB
Uncorrelated
Correlated
BEAMWIDTH (2*σ) [DEG.]
INPUT SNR [DB]
25
20
15
10
5
0
-15
-12
-9
-6
-3
0
3
6
9
12
15
18
21

Figure V-5

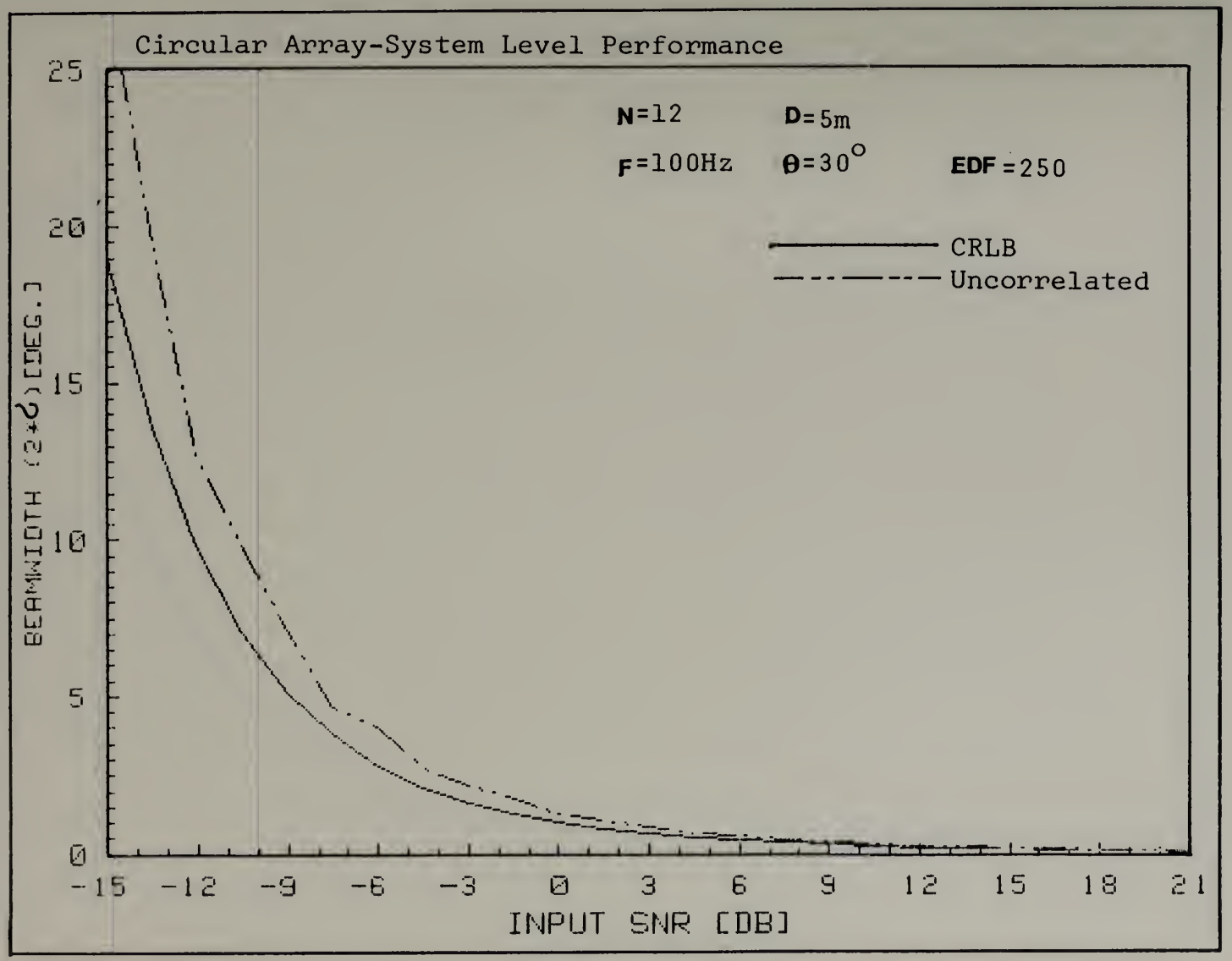
Circular Array-System Level Performance
N=12
D=5m
F=100Hz
θ=30°
EDF=250
CRLB
Uncorrelated
BEAMWIDTH (2*σ)[DEG.]
INPUT SNR [DB]
25
20
15
10
5
0
-15
-12
-9
-6
-3
0
3
6
9
12
15
18
21

Figure V-6

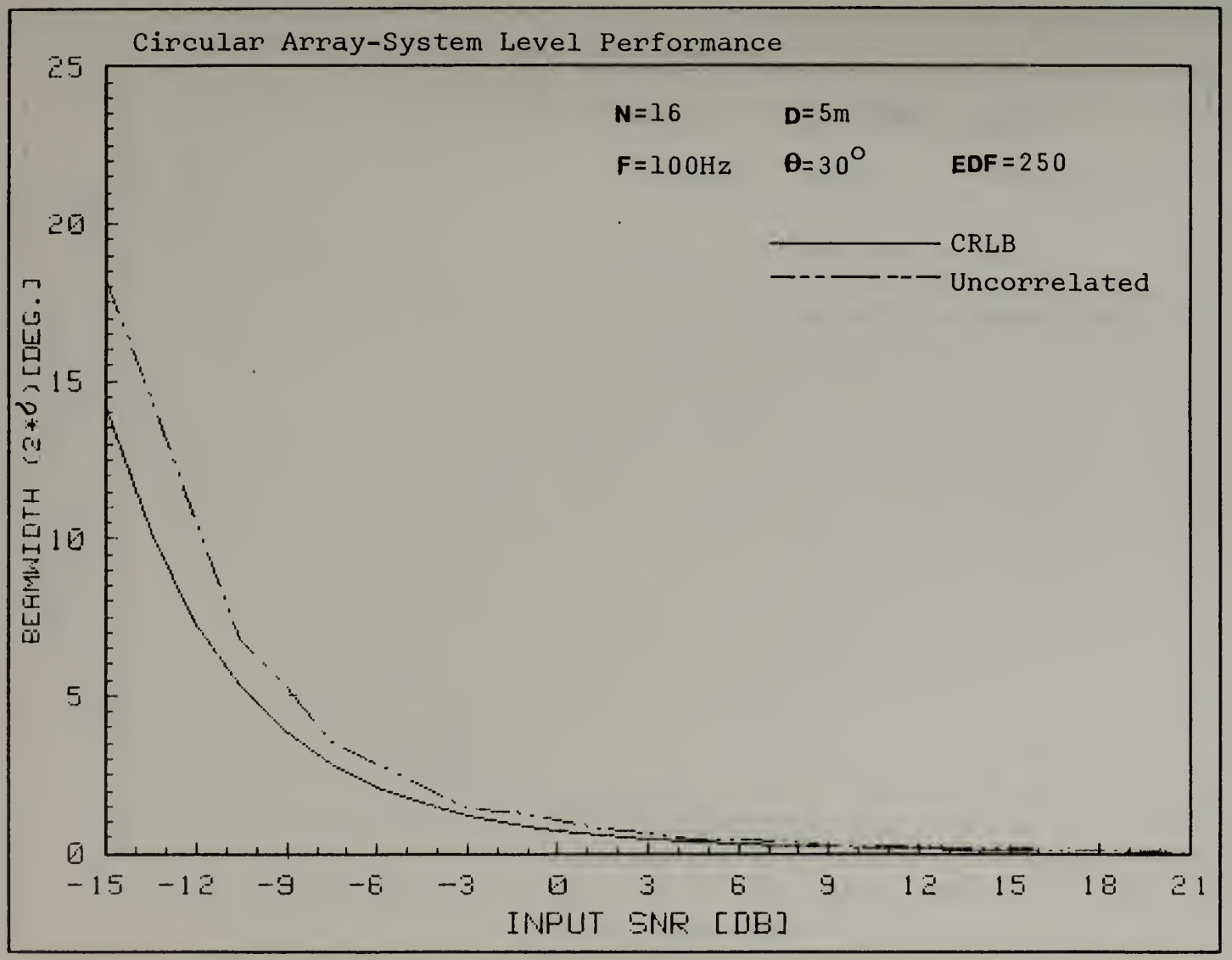
Circular Array-System Level Performance
N=16
D=5m
F=100Hz
θ=30°
EDF=250
CRLB
Uncorrelated
BEAMWIDTH (2*σ) [DEG.]
INPUT SNR [DB]
25
20
15
10
5
0
-15
-12
-9
-6
-3
0
3
6
9
12
15
18
21

Figure V-7

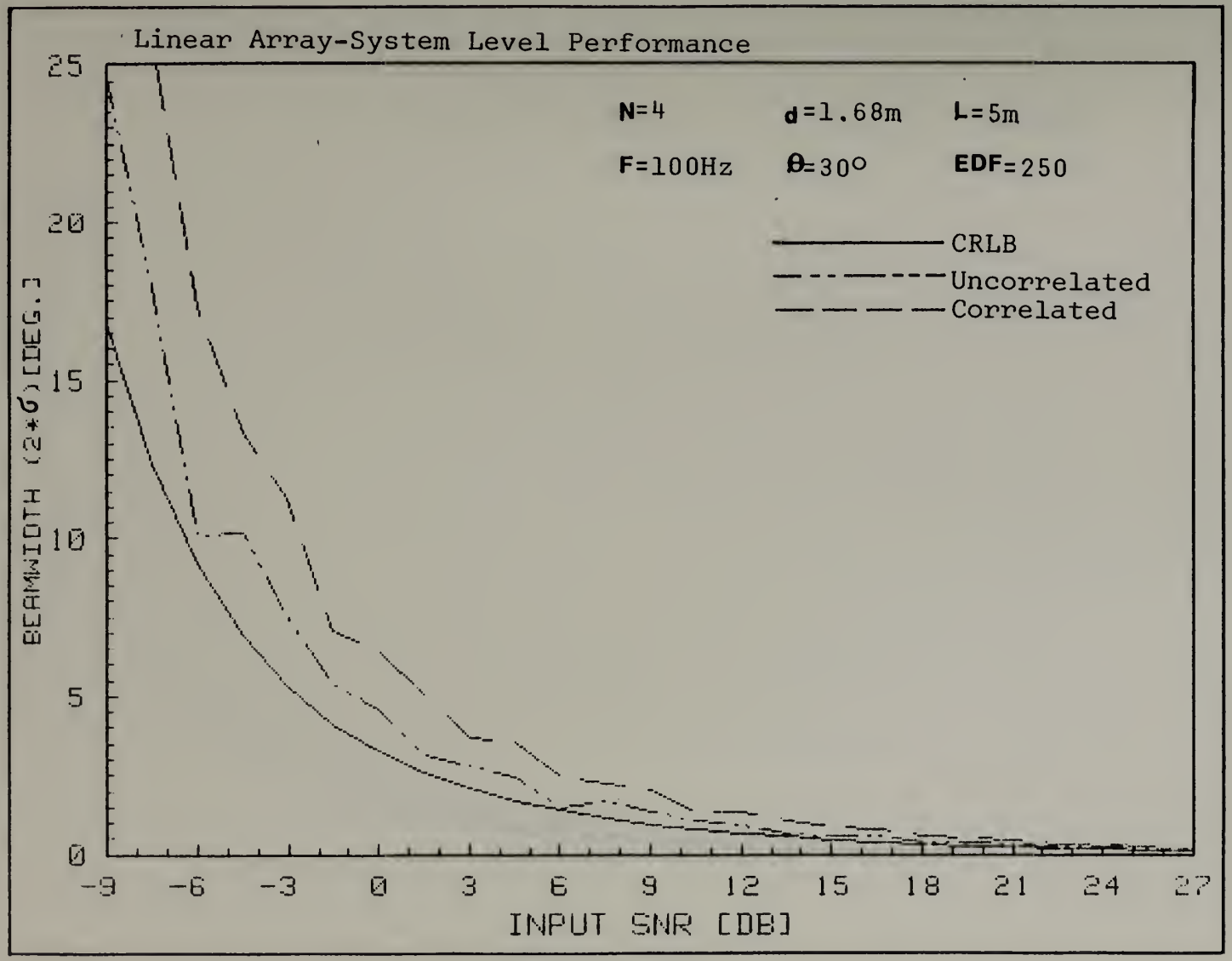
Linear Array-System Level Performance
N=4
d=1.68m
L=5m
F=100Hz
θ=30°
EDF=250
CRLB
Uncorrelated
Correlated
BEAMWIDTH (2*σ)[DEG.]
INPUT SNR [DB]
25
20
15
10
5
0
-9
-6
-3
0
3
6
9
12
15
18
21
24
27

Figure V-8

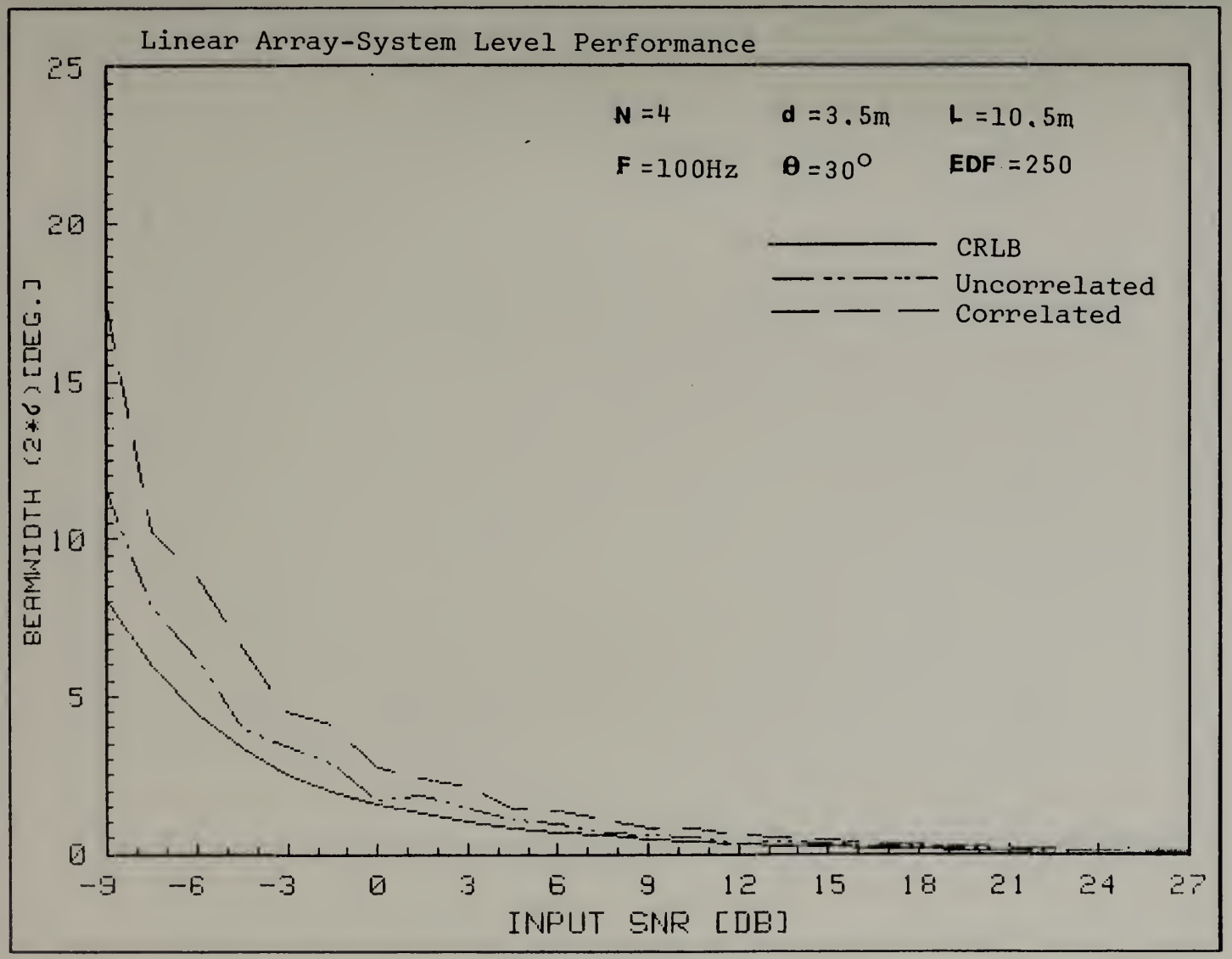
Linear Array-System Level Performance
N =4
d =3.5m
L =10.5m
F =100Hz
θ =30°
EDF =250
CRLB
Uncorrelated
Correlated
BEAMWIDTH (2*σ)[DEG.]
INPUT SNR [DB]
25
20
15
10
5
0
-9
-6
-3
0
3
6
9
12
15
18
21
24
27

Figure V-9

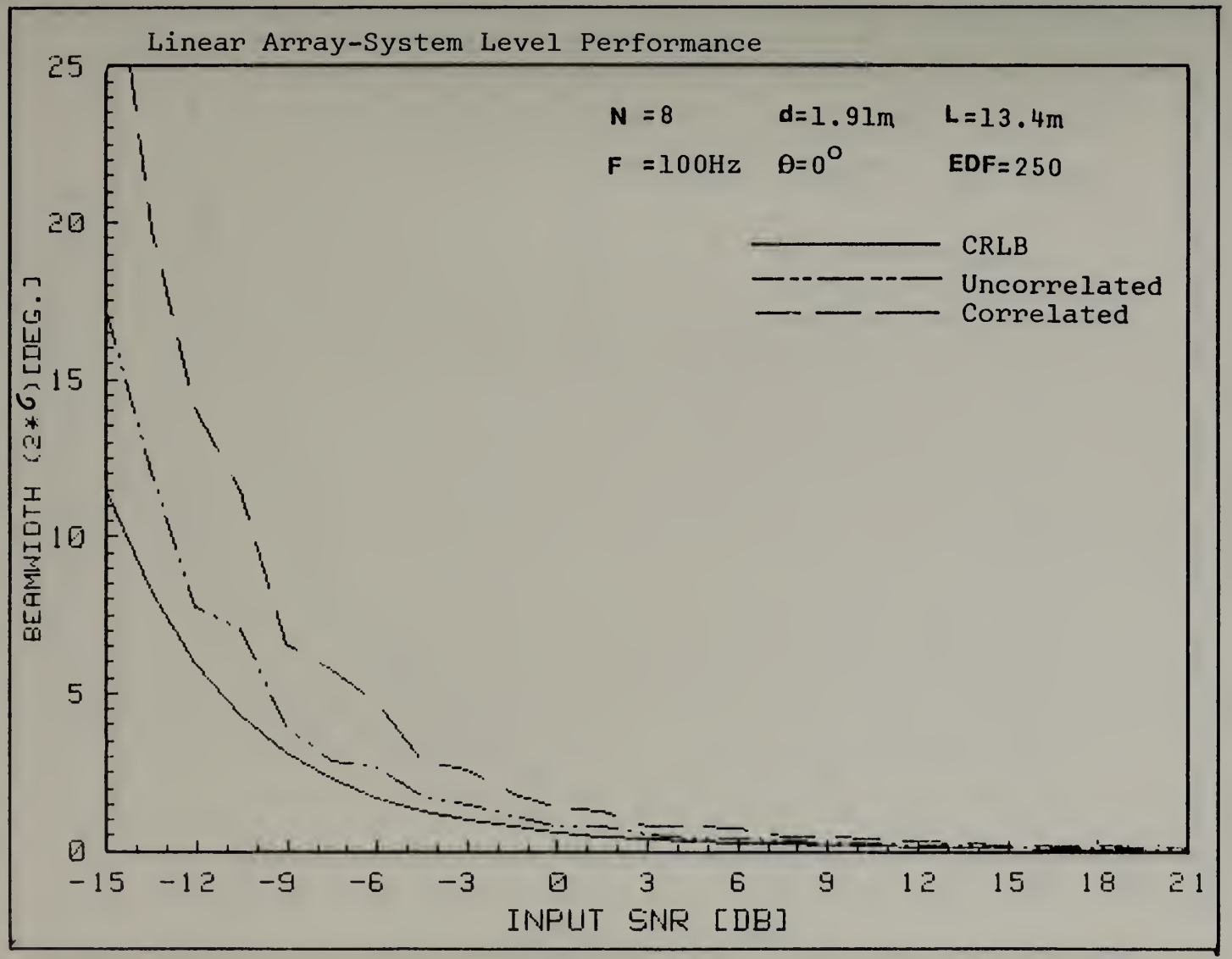
Linear Array-System Level Performance
N =8
d=1.91m
L=13.4m
F =100Hz
θ=0°
EDF=250
CRLB
Uncorrelated
Correlated
BEAMWIDTH (2*σ)[DEG.]
25
20
15
10
5
0
-15
-12
-9
-6
-3
0
3
6
9
12
15
18
21
INPUT SNR [DB]

Figure V-10

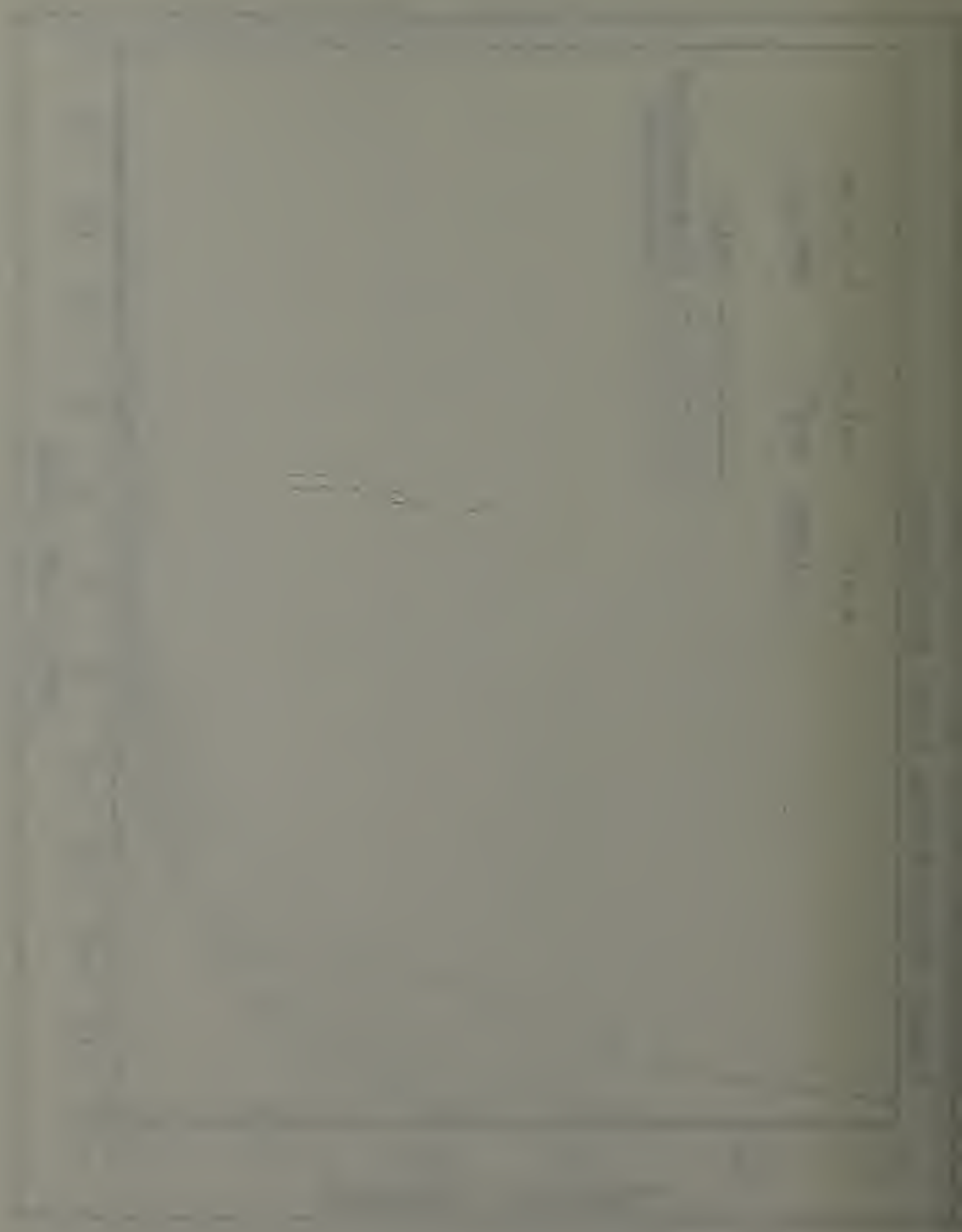

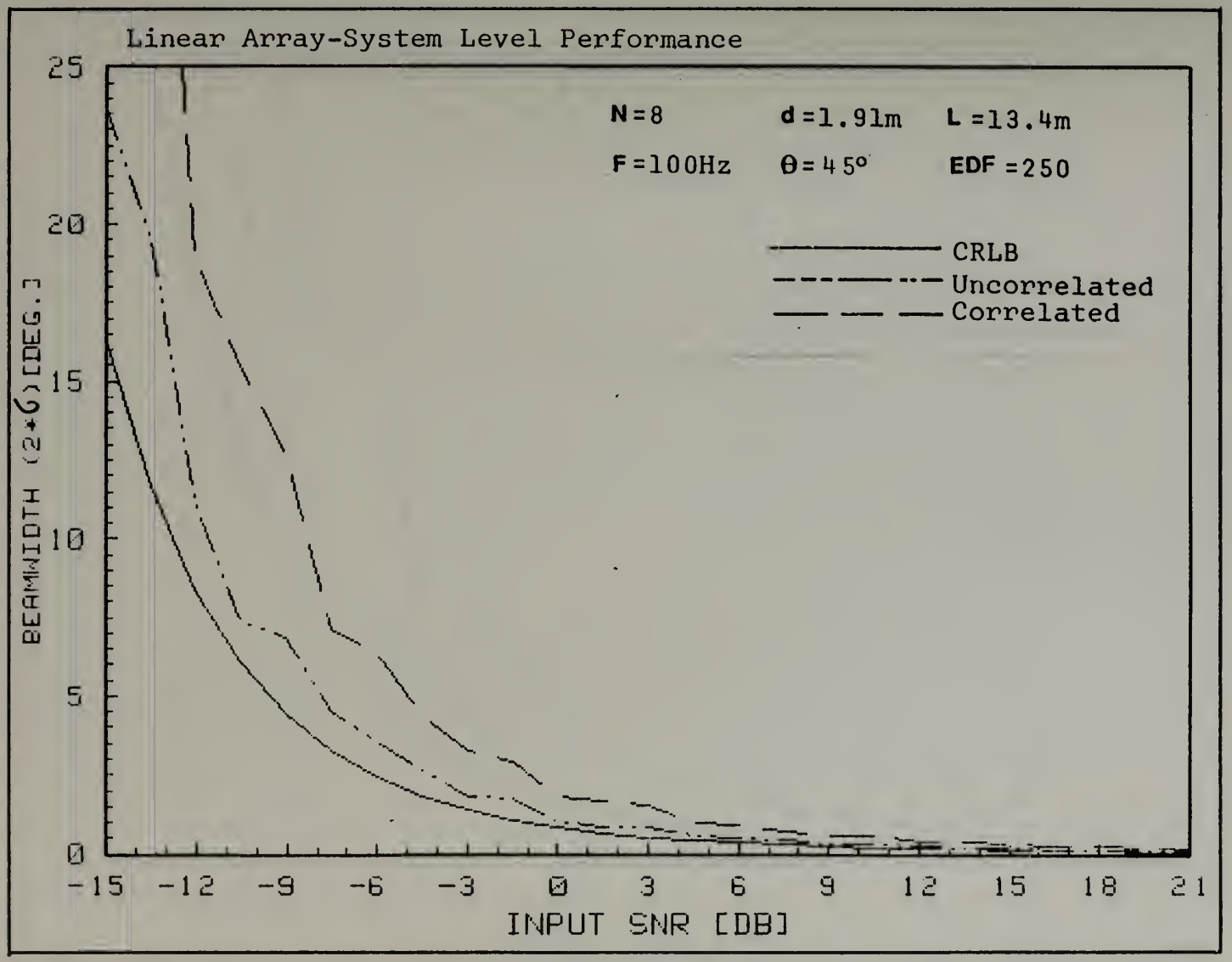
Linear Array-System Level Performance
N=8
d=1.91m
L=13.4m
F=100Hz
θ=45°
EDF=250
CRLB
Uncorrelated
Correlated
BEAMWIDTH (2*σ) [DEG.]
INPUT SNR [DB]
25
20
15
10
5
0
-15
-12
-9
-6
-3
0
3
6
9
12
15
18
21

Figure V-11

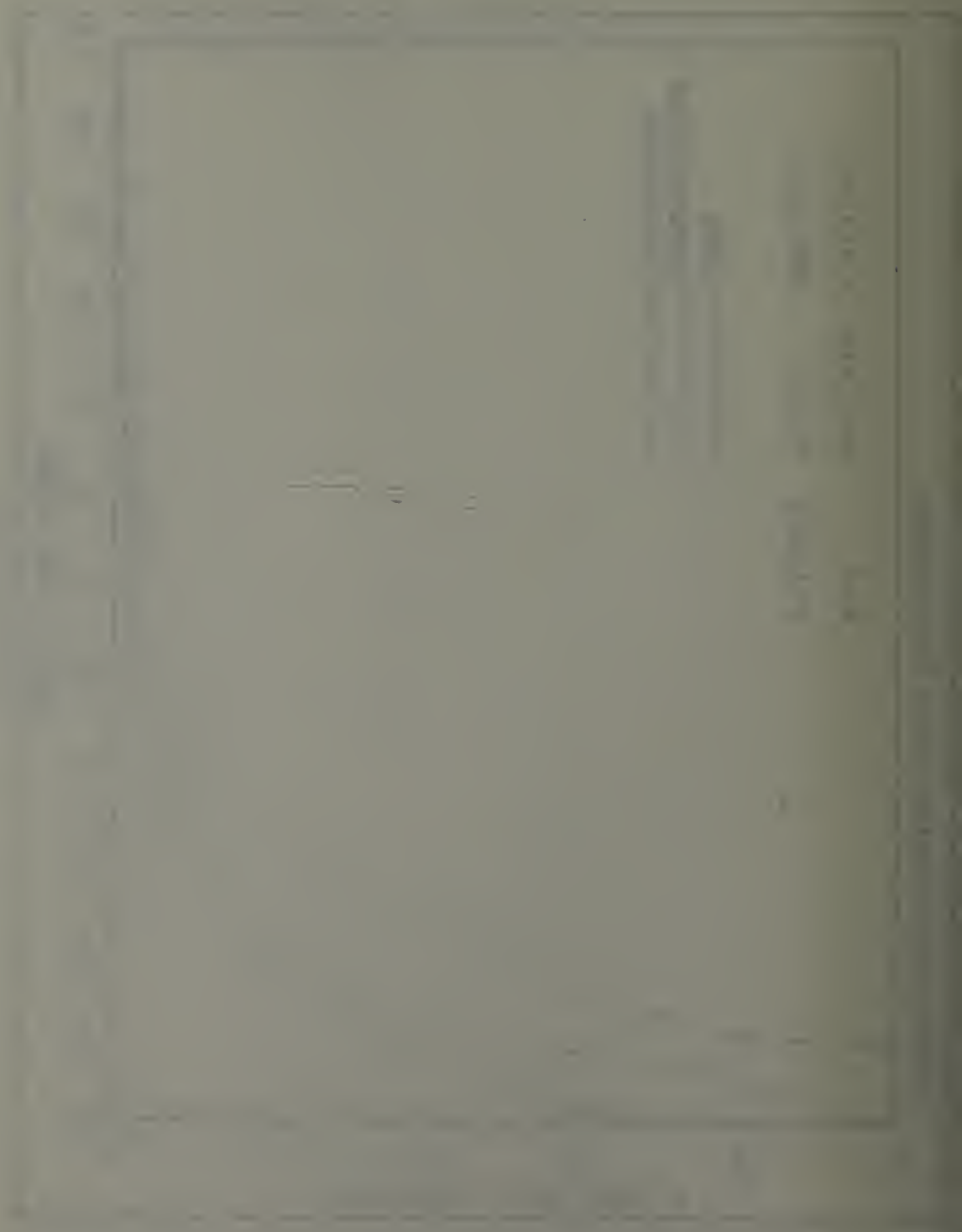

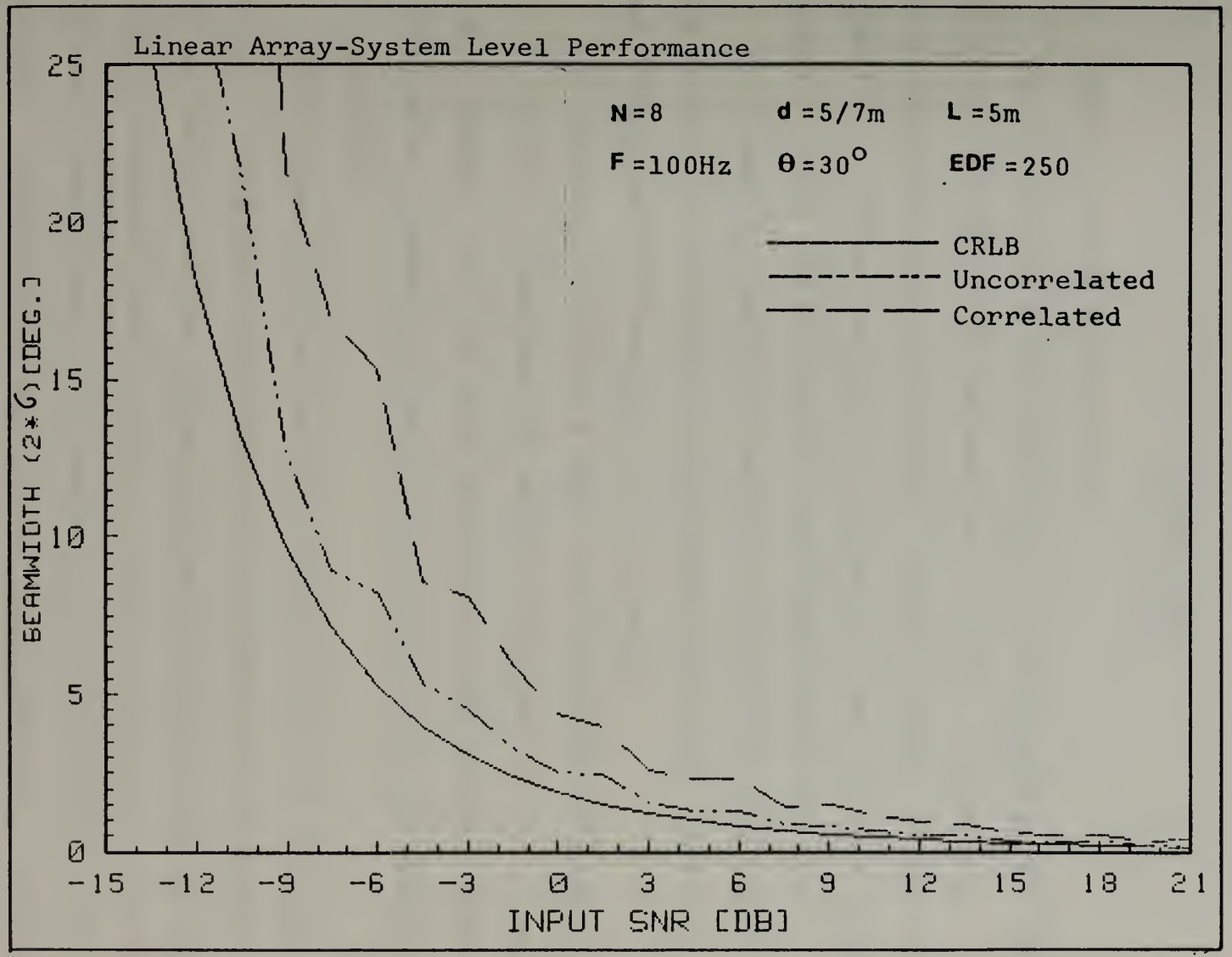
Linear Array-System Level Performance
N=8
d=5/7m
L=5m
F=100Hz
θ=30°
EDF=250
CRLB
Uncorrelated
Correlated
BEAMWIDTH (2*σ)[DEG.]
INPUT SNR [DB]
25
20
15
10
5
0
-15
-12
-9
-6
-3
0
3
6
9
12
15
18
21

Figure V-12

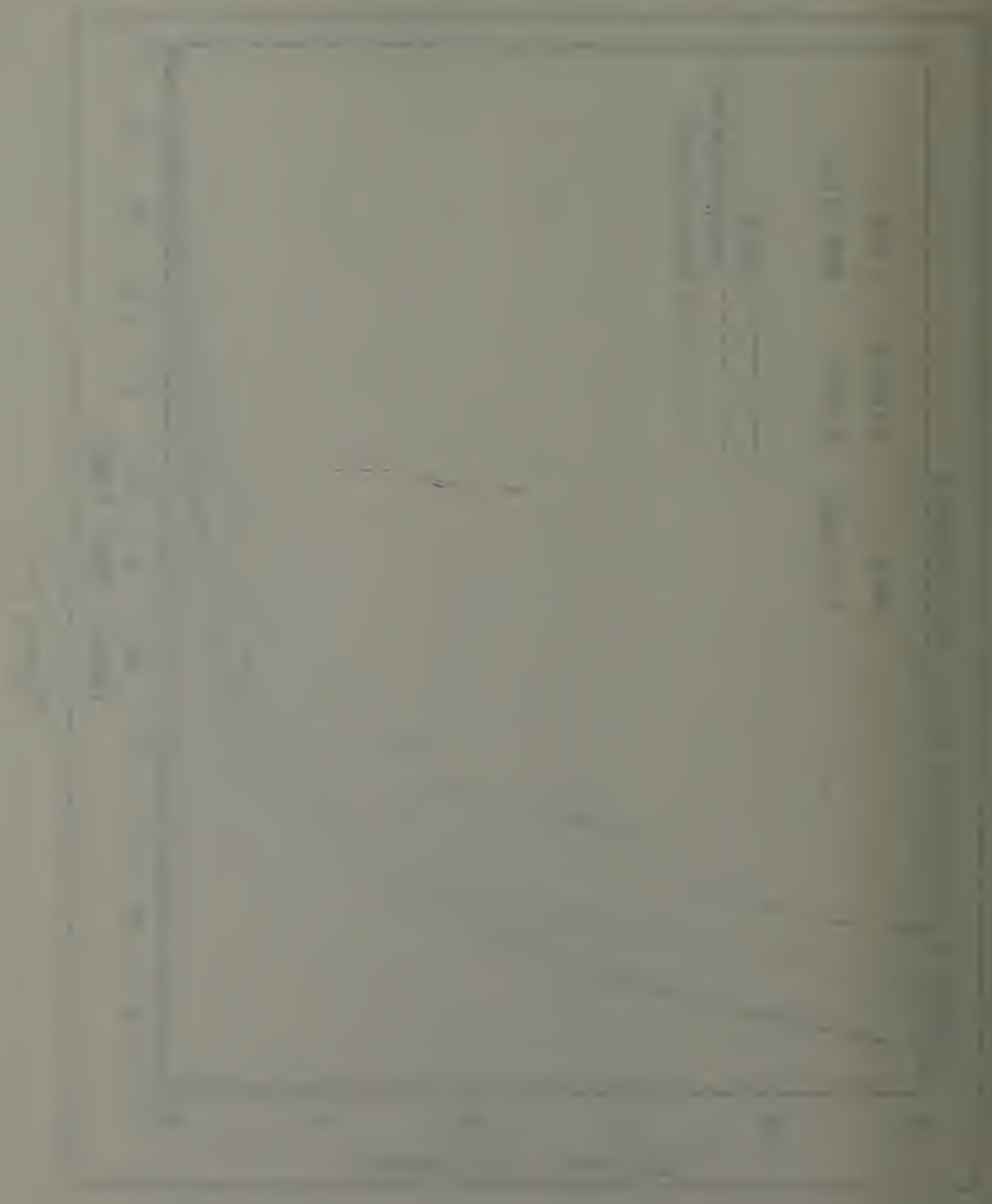

# VI. CONCLUSION

## A. SUMMARY OF THE PRESENT WORK

The aim of the work performed in this dissertation was to develop a solution to the problem of signal processing, particularly spatial processing, of small arrays at low frequencies. Special emphasis was given to the circular array geometry which was motivated by its wide practical use.

As presently available methods looked unsatisfactory to the author, a new concept called here the "trace function" was formulated and developed in this work.

It is based on the fact that the directional information of an incoming plane wave is mainly contained in the received signal phases, or to be more precise, in the relative phase differences between received signals at the various elements of the array.

Those phase differences are representative of the time delay of the plane wave between the elements of the array. The notion is that the phase differences/time delays of the signals received from an array of sensors which has a given defined geometry describe a certain "trace function" which is constant for that array at a given look direction. If one can find a geometry for which the trace function's basic shape is not dependent on the look direction, but only some of its parameters are, then one has a powerful method to correlate

(compare) the trace function of the received signal to a stored replica.

The concept of the trace function was formalized and its application to some typical array geometries was demonstrated. Furthermore, it was shown that for highly symmetric arrays like the circular and linear arrays the trace function reduces to a particularly simple form.

This characteristic was used to derive a relatively simple and manageable MMSE estimator for the bearing of the incoming signal. The estimator is applicable to either narrow band signal by use of phase difference trace function or to the wide band signal using time delay trace function.

The performance of the estimator was checked by simulation and compared to the CRLB as adapted to this application.

A brief performance summary is:

- The estimator exhibits a threshold phenomena called "lock-on" with respect to the variance of the phase difference measurements.
- Within the "lock-on" range the estimator is practically unbiased.
- With respect to beamwidth performance the estimator is asymmtotically efficient.
- It exhibits a saturation point in the number of elements at constant diameter or in the diameter at constant number of element, beyond which only marginal improvement is achieved in beamwidth.

The estimator was applied to both circular and linear arrays and its performance was equally good except for differences imposed by the geometry. (symmetry)

Finally, a system configuration applying trace function principles was outlined and the major problem areas caused by the specific application were identified, reviewed and some suggestions to solutions were made.

As a final conclusion it can be said that this work presented a new way of looking at the available information from an array of sensors. It is clear that the use of the above concept in a generalized replica correlation model is effective for highly symmetrical arrays. As such the circular array is a natural one to be treated this way. For this array the derivations of the bearing estimator is simple and its performance appears to be very good.

However, it should be emphasized that the trace function concept is applicable to any array geometry and for both narrow and wideband processing schemes.

## B. OTHER POSSIBLE APPLICATIONS

The trace function concept and the estimators derived in this work are not limited in their application to the passive sonar case.

They can be applied to related areas like seismic, and ocean wave analysis as well.

In addition the principle can be applied to any other situation in which phase differences and/or time delays within an array of sensor can be measured. The performance curves show that the trace function bearing estimator is very tolerant to phase difference measurement noise, even $30^{\circ}$-$40^{\circ}$ of standard deviation in the measurements can give very good results with reasonable number of elements. This suggests that even in areas where F.F.T. techniques for cross spectral estimation are still beyond the state-of-the-art (like microwave frequencies) available hardware exists for phase difference or time of arrival measurements which may be sufficient to allow application of the trace function concept.

## C. PROPOSED FUTURE WORK

Although the trace function principle was developed in this work there are a vast number of points to be checked. In addition several extensions and applications should be investigated.

Some proposed topics are:

1. Testing the concept of 3 possible ways:
   a. Computer simulation of a <u>whole</u> system (similar to Figure V-1) including model of the sea.
   b. Laboratory simulation.
   c. Testing on real data at sea.
2. Investigation of the weighted MMSE , optimization of the weights and their possible adaptive derivation.

3. Derivation of a minimization algorithm for "non-analytic" trace function.
4. Further formalization and development of the phase preserving spatial decorrelation.
5. Investigation of the multiple target discrimination for both narrow and wide band targets.

The above are only a few of the possible topics opened up by the introduction of the trace function principle.

## APPENDIX A

## TRACE FUNCTION DERIVATIONS

### 1. Circular Array

This derivation is related to Figure II-4. Using Eq. (II-2) the following is the interpretation of the parameters for circular arrays:

$$\bar{\alpha} = -\sin\theta\hat{x} + \cos\theta\hat{y}$$

$$\bar{r}_i = R\left[-\sin\theta\frac{2\pi}{N}\, i\hat{x} + \cos\frac{2\pi}{N}\, i\hat{y}\right]$$

where $\hat{x}$, $\hat{y}$ are unit vectors in x and y directions.

Inserting in Equation (II-6):

$$\Delta\tau_{ij} = \frac{R}{C}\,(-\sin\theta\hat{x} + \cos\theta\hat{y})\cdot\left[-\left(\sin\frac{2\pi}{N}\, i - \sin\frac{2\pi}{N}\, j\right)\hat{x}\right.$$

$$\left. + \left(\cos\frac{2\pi}{N}\, i - \cos\frac{2\pi}{N}\, j\right)\hat{y}\right]$$

$$= \frac{R}{C}\left[\cos\theta\left(\cos\frac{2\pi}{N}\, i - \cos\frac{2\pi}{N}\, j\right) + \sin\theta\left(\sin\frac{2\pi}{N}\, i - \sin\frac{2\pi}{N}\, j\right)\right]$$

$$= \frac{R}{C}\left[\cos\left(\frac{2\pi}{N}\, i - \theta\right) - \cos\left(\frac{2\pi}{N}\, j - \theta\right)\right]$$

$$= -2\frac{R}{C}\sin\left[\frac{\pi}{N}\,(i+j) - \theta\right]\sin\left[\frac{\pi}{N}\,(i-j)\right] \qquad \text{(A-1)}$$

and for phase difference Eq. (II-5):

$$\Delta\phi_{ij,\ell} = \Delta\tau_{ij}\,\omega_\ell = -\frac{2\pi D}{\lambda_\ell}\sin\left[\frac{\pi}{N}(i+j) - \theta\right]\sin\left[\frac{\pi}{N}(i-j)\right] \quad \text{(A-2)}$$

2. Linear Array

This derivation is related to Figure II-15. The following are the various terms:

$$\bar{\alpha} = \sin\theta\hat{x} + \cos\theta\hat{y}$$

$$\bar{r}_i = d\,i\,\hat{x}$$

Inserting in Eq. (II-6):

$$\Delta\tau_{ij} = \frac{d}{c}(\sin\theta\hat{x} + \cos\theta\hat{y})\cdot[(i-j)\hat{x}]$$

$$= \frac{d}{c}\sin\theta(i-j) \quad \text{(A-3)}$$

and for phase difference Eq. (II-5):

$$\Delta\phi_{ij,\ell} = \Delta\tau_{ij}\,\omega_\ell = \frac{2\pi d}{\lambda_\ell}(i-j)\sin\theta \quad \text{(A-4)}$$

# APPENDIX B

## 1. Computer Program for Three Dimensional Plotting of the Trace Functions for Circular Arrays.

The following computer program as well as all the other programs in this dissertation were developed and executed on a Hewlett-Packard 9845T computer.

```
10    ! ************************************************************************
20    ! *  THREE DIMENSIONAL TRACE FUNCTION PLOTTING FOR CIRCULAR ARRAY        *
30    ! *        PARAMETER DEFINITION                                          *
40    ! *        N - Number Of Elements                                        *
50    ! *        A - Inclination Angle Of The Plot (From the vertical)         *
60    ! *        F - Frequency                                                 *
70    ! *        C - Speed Of Sound                                            *
80    ! *        D - Diameter                                                  *
90    ! *        Theta - Bearing                                               *
100   ! *                                                                      *
110   ! *        NOTE: If parameters are changed, it may be necessary to       *
120   ! *              change scaling !                                        *
130   ! ************************************************************************
140   N=32
150   A=PI/8
160   F=250
170   C=1500
180   D=5
190   Theta=PI/4
200   A1=TAN(A)
210   PLOTTER IS 13,"GRAPHICS"
220   GRAPHICS
230   FRAME
240   PRINTER IS 0
250   RAD
260   LOCATE 10,10+84*N*(1+SIN(A))/((N+2)*COS(A)),10,90
270   K=2*PI*F*D/C
280   Xmin=0
290   Xmax=N*(1+SIN(A))+4
300   Ymin=-6
310   Ymax=N+6
320   SCALE Xmin,Xmax,Ymin,Ymax
330   AXES 1,1/2,0,-6,N/2+1,6
340   CSIZE 3.3
```

```
350   LORG 5
360   FOR X=1 TO 32 STEP 4
370   MOVE X,-7.5
380   LABEL X
390   NEXT X
400   LORG 2
410   CSIZE 3.2
420   MOVE 33,-8
430   LABEL "i[Element #]"
440   CSIZE 3.3
450   LORG 8
460   FOR Y=-6 TO 6 STEP 3
470   MOVE -.25,Y
480   LABEL Y
490   NEXT Y
500   LORG 1
510   MOVE -4,7.5
520   LABEL "[Rad]"
530   LORG 5
540   CSIZE 3.2
550   LORG 8
560   MOVE 13.5,34
570   LABEL "j"
580   MOVE 13.5,32
590   LABEL "[Element #]"
600   LORG 1
610   CSIZE 3.5
620   MOVE -2.5,N+8.5
630   LABEL "PHASE DIFFERENCE TRACE FUNCTION FOR A CIRCULAR ARRAY "
640   CSIZE 3.2
650   MOVE 0,N+6.6
660   LABEL "Bearing=";Theta*180/PI;"DEG.";"    Frequency=";F;"Hz";"    Diameter
=";D;"Meter"
670   FOR J=0 TO N-1
680   MOVE J*A1+1,J
```

```
690   DRAW J*A1+1,-K*SIN(PI*J/N-Theta)*SIN(PI*-J/N)+J
700   MOVE J*A1+1,J
710   FOR I=0 TO N-1
720   RPLOT I,-K*SIN(PI*(I+J)/N-Theta)*SIN(PI*(I-J)/N),1
730   NEXT I
740   DRAW J*A1+N,J
750   NEXT J
760   FOR I=0 TO N-1
770   MOVE I+1,0
780   FOR J=0 TO N-1
790   DRAW J*A1+I+1,J-K*SIN(PI*(I+J)/N-Theta)*SIN(PI*(I-J)/N)
800   NEXT J
810   NEXT I
820   END
```

2. Computer Program for Three Dimensional Plotting of the Trace Function for Linear Arrays.

Following is the listing of the computer program for the plotting of the trace function for linear arrays.

```
10    ! ************************************************************************
20    ! *  THREE DIMENSIONAL TRACE FUNCTION PLOTTING FOR LINEAR ARRAY          *
30    ! *        PARAMETER DEFINITION                                          *
40    ! *        N - Number Of Elements                                        *
50    ! *        A - Inclination Angle Of The Plot (From the vertical)         *
60    ! *        F - Frequency                                                 *
70    ! *        C - Speed Of Sound                                            *
80    ! *        D - Interelement Spacing                                      *
90    ! *        Theta - Bearing                                               *
100   ! *                                                                      *
110   ! *        NOTE: If parameters are changed, it may be necessary to       *
120   ! *              change scaling !                                        *
130   ! ************************************************************************
140   N=32
150   A=PI/8
160   F=250
170   C=1500
180   D=.1613
190   Theta=3*PI/2
200   A1=TAN(A)
210   PLOTTER IS 13,"GRAPHICS"
220   GRAPHICS
230   FRAME
240   PRINTER IS 0
250   RAD
260   LOCATE 10,10+84*N*(1+SIN(A))/((N+2)*COS(A)),10,90
270   K=2*PI*F*D/C
280   Xmin=0
290   Xmax=N*(1+SIN(A))+4
300   Ymin=-6
310   Ymax=N+6
320   SCALE Xmin,Xmax,Ymin,Ymax
330   AXES 1,1/2,0,-6,N/2+1,6
340   CSIZE 3.3
350   LORG 5
```

```
360   FOR X=1 TO 32 STEP 4
370   MOVE X,-7.5
380   LABEL X
390   NEXT X
400   LORG 2
410   CSIZE 3.2
420   MOVE 33,-8
430   LABEL "i[Element #]"
440   CSIZE 3.3
450   LORG 8
460   FOR Y=-6 TO 6 STEP 3
470   MOVE -.25,Y
480   LABEL Y
490   NEXT Y
500   LORG 1
510   MOVE -4,7.5
520   LABEL "[Rad]"
530   LORG 5
540   CSIZE 3.2
550   LORG 8
560   MOVE 11.5,34
570   LABEL "j"
580   MOVE 11.5,32
590   LABEL "[Element #]"
600   LORG 1
610   CSIZE 3.5
620   MOVE -2.5,N+8.5
630   LABEL "PHASE DIFFERENCE TRACE FUNCTION FOR A LINEAR ARRAY "
640   CSIZE 3.2
```

```
650   MOVE 0,N+6.6
660   LABEL "Bearing=";Theta*180/PI;"DEG.";"    Frequency=";F;"Hz";"    Length="
;5;"Meter"
670   FOR J=0 TO N-1
680   MOVE J*A1+1,J
690   DRAW J*A1+1,J+K*-J*SIN(Theta)
700   MOVE J*A1+1,J
710   FOR I=0 TO N-1
720   RPLOT I,K*(I-J)*SIN(Theta)
730   NEXT I
740   DRAW J*A1+N,J
750   NEXT J
760   FOR I=0 TO N-1
770   MOVE I+1,0
780   FOR J=0 TO N-1
790   DRAW J*A1+I+1,J+K*(I-J)*SIN(Theta)
800   NEXT J
810   NEXT I
820   END
```

3. Computer Program for Three Dimensional Plotting of the Trace Function for Random Arrays.

Following is the listing of the computer program for the plotting of the trace function for random arrays. The same program may be used for conformal arrays.

```
10    ! ************************************************************************
20    ! *  THREE DIMENSIONAL TRACE FUNCTION PLOTTING FOR RANDOM ARRAY          *
30    ! *        PARAMETER DEFINITION                                          *
40    ! *        N - Number Of Elements                                        *
50    ! *        A - Inclination Angle Of The Plot (From the vertical)         *
60    ! *        F - Frequency                                                 *
70    ! *        C - Speed Of Sound                                            *
80    ! *        Arr(i,j) - Array Of The Vectors Deffining The Element         *
90    ! *                   Locations In Polar Coordinates                     *
100   ! *              Where  Arr(i,1) - Vector Length In Meters               *
110   ! *                     Arr(i,2) - Vector Direction In Radians           *
120   ! *        Theta - Bearing                                               *
130   ! *                                                                      *
140   ! *        NOTE: If parameters are changed, it may be necessary to       *
150   ! *              change scaling !                                        *
160   ! ************************************************************************
170   OPTION BASE 1
180   DIM Arr(19,2)
190   Arr(1,1)=2
200   Arr(2,1)=.625
210   Arr(3,1)=1.25
220   Arr(4,1)=2.125
230   Arr(5,1)=.752
240   Arr(6,1)=1.625
250   Arr(7,1)=2.25
260   Arr(8,1)=1
270   Arr(9,1)=1.5625
280   Arr(10,1)=2.075
290   Arr(11,1)=1.6875
300   Arr(12,1)=.6875
310   Arr(13,1)=1.45
320   Arr(14,1)=2.1875
330   Arr(15,1)=.9375
340   Arr(16,1)=2.2
350   Arr(17,1)=1.4375
```

```
360   Arr(18,1)=1.75
370   Arr(19,1)=2.5
380   Arr(1,2)=13*PI/180
390   Arr(2,2)=31.5*PI/180
400   Arr(3,2)=52*PI/180
410   Arr(4,2)=86*PI/180
420   Arr(5,2)=90*PI/180
430   Arr(6,2)=103*PI/180
440   Arr(7,2)=127.5*PI/180
450   Arr(8,2)=141*PI/180
460   Arr(9,2)=167.5*PI/180
470   Arr(10,2)=194*PI/180
480   Arr(11,2)=210*PI/180
490   Arr(12,2)=233*PI/180
500   Arr(13,2)=261*PI/180
510   Arr(14,2)=281*PI/180
520   Arr(15,2)=290*PI/180
530   Arr(16,2)=313*PI/180
540   Arr(17,2)=321*PI/180
550   Arr(18,2)=347*PI/180
560   Arr(19,2)=355*PI/180
570   N=19
580   A=PI/8
590   F=250
600   C=1500
610   Theta=PI/6
620   A1=TAN(A)
630   PLOTTER IS 13,"GRAPHICS"
640   GRAPHICS
650   FRAME
660   PRINTER IS 0
```

```
670   RAD
680   LOCATE 12,12+84*N*(1+SIN(A))/((N+2)*COS(A)),12,88
690   K=2*PI*F/C
700   Xmin=0
710   Xmax=N*(1+SIN(A))+1
720   Ymin=-6
730   Ymax=N+6
740   SCALE Xmin,Xmax,Ymin,Ymax
750   AXES 1,1/2,0,Ymin,1,6
760   CSIZE 3.3
770   LORG 5
780   FOR X=1 TO 19 STEP 2
790   MOVE X,-7
800   LABEL X
810   NEXT X
820   LORG 2
830   CSIZE 3.2
840   MOVE 20,-7.5
850   LABEL "i[Element #]"
860   CSIZE 3.3
870   LORG 8
880   FOR Y=Ymin TO -Ymin STEP 3
890   MOVE -.25,Y
900   LABEL Y
910   NEXT Y
920   LORG 1
930   MOVE -2.5,7.5
940   LABEL "[Rad]"
950   LORG 5
960   CSIZE 3.2
970   LORG 8
980   MOVE 7,N+3
990   LABEL "j"
1000  MOVE 7,N+1.5
1010  LABEL "[Element #]"
```

```
1020  LORG 1
1030  CSIZE 3.5
1040  MOVE -2,N+7.5
1050  LABEL "PHASE DIFFERENCE TRACE FUNCTION FOR A RANDOM ARRAY "
1060  CSIZE 3.3
1070  MOVE 5,N+6
1080  LABEL "Bearing=";Theta*180/PI;"DEG.";"    Frequency=";F;"Hz"
1090  FOR J=0 TO N-1
1100  MOVE J*A1+1,J
1110  DRAW J*A1+1,K*(Arr(1,1)*COS(Arr(1,2)-Theta)-Arr(J+1,1)*COS(Arr(J+1,2)-Thet
a))+J
1120  MOVE J*A1+1,J
1130  FOR I=0 TO N-1
1140  RPLOT I,K*(Arr(I+1,1)*COS(Arr(I+1,2)-Theta)-Arr(J+1,1)*COS(Arr(J+1,2)-Thet
a))
1150  NEXT I
1160  DRAW J*A1+N,J
1170  NEXT J
1180  FOR I=0 TO N-1
1190  MOVE I+1,0
1200  FOR J=0 TO N-1
1210  DRAW J*A1+I+1,J+K*(Arr(I+1,1)*COS(Arr(I+1,2)-Theta)-Arr(J+1,1)*COS(Arr(J+1
,2)-Theta))
1220  NEXT J
1230  NEXT I
1240  END
```

## APPENDIX C

## SIMULATION AND THE NOISE MODEL

The simulation of the performance was done by generating a noisy trace function (Eq. III-1).

$$\hat{\Delta\phi}_{ij} = f_{Tr}(i,j,\theta) + v(i,j) \qquad \text{(C-1)}$$

and applying the MMSE estimator.

The trace function $f_{Tr}(i,j,\theta)$ is generated simply by calculating its value for all "i" and "j" at a given bearing "$\theta$". The additive noise v(i,j) is the more problematic term and its definitions will be discussed next.

### 1. Noise Model

In Ref. [29] it was shown that for high SNR or conversely for low SNR with long averaging time (high K) the error in the phase difference estimate may be considered approximately as a gaussian distributed noise with zero mean and the variance given by Eq. (V-35)

$$\sigma^2_{\hat{\Delta\phi}_{ij}} = \frac{1-|\gamma_{ij}|^2}{|\gamma_{ij}|^2 K_A} \qquad \text{(C-2)}$$

at a specific frequency.

This assumption of gaussian noise was used throughout the simulation and to validate it $K_A$ was chosen to be 250.

This K corresponds, by using Eq. (V-37), to a T (data stationarity time) of approximately 85 seconds when assuming one hertz frequency resolution in processing. This figure is a reasonable one for real data in the ocean.

The values of coherence square used were in range ~ $10^{-3}$ to 0.985 which corresponds to input SNR of -15 to +21 dB (using Eq. (V-46)).

The next point to be considered is the covariance between the various noise terms. In the phase difference estimation process each element is used in 2N-1 pairs so that obviously there is a certain correlation between these pairs. The following model is assumed for the covariance matrix which takes in consideration the various pairs of terms of the trace function. Table C-1 summarizes the above model.

| # | DESCRIPTION | TERM FORM | COVARIANCE |
|---|---|---|---|
| 1 | Pairs without common elements | $\Delta\hat{\phi}_{ij}$ and $\Delta\hat{\phi}_{k\ell}$ | 0 |
| 2 | Pairs with one common element | $\Delta\hat{\phi}_{ij}$ and $\Delta\hat{\phi}_{ik}$ | 0.5 |
| | | $\Delta\hat{\phi}_{ij}$ and $\Delta\hat{\phi}_{ki}$ | -0.5 |
| 3 | Pairs with two common elements | $\Delta\hat{\phi}_{ij}$ and $\Delta\hat{\phi}_{ii}$ | 0 |
| | | $\Delta\hat{\phi}_{ij}$ and $\Delta\hat{\phi}_{jj}$ | 0 |
| 4 | Pairs with all common elements | $\Delta\hat{\phi}_{ij}$ and $\Delta\hat{\phi}_{ji}$ | -1 |
| | | $\Delta\hat{\phi}_{ij}$ and $\Delta\hat{\phi}_{ij}$ | 1 |

Table C-1

The covariance array is basically a four dimensional array which takes in consideration all the above pairs of terms. But for ease of perception and calculation this array was described as a two dimensional array which is composed of submatrices.

This covariance matrix is of order $N^2 x N^2$ and corresponds to the $N^2$ noise terms of the trace function.

An example of such a covariance matrix for a 4 element array (16 term trace function) is shown in Figure C-1.

The method in Ref. [4] was used to obtain correlated gaussian random variables having a specified covariance matrix. Specifically, defining the above $N^2 x N^2$ covariance matrix as Q then

$$Q = U \Lambda U^t \qquad \text{(C-3)}$$

where U - is a matrix whose columns are the eigenvectors of Q

$\Lambda$ - is a diagonal matrix whose elements on the diagonal are the eighenvalues of Q

$U^t$ - transpose

The next step will be to generate $N^2$ independent gaussian random variables with zero mean and unity variance.

This operation can be done by several methods, in the present case the polar transformation method was used [4] to generate a pair of gaussian independent random variables from a pair of uniform random variables which are available as a built-in function in the computer.

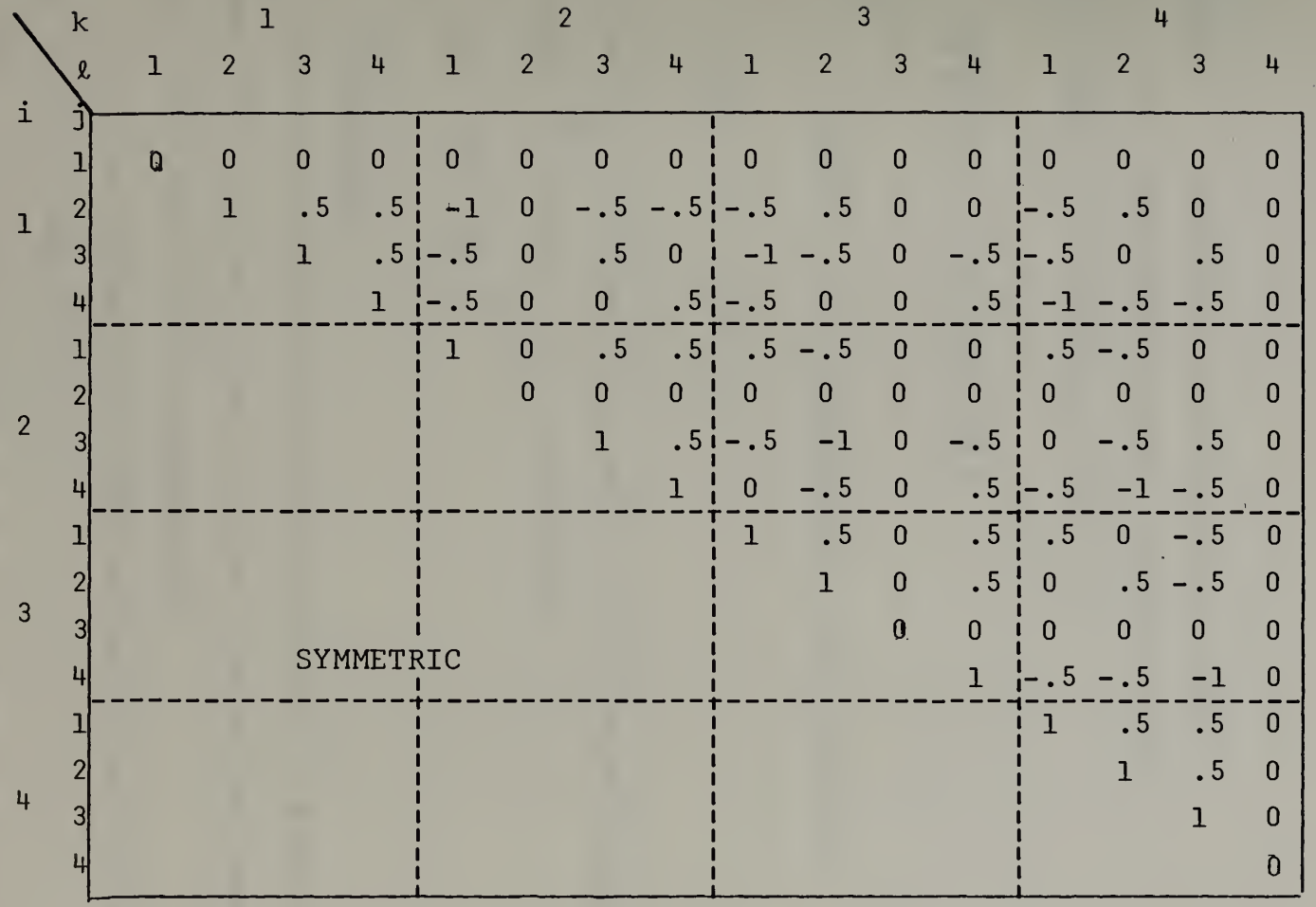


| i | j | k=1, ℓ=1 | k=1, ℓ=2 | k=1, ℓ=3 | k=1, ℓ=4 | k=2, ℓ=1 | k=2, ℓ=2 | k=2, ℓ=3 | k=2, ℓ=4 | k=3, ℓ=1 | k=3, ℓ=2 | k=3, ℓ=3 | k=3, ℓ=4 | k=4, ℓ=1 | k=4, ℓ=2 | k=4, ℓ=3 | k=4, ℓ=4 |
|---|---|---|---|---|---|---|---|---|---|---|---|---|---|---|---|---|---|
| 1 | 1 | 0 | 0 | 0 | 0 | 0 | 0 | 0 | 0 | 0 | 0 | 0 | 0 | 0 | 0 | 0 | 0 |
| | 2 | | 1 | .5 | .5 | -1 | 0 | -.5 | -.5 | -.5 | .5 | 0 | 0 | -.5 | .5 | 0 | 0 |
| | 3 | | | 1 | .5 | -.5 | 0 | .5 | 0 | -1 | -.5 | 0 | -.5 | -.5 | 0 | .5 | 0 |
| | 4 | | | | 1 | -.5 | 0 | 0 | .5 | -.5 | 0 | 0 | .5 | -1 | -.5 | -.5 | 0 |
| 2 | 1 | | | | | 1 | 0 | .5 | .5 | .5 | -.5 | 0 | 0 | .5 | -.5 | 0 | 0 |
| | 2 | | | | | | 0 | 0 | 0 | 0 | 0 | 0 | 0 | 0 | 0 | 0 | 0 |
| | 3 | | | | | | | 1 | .5 | -.5 | -1 | 0 | -.5 | 0 | -.5 | .5 | 0 |
| | 4 | | | | | | | | 1 | 0 | -.5 | 0 | .5 | -.5 | -1 | -.5 | 0 |
| 3 | 1 | | | | | | | | | 1 | .5 | 0 | .5 | .5 | 0 | -.5 | 0 |
| | 2 | | | | | | | | | | 1 | 0 | .5 | 0 | .5 | -.5 | 0 |
| | 3 | | | | | | | | | | | 0 | 0 | 0 | 0 | 0 | 0 |
| | 4 | | | | | | | | | | | | 1 | -.5 | -.5 | -1 | 0 |
| 4 | 1 | | | | | | | | | | | | | 1 | .5 | .5 | 0 |
| | 2 | | | | | | | | | | | | | | 1 | .5 | 0 |
| | 3 | | | | | | | | | | | | | | | 1 | 0 |
| | 4 | | | | | | | | | | | | | | | | 0 |

Figure C-1

Trace Function Noise Covariance Matrix

To generate the dependent gaussian variables:

$$V = U \Lambda^{\frac{1}{2}} Z \tag{C-4}$$

where V - dependent random variable vector

Z - independent random variable vector

As a result the covariance of V is:

$$E\{VV^t\} = V \Lambda^{\frac{1}{2}} E\{ZZ^t\} \Lambda^{\frac{1}{2}} U^t \tag{C-5}$$

$E\{ZZ^t\} = I$ - independent, unity variance

$$E\{VV^t\} = U \Lambda U^t = Q \tag{C-6}$$

To get the required noise power V will be multiplied by the scalar $\sqrt{Np}$ (noise r.m.s. amplitude):

$$No = \sqrt{Np}\, U \Lambda^{\frac{1}{2}} Z \tag{C-7}$$

2. Simulation

Once the additive noise was generated it was added to the trace function calculated for the circular or linear array Eq. (II-8) and (II-10) respectively.

Next the corresponding MMSE estimator was applied to Eq. (III-23) and (III-24).

The above operations were run 48 times and the mean and variance of the resultant bearing estimates were calculated and printed out. In addition a plot of the beamwidth versus input SNR was done.

The CRLB Eq. (IV-3) and (IV-4) respectively are given only with the simulation results for comparison purposes.

Following is a listing of the simulation program for an 8 element circular array. In order to change the number of elements in addition to change of the parameter N the relevant arrays in the main program have to be redimensioned. (line 240)

In order to change to a linear array, equations have to be changed to the applicable ones in the generation of the signals, the estimators and the CRLB (lines 200, 360, 680, 1270, 1670, 1680, 1710, 1760, 1770, 1800).

The transformation matrix for the generation of the correlated random variable ($t = U \Lambda^{\frac{1}{2}}$) has to be calculated only once for a given number of elements, then this part of the program can be skipped (lines 260 to 290). Care should be taken to have a data file (TRAN) defined for the storage of the transformation matrix. The subroutine "Symqr" (line 2170) for the eigen-analysis can be found in the Hewlett-Packard Numerical Analysis Software Package.

```
10    ! ************************************************************************
20    ! *  PHASE DIFFERENCE TRACE FUNCTION ESTIMATION - SIMULATION PROGRAM     *
30    ! *        PARAMETER DEFINITION                                          *
40    ! *        D - Array Diameter                                            *
41    ! *        F - Freqency                                                  *
60    ! *        C - Speed Of Sound                                            *
70    ! *        N - Number Of Elements                                        *
80    ! *        Ro - Correlation Coeff. For The Correlated Noise Generator    *
90    ! *        It - Number Of Runs For Statistical Averaging                 *
100   ! *        Edf - Equivalent # Of Degrees Of Freedom                      *
110   ! *        Theta - Bearing                                               *
120   ! ************************************************************************
130   OPTION BASE 1
140   D=5
150   F=100
160   C=1500
170   Lambda=C/F
180   N=8
190   Ro=.5
200   K1=-2*PI*D/Lambda
210   It=48
220   Edf=250
230   Theta=PI/6
240   DIM Meas(8,8),Out(25,4),Tran(64,64),Meascor(8,8)
250   OVERLAP
260   ASSIGN #1 TO "TRAN"
270   CALL Transf(Tran(*),N,Ro)
280   MAT PRINT #1;Tran
290   GOTO 320
300   ASSIGN #2 TO "TRAN"
310   MAT READ #2;Tran
320   A1=2*PI/N
330   Sum=0
340   FOR J=1 TO N-1
350   FOR I=J+1 TO N
360   Sum=Sum+(COS(PI*(J+I)/N-Theta)*SIN(PI*(J-I)/N))^2
370   NEXT I
380   NEXT J
```

```
390   FOR M=0 TO 24
400   Sn=1/32*SQR(2)^M
410   Out(M+1,1)=10*LGT(Sn)
420   Cohsq=(Sn/(Sn+1))^2
430   Np=SQR((1-Cohsq)/(Cohsq*Edf))
440   PRINT "POINT # ";M,LIN(1)
450   PRINT "S/N=";10*LGT(Sn);"DB(";Sn;")"
460   PRINT "COH=";Cohsq;"   VAR(Noise on phase)=";Np^2;"RAD**2";LIN(1),"STD DEV
=";Np*180/PI;"DEG"
470   PRINT LIN(1)
480   Out(M+1,2)=Np^2*C^2/((D*F*PI*2)^2*2*Sum)
490   Sume1=Sumv1=Sume2=Sumv2=0
500   FOR Ii=1 TO It
510   RANDOMIZE
520   CALL Dat(Meas(*),N,K1,Theta,Np,Tran(*),Meascor(*))
530   CALL Est(Meas(*),N,A1,Th1est,K1,Th2est,Meascor(*))
540   Sume1=Sume1+Th1est
550   Sumv1=Sumv1+Th1est^2
560   Sume2=Sume2+Th2est
570   Sumv2=Sumv2+Th2est^2
580   NEXT Ii
590   The1=Sume1/It
600   Var1=(Sumv1-It*The1^2)/(It-1)
610   The2=Sume2/It
620   Var2=(Sumv2-It*The2^2)/(It-1)
630   Out(M+1,3)=Var1
640   Out(M+1,4)=Var2
650   PRINT "(1)  Bearing(Trace Function)=";The1*180/PI;"DEG",LIN(1),"VAR=";Var1
;" BEAMWIDTH=";2*SQR(Var1)*180/PI;"DEG",LIN(1),"BIAS=";(The1-Theta)*180/PI;"DEG"
660   PRINT "(2)  Bearing(Corr.Trace Fun)=";The2*180/PI;"DEG";LIN(1);"VAR=";Var2
;" BEAMWIDTH=";2*SQR(Var2)*180/PI;"DEG",LIN(1),"BIAS=";(The2-Theta)*180/PI;"DEG"
670   PRINT "(3)  OPTIMAL(CRLB) ",LIN(1),"VAR=";Out(M+1,2);"RAD**2";"  BEAMWIDTH
=";2*SQR(Out(M+1,2))*180/PI;"DEG"
680   PRINT LIN(1)
690   NEXT M
700   PLOTTER IS 13,"GRAPHICS"
```

```
710   GRAPHICS
720   FRAME
730   PRINTER IS 0
740   RAD
750   LOCATE 10,120,10,90
760   Xmin=-15
770   Xmax=21
780   Ymin=0
790   Ymax=25
800   SCALE Xmin,Xmax,Ymin,Ymax
810   AXES 1,.5,Xmin,Ymin,3,10
820   FRAME
830   MOVE Out(1,1),2*SQR(Out(1,2))*180/PI
840   FOR I=1 TO 25
850   DRAW Out(I,1),2*SQR(Out(I,2))*180/PI
860   NEXT I
870   LINE TYPE 8
880   MOVE Out(1,1),2*SQR(Out(1,3))*180/PI
890   FOR I=1 TO 25
900   DRAW Out(I,1),2*SQR(Out(I,3))*180/PI
910   NEXT I
920   LINE TYPE 5
930   MOVE Out(1,1),2*SQR(Out(1,4))*180/PI
940   FOR I=1 TO 25
950   DRAW Out(I,1),2*SQR(Out(I,4))*180/PI
960   NEXT I
970   LINE TYPE 1
980   CSIZE 3.5
990   LORG 5
1000  FOR X=Xmin TO Xmax STEP 3
1010  MOVE X,-1
1020  LABEL X
1030  NEXT X
1040  MOVE 3,-2.2
1050  LABEL "INPUT SNR [DB]"
1060  LORG 8
```

```
1070  FOR Y=Ymin TO Ymax STEP 5
1080  MOVE Xmin-.1,Y
1090  LABEL Y
1100  NEXT Y
1110  CSIZE 3
1120  LORG 5
1130  MOVE Xmin-2.50,(Ymax-Ymin)/2
1140  LDIR PI/2
1150  LABEL "BEAMWIDTH (2* )[DEG.]"
1160  PRINT PAGE
1170  DUMP GRAPHICS
1180  PRINT PAGE
1190  DUMP GRAPHICS
1200  PRINT LIN(2)
1210  END
1220  SUB Dat(Meas(*),N,K,Theta,Np,Tran(*),Meascor(*))
1230  OPTION BASE 1
1240  DIM Fi(N,N),No(N,N),Z(N^2),X(N^2)
1250  FOR I=1 TO N
1260  FOR J=1 TO I
1270  Fi(I,J)=K*SIN(PI*(I+J)/N-Theta)*SIN(PI*(I-J)/N)
1280  Fi(J,I)=-Fi(I,J)
1290  NEXT J
1300  NEXT I
1310  Up=N^2-1
1320  FOR P=1 TO Up STEP 2
1330  Temp1=SQR(-2*LOG(RND))
1340  Temp2=2*PI*RND
1350  Z(P)=Temp1*COS(Temp2)
1360  Z(P+1)=Temp1*SIN(Temp2)
1370  NEXT P
1380  Cnt=0
1390  FOR I=0 TO N-1
1400  FOR J=1 TO I+1
1410  Cnt=Cnt+1
1420  No(I+1,J)=Z(Cnt)
```

```
1430  No(J,I+1)=-No(I+1,J)
1440  NEXT J
1450  NEXT I
1460  Kk=1
1470  MAT No=No*(Np)
1480  MAT Fi=Fi*(Kk)
1490  MAT Meas=Fi+No
1500  MAT X=Tran*Z
1510  FOR I=0 TO N-1
1520  FOR J=1 TO N
1530  No(I+1,J)=X(N*I+J)
1540  NEXT J
1550  NEXT I
1560  MAT No=No*(Np)
1570  MAT Fi=Fi*(Kk)
1580  MAT Meascor=Fi+No
1590  SUBEND
1600  !
1610  !
1620  SUB Est(Meas(*),N,A,Th1est,K,Th2est,Meascor(*))
1630  OPTION BASE 1
1640  DIM Si(N,N),Co(N,N)
1650  FOR I1=1 TO N
1660  FOR J1=I1 TO N
1670  Si(I1,J1)=Meas(I1,J1)*(SIN(A*I1)-SIN(A*J1))
1680  Co(I1,J1)=Meas(I1,J1)*(COS(A*I1)-COS(A*J1))
1690  NEXT J1
1700  NEXT I1
1710  Th1est=ATN(SUM(Si)/SUM(Co))
1720  MAT Si=ZER
1730  MAT Co=ZER
1740  FOR I1=1 TO N
1750  FOR J1=I1 TO N
1760  Si(I1,J1)=Meascor(I1,J1)*(SIN(A*I1)-SIN(A*J1))
1770  Co(I1,J1)=Meascor(I1,J1)*(COS(A*I1)-COS(A*J1))
1780  NEXT J1
```

```
1790  NEXT I1
1800  Th2est=ATN(SUM(Si)/SUM(Co))
1810  SUBEND
1820  SUB Transf(Tran(*),N,Ro)
1830  OPTION BASE 1
1840  DIM C(N^2,N^2),D(N^2),E(N^2),Ev(N^2,N^2)
1850  FOR I=0 TO N-1
1860  FOR J=1 TO N
1870  FOR L=0 TO N-1
1880  FOR K=1 TO N
1890  P=N*I+J
1900  Q=N*L+K
1910  IF (I=L) AND (J=K) THEN 2020
1920  IF (I+1=K) AND (J=L+1) THEN 2000
1930  IF (I+1=J) AND (L=I) OR (L+1=K) AND (L=I) THEN 2040
1940  IF (I+1=J) AND (J=K) OR (L+1=K) AND (J=K) THEN 2060
1950  IF (I+1=K) OR (L+1=J) THEN 2080
1960  IF (I=L) OR (J=K) THEN 1980
1970  GOTO 2100
1980  C(P,Q)=Ro
1990  GOTO 2110
2000  C(P,Q)=-1
2010  GOTO 2110
2020  C(P,Q)=1
2030  GOTO 2110
2040  C(P,Q)=0
2050  GOTO 2110
2060  C(P,Q)=0
2070  GOTO 2110
2080  C(P,Q)=-Ro
2090  GOTO 2110
2100  C(P,Q)=0
2110  NEXT K
2120  NEXT L
2130  NEXT J
2140  NEXT I
```

```
2150  PRINT "******* COVARIANCE MATRIX ***********"
2160  MAT PRINT C
2170  CALL Symqr(C(*),D(*),E(*),0,N^2,1E-20,0,1,0,1)
2180  PRINT "************ EIGENVALUES ************"
2190  MAT PRINT D
2200  PRINT "************ EIGENVECTORS ***********"
2210  MAT PRINT C
2220  MAT Ev=ZER
2230  FOR I=1 TO N^2
2240  IF ABS(D(I))<1E-6 THEN D(I)=0
2250  Ev(I,I)=SQR(D(I))
2260  NEXT I
2270  MAT Tran=C*Ev
2280  PRINT "****** TRANSFORMATION MATRIX ********"
2290  MAT PRINT Tran
2300  SUBEND
```

# BIBLIOGRAPHY

This section consists of two parts:

- References which are explictely mentioned in this work.
- Additional subject related bibliography which is an outcome of an extensive bibliographical search done during the course of this work.

## A. LIST OF REFERENCES


1. Baggeroer, A. B., "Space/Time Random Processes and Optimum Array Processing", Naval Undersea Center, NUC TP506, April 1976.

2. Bangs, W. J. and Schultheiss, P. M., "Space-Time Processing for Optimal Parameter Estimation", in Signal Processing, p. 577-590, J.W.R. Griffiths, P. L. Stocklin, and C. VanSchooneveld (Ed), Academic Press, 1973.

3. Bennett, C. M., "The Directional Analysis of Ocean Waves: An Introductory Discussion", Naval Coastal System Laboratory Report NCSL-144-72, Dec. 1972.

4. Bernnan, L. E. and Mallett, J. D., "Efficient Simulation of External Noise Incident on Arrays", IEEE Trans. Ant. Prop., p. 740, Sept. 1976.

5. Bryn, F., "Optimum Signal Processing of Three Dimensional Arrays Operating on Gaussian Signals and Noise", Journal Acoust. Soc. Am., v. 34, No. 3, p. 289, 1962.

6. Carter, G. C., "Time Delay Estimation", University of Connecticut, Ph.D. Thesis, 1976.

7. Carter, G. C., "Receiver Operating Characteristics for a Linearly Thresholded Coherence Estimation Detector", IEEE Trans. Acoust. Speech and Sig. Proc., p. 90, February 1977.

8. Carter, G. C., Nuttall, A. H., and Cable, P. G., "The Smoothed Coherence Transform", IEEE Proc., V. 61, No. 10, p. 1497, 1973.

9. Chan, Y. T., Hattin, R. V., and Plant, J. B., "The Least Squares Estimation of Time Delay and Its Use in Signal Detection", IEEE Trans. Acoust. Speech Signal Proc., ASSP-26, No. 3, p. 217, 1978.

10. Dawoud, M. M. and Anderson, A. P., "Design of Super-directive Arrays with High Radiation Efficiency", IEEE Trans. Ant. Prop., AP-26, No. 6, p. 819, 1978.

11. Faran, J. J. and Hills, R., "Wide Band Directivity of Receiving Arrays", Journal Acoust. Soc. Am., V. 57, No. 6, p. 1300, 1975.

12. Frost, O. L., "An Algorithm for Linearly Constrained Adaptive Array Processing", IEEE Proc., V. 60, No. 8, p. 926, 1972.

13. Hahn, W. R., "Optimum Signal Processing for Passive Sonar Range and Bearing Estimation", Journal Acoust. Soc. Am., V. 58, No. 1, July 1975.

14. Hamon, B. V. and Hannan, E. J., "Spectral Estimation of Time Delay for Dispersive and Non Dispersive Systems", Appl. Statist., V. 23, No. 2, p. 134, 1974.

15. Hassab, J. C. and Boucher, R. E., "Optimum Estimation of Time Delay By a Generalized Correlator", IEEE Trans. on Acoust., Speech and Sig. Proc., V. ASSP-27, No. 4, p. 373, Aug. 1979.

16. Hodgkiss, W. S. and Nolte, L. W., "Covariance Between Fourier Coefficients Representing the Time-Waveforms Observed from an Array of Sensors", Journal Acoust. Soc. Am., V. 59, No. 3, p. 582, 1976.

17. Jacobson, M. J., "Analysis of a Multiple Receiver Correlation System", Journal Acoust. Soc. Am., V. 29, No. 12, p. 1342, 1957.

18. Jenkins, G. M. and Watts, D. G., "Spectral Analysis and Its Applications", Holden-Day Inc., 1969.

19. Knapp, C. H. and Carter, G. C., "The Generalized Correlation Method for Estimation of Time Delay", IEEE Trans. Acoust. Speech, Sig. Proc., V. ASSP-24, No. 4, p. 320, 1976.

20. Knapp, C. H., "An Algorithm for Estimation of the Inverse Spectral Matrix", General Dynamics Corp., Electric Boat Div. Report, U417-70-010, 1970.

21. Miller, L., "Signal Detection and Bearing Estimation Capabilities of Multiplicative Array Processors", The Catholic University of America, Ph.D., Thesis, 1973.

22. Munk, W. H., Miller, G. R., Snodgrass, F. E., and Barber, N. F., "Directional Recording of Swell from Distant Storms", Philosophical Transactions of the Royal Society of London, Series A., V. 255, No. 1062, p. 505-584, April 1963.

23. Nahi, N. E., "Estimation Theory and Applications", Wiley, 1969.

24. Newman, E. H., et. al. "Superdirective Receiving Arrays", IEEE Trans. Ant., Prop., V. AP-26, No. 5, p. 629, 1978.

25. Nuttall, A. H., "Spectral Estimation by Means of Overlapped F.F.T. Processing of Windowed Data", Naval Underwater System Center, TR-4169, 1971.

26. Nuttall, A. H., "Estimation of Cross-Spectra Via Overlapped F.F.T. Processing", Naval Underwater System Center, TR-4169-S, 1975.

27. Nuttall, A. H., "Probability Distribution of Spectral Estimates Obtained via Overlapped F.F.T. Processing of Windowed Data", Naval Underwater System Center, TR-5529, 1976.

28. Nuttall, A. H. and Carter, G. C., "Bias of the Estimate of Magnitude Squared Coherence", IEEE Trans. Acoust., Speech Sig. Proc., p. 582 (corresp.), December 1976.

29. Nuttall, A. H., "On the Variance of the Phase Estimate of the Cross Spectrum and Coherence", Naval Underwater System Center, TM 771112, 10 June 1977.

30. Sackman, G. L. and Shelef, S. C., "The Use of Time Delay/Phase Difference Trace Functions for Bearing Estimation in Arrays", Proceedings of the Time Delay Estimation and Application Conference, Vol. 1, p. D-1, Naval Underwater Systems Center, 16 July 1979.

31. Sackman, G. L. and Shelef, S. C., "The Use of Time Delay/Phase Difference Trace Functions for Bearing Estimation in Arrays", Proceedings of the Asilomar Conference on Circuits, Systems and Computers, Nov. 1979. (To be published)

32. Shensa, M. and Black, C., "Passive Bearing Estimation: The Removal of Bias and $2\pi$ Ambiguities", Journal Acoust. Soc. Am., V. 63, No. 1, p. 91, 1978.

33. Speiser, J. M., "Beamformer Architectures", NOSC Symposium, Oct. 1977.

34. Stradling, C. S. and Baggeroer, A. B., "Joint Active and Passive Sonar Signal Processing Using Arrays", Naval Undersea Center, TP-121, 1969.

35. Steinberg, B. D., "Principles of Aperture and Array System Design", John Wiley & Sons, 1976.

36. Tribolet, J. M., "A New Phase Unwrapping Algorithm", IEEE, Trans. Acoust. Speech Sig. Proc., V. ASSP-25, No. 2, p. 170, 1977.

37. Urick, R. J., "Principles of Underwater Sound", McGraw-Hill, Inc., 1975.

38. VanTrees, H. L., "Detection, Estimation, and Modulation Theory", Part 1, Wiley, 1968.

39. VanTrees, H. L., "A Unified Theory for Optimum Array Processing", Arthur D. Little, Inc., (AD 649-929), 1966.

40. Welch, P. D., "The Use of Fast Fourier Transform for the Estimation of Power Spectra: A Method Based on Time Averaging Over Short Modified Periodograms", IEEE, Trans. Audio Electroacoust, V. AU-15, No. 2, p. 70, 1967.

41. Whalen, A. D., "Detection of Signals in Noise", Academic Press, 1971.

42. Widrow, B., et. al., "Adaptive Antenna Systems", IEEE. Proc., V. 55, No. 12, p. 2143, 1967.

## B. ADDITIONAL SUBJECT RELATED BIBLIOGRAPHY


1. Adams, S. L., and Nolte, L. W., "Bayes Optimum Array Detection of Targets of Known Location", Journal Acoust. Soc. Am., V. 58, No. 3, p. 656, Sept. 1975.

2. Adams, S. L., and Nolte, L. W., "Optimum Array Detection in Fluctuating Ambient Noise Fields", Journal Acoust. Soc. Am., V. 58, No. 3, Sept. 1975.

3. Applebaum, S. P., "Adaptive Arrays", IEEE Trans. Ant. Prop., V. AP-24, No. 5, p. 585, Sept. 1976.

4. Applebaum, S. P., and Chapman, D. J., "Adaptive Arrays with Main Beam Constraints", IEEE Trans. Ant. Prop., V. AP-24, No. 5, p. 650, Sept. 1976.

5. Autrey, S. W., "Design of Arrays to Achieve Specified Spatial Characteristics over Broad Bands", in Signal Processing, p. 507-527, J.W.R. Griffiths, P.L. Stocklin, and C. VanSchooneveld (Ed.), Academic Press, 1973.

6. Anderson, V. C., and Munson, J. C., "Directivity of Spherical Receiving Arrays", Journal Acoust. Soc. Am., V. 35, No. 8, p. 1162, Aug. 1963.

7. Arase, E. M., and Arase, T., "Correlation of Ambient Sea Noise", Journal Acoust. Soc. Am., V. 40, No. 1, 1966.

8. Handbook of Array Design Technology, V-I, prepared by Applied Hydro-Acoustics Research, Inc., June 30, 1976.

9. Abraham, P. B., and Carter, G. C., "Determination of Source Motion from Relative Time Compressions and Time Delays to Three Sensors", U.S. Navy Journal of Underwater Acoustics, V. 28, No. 1, Jan. 1978.

10. Bucker, H. P., "High-Resolution Cross-Sensor Beamforming for a Uniform Line Array", Journal Acoust. Soc. Am., V. 63, No. 2, p. 420, Feb. 1978.

11. Bershad, N. J., and Teintuch, P. L., "Sonar Array Detection of Gaussian Signals in Gaussian Noise of Unknown Power", IEEE Trans. Aerosp. Elect. Syst., V. AES-10, No. 1, p. 94, Jan. 1974.

12. Bucker, H. P., "Comparison of FFT and Prony Algorithms for Bearing Estimation of Narrow-Band Signals in a Realistic Ocean Environment", Journal Acoust. Soc. Am., V. 61, No. 3, p. 756, March 1977.

13. Bucker, H. P., "Cross-Sensor Beam Forming with a Sparse Line Array", Journal Acoust. Soc. Am., V. 61, No. 2, p. 494, Feb. 1977.

14. Baird, C. A., and Rassweiler, G. G., "Adaptive Sidelobe Nulling Using Digitally Controlled Phase-Shifters", IEEE Trans. Ant. Prop., V. AP-24, No. 5, p. 638, Sept. 1976.

15. Brown, J. L., Jr., "Variation of Array Performance with Respect to Statistical Phase Fluctuations", Journal Acoust. Soc. Am., V. 34, No. 12, p. 1927, Dec. 1962.

16. Burg, J. P., "Three-Dimensional Filtering with an Array of Seismometers", Geophysics, V. XXIX, No. 5, p. 693, Oct. 1964.

17. Brillinger, D. R., "Fourier Analysis of Stationary Processes", IEEE Proc., V. 62, No. 12, Dec. 1974.

18. Berman, A., and Clay, C. S., "Theory of Time-Averaged-Product Arrays", Journal Acoust. Soc. Am., V. 29, No. 7, July 1957.

19. Cron, B. J., and Sherman, C. H., "Spatial-Correlation Functions for Various Noise Models", Journal Acoust. Soc. Am., V. 13, No. 11, p. 1732, Nov. 1962.

20. Carter, G. C., "Estimation of the Magnitude-Squared Coherence Function (Spectrum)", Naval Underwater Systems Center, T.R. 4343, 19 May 1972.

21. Carter, G. C., "The Role of Coherence in Time Delay Estimation", in Aspects of Signal Processing, p. 251-256, G. Tacconi (Ed), D. Reidel Publishing Company, 1976.

22. Carter, G. C., "Optimum Element Placement for Passive Localization", Naval Underwater Systems Center, TD 5689, 6 July 1977.

23. Carter, G. C., "A Brief Description of the Fundamental Difficulties in Passive Ranging" (Communications), IEEE Journal of Oceanic Engineering, V. OE-3, No. 3, July 1978.

24. Carter, G. C., Knapp, C. H., and Nuttall, A. H., "Estimation of the Magnitude-Squared Coherence Function Via Overlapped Fast Fourier Transform Processing", IEEE Trans. Audio Elect. Acoust., V. AU-21, No. 4, Aug. 1973.

25. Carter, G. C., "Variance Bounds for Passively Locating an Acoustic Source with a Symmetric Line Array", Journal Acoust. Soc. Am., V. 62, No. 4, p. 922, Oct. 1977.

26. Carter, G. C., "Bias in Bearing Estimation Resulting from Source Motion", Journal Acoust. Soc. Am., V. 62 No. 6, p. 1447, Dec. 1977.

27. Carter, G. C., "Optimum Element Placement for Passive Bearing Estimation in Unequal Signal-to-Noise Ratio Environment" (Correspondence), IEEE Trans. Acoust. Speech Sig. Proc., V. ASSP-26, No. 4, p. 365, Aug. 1978.

28. Carter, G. C., Knapp, C. H., and Nuttall, A. H., "Statistics of the Estimate of the Magnitude-Coherence Function", IEEE Trans. Audio Elect. Acoust., V. AU-21, No. 4, p. 388, Aug. 1973.

29. Carter, G. C., and Knapp, C. H., "Coherence and its Estimation via the Partitioned Modified Chirp-Z Transform", IEEE Trans. on Acoust. Speech Sig. Proc., V. ASSP-23, No. 3, p. 257, June 1975.

30. Carter, G. C., "Coherence Estimation as Affected by Weighting Functions and Fast Fourier Transform Size", Naval Underwater Systems Center, TR 4423, 12 Oct 1972.

31. Cox, H., "Sensitivity Considerations in Adaptive Beaforming", in Signal Processing, p. 619-646, J.W.R. Griffiths, P.L. Stocklin, and C. Van Schooneveld (Ed.), Academic Press, 1973.

32. Cox, H., "Optimum Arrays and the Schwartz Inequality", Journal Acoust. Soc. Am., V. 45, No. 1, p. 228, 1969.

33. Cox, H., "Spatial Correlation in Arbitrary Noise Fields with Application to Ambient Sea Noise", Journal Acoust. Soc. Am., V. 54, No. 5, p. 1289, 1973.

34. Cox, H., "Line Array Performance when the Signal Coherence is Spatially Dependent", Journal Acoust, Soc. Am., V. 54, No. 6, p. 1743, 1973.

35. Cox, H., "Resolving Power and Sensitivity to Mismatch of Optimum Array Processors", Journal Acoust. Soc. Am., V. 54, No. 3, p. 771, 1973.

36. Cheng, D. K., "Optimization Techniques for Antenna Arrays", IEEE Proc., V. 59, No. 12, p. 1664, Dec. 71.

37. Capon, J., "High-Resolution Frequency-Wavenumber Spectrum Analysis", IEEE Proc., V. 57, No. 8, p. 1408, Aug. 1969.

38. Clay, C. S., Hinich, M. J., and Shaman, P., "Error Analysis of Velocity and Direction Measurements of Plane Waves Using Thick Large-Aperture Arrays", Journal Acous. Soc. Am., V. 53, No. 4, p. 1161, 1973.

39. Clay, C. S., and Hinich, M. J., "Use of a Two-Dimensional Array to receive an Unknown Signal in a Dispersive Waveguide", Journal Acoust. Soc. Am., V. 47, No. 2, p. 435, 1970.

40. Childers, D. G., and Reed, I. S., "On the Theory of Continuous Array Processing", IEEE Trans. Aerosp. Nav. Elect., p. 103, June 1965.

41. Cron, B. F., Hassell, B. C., and Keltonic, F. J., "Comparison of Theoretical and Experimental Values of Spatial Correlation", Journal Acoust. Soc. Am., V. 37, No. 3, p. 523, March 1965.

42. Cleveland, W. S., and Parzen, E., "The Estimation of Coherence, Frequency Response, and Envelope Delay", Technometrics, V. 17, No. 2, p. 167, May 1975.

43. Crochiere, R. E., Rabiner, L. R., and Shively, R. R., "A Novel Implementation of Digital Phase Shifters", The Bell System Technical Journal, p. 1497, Oct. 1975.

44. Davis, R. C., Brennan, L. E., and Reed, L. S., "Angle Estimation with Adaptive Arrays in External Noise Fields", IEEE Trans. Aerosp. Elect. Syst., V. AES-12, No. 2, p. 179, March 1976.

45. Davies, D.E.N., and McCartney, B. S., "Cylindrical Arrays with Electronic Beam Scanning", IEEE Proc., V. 112, No. 3, p. 497, March 1965.

46. Edelblute, D. J., Fisk, J. M., and Kinnison, G. L., "Criteria for Optimum-Signal-Detection Theory for Arrays", Journal Acoust. Soc. Am., V. 41, No. 1, p. 199, 1967.

47. Feintuch, P. L., and Weber, C. L., "Specification and Performance of Passive Sonar Spectral Estimators", IEEE Trans. Aerosp. Elect. Syst., V. AES-9, No. 6, p. 889, Nov. 1973.

48. Farrier, D. R., Durrani, T. S., and Nightingale, J. M., "Fast Beamforming Techniques for Circular Arrays", Journal Acoust. Soc. Am., V. 58, No. 4, p. 920, Oct. 1975.

49. Frank, T. H., Kesner, J. W., and Gruen, H. M., "Conformal Array Beam Patterns and Directivity Indices", Journal Acoust. Soc. Am., V. 63, No. 3, p. 841, March 1978.

50. Fitelson, M. M., "Correlation Function of the Field Between Arbitrarily Oriented Points for a Plane Wave in a Random Medium", Journal Acoust. Soc. Am., V. 58, No. 3, p. 679, Sept. 1975.

51. Fischer, W. K., "An Alternate Approach To Optimum Bearing Estimation", Naval Underwater Systems Center, TR-5439, 27 Sept 1976.

52. Feintuch, P., "Passive Sonar Spectral Estimation", Ph.D. Thesis, University of Southern California, June 1972.

53. Frank, T., "A Linear Transformation Superresolution Processor and a Modified Sampling Array Bearing Estimator", Ph.D. Thesis, The Catholic University of America, 1978.

54. Gilbert, E. N., and Morgan, S. P., "Optimum Design of Directive Antenna Arrays Subject to Random Variations", The Bell System Technical Journal, p. 637, May 1955.

55. Gabriel, W. F., "Adaptive Arrays-An Introduction", IEEE Proc., V. 64, No. 2, p. 239, Feb. 1976.

56. Goode, B. B., "Adaptive Sensor Array Processing", Naval Undersea Center, TP. 259, Sept. 1971.

57. Griffiths, L. J., "A Simple Adaptive Algorithm for Real-Time Processing in Antenna Arrays", IEEE Proc., V. 51, No. 10, p. 1696, Oct. 1969.

58. Gaarder, N. T., "The Design of Point Detector Arrays, I", IEEE Trans. Inf. Theory, V. IT-13, No. 1, p. 42, Jan. 1966.

59. Gaarder, N. T., "The Design of Point Detector Arrays, II", IEEE Trans. Inf. Theory, V. IT-12, No. 2, p. 112, Apr. 1966.

60. Geist, J. M., "Computer Generation of Correlated Gaussian Random Variables", IEEE Proc., V. 67, No. 5, p. 862, May 1979.

61. Hahm, R. H., and Trelter, S. A., "Optimum Processing for Delay-Vector Estimation in Passive Signal Arrays", IEEE Trans. Inf. Theory, V. IT-19, No. 3, p. 608, Sept. 1973.

62. Hodgkiss, W. S., and Nolte, L. W., "Adaptive Optimum Array Processing", Journal Acoust. Soc. Am., V. 61, No. 3, p. 763, March 1977.

63. Hansen, W. W., and Woodyard, J. R., "A New Principle in Directional Antenna Design", I.R.E. Proc., V. 26, No. 3, p. 333, March 1938.

64. Hinich, M. J., "Processing Spatially Aliased Arrays", Journal Acoust. Soc. Am., V. 63, No. 3, p. 792, Sept. 1978.

65. Hinich, M. J., and Shaman, P., "Parameter Estimation for an R- Dimensional Plane Wave Observed with Additive Independent Gaussian Errors", The Annals of Mathematical Statistics, V. 43, No. 1, p. 153, 1972.

66. Hannan, E. J., and Thomson, P. J., "The Estimation of Coherence and Group Delay", Biometrika, V. 58, No. 3, p. 469, 1971.

67. Hannan, E. J., and Thomson, P. J., "Estimating Group Delay", Biometrika, V. 60, No. 2, p. 241, 1973.

68. Horton, C. W., "Signal Processing Of Underwater Acoustic Waves", U. S. Printing Office, 1969.

69. Jacobson, M. J., "Space-Time Correlation in Spherical and Circular Noise Fields", Journal Acoust. Soc. Am., V. 37, No. 7, p. 971, July 1962.

70. Kooij, T., "Adaptive Array Processors for Sensitivity Constrained Optimization", Ph.D. Thesis, The Catholic University of America, 1977.

71. Kirlin, L., "Augmenting the Maximum Likelihood Delay Estimator to Give Maximum Likelihood Direction", (Correspondence), IEEE Trans. Acoust. Speech Sig. Proc., V. ASSP-20, No. 1, p. 107, Feb. 1978.

72. Knapp, C. H., and Carter, G. C., "Estimation of Time Delay in the Presence of Source or Receiver Motion", Journal Acoust. Soc. Am., V. 61, No. 6, p. 1545, June 1977.

73. Liu, C. S., and Nolte, L. W., "Performance Sensitivity of Array Detectors to a priori Spatial Knowledge", Journal Acoust. Soc. Am., V. 63, No. 3, p. 848, Mar. 1978.

74. Lo, Y. T., Lee, S. W., and Lee, Q. H., "Optimization of Directivity and Signal-to-Noise Ratio of an Arbitrary Antenna Array", IEEE Proc., V. 54, No. 8, p. 1033, Aug. 1966.

75. Lee, S., "Relationships Between Detection and Estimation Scalar and Array Processing", Ph.D. Thesis, Duke University, 1976.

76. Longstaff, I. D., Chow, P.E.K., and Davies, D.E.N., "Directional Properties of Circular Arrays", IEEE Proc., V. 114, No. 6, p. 713, June 1967.

77. Levin, M. J., "Least-Squares Array Processing for Signals of Unknown Form", The Radio and Electronic Engineer, p. 213, April 1965.

78. Lunde, E. B., "Estimation of Signal Phase", Naval Underwater Systems Center, TC-7-75, 12 Sept. 1975.

79. Liggett, W. S., Jr., and Jacobson, M. J., "Noise Covariance and Vertical Directivity in a Deep Ocean", Journal Acoust. Soc. Am., V. 39, No. 2, p. 280, 1966.

80. Lewis, J. B., and Schultheiss, P. M., "Optimum and Conventional Detection Using a Linear Array", Journal Acoust. Soc. Am., V. 49, No. 4, p. 1083, 1971.

81. McDonough, R. N., "Maximum-Entropy Spatial Processing of Array Data", Geophysics, V. 39, No. 6, p. 843, Dec. 1974.

82. McCartney, B. S., "Proposals for an Electronically Scanned Circular Array", IEE Proc., V. 110, No. 7, p. 1220, July 1963.

83. Maksym, J. N., "Directional Accuracy of Small Ring Arrays", Journal Acoust. Soc. Am., V. 61, No. 1, p. 105, Jan. 1977.

84. MacDonald, V. H., and Schultheiss, P. M., "Optimum Passive Bearing Estimation in a Spatially Incoherent Noise Environment", Journal Acoust. Soc. Am., V. 46, No. 1, p. 37, 1969.

85. MacDonald, V. H., "Optimum Bearing Estimation with Passive Sonar Systems", Ph.D. Thesis, Yale, 1971.

86. McMahon, G. W., Hubley, B., and Mohammed, A., "Design of Optimum Directional Arrays Using Linear Programming Techniques", Journal Acoust. Soc. Am., V. 51, No. 1, p. 304, 1972.

87. Middleton, D., and Esposita, R., "Simultaneous Optimum Detection and Estimation of Signals in Noise", IEEE Trans. Inf. Theory, V. IT-14, No. 3, p. 434, May 1968.

88. McGarty, T. P., "The Effect of Interfering Signals on the Performance of Angle of Arrival Estimates", IEEE Trans. Aerosp. Elect. Syst., V. AES-10, No. 1, p. 70, Jan. 1974.

89. Maksym, J. N., "A Robust Formulation of an Optimum Cross-Spectral Beamformer for Line Arrays", Journal Acoust. Soc. Am., V. 65, No. 4, p. 971, Apr. 1979.

90. Nuttall, A. H., Carter, G. C., and Montavon, E. M., "Estimation of the Two-Dimensional Spectrum of the Space-Time Noise Field for a Sparce Line Array", Journal Acoust. Soc. Am., V. 55, No. 5, p. 1034, May 1974.

91. Nuttall, A. H., Estimation of Noise Directionality Spectrum, Naval Underwater Systems Center, TR-4345, 1 Sept. 1972.

92. Nolte, L. W., "Adaptive Processing: Time-Varying Parameters", in Signal Processing, p. 641-656, J.W.R. Griffiths, P. L. Stocklin, and C. Van Schooneveld (Ed.), Academic Press, 1973.

93. Nuttall, A. H., Resolving the Directional Ambiguities of a Line Array of Hydrophones, Naval Underwater Systems Center, TR-4385, 14 Sept. 1972.

94. Nuttall, A. H., and Cable, P. G., "Operating Characteristics for Maximum Likelihood Detection of Signals in Gaussian Noise of Unknown Level - I. Coherent Signals of Unknown Level", Naval Underwater Systems Center, TR-4243, 27 March 1972.

95. Nuttall, A. H., and Cable, P. G., "Operating Characteristics for Maximum Likelihood Detection of Signals in Gaussian Noise of Unknown Level - II. Phase-Incoherent Signals of Unknown Level", Naval Underwater Systems Center, TR-4683, 22 April 1974.

96. Nuttall, A. H., and Cable, P. G., "Operating Characteristics for Maximum Likelihood Detection of Signals in Gaussian Noise of Unknown Level - III. Random Signals of Unknown Level", Naval Underwater Systems Center, TR-4783, 31 July 1974.

97. Nuttall, A. H., "Detection Capabilities of Several Phase-Processing Receivers", Naval Underwater Systems Center, TR-4529, July 1973.

98. Owsley, N. L., "A Recent Trend in Adaptive Spatial Processing for Sensor Arrays: Constrained Adaptation", in Signal Processing, J.W.R. Griffiths, P. L. Stocklin, and C. Van Schooneveld (Ed.), Academic Press, 1973.

99. Owsley, N., "Source Location with an Adaptive Antenna Array", Naval Underwater Systems Center, NL-3015, 6 Jan 1971.

100. Owsley, N., "A Technique for Coherent Detection and Relating of Spectral Signals", Naval Underwater Systems Center, 7 April 1977.

101. Owsley, N., "Adaptive Spatial Processing for the Sonar Noise Environment", U.S. Navy Journal of Underwater Acoustics, V. 25, No. 1, p. 159, Jan. 1975.

102. Oppenheim, A. V. (Ed.), "Applications of Digital Signal Processing", Prentice-Hall, 1978.

103. Patrick, E. A., and Carayannopoulos, G. L., "Bearing Estimation Utilizing Intervalized Basis Functions", Journal Acoust. Soc. Am., V. 56, No. 2, p. 548, Aug. 1974.

104. Page, C. G., "Beamforming of Sensor Arrays by Computer", Royal Aircraft Establishment, TR-73176, Dec. 1973.

105. Pitt, S. P., Adams, W. T., and Vaughan, J. K., "Design and Implementation of a Digital Phase Shift Beamformer", Journal Acoust. Soc. Am., V. 64, No. 3, p. 808, Sept. 1978.

106. Patzewitsch, J. T., Srinath, M. D., and Black, C. I., "Nearfield Performance of Passive Correlation Processing Sonars", Journal Acoust. Soc. Am., V. 64, No. 5, p. 1412, Nov. 1978.

107. Pohler, R. F., "Statistics of the Angle Between Two-Gaussian Phasors", Short, Breed, Pohler, & Cohagan Ass., TN-76-11-01, Sept. 1976.

108. Pridham, R. G., and Mucci, R. A., "Digital Interpolation Beamforming for Low-Pass and Bandpass Signals", IEEE Proc., V. 67, No. 6, p. 906, June 1979.

109. Pridham, R. G., and Mucci, R. A., "A Novel Approach to Digital Beamforming", Journal Acoust. Soc. Am., V. 63, No. 2, p. 425, Feb. 1978.

110. Queen, W. C., "Directional Characteristics Of Cylindrical Receiving Arrays With Nonuniform Hydrophone Response", Journal Acoust. Soc. Am., V. 62, No. 2, p. 400, August, 1977.

111. Queen, W. C., "The Directivity of Sonar Receiving Arrays", Journal Acoust. Soc. Am., V. 47, No. 3, p. 711, 1970.

112. Raabe, H. P., "Fast Beamforming With Circular Receiving Arrays", IBM J. Res. Develop, p. 398, July 1976.

113. Robertson, G. D., "Small Aperture Directional Hydrophones", Proc. EASCON 78, p. 278, 1978 (IEEE).

114. Robinson, A. Z., "A New Approach To Superdirective Arrays", Naval Research Laboratory, Report 7241, Jan. 1971.

115. Roth, P. R., "Effective Measurements Using Digital Signal Analysis", IEEE Spectrum, p. 62, April 1971.

116. Reed, I. S., Mallett, J. D., and Brennan, L. E., "Rapid Convergence Rate In Adaptive Arrays", IEEE Trans. Aerosp. Elect. Sys., V. AES 10, No. 6, p. 853, November 1974.

117. Stocklin, P. L., "Relation of Decision and Physical Wavefield Spaces: Concept and Example", in Signal Processing, p. 347, J.W.R. Griffiths, P. L. Stocklin, and C. Van Schooneveld (Ed.), Academic Press, 1973.

118. Schultheiss, P. M., "Frequency Estimation Using An Array", Proc. EASCON 77, p. 34-1A, 1977.

119. Sullivan, E. J., Jr., "Amplitude Shading Of Irregular Acoustic Arrays", Journal Acoust. Soc. Am., V. 63, No. 6, p. 1873, June 1978.

120. Schweppe, F. C., "Sensor Array Data Processing For Multiple Signal Sources", IEEE Trans. Inf. Theory, V. IT-14, No. 2, p. 294, March 1968.

121. Sheehy, J. J., "Optimum Detection of Signals in Non-Gaussian Noise", Journal Acoust. Soc. Am., V. 63, No. 1, p. 81, January 1978.

122. Sheehy, J. J., "Optimum Estimation of Signal Parameter In Non-Gaussian Noise", Journal Acoust. Soc. Am., V. 64, No. 6, p. 1602, December 1978.

123. Stremler, F. G., and Brown, W. M., "Phase Analysis in Multiple Sensor Receivers with High Signal To Noise Ratio", IEEE Trans. Aerosp. Elect. Syst., V. AES-5, No. 2, p. 163, March 1969.

124. Stremler, F. G., "Estimation of Phase Differences in Multiple Sensor Arrays", IEEE Trans. Aerosp. Elect. Syst., V. AES-6, No. 4, p. 528, July 1970.

125. Skinner, D. P., Hedlicka, S. M. and Matthews, A. D., "Maximum Entropy Array Processing", Journal Acoust. Soc. Am., V. 66, No. 2, p. 488, August 1979.

126. Takao, K., Fujita, M., and Nishi, T., "An Adaptive Antenna Array Under Directional Constraint", IEEE Trans. Ant. Prop., V. AP-24, No. 5, p. 662, September 1976.

127. Taheri, S. H., and Steinberg, B. D., "Tolerances In Self-Cohering Antenna Arrays of Arbitrary Geometry", IEEE Trans. Ant. Prop., V. AP-24, No. 5, p. 733, September 1976.

128. Trider, R. C., "A Fast Fourier Transform (FFT) Based Sonar Signal Processor", IEEE Trans. Acoust. Speech Sig. Proc., V. ASSP-26, No. 1, p. 15, February 1978.

129. Ulrych, T., and Jensen, O., "Cross Spectral Analysis Using Maximum Entropy", Geophysics, V. 39, No. 3, p. 353, June 1974.

130. Vanderkulk, W., "Optimum Processing For Acoustic Arrays", Journal Brit. I.R.E., p. 285, October 1963.

131. Widrow, B., "Adaptive Filters", from Aspects Of Network and System Theory, Kalman, R. E., and DeClaris, 1970.

132. Woods, J. W., Lintz, P. R., "Plane Waves At Small Arrays", Geophysics, V. 38, No. 6, p. 1023, Dec. 1973.

133. Williams, J. R., "Fast Beamforming Algorithm", Journal Acoust. Soc. Am., V. 44, No. 5, p. 1454, 1968.

134. Welkowitz, W., "Directional Circular Arrays of Point Sources", Journal Acoust. Soc. Am., V. 28, No. 3, p. 362, May 1956.

135. Wagstaff, R. A., "Iterative Technique For Ambient Noise Horizontal Directionality Estimation From Towed Line-Array Data", Journal Acoust. Soc. Am., V. 63, No. 3, p. 863, March 1978.

136. Wang, H.S.C., "Amplitude Shading of Sonar Transducer Arrays", Journal Acoust. Soc. Am., V. 57, No. 5, p. 1076, May 1975.

137. Winder, A. A., "Sonar System Technology", IEEE Trans. Sonics Ultrason, V. S4-22, No. 5, p. 291, September 1975.

138. Wirth, W. D., "Suboptimal Suppression of Directional Noise By a Sensor Array Before Beamforming" (Communication), IEEE Trans. Ant. Prop., p. 741, September 1976.

139. Winkler, L. P., and Schwartz, M., "Constrained Array Optimization By Penalty Function Techniques", Journal Acoust. Soc. Am., V. 55, No. 5, p. 1042, May 1974.

140. Wilson, J. H., "Application of the Fourier Series Method To The Detection and Localization of Signals Embedded In A Noise Background", Journal Acoust. Soc. Am., V. 64, No. 4, p. 1046, October 1978.

141. Wenz, G. M., "Acoustic Ambient Noise In The Ocean: Spectra and Sources", Journal Acoust. Soc. Am., V. 34, No. 12, p. 1936, December 1962.

142. Yaru, N., "A Note On Supergain Antenna Arrays", Proc. IRE, p. 1081, September 1951.

143. Ziehm, G., "Optimum Directional Pattern Synthesis of Circular Arrays", The Radio and Electronic Engineer, p. 341, November 1964.

INITIAL DISTRIBUTION LIST

| | | No. Copies |
|---|---|---|
| 1. | Defense Documentation Center<br>Cameron Station<br>Alexandria, Virginia 22314 | 2 |
| 2. | Library, Code 0142<br>Naval Postgraduate School<br>Monterey, California 93940 | 2 |
| 3. | Electrical Engineering Department Chairman, Code 62<br>Department of Electrical Engineering<br>Naval Postgraduate School<br>Monterey, California 93940 | 2 |
| 4. | Professor G. L. Sackman, Code 62Sa<br>Department of Electrical Engineering<br>Naval Postgraduate School<br>Monterey, California 93940 | 20 |
| 5. | Professor S. R. Parker, Code 62Px<br>Department of Electrical Engineering<br>Naval Postgraduate School<br>Monterey, California 93940 | 1 |
| 6. | Professor R. Panholzer, Code 62Pz<br>Department of Electrical Engineering<br>Naval Postgraduate School<br>Monterey, California 93940 | 1 |
| 7. | Professor R. W. Hamming, Code 52Hg<br>Department of Computer Science<br>Naval Postgraduate School<br>Monterey, California 93940 | 1 |
| 8. | Professor A. B. Coppens, Code 61Cz<br>Department of Physics and Chemistry<br>Naval Postgraduate School<br>Monterey, California 93940 | 1 |
| 9. | Professor H. A. Titus, Code 62Ts<br>Department of Electrical Engineering<br>Naval Postgraduate School<br>Monterey, California 93940 | 10 |
| 10. | Professor J. Rockmore, Code 62Rr<br>Department of Electrical Engineering<br>Naval Postgraduate School<br>Monterey, California 93940 | 1 |

| | | |
|---|---|---|
| 11. | Lieutenant Commander S. C. Shelef<br>20 Hasharon Street<br>Raanana<br>Israel | 5 |
| 12. | Commodore H. Ben Eliahu<br>Israeli Navy<br>c/o Embassy of Israel<br>1621 22nd Street N.W.<br>Washington, D.C. 20008 | 1 |
| 13. | Captain I. Almog<br>Israeli Navy<br>c/o Embassy of Israel<br>1621 22nd Street N.W.<br>Washington, D.C. 20008 | 1 |
| 14. | Lieutenant Commander S. C. Shelef<br>Israeli Navy<br>c/o Embassy of Israel<br>1621 22nd Street N.W.<br>Washington, D.C. 20008 | 5 |
| 15. | Lieutenant Colonel A. Feit<br>SMC #1073<br>Naval Postgraduate School<br>Monterey, California 93940 | 1 |
| 16. | Lieutenant H. Amir<br>SMC #2641<br>Naval Postgraduate School<br>Monterey, California 93940 | 1 |

Thesis
S44219 Shelef
c.1
186099
Phase difference/time delay trace functions and their application to bearing estimation in arrays.